# Optimization-based Solutions to Constrained Trajectory-tracking and Path-following Problems

**Dissertation**
zur Erlangung des akademischen Grades
**Doktoringenieur (Dr.-Ing.)**

von
**Timm Faulwasser**
geboren am 5. Mai 1981 in Erfurt

genehmigt durch die Fakultät für Elektrotechnik und Informationstechnik der
Otto-von-Guericke-Universität Magdeburg

Gutachter:
Prof. Dr.-Ing. Rolf Findeisen
Prof. Dr. techn. Andreas Kugi
Prof. Colin Jones, PhD

eingereicht am 23. März 2012
Promotionskolloquium am 5. Oktober 2012

# Acknowledgments

This thesis is the result of my PhD studies in the Systems and Control Group of Rolf Findeisen at the Institute for Automation Engineering, Faculty of Electrical Engineering and Information Technology at the Otto-von-Guericke-Universität Magdeburg, Germany. I would like to express my gratitude to the people who have made this thesis possible.

I am indebted to my supervisor Prof. Dr.-Ing. Rolf Findeisen for leaving large scientific freedom, the opportunity to learn about the administrative aspects of academia, and many lively discussions about scientific and non-scientific topics. Furthermore, I would like to thank Prof. Dr. techn. Andreas Kugi from the Technische Universität Wien, Austria, and Prof. Colin Jones, PhD from the École Polytechnique Fédérale de Lausanne, Switzerland for their willingness to act as external reviewers of this thesis.

In the first months of my time in Magdeburg, when the lab had to be filled with life, and many administrative issues had to be solved, scientific progress would have been impossible without the excellent collaboration in the team of the research assistants in the lab. In particular, I would like to thank Philipp Rumschinski and Paolo Varutti for their excellent cooperation and teamwork not only in these early days. Later on, as the lab grew in terms of team members, I enjoyed working with Jürgen Ihlow, Friedrich von Haeseler, and Stefan Streif as well as with the fellow PhD students: Benjamin Kern, Steffen Borchers, Juan Pablo Zometa, Markus Kögel, Anton Shavchenko, Solvey Maldonado, Petar Andonov, Tobias Bäthge, Nadine Strobel, and Michael Maiworm. The support of Ulrike Thürmer with respect to all non-scientific issues was extremely valuable.

Aside from the persons mentioned I would like to acknowledge the fruitful discussions with Veit Hagenmeyer (BASF), and Friedrich von Haeseler. Their willingness to discuss scientific ideas was a great help. Furthermore, I had the pleasure to learn a lot from the cooperations with Denise Lam (University of Melbourne, Australia), as well as Johann Dauer and Sven Lorenz (Institute for Flight Systems, DLR Braunschweig, Germany).

It is much easier to focus on scientific problems if you can rely on your family and friends. Thus I am indebted to my parents, to my brothers and their families, and to Sophia Hengst for their great support and patience.

December 2012 Timm Faulwasser

# Contents

# Abstract

Systems and control theory is of great importance for the analysis, the design, and the operation of complex dynamical systems. The prototypical problem in control theory is the *stabilization of a set point.* This is the problem of designing a feedback such that the closed-loop solutions stay in a neighborhood of the set point and converge to it. When, instead of a set point, a time-varying reference needs to be stabilized—i.e., the closed-loop solutions shall converge to a time-varying reference trajectory—then the problem is called *trajectory tracking.* Typical examples of trajectory-tracking problems are set point changes along precomputed references, synchronization tasks or startup of processes. While stabilization and trajectory tracking are well-understood for a wide range of systems, not all control tasks arising in practise belong to these categories.

For example, consider the case of steering a car automatically along a road. Usually, the driving velocity is not predetermined. The only requirements are to keep the car on the road while driving sufficiently fast. Formally, we can reformulate this task as follows: the system state or output should converge to a known geometric curve and follow it along in a specific direction. These kinds of control tasks are known as *path-following problems.* The major difference to trajectory tracking is that the speed along the path along is not fixed a priori. Instead it is an additional degree of freedom which can be tuned to achieve fast convergence, and small deviations of the system state or output to the path. Path-following problems typically arise in robotics and vehicle-like applications, such as unmanned aerial vehicles, robots, or milling machines. Moreover, some process control problems can be formulated as path following, for example, the task of steering a batch reactor along a temperature profile while maximizing the process productivity.

This thesis deals with the design of optimization-based control schemes for trajectory-tracking and path-following problems in the presence of constraints. We present novel results on the design of nonlinear model predictive control (NMPC) schemes for both problem classes.

Sufficient conditions for the stability of NMPC for trajectory tracking based on time-varying terminal regions are derived. The key feature of our approach is the introduction of positive invariant time-varying level sets of Lyapunov functions as terminal regions. These sets allow enlarging the region of attraction of the proposed control schemes and thereby improve the control performance.

Furthermore, we discuss path-following problems for constrained nonlinear systems. We propose using a nonlinear normal form of an augmented system to analyze these problems. We investigate sufficient conditions for exact path followability of unconstrained and constrained nonlinear systems. Based on these results we present tailored predictive control schemes for path following. We derive sufficient conditions which guarantee the convergence of the system output to the path. In contrast to previous works—for example, in the field of robotics—our schemes can handle constraints on states and inputs as well as situations where the system does not start on the path. In other words, using the proposed control schemes makes it possible to stabilize the motion of a system in the presence of constraints with respect to a path defined in an output space. Examples from robotics and chemical engineering are drawn upon to support our results.

The main intention of this thesis is twofold: Firstly, we show that nonlinear model predictive control is very well applicable to problems beyond set point stabilization. Secondly, we demonstrate that path-following concepts provide a suitable framework for many challenging control problems ranging from robotics to chemical engineering.

# Deutsche Kurzfassung

Die Bedeutung der Regelungstechnik und Systemtheorie für die Analyse, den Entwurf und den Betrieb komplexer dynamischer Systeme ist immens. Das prototypische Problem des Reglerentwurfs ist die *Stabilisierung eines Arbeitspunktes*. Dabei ist es das Ziel, durch Wahl einer geeigneten Rückführung, die Trajektorien eines dynamischen Systems in der Umgebung eines festen Arbeitspunktes zu halten und die Konvergenz der Lösungen des geregelten Systems gegen diesen Arbeitspunkt sicherzustellen. Wenn anstelle eines festen Arbeitspunktes eine zeitveränderliche Referenztrajektorie stabilisiert werden soll, so spricht man von einem *Trajektorienfolgeproblem*. Typischerweise werden Anfahrprozesse von Reaktoren, Synchronisationsaufgaben oder Wechsel zwischen Arbeitspunkten entlang vorab berechneter Verläufe als Trajektorienfolgeprobleme formuliert. Für den Entwurf stabilisierender Rückführungen und Folgeregelungen sind verschiedene Methoden und Lösungsansätze bekannt. Jedoch lassen sich bei weitem nicht alle in der Praxis auftretenden Fragestellungen als Probleme der Stabilisierung von Arbeitspunkten oder der Trajektorienfolge auffassen.

Falls beispielsweise ein autonomes Fahrzeug einer Straße folgen soll, so ist nicht notwendigerweise auch die Geschwindigkeit vorgegeben. Stattdessen reicht es aus, das Fahrzeug auf der Straße zu halten und hinreichend schnell die Strasse entlang zu führen. Abstrakter gesprochen: Der Zustand oder der Ausgang eines Systems soll gegen eine geometrische Kurve konvergieren und dieser Kurve in vorgegebener Richtung folgen. Solche Fragestellungen bezeichnet man als *Pfadverfolgungsprobleme*. Der maßgebliche Unterschied zur Trajektorienfolge ist, dass die Geschwindigkeit der Bewegung entlang der Kurve, beziehungsweise entlang des Pfades, nicht fest vorgegeben ist. Vielmehr kann dieser Freiheitsgrad genutzt werden, um eine schnellere Konvergenz gegen den Pfad und eine geringere Abweichung zu erzielen. Typische Anwendungsbeispiele für Pfadverfolgungsprobleme sind die angesprochenen autonomen Fahrzeuge, unbemannte Fluggeräte, Roboter oder Fräs- und Werkzeugmaschinen. Weiterhin kann das Abfahren von Temperatur- oder Konzentrationsprofilen in verfahrenstechnischen Prozessen als Pfadverfolgungsproblem aufgefasst werden.

Die vorliegende Arbeit beschäftigt sich mit dem Entwurf von optimierungsbasierten Regelungsverfahren für Trajektorien- und Pfadverfolgungsprobleme unter Berücksichtigung von Beschränkungen der Stell- und Zustandsgrößen. Es werden neue, nichtlineare, modell-basierte, prädiktive Regelungsverfahren für beide Problemklassen vorgestellt. Unter anderem werden hinreichende Bedingungen für die Stabilität, beziehungsweise die Konvergenz, der vorgeschlagenen Verfahren entwickelt.

Als Hilfsmittel für den Entwurf prädiktiver Regler für Probleme der Trajektorienfolge werden dabei vorwärtsinvariante, zeitveränderliche Niveaumengen von Lyapunovfunktionen eingeführt. Dies erlaubt es, den Einzugsbereich der Regler deutlich zu vergrößern und dadurch die Regelgüte zu verbessern.

Außerdem werden Beiträge zur Beschreibung, Analyse und Lösung von Pfadverfolgungsproblemen mit Hilfe erweiterter Systemdynamiken und geeigneter Normalformkoordinaten geleistet. Es werden hinreichende Bedingungen für die exakte Verfolgbarkeit von Pfaden in Ausgangsräumen vorgestellt. Insbesondere wird auf Fragestellungen der Verfolgbarkeit von Pfaden unter Beschränkungen der Stell- und Zustandsgrößen eingegangen.

Aufbauend auf diese Ergebnisse zur Analyse werden neue, modell-basierte, prädiktive Regelungsansätze für Pfadverfolgungsprobleme unter Berücksichtigung von Beschränkungen entwickelt. Im Gegensatz zu existierenden Ansätzen für diese Probleme, zum Beispiel aus dem Bereich der Robotik, können hierbei Fälle berücksichtigt werden, bei denen das System nicht direkt auf dem Pfad startet. Es werden rigorose Bedingungen vorgestellt, welche garantieren, dass die Anwendung der vorgeschlagenen prädiktiven Regelungsschemata zur Konvergenz des Ausgangs gegen den zu verfolgenden Pfad führt. Die Ergebnisse der Arbeit werden anhand verschiedener Beispiele aus der Robotik und der Verfahrenstechnik illustriert.

Die Anliegen dieser Arbeit können in zwei Punkten zusammengefasst werden: Zum einen ist es das Ziel, die Anwendbarkeit der nichtlinearen modell-prädiktiven Regelung auf Probleme jenseits typischer Arbeitspunktstabilisierung aufzuzeigen. Zum anderen soll verdeutlicht werden, dass die Pfadverfolgung einen geeigneten Rahmen für die Formulierung und Lösung herausfordernder Fragestellungen aus verschiedenen Anwendungsgebieten – von der Robotik bis hin zur Verfahrenstechnik – bietet.

# Index of Notation

## Abbreviations and Acronyms

This list serves as a reference for abbreviations and acronyms.

| | |
|---|---|
| CSTR | continuously stirred tank reactor |
| DAE | differential algebraic equation |
| LTI | linear time invariant |
| LTV | linear time-varying |
| LP | linear program |
| LQR | linear quadratic regulator |
| MIMO | multiple input multiple output |
| MPC | model predictive control |
| MPFC | model predictive path-following control |
| NMPC | nonlinear model predictive control |
| OCP | optimal control problem |
| ODE | ordinary differential equation |
| RDE | Riccati differential equation |
| QP | quadratic program |
| SISO | single input single output |
| w.l.o.g. | without loss of generality |

## Mathematical Notation

The following symbols are used throughout the thesis.

| | |
|---|---|
| $t$ | time variable |
| $\theta$ | scalar path parameter |
| $x$ | state vector $x \in \mathbb{R}^{n_x}$ |
| $y$ | output vector $y \in \mathbb{R}^{n_y}$ |
| $u$ | input vector $u \in \mathbb{R}^{n_u}$ |
| $n_x$ | dimension of the real valued state vector $x$ |
| $n_u$ | dimension of the real valued input vector $u$ |
| $n_y$ | dimension of the real valued output vector $y$ |
| $f$ | vector field describing the system dynamics |
| $x_0$ | initial condition of the system dynamics |

| | |
|---|---|
| $x(\cdot, t_0, x_0 \vert u(\cdot))$ | state trajectory starting at $t_0$ at $x_0$ driven by an signal $u(\cdot)$; if an autonomous system is considered, we drop $t_0$ and write $x(\cdot, x_0 \vert u(\cdot))$ |
| $\frac{\partial f_j(x)}{\partial x_i}$ | partial derivative of the $j$-th component of $f$ with respect to the $i$-th component of $x = (x_1, \ldots, x_i, \ldots, x_{n_x})^T$ |
| $\nabla E(x)$ | gradient of $E : \mathbb{R}^k \to \mathbb{R}$. $\nabla E = \left(\frac{\partial E}{\partial x_1}, \ldots, \frac{\partial E}{\partial x_k}\right)^T$ |
| $\frac{\partial E(x)}{\partial x}$ | transposed gradient $\frac{\partial E(x)}{\partial x} = (\nabla E(x))^T$ |
| $\mathrm{L}_f\, h_i$ | Lie derivative of $h_i$ along $f$, i.e. $\mathrm{L}_f\, h_i = \frac{\partial h_i}{\partial x} f(x, u)$ whereby $h_i : \mathbb{R}^{n_x} \to \mathbb{R}$ and $f : \mathbb{R}^{n_x} \times \mathbb{R}^{n_u} \to \mathbb{R}^{n_x}$ |
| $\mathbf{I}^{n \times n}$ | identity matrix of $\mathbb{R}^n$ |
| $\mathbf{0}^{n \times m}$ | zero matrix of $\mathbb{R}^{n \times m}$ |
| $\mathrm{diag}(q_1, \ldots, q_n)$ | diagonal matrix with entries $q_1, \ldots, q_n$ |
| $Q \geq 0$ | positive semi-definite matrix $Q$ |
| $R > 0$ | positive definite matrix $R$ |
| $\Vert x \Vert$ | 2-norm of a vector $x \in \mathbb{R}^n$ |
| $\Vert x \Vert_Q^2$ | brief notation for $x^T Q x$, $Q \geq 0$ |
| $\mathcal{X}$ | set describing the state constraints $\mathcal{X} \subseteq \mathbb{R}^{n_x}$ |
| $\mathcal{U}$ | set describing the input constraints $\mathcal{U} \subseteq \mathbb{R}^{n_u}$ |
| $\mathrm{int}\, \mathcal{A}$ | interior of a set $\mathcal{A}$ |
| $\partial \mathcal{A}$ | boundary of a set $\mathcal{A}$ |
| $\mathcal{K}$ | set of class $\mathcal{K}$ functions, cf. Definition B.1, Appendix B |
| $\mathcal{KL}$ | set of class $\mathcal{KL}$ functions, cf. Definition B.2, Appendix B |
| $\mathcal{C}^k$ | set of $k$-times continuously differentiable functions mapping from $[t_0, t_1] \subseteq \mathbb{R}$ to $\mathbb{R}^n$ [1] |
| $\mathcal{PC}(\mathcal{A})$ | set of piecewise continuous and right continuous functions mapping from $[t_0, t_1] \subseteq \mathbb{R}$ to $\mathcal{A} \subseteq \mathbb{R}^n$ [1] |
| $\mathcal{L}^p$ | set of $p$-integrable functions—with $p \in [1, \infty)$—mapping from $[t_0, t_1] \subseteq \mathbb{R}$ to $\mathbb{R}^n$ [1] |
| $\mathcal{BC}(\mathbb{R}^{n \times n})$ | set of elementwise bounded and elementwise continuous time-varying matrices on $\mathbb{R}^{n \times n}$ |
| $\mathcal{BC}^+(\mathbb{R}^{n \times n})$ | set of elementwise bounded and elementwise continuous time-varying matrices on $\mathbb{R}^{n \times n}$ which are symmetric and strictly positive definite |
| $\mathcal{BC}_0^+(\mathbb{R}^{n \times n})$ | set of elementwise bounded and elementwise continuous time-varying matrices on $\mathbb{R}^{n \times n}$ which are symmetric and positive semi-definite |

[1]The dimension $n < \infty$ and the size of the domain $[t_0, t_1]$ follow from the context.

# Part I

# Basics and Introduction

# 1 Set Point Stabilization, Trajectory Tracking, and Path Following

Feedback is a fundamental concept, which is present in many technical, as well as non-technical systems. It is of great importance for the solution to manifold automation and control problems. An omnipresent and prototypical problem in control is *set point stabilization*. Consider a dynamical system with control

$$\dot{x}(t) = f(x(t), u(t)), \quad x(t_0) = x_0 \tag{1.1}$$

where $t \in \mathbb{R}$ is the time, $x \in \mathbb{R}^{n_x}$ is the state, $u \in \mathbb{R}^{n_u}$ is the input, and $x_s$ is a set point to be stabilized. The stabilization problem can be stated as follows: Design a feedback $k : x \mapsto u$ such that the solutions $x(t, x_0|k(x))$—i.e., the solutions of (1.1) starting at $x_0$ driven by the feedback $u = k(x)$—stay close to the desired set point $x_s$ and converge

$$\lim_{t\to\infty} \|x(t) - x_s\| = 0. \tag{1.2}$$

The stabilization problem is well understood for a wide range of systems: linear and nonlinear, continuous and discrete time, finite and infinite dimensional. Any many control tasks belong to this class. Typical examples are temperature control in building automation or the task to keep an unstable vehicle like a *SEGWAY*® in an upright position. Yet, not all control problems arising in applications are set point stabilization problems.

For example, consider the task of driving a car automatically along a road. From the driver's point of view two main objectives are evident. Keep the car on the road, *and* ensure that the car moves forward sufficiently fast. One can break this task down into two subproblems: control of the lateral position of the car on the road, and assignment of an admissible speed. Often both subproblems are solved as decoupled stabilization problems: One controller stabilizes the lateral position by using the steering angle as input. Another controller stabilizes the vehicle speed via engine thrust. Although quite simplistic this approach is successfully employed in practice. Modern drivers assistance systems such as cruise control, and lane assistance systems are instances of this decomposition approach. The achievable performance is, however, limited due to the problem reformulation.

Not necessarily it is required to keep the car in the middle of the road. It might suffice to stay on the road. If this is the case, one can take another point of view to formulate the problem. Firstly, compute *offline* a reference motion $x_r : [t_0, \infty) \to \mathbb{R}^{n_x}$ for the car along the road. And secondly, design a controller which tracks online this reference motion such that

$$\lim_{t\to\infty} \|x(t) - x_r(t)\| = 0. \tag{1.3}$$

This means that we determine the velocity along the road offline and design a controller to track this reference motion online. Literally speaking the trajectory $x_r : [t_0, \infty) \to \mathbb{R}^{n_x}$ is an explicit requirement *when to be where* on the road. Following this concept automatic car control is considered as a *trajectory-tracking problem.*[1]

In the control literature the aforementioned two problems of stabilization and tracking are predominant. Nevertheless, one can take a third point of view on the problem of driving a car automatically. Instead of breaking the problem down—either into two control tasks or into reference trajectory generation and tracking—we can consider it in the original form. This means that we regard the road as a geometric reference curve without any preassigned timing information. Let us assume we are given a description of the road as a geometric curve

$$\mathcal{P} = \{x \in \mathbb{R}^{n_x} \mid \theta \mapsto p(\theta)\}$$

whereby $p : \mathbb{R} \to \mathbb{R}^{n_x}$ is a parametrization of $\mathcal{P}$ and increasing values of $\theta$ denote forward movement on the road. Then the task can be formulated as

$$\lim_{t\to\infty} \|x(t) - p(\theta(t))\| = 0 \quad \text{and} \quad \dot{\theta} \geq 0. \tag{1.4}$$

Here, the first part reflects the objective of staying on the road. And the second part expresses the objective of moving forward. Clearly, the challenge of this problem formulation is that the timing along the track or specifically the map $t \mapsto \theta(t)$ is not given a priori. Rather it needs to be determined online in the controller. In other words, we have to design a controller which keeps the car on track and assigns a reference velocity online. Taking this point of view, automatic car control is considered as a *path-following problem.* While literally being more complicated, this formulation introduces additional freedom to the controller design—the speed to move along the curve—and does not limit the performance from the beginning.

[1] The terminology with respect to trajectory-tracking problems is not unified. We follow along the classic lines of [Athans and Falb 1966]. If the task is to track a trajectory defined in an output space and this reference trajectory is generated by an exogenous system—a so-called exo-system—then one denotes the problem either as *model-following problem, servo problem*, or as *output regulation problem.* The first two denominations stem from optimal control approaches towards the problem [Anderson and Moore 1990]. The latter is common if one refers to geometric approaches to tracking problems [Isidori 1995].

## 1.1 Stabilization, Tracking, Path Following, and Model Predictive Control

For set point stabilization problems a large variety of suitable control methods with specific properties exist: from classic techniques for linear systems in time and frequency domain, via optimization-based approaches, to advanced differential geometric tools for nonlinear systems. If an application requires the design of controllers with explicit consideration of constraints on states and inputs, or if a prediction of the future system behavior is required, only a few suitable design techniques are known. Nowadays, intensive research efforts on *model predictive control* (MPC) try to shrink this gap in the set of controller design techniques. Basically, MPC is built upon the idea of choosing the current control actions on the basis of repeated predictions of the future system behavior. To do so, one needs a suitable model of the system to be controlled as well as a strategy on how to predict its behavior and decide on control actions.

Since the 1960s optimal control has been proven to be very powerful. Mainly, it allows computation of constraint-consistent open-loop control actions based on a model and a cost criterion [Athans and Falb 1966; Berkovitz 1974; Bryson and Ho 1969; Lee and Markus 1967]. Usually, these methods are employed in the prediction and decision step of MPC, and hence MPC can be understood as repetitive optimal control. From a systems and control point of view MPC has several advantageous properties [Findeisen et al. 2003]:

- Consideration of nonlinear systems with multiple inputs and outputs.
- Online performance optimization with respect to a cost criterion.
- Consideration of constraints on states and inputs.
- Rigorous stability and robustness conditions.

In view of the introductory distinction between set point stabilization, trajectory tracking, and path following, one can say that the vast majority of MPC results consider set point stabilization, see i.a. [Chen and Allgöwer 1998; Findeisen 2006; Mayne et al. 2000]. The problem of steering a system from one set point to another without the specification of a specific continuous transition trajectory is often called set point tracking [Grüne and Pannek 2011; Rawlings and Mayne 2009]. It can be regarded as an intermediate problem between stabilization and trajectory tracking. If one regards the step-wise change of the set point as reference trajectory, then set point tracking is a tracking problem. If one treats the change of the set point as a disturbance which instantaneously leads to a big set point deviation, then it is a stabilization problem. Hence we call it an intermediate problem. This problem is frequently discussed in the context of MPC, see [Broeck 2011; Ferramosca et al. 2009; Limon et al. 2008; Magni and Scattolini 2005] and the corresponding chapters in the recent monographs [Grüne and Pannek 2011; Rawlings and Mayne 2009].

Although trajectory tracking can be considered as a classic problem [Athans and Falb 1966; Kalman 1963; Kreindler 1969], only a few works consider explicitly the design of MPC schemes for trajectory tracking [Gu and Hu 2006; Magni and Scattolini 2007; Magni et al. 2001; Michalska 1996]. These results have shortcomings. Constraints are only sparsely considered, and if so very long prediction horizons are required. One reason for the lack of results on MPC for trajectory tracking might be as follows: Even for time-invariant systems, the standard approach of reformulating trajectory-tracking as set point stabilization in error coordinates leads to inherently time-varying error dynamics. Due to the technical challenges, MPC schemes which allow the consideration of time-varying systems are sparsely available. Among the exceptions are [Fontes 2001; Gondhalekar and Jones 2011; Kern et al. 2009]. This lack of results is the motivation to investigate MPC for trajectory tracking in this work, see Chapter 3.

Path-following problems arise in many different applications as control of robots or autonomous vehicles, ships, and aircrafts. Additionally, some control concepts in process engineering implicitly rely on structures similar to path-following problems, for example, super saturation control of crystallization processes [Fujiwara et al. 2005; Nagy et al. 2008]. There the primary objective is to steer a batch crystallization reactor as close as possible along the solubility curve. The end time of the batch process is secondary.

Surprisingly, path following was mainly considered in robot control until the mid 1990s [Dahl and Nielsen 1990; Shin and McKay 1985; Slotine and Yang 1989]. There the task of assigning feedforward inputs such that the robot follows the path exactly and in minimum time is considered. Stabilization of the motion of a robot with respect to the path is not discussed. Beginning with [Banaszuk and Hauser 1995; Hauser and Hindman 1995] path following is regarded as a challenging control problem itself and beyond specific robot control applications. Two reasons have been decisive for these developments. In contrast to trajectory tracking, path following for non-minimum phase systems is not subject to fundamental performance limits [Aguiar et al. 2004, 2005]. Additionally, path-following problems are accessible via geometric and Lyapunov based nonlinear feedback control methods [Banaszuk and Hauser 1995; Nielsen and Maggiore 2004; Skjetne et al. 2004]. Consequently, these methods are the dominant controller design techniques used in the existing path-following literature. The pitfall of these methods is that constraints cannot be considered in a structured way. However, consideration of constraints is an intrinsic feature and novelty of MPC. This is the motivation to investigate the path-following problem in the presence of constraints as well as the design of predictive path-following controllers in Chapters 4 and 5, respectively.

## 1.2 Outline

This thesis is devided into three parts. In Part I Chapters 1 and 2 give an introduction. In the remainder of this part we provide a brief review on sampled-data MPC for set point stabilization problems in Chapter 2. We introduce different approaches to rigorous stability conditions and restate an important result on sufficient stability conditions.

Part II of the thesis deals with predictive control schemes for trajectory-tracking problems. We begin with a formal problem description in Section 3.1 and an overview of existing results in Section 3.2. Based on this we consider tracking of output reference signals in Section 3.3. We focus on tracking of state space trajectories in Section 3.4, where we introduce the notion of a time-varying level set of a Lyapunov function to derive computable candidates for the time-varying terminal regions. Background information on positive invariance of general time-varying sets is provided in Appendix C. For asymptotically constant reference trajectories we show how positive invariant time-varying level sets can be computed via an optimal control problem based on scalar dynamics, affine constraints and an affine cost function, see Section 3.5. As an example we consider trajectory tracking of a nonlinear chemical reactor in Section 3.5.5.

Finally, in Part III of the thesis (Chapters 4 & 5) we consider the path-following problem and the design of predictive control schemes for this problem. In Chapter 4 we state the problem to be solved. We provide an extensive overview of existing results on the problem analysis as well as on synthesis of path-following controllers in Section 4.2. A framework to analyze path-following problems via an augmented system description is presented in Section 4.3. There we show that output path following is not a typical stabilization problem but rather a special manifold or set stabilization problem. Moreover, we investigate constrained path-followability problems for the special case of differentially flat systems, see Section 4.4. This concept is illustrated by a simulation study of a nonlinear chemical reactor in Section 4.4.2.

These investigations on the problem structure allow the introduction of predictive control schemes for path-following problems in Chapter 5. We present results on the slightly simplifed problem of following paths directly in the state space in Section 5.1. Section 5.1.4 deals with the design of a predictive control scheme for path-following of a simple autonomous robot. In Section 5.2 we transfer these results to the more general problem of following paths in output spaces. In Sections 5.2.2–5.2.3 we illustrate our predictive control approach to path-following problems by examples. We consider a robot control problem in Section 5.2.2. The applicability to non-square input-output structures is shown by means of a ship course control problem in Section 5.2.3.

This thesis ends with a brief summary and an outlook on open issues in Chapter 6.

## 1.3 Contributions

As mentioned we investigate the design of predictive controllers for control tasks beyond set point stabilization. Specifically, we discuss the design of predictive controllers for constrained trajectory-tracking and path-following problems. We derive new theoretical results with respect to these problems. The contributions are presented in Chapters 3–5.

### Chapter 3—MPC for Trajectory Tracking

In this chapter we discuss a model predictive control approach to trajectory-tracking problems of constrained nonlinear continuous time systems. The main idea is to use time-varying level sets as terminal regions. In the context of (offline) discrete time robust MPC the use of time-varying level sets has been previously proposed in [Wan and Kothare 2003]. However, in the context of MPC for trajectory tracking usually time-invariant terminal sets are employed [Gu and Hu 2006; Magni and Scattolini 2007]. Time-invariant terminal regions are conservative, since the trajectory-tracking problem is inherently time-varying.

Specifically, we adapt a notion of time-varying sets [Michel and Miller 1977] and propose to use time-varying level sets of Lyapunov functions as terminal regions to gurantee stability. In contrast to a usual level set $\{x \mid V(t,x) \leq c^2\}$ of a time-varying Lyapunov function $V(t,x)$ a time-varying level set $\{x \mid V(t,x) \leq \pi^2(t)\}$ employs a time-varying diameter function $\pi(t)$. The nice feature about these sets is that the function $\pi(t)$ does not necessarily need to be monotonously decreasing. We prove necessary and sufficient conditions for positive invariance of these sets.

To determine locally attractive trajectories of uncontrolled systems a concept similar to time-varying level sets was proposed in [Tobenkin et al. 2011]. In contrast to our approach, the structure of polynomial systems is exploited, yet inputs are not considered. Another related approach considers Lyapunov functions for periodic discrete-time systems [Böhm et al. 2010a,b]. There periodic Lyapunov functions which decrease only from period to period and not monotonously are considered. Furthermore, the use of inequalities with time-varying levels $\pi(t)$ is mentioned but not further elaborated in [Böhm 2010].

For the special case of asymptotically constant state space reference trajectories we show how the level sets $\{x \mid V(t,x) \leq \pi^2(t)\}$ can be computed efficiently. We propose solving an optimal control problem with scalar dynamics, affine constraints, and linear cost in order to compute maximum volume time-varying terminal regions. The computational approach can be considered as a numerical approximation of the region of attraction of a two-degrees-of-freedom control scheme in the presence of constraints. Parts of the results of Chapter 3 have appeared in [Faulwasser and Findeisen 2011].

## Chapter 4—Path Followability

In this chapter we analyze path-following problems from a geometric point of view. In contrast to previous approaches we work directly with a parametrization of the reference paths and do not rely on the descriptions of paths as level sets as in [Nielsen and Maggiore 2006, 2008; Nielsen et al. 2010]. The main idea is to use an augmented system to describe and analyze path-following problems.

Based on this we discuss the path-followability problem, i.e., the question of whether a given path in the output space of a nonlinear system is exactly followable. Additionally, we investigate path-followability problems of differentially flat systems in the presence of constraints on states and inputs. We derive a novel approach for general flat systems using an approach similar to results from robotics [Dahl and Nielsen 1990; Shin and McKay 1985; Slotine and Yang 1989]. The notion of paths and trajectories is not completely new in the context of flat systems [Martin et al. 1997; Raczy and Jacob 1999; Rothfuß et al. 1996; Rouchon et al. 1993]. In contrast to these works we state sufficient conditions for exact path followability of constrained flat systems. Moreover, we show how to compute feedforward controls ensuring exact path following via a low dimensional optimal control problem subject to single input dynamics in Brunovský normal form. These results have been published in [Faulwasser et al. 2011].

## Chapter 5—Model Predictive Path-following Control (MPFC)

We present novel MPC schemes which are tailored to path-following tasks subject to constraints. Compared to previous approaches to the problem in context of robotics [Dahl and Nielsen 1990; Shin and McKay 1985; Slotine and Yang 1989] the main advantage is to directly ensure path stabilization. The usual results in robotics merely allow the computation of feedforward inputs which guarantee nominal path following. In contrast to geometric approaches we consider constraints on states and inputs [Aguiar 2005; Nielsen et al. 2010; Skjetne et al. 2004, 2005]. Furthermore, we do not rely on a decomposition of the problem into stabilization of the zero-path-error manifold and assignment of a forward velocity to the path as in [Nielsen et al. 2010].

Different to other works dealing with MPC for path-following problems, we give rigorous stability conditions for both path following in the state space as well as path following in an output space of a nonlinear system, cf. [Ghaemi et al. 2010; Li et al. 2009]. One of the rare works giving stability conditions on MPC for path following is [Lam et al. 2010]. However, these conditions utilize concepts from contractive MPC [de Oliveira Kothare and Morari 2000] and hence guaranteed recursive feasibility is lost. That means that feasibility of the optimal control problem for one prediction step does not imply the feasibility of the optimal control problem at the next step. In contrast to that our results guarantee recursive feasibility in the presence of input and state constraints. We show how to obtain stabilizing terminal regions and end penalties. A genuine advantage of our approach is to directly tackle the path-following problem and to not rely on preassignment of reference trajectories to the path geometry. The presented results have been published in [Faulwasser and Findeisen 2009a,b, 2010; Faulwasser et al. 2009a]

# 2 Brief Review of Model Predictive Control for Set Point Stabilization

During the last decades manifold research efforts have been dedicated to model predictive control or receding horizon control. And still today MPC is a very active field of research. One reason for this might be the following observation [Maciejowski 2002, p. *xi*]:

> *Predictive Control [...] is the only advanced control technique—that is, more advanced than standard PID control—to have had a significant and widespread impact on industrial process control.*

The goal of this chapter is a brief introduction into sampled-data nonlinear model predictive control (NMPC) for set point stabilization problems of continuous time systems.[1] Due to the vast and steadily increasing amount of results published in the field of MPC, the objective of giving a brief introduction contradicts any attempt of being complete in terms of a literature review. We focus on the aspects of NMPC which are relevant for later chapters, i.e., we work in a continuous time sampled-data setting. We do not discuss discrete time, offline, and tube-based NMPC or explicit MPC approaches in detail. For a broader and general introduction to these and other aspects of MPC the reader is referred to the recent research monographs [Grüne and Pannek 2011; Rawlings and Mayne 2009] and the miscellanies [Allgöwer and Zheng 2000; Findeisen et al. 2007; Magni et al. 2009].

## 2.1 Principle of Model Predictive Control

The main idea of MPC is to use a model of a system to predict and to optimize its future behavior, i.e., to choose the inputs such that the predicted behavior is optimized. Consequently, MPC relies on a (dynamical) model of the system to be controlled as well as on a cost criterion to be minimized. Basically, MPC is built upon the iterative scheme:

1. At a sampling time $t_k$ obtain a state measurement $x(t_k)$.

[1] There is a slight difference between the terms model predictive control and receding horizon control. While the former refers to the model-based nature the later refers to the iterative aspects of predictive or receding horizon control algorithms. Here we use the terms synonymously as in [Grüne and Pannek 2011; Rawlings and Mayne 2009]. Also note that the acronym NMPC is commonly used to emphasize the use of nonlinear models.

2. Predict the system behavior by means of a system model, a set of admissible open-loop control actions, and a cost criterion to be minimized.
3. Apply the optimal open-loop input signal $u_k^\star(\cdot)$. Go back to 1.

This conceptual idea was already formulated in the 1960s, when optimal control attracted a lot of research attention, see [Lee and Markus 1967, p. 423]. Therefore, one can claim that "[MPC] has its roots in optimal control[...]", cf. [Rawlings and Mayne 2009, p. 1]. Although the above description is (intentionally) simplified it shows several important features. In essence MPC is built upon the repetitive solution of an optimal control problem. One could aim at deriving an optimal feedback controller and thereby avoid the repetitive optimal control. This is often not feasible for nonlinear systems, since the computation of an optimal feedback involves the Hamilton-Jacobi-Bellman equation, and solving this partial differential equation is, in general, difficult. Instead MPC aims at the easier computation of an optimal open-loop input trajectory for the given state at each step. In order to perform the optimization-based prediction, MPC requires three main ingredients: a model, a cost criterion to be minimized as well as state information at each sampling time.

Despite the simplicity of the basic MPC formulation manifold system theoretic issues arise immediately: Under which conditions does the repetitive application of open-loop inputs lead to stability? How robust is such a scheme with respect to a mismatch between the model used for prediction and the system/plant to be controlled? Is it necessary to compute the optimal input trajectory or does a suboptimal solution suffice? How can one handle computational delay in the prediction steps? Is the basic idea applicable to control problems beyond set point stabilization?

### 2.1.1 Mathematical Formulation of Predictive Control

To set the basis for this work we shift to a formal description of NMPC. We work in a sampled-data continuous time setting similar to the ones used in [Findeisen 2006; Fontes 2001]. However, the general ideas transfer to discrete time, see [Grüne and Pannek 2011; Mayne et al. 2000; Rawlings and Mayne 2009].

Assume that the model of the system to be controlled is a time-varying differential equation

$$\dot{x}(t) = f(t, x(t), u(t)), \quad x(t_0) = x_0 \in \mathcal{X}_0 \subset \mathbb{R}^{n_x}. \tag{2.1}$$

The system states and inputs are subject to constraints. The system states $x$ are restricted to the simply connected and closed set $\mathcal{X} \subseteq \mathbb{R}^{n_x}$ with $0 \in \mathcal{X}$. The inputs are piecewise continuous functions with values in the compact set $\mathcal{U} \subset \mathbb{R}^{n_u}$ and $0 \in \mathcal{U}$. These input signals are briefly written as $u(\cdot) \in \mathcal{PC}(\mathcal{U})$. If a solution to (2.1) at time $t \geq t_0$, starting at time $t_0$ at $x(t_0)$, driven by an input $u(\cdot)$ exists, we denote it as $x(t, t_0, x(t_0)|u(\cdot))$. To explain the concept of NMPC we consider a set-point stabilization problem. In other words, the control task is to steer the system state

$x$ to the set point $x_s$, and to stabilize the system against disturbances. For sake of simplicity we assume that for all $t \geq t_0 : \; f(t, x_s, u_s) = 0$, and $x_s = 0, u_s = 0$, i.e., the origin is a steady state to be stabilized.

In order to distinguish between the real system variables $x, u$ and predicted variables the latter are denoted by $\bar{x}, \bar{u}$. The performance criterion to be optimized at each prediction step is given as a cost functional of the form

$$J\left(t_k, x(t_k), \bar{x}(\cdot), \bar{u}(\cdot)\right) = \int_{t_k}^{t_k+T_p} F\left(\tau, \bar{x}(\tau), \bar{u}(\tau)\right) d\tau + E\left(t_k + T_p, \bar{x}(t_k + T_p)\right). \quad (2.2)$$

Commonly, $F : \mathbb{R}_0^+ \times \mathcal{X} \times \mathcal{U} \to \mathbb{R}_0^+$ is denoted as cost function, and $E : \mathbb{R}_0^+ \times \mathcal{X} \to \mathbb{R}_0^+$ is called end or terminal penalty. At each sampling instance $t_k = t_0 + k\delta, k \in \mathbb{N}$, where $\delta > 0$ is the sampling time, the prediction is performed via the solution of the optimal control problem (OCP)

$$\underset{\bar{u}(\cdot) \in \mathcal{PC}(\mathcal{U})}{\text{minimize}} \; J\left(t_k, x(t_k), \bar{x}(\cdot), \bar{u}(\cdot)\right) \quad (2.3a)$$

subject to

$$\forall \tau \in [t_k, t_k + T_p] : \; \dot{\bar{x}}(\tau) = f(\tau, \bar{x}(\tau), \bar{u}(\tau)), \quad \bar{x}(t_k) = x(t_k) \quad (2.3b)$$

$$\bar{x}(\tau) \in \mathcal{X} \quad (2.3c)$$

$$\bar{u}(\tau) \in \mathcal{U} \quad (2.3d)$$

$$\bar{x}(t_k + T_p) \in \mathcal{E} \subseteq \mathcal{X} \subseteq \mathbb{R}^{n_x}. \quad (2.3e)$$

The optimal solution to this problem—denoted by superscript $\cdot^\star$—is the input trajectory[2]

$$u_k^\star(\cdot) = \underset{\bar{u}(\cdot) \in \mathcal{PC}(\mathcal{U})}{\text{argmin}} \; J\left(t_k, x(t_k), \bar{x}(\cdot), \bar{u}(\cdot)\right). \quad (2.4)$$

The subscript $\cdot_k$ indicates that the input signal $\bar{u}_k^\star(\cdot)$ is computed using the state information $x(t_k)$. The basic principle of an NMPC scheme built upon (2.3) is illustrated in Figure 2.1. At each sampling time $t_k$ we predict the system behavior over the horizon $[t_k, t_k + T_p]$ by computation of the input (2.4) and $\bar{x}(\cdot, t_k, x(t_k)|u_k^\star(\cdot))$. During the time span $[t_k, t_k + \delta)$ the optimal input $u_k^\star(\cdot)$ is applied to the system (2.1). The remaining part of $u_k^\star(\cdot)$ is discarded. Then the prediction horizon is shifted forward to $[t_{k+1}, t_{k+1} + T_p]$, and the whole procedure is repeated.

A predicted input $\bar{u}(\cdot)$ is called admissible, if it satisfies the input constraints (2.3d) and the corresponding state trajectory $\bar{x}(\cdot, t_k, x(t_k)|\bar{u}(\cdot))$ satisfies the following: for all $t \in [t_k, t_k + T_p] : \bar{x}(t, t_k, x(t_k)|\bar{u}_k(\cdot)) \in \mathcal{X}$ and $\bar{x}(t_k + T_p, t_k, x(t_k)|\bar{u}_k(\cdot)) \in \mathcal{E}$. That is,

[2] From the optimal control point of view, it is fair to ask under which conditions an optimal solution to (2.3) exists. Here, we assume for sake of simplicity that the minimum is attained and write min instead of inf. Guaranteeing this is in general challenging. However, under certain convexity assumptions the existence of optimal solutions can be guaranteed. We refer to Theorem E.1 in Appendix E, and to [Berkovitz 1974; Bryson and Ho 1969; Lee and Markus 1967].

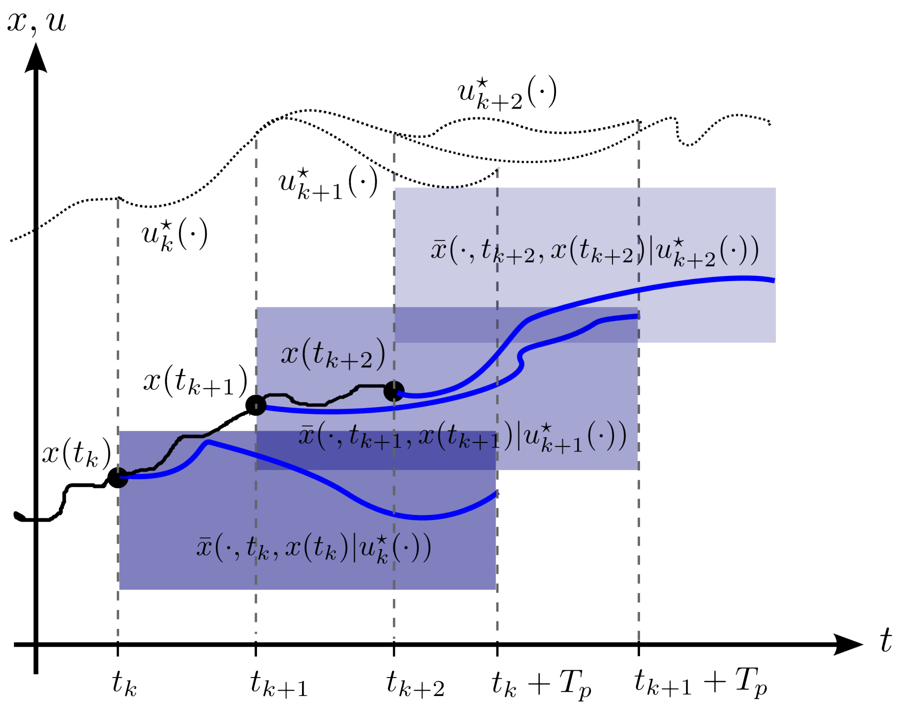


**Figure 2.1:** Basic principle of NMPC.

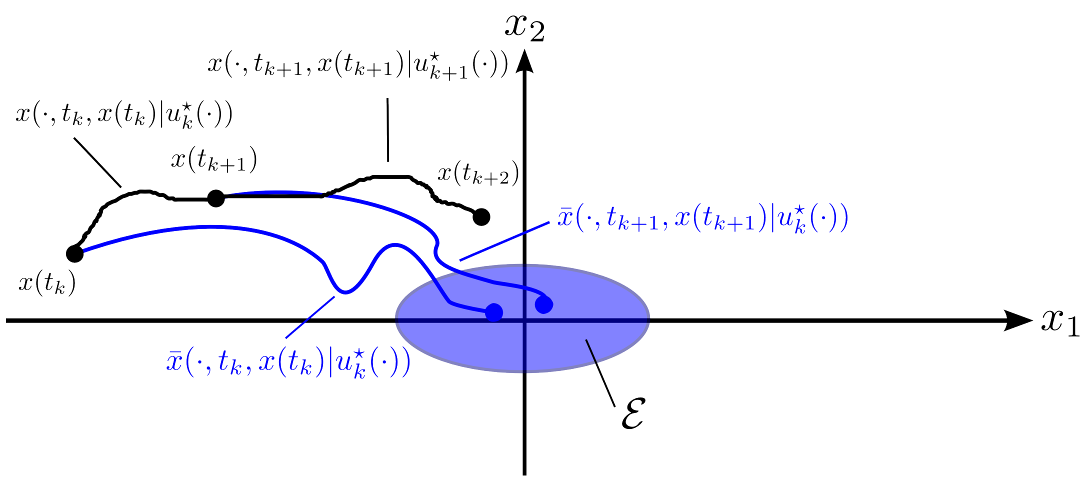


**Figure 2.2:** Role of terminal constraint (2.3e) in NMPC.

the predicted trajectories have to fulfill the state constraint (2.3c) and the terminal constraint (2.3e). The application of the optimal input $u^\star_k(\cdot)$ during the time interval $[t_k, t_k+\delta)$ leads to a trajectory $x(\cdot, t_k, x(t_k)|u^\star_k(\cdot))$ which in general will not be identical to the predicted trajectory $\bar{x}(\cdot, t_k, x(t_k)|u^\star_k(\cdot))$. This situation is depicted in Figure 2.2.

While the OCP (2.3) is solved *online* at each sampling instance several design parameters of the NMPC scheme need to be determined *offline* to guarantee stability and performance. In principle, the sampling or recalculation time $\delta > 0$ should be as short as possible to use as much feedback information as possible. However, the achievable sampling rate is often limited by the available computational resources. If the system model is sufficiently accurate, the prediction horizon $T_p$ should be as large as possible to guarantee good control performance. Clearly, long prediction horizons increase the computational burden. Of course we cannot compute the solution to the OCP (2.3) arbitrarily fast. This leads to a trade-off between fast sampling (small $\delta$) and long prediction horizon (large $T_p$). Hence, in applications one needs to take computation times and possible computational and/or communication delays into account. Closely related to this issue is the possibility to asynchronously trigger the solution of the OCP by system specific events online. The computation can, for example, be triggered by error and performance thresholds or disturbance measurements. Both aspects are beyond the scope of this work. We refer the interested reader to [Faulwasser et al. 2009b; Findeisen et al. 2011; Varutti et al. 2009] and the references therein. Additionally, one has to choose the cost function $F$, the terminal penalty $E$, as well as the terminal region $\mathcal{E}$ as design parameters. Often the cost function $F$ reflects performance aspects like a trade-off between input energy and set point deviation, or economical and ecological aspects of system operation. The choices for $F, E, \mathcal{E}$, and $T_p$ are not completely free, since stability depends one their choice. This is discussed in the next section.

### 2.1.2 Approaches to Nominal Stability

As is well-known optimization of input or feedback signals does not necessarily lead to stability [Kalman 1960]. Consequently, the design of NMPC schemes with stability guarantees is of major interest. One can distinguish two approaches to guarantee stability of NMPC schemes for set point stabilization. Either, one enforces stability via suitable terminal regions $\mathcal{E}$ and terminal penalties $E$, or one imposes controllability-like conditions and sufficiently long prediction horizons. While the former is often called a *classical* NMPC approach the latter is—easily misleading, since constraints on states and inputs are considered—referred to as an *unconstrained* NMPC approach.
The main idea of classical NMPC schemes relying on terminal constraints can be divided into two parts. The first part is to determine an admissibe control, which is valid in a set containing the set point to be stabilized. During the optimization it is enforced that the predicted trajectories end in this *terminal* set, which leads to the constraint (2.3e). Due to this constraint recursive feasibility is enforced, i.e., the existence of an admissible solution to (2.3) at $t_0$ implies the existence of admissible solutions for all later sampling instance $t_k = t_0 + k\delta, k \in \mathbb{N}$. The second part is to ensure convergence to the set point by construction of a strictly decreasing bound on the cost implied by the closed-loop trajectories $x(\cdot, t_k, x(t_k)|u_k^\star(\cdot))$ which arise from the NMPC scheme (2.3). To construct such a bound one often requires that inside the set $\mathcal{E}$ the end penalty $E$ is a local control Lyapunov function.

For autonomous systems early NMPC schemes with terminal constraints are presented in [Keerthi and Gilbert 1988; Mayne and Michalska 1990]. In these works the terminal equality constraint $x(t_k + T_p) = 0$ is used in conjunction with the trivial terminal penalty $E(x) = 0$ to enforce stability. Such a minimal choice of a terminal region is also called *zero-terminal constraint*. However, zero-terminal constraints increase the computational burden of solving the OCP (2.3) dramatically. To alleviate this major drawback one can rely on a dual-mode strategy [Michalska and Mayne 1993]. There the predicted system state $x(t_k+T_p)$ is required to be contained in a neighborhood $\mathcal{E}$ of the set point to be stabilized. As soon as the real system state enters this neighborhood the control strategy switches from the application of the predicted inputs (2.4) to a local feedback law. The local feedback ensures constraint satisfaction, positive invariance of $\mathcal{E}$, and convergence to the set point.

Also in so-called *quasi infinite horizon* NMPC schemes a terminal region or terminal inequality constraint is used to enforce stability [Chen and Allgöwer 1998]. As depicted in Figure 2.2, the terminal region is a neighborhood of the desired set point. Moreover, a terminal feedback law guarantees constraint satisfaction and convergence inside $\mathcal{E}$. In contrast to the dual-mode strategy the terminal feedback is never applied to the real system. Its value is merely conceptual in the sense that it allows the construction of a local Lyapunov function which is valid on $\mathcal{E}$. Using this local Lyapunov function one can guarantee the decrease of the optimal value function of the OCP (2.3) and show stability of the closed NMPC loop. A seminal overview on these approaches covering discrete and continuous time formulations is provided in [Mayne et al. 2000]. More general formulations allowing consideration of non-autonomous systems and relaxed controls have been proposed, for example, in [Findeisen 2006; Fontes 2001]. There generalized terminal penalties—not necessarily local Lyapunov functions—are employed. It should be noted that a terminal region implies a rather strong requirement on the controllability properties in the presence of constraints: in a finite time span $T_p$ the predicted state needs to be steered into the terminal set $\mathcal{E}$. Hence the main challenge of the classical approaches is to determine a terminal region which is as large as possible. The results in [Chen et al. 2003; Yu et al. 2009] directly aim in this direction.

Approaches employing a terminal constraint have several advantages, i.e., input and state constraints can be considered and recursive feasibility can be shown. Furthermore, for stable systems the computation of suitable terminal regions is simplified. In case of globally asymptotically stable systems they can be completely dropped [Chen and Allgöwer 1997]. Additionally, the prediction horizon $T_p$ can be chosen rather short without a severe loss of performance as long as the terminal region constraint (2.3e) can be satisfied [Chen and Allgöwer 1998]. The typical drawback of classical NMPC approaches is the computational burden of terminal constraints (equality or inequality). In practice implemented NMPC schemes, however, often work well without terminal constraints, see [Dittmar and Pfeiffer 2006; Ferreau et al. 2007; Qin and Badgwell 2000; Santos et al. 2001; Simon et al. 2009]. One of the rare works showing the necessity of a terminal constraint in an application is [Raff et al. 2006].

Consequently, there are efforts to overcome terminal region constraints. Early results for discrete time NMPC without terminal constraints are, for example, [Alamir and Bornard 1995; Parisini and Zoppoli 1995]. In continuous time settings [Jadbabaie 2000; Jadbabaie et al. 2001] use a control Lyapunov function as terminal cost, however, no constraints on inputs and states are considered. An extension considering input constraints and generalized terminal costs is [Jadbabaie and Hauser 2005]. The aspect that usually only suboptimal solutions to the OCP are computed is discussed in [Graichen and Kugi 2010]. Based on an asymptotic controllability assumption one can also establish the existence of a finite stabilizing horizon length for discrete time NMPC [Grimm et al. 2005]. The last three results suffer from the drawback that merely the existence of a stabilizing horizon length $T_p$ is shown. They do not provide a constructive way to determine the minimal stabilizing horizon length. To overcome this limitation a discrete time approach, based on similar controllability assumptions as in [Grimm et al. 2005], is presented in [Grüne 2009]. The main idea is to derive a bound on the suboptimality of an NMPC scheme with a finite horizon compared to a scheme with an infinite horizon. Input constraints are included in this framework. A remarkable feature of this approach is the possibility to explicitly compute a stabilizing horizon length. Additionally, the relation between the stabilizing horizon length and the cost function is investigated in [Grüne et al. 2010]. A drawback of these works is that a rather strong assumption of an asymptotically controllable cost function is required. In general, the verification of such an assumption for a given nonlinear system is very challenging. First steps towards an extension to continuous time systems are discussed in [Reble and Allgöwer 2011, 2012].

A different route to overcome terminal constraints for autonomous discrete time systems is presented, for example, in [Limon et al. 2006; Pannocchia et al. 2011; Rawlings and Mayne 2009]. There the argumentation begins with a stabilizing terminal region which is a level set of the end penalty $\mathcal{E} = \{x \mid E(x) \leq \alpha\}$. Based on this and on an assumption on the reachability of the terminal region a modified terminal penalty $\tilde{E}(x) = \beta E(x), \beta \geq 0$ is constructed, which ensures that the terminal region constraint is fulfilled without explicitly being a constraint in the OCP. The major advantage of NMPC schemes without terminal constraints is the reduced computational burden. However, if state constraints are present, it is in general very difficult to guarantee recursive feasibility.

### 2.1.3 Explicit Stability Conditions

In the remainder of this work we aim at sampled-data NMPC schemes with terminal constraints which are applicable to control problems beyond set point stabilization. To prove stability for the NMPC scheme based on (2.3) we use similar assumptions as in [Chen and Allgöwer 1998; Findeisen 2006; Fontes 2001; Mayne et al. 2000].

**Assumption 2.1** (Input constraints).
*The input constraint set* $\mathcal{U} \subset \mathbb{R}^{n_u}$ *is compact and* $0 \in \mathcal{U}$. *The input functions* $u(\cdot)$ *are piecewise continuous or right continuous and take values in* $\mathcal{U}$: $u(\cdot) \in \mathcal{PC}(\mathcal{U})$.[3]

**Assumption 2.2** (State constraints).
*The state constraint set* $\mathcal{X} \subseteq \mathbb{R}^{n_x}$ *is closed, simply connected, and* $0 \in \mathcal{X}$.

**Assumption 2.3** (System dynamics).
*The vector field* $f : \mathbb{R}_0^+ \times \mathbb{R}^{n_x} \times \mathbb{R}^{n_u} \to \mathbb{R}^{n_x}$ *from* (2.1) *is continuous and locally Lipschitz for any pair* $(t, u)$ *with* $u \in \mathcal{U}$. *Additionally,* $f(t, 0, 0) = 0$.

**Assumption 2.4** (Continuity of system trajectories).
*For any* $x_0 \in \mathcal{X}_0$, $t_0 \in \mathbb{R}$, *and any input function* $u(\cdot) \in \mathcal{PC}(\mathcal{U})$ *the system* (2.1) *has an absolutely continuous solution.*

**Assumption 2.5** (Cost function).
*The cost function* $F : \mathbb{R}_0^+ \times \mathcal{X} \times \mathcal{U} \to \mathbb{R}_0^+$ *is continuous, and* $F(t, 0, 0) = 0$. *Furthermore,* $F$ *is lower bounded by a class* $\mathcal{K}$ *function such that for all* $(t, x, u) \in \mathbb{R}_0^+ \times \mathcal{X} \times \mathcal{U}$ : $\underline{\psi}(\|x\|) \leq F(t, x, u)$.[4]

Assumptions 2.1 and 2.4 ensure that the solutions obtained from the NMPC scheme based on (2.3) exist and are sufficiently smooth. The lower boundedness of the cost $F$ is an assumption typically required for set point stabilization. It enforces that minimizing $F$ leads to convergence of the state to the desired set point ($x_s = 0$). In the remainder of this work we refer to Assumptions 2.1–2.5 as standard assumptions. Following along the lines of [Fontes 2001, Theorem 3] and [Findeisen 2006, Theorems 2.2 and 4.3] one can state the following result.

**Theorem 2.1** (Convergence of sampled-data NMPC for set point stabilization).
*Given system* (2.1), *the NMPC scheme based on* (2.3) *with sampling time* $\delta > 0$, *and Assumptions 2.1-2.5 hold. Suppose that a terminal region* $\mathcal{E}$, *and a terminal penalty* $E$ *exist such that the following holds:*

*i)* $\mathcal{E} \subset \mathcal{X}$ *is closed, and* $E : \mathbb{R}_0^+ \times \mathcal{X} \to \mathbb{R}_0^+$ *is continuously differentiable in* $t$ *and* $x$.
*ii) For all* $x_t \in \mathcal{E}$ *and all* $t \in [t_0, \infty)$ *there exist a scalar* $\epsilon \geq \delta > 0$ *and a control signal* $u_{\mathcal{E}}(\cdot) \in \mathcal{PC}(\mathcal{U})$ *such that for all* $\tau \in [t, t + \epsilon]$

$$\frac{\partial E}{\partial \tau} + \frac{\partial E}{\partial x} f(\tau, x(\tau, t, x_t | u_{\mathcal{E}}(\cdot)), u_{\mathcal{E}}(\tau)) + F(\tau, x(\tau, t, x_t | u_{\mathcal{E}}), u_{\mathcal{E}}(\tau)) \leq 0, \tag{2.5}$$

*and the trajectory* $x(\tau, t, x_t | u_{\mathcal{E}}(\cdot)) \in \mathcal{E}$.
*iii) The OCP* (2.3) *is feasible for* $t_0$ *and all* $x_0 \in \mathcal{X}_0$.

[3] Extending this assumption to more general classes of input functions—also called relaxed controls—is possible, cf. [Berkovitz 1974; Fontes 2001].
[4] The properties of a class $\mathcal{K}$ function are stated in Definition B.1 in Appendix B.

*Then*

a) *OCP* (2.3) *is feasible for all sampling instances* $t_k = t_0 + k\delta,\ k \in \mathbb{N}$*;*

b) *and the system states converge to the steady state* $\lim_{t \to \infty} \|x(t)\| = 0$.

A detailed proof of this result is given in Appendix A. Subsequently, we derive convergence results on NMPC for trajectory-tracking and path-following problems which are similar to the previous prototypical theorem for set point stabilization. Note that Assumptions 2.1–2.5 are valid unless we explicitly comment on modifications.

## 2.2 Open Issues and Challenges

In the remainder of this thesis we discuss the design of NMPC schemes beyond set point stabilization. However, beyond this scope there are further open issues of model predictive control.

By nature NMPC is a state-feedback control approach. Hence in practice an NMPC scheme has to be combined with a suitable observer. In general, a separation principle does not hold for nonlinear systems. Consequently, there is a lack of results on the stability of NMPC based on observed state information and on output feedback. A review on existing schemes is given in [Findeisen et al. 2003]. Additionally, one should note that Theorem 2.1 is merely a result on nominal stability, i.e., no model-plant mismatch and no exogenous disturbances are considered. Therefore, the question of robustness of NMPC is of vital interest. In discrete time settings different approaches to robust NMPC schemes have been proposed, see i.a. [Bemporad and Morari 1999; Grimm et al. 2007; Magni et al. 2009; Pannocchia et al. 2011; Rawlings and Mayne 2009] and the references therein. The robustness of NMPC in continuous time is investigated, for example, in [Findeisen 2006; Yu 2011]. As pointed out, two main branches of stability results can be identified, i.e., schemes with and without terminal constraints. Both approaches implicitly require strong controllability properties in the presence of constraints. The relation between the terminal region condition (2.5) and the asymptotic controllability properties required in [Grüne 2009; Reble and Allgöwer 2012] has not been closely investigated yet.

Besides trajectory tracking and path following also *economic* MPC deals with questions beyond set point stabilization. The conceptual idea of economic MPC is to consider economically induced cost functions and no a priori fixed set point to be stabilized. Essentially, it deals with predictive controls schemes that rely on cost functions, which are not necessarily measuring the distance to a desired steady state. Often these cost functions are linear and hence Assumption 2.5, which implies lower boundedness of $F$ by a positive definite function, has to be dropped. The aim is to optimize the performance with respect to the economic cost, and to converge to an—implicitly defined—set point only in the long term. For more details see [Angeli et al. 2009; Diehl et al. 2011; Rawlings and Amrit 2009]. It is also possible to interpret this as a kind of set stabilization approach [Grüne 2011]. Furthermore, the control of decentralized and large scale systems via predictive control methods is a field of intensive research activities, cf. [Magni and Scattolini 2006; Raimondo et al. 2007].

From the applications point of view fast and robust implementations of MPC schemes are needed. As discussed in [Dittmar and Pfeiffer 2006; Qin and Badgwell 1997, 2000] most the of commercial MPC applications focus on linear systems, since for MPC based on discrete time linear models industrial *off-the-shelf* solutions are available. Often these industrial tools are applied for process control, where dynamics are rather slow and sufficient computational resources are available. In case of linear MPC for mechatronic systems, where controllers are implemented on embedded platforms, industrial off-the-shelf tools are not yet available. Often mechatronic systems are governed by fast dynamics and require sampling times in the order of milliseconds. Moreover, embedded platforms offer only limited computational resources. A lot of ongoing research tries to exploit the structure of the quadratic programs arising in discrete time linear MPC to speed up the computations, see i.a. [Ferreau et al. 2008; Kögel and Findeisen 2011; Richter et al. 2009, 2010; Zometa et al. 2012]. For NMPC of continuous time systems academic as well as commercial tools are available, for example [Ariens et al. 2010-2011; Houska et al. 2011; Nagy 2007; Rutquist and Edvall 2009]. However, the industrial use of these tools in applications under explicit consideration of nonlinearities is still out of reach and requires development of customized software.

## 2.3 Summary

In this chapter we gave a brief introduction to NMPC. Additionally, we presented a concise overview on the existing approaches to stability guarantees for NMPC. We recalled a stability result based on terminal regions and end penalties which serves as the basis for our subsequent developments on NMPC for trajectory-tracking and path-following problems.

# Part II

# Predictive Trajectory Tracking

# 3 Predictive Control for Trajectory-tracking Problems

In this chapter we investigate the design of NMPC schemes for trajectory-tracking problems. We begin with a concise statement of the output-tracking problem. We briefly review existing results on NMPC for trajectory tracking. Furthermore, we present a general NMPC scheme for tracking of reference trajectories defined in an output space. The main parts of this chapter in Sections 3.4 and 3.5 deal with state space trajectory-tracking problems. We show how stabilizing time-varying terminal regions and terminal penalties can be derived. A key element in our developments is the notion of time-varying level sets of Lyapunov functions which we employ as terminal regions. Parts of the results have appeared in [Faulwasser and Findeisen 2011].

## 3.1 The Constrained Trajectory-tracking Problem

We consider autonomous, continuous time systems

$$\dot{x}(t) = f(x(t), u(t)), \quad x(0) = x_0, \tag{3.1a}$$

$$y(t) = h(x(t)) \tag{3.1b}$$

where $x \in \mathcal{X} \subseteq \mathbb{R}^{n_x}$, $u \in \mathcal{U} \subset \mathbb{R}^{n_u}$ are state and input constraints. The map $h : \mathbb{R}^{n_x} \to \mathbb{R}^{n_y}$ (3.1b) defines the output $y \in \mathbb{R}^{n_y}$ and is assumed to be suffciently often continuously differentiable. Moreover, we assume that the system and the constraints fulfill our standard assumptions from Chapter 2. Subsequently, we consider the output trajectory-tracking problem.

**Problem 3.1** (Constrained output trajectory tracking).
*Given system* (3.1)*, and an a priori known output reference trajectory* $y_r : [0, \infty) \to \mathbb{R}^{n_y}$*, design a controller that achieves:*

*i)* ***Reference Convergence:*** *The system output* $y$ *from* (3.1b) *converges to the reference:* $\lim_{t \to \infty} \|y(t) - y_r(t)\| = 0$.

*ii)* ***Constraint Satisfaction:*** *The state and input constraints are satisfied for all* $t \geq 0 : x(t) \in \mathcal{X}, u(t) \in \mathcal{U}$.

With the denomination of this problem as *trajectory tracking* we follow along the lines of [Athans and Falb 1966]. If the reference trajectory is generated by an exogenous system, then one denotes the problem of tracking its output either as *model following, servo problem*, or as *output regulation problem*. The first two denominations stem from optimal control approaches towards the problem [Anderson and Moore 1990]. The latter is common, if one refers to geometric approaches to tracking problems [Isidori 1995].

One should note that even the unconstrained trajectory-tracking problem is in general difficult. The objective of tracking a time-varying reference signal as well as possible is subject to fundamental performance limits, if the system is non-minimum phase. In case of linear systems these limits are induced by the right half plane zeros, see [Seron et al. 1999; Su et al. 2003]. These performance limits are closely connected to the *cheap control problem* [Kwakernaak and Sivan 1972a,b]. However, this issue is beyond the scope of this thesis.

## 3.2 Existing NMPC Approaches to Trajectory Tracking

Stability results for NMPC applied to trajectory-tracking problems are only sparsely available. In the early work [Michalska 1996] the tracking of output reference trajectories via NMPC is discussed. No state or input constraints are considered. These results suffer from the major drawback of an output trackability assumption. This assumption requires that a zero output tracking error $y(t_1) - y_r(t_1) = 0$ at some time $t_1$ implies the existence of admissible controls for all $t \geq t_1$ such that the output tracking error remains zero for $t \geq t_1$. We show in Section 3.3.2 that such an assumption often does not hold. Furthermore, output trackability assumptions imply an output terminal equality constraint $y(t_k + T_p) - y_r(t_k + T_p) = 0$, which increases the computational burden.

In [Magni et al. 2001] an approach to general output tracking problems, where the reference is generated by an exogenous system, is outlined. This work is related to geometric approaches to tracking of exogenous reference signals, cf. [Isidori 1995]. A limitation is that neither input nor state constraints are considered. The tracking of asymptotically constant output references in the presence of constraints is considered in [Magni and Scattolini 2007]. A pitfall of this work is that the prediction horizon has to cover the full length of the reference trajectory. The use of long prediction horizons is computationally demanding. Moreover, it limits the achievable sampling rate and hence also the robustness of the predictive controller. In Section 3.4 we present an approach for tracking of state space reference trajectories which overcomes this limitation. The trajectory-tracking problem for the kinematic unicycle is dealt with in [Gu and Hu 2006]. There a stabilizing terminal region for the unicycle is derived. However, the approach relies on the specific system structure and its generalization is not straightforward.

It might be surprising that only a few results on stability of NMPC for tracking problem are available. One reason for this is that the tracking problem is inherently time-varying for time-varying $y_r(t)$. For an a priori given reference consider the tracking error as $e(t) = y(t) - y_r(t)$. Using this variable the task to stabilize the error is equivalent to stabilizing a non-autonomous system at $e = 0$. While the stabilization of time-invariant systems has been extensively considered in discrete as well as in continuous time, the same is not true for time-varying systems. This can be explained as follows. As outlined in Chapter 2 often local control Lyapunov functions are used as stabilizing terminal penalties, cf. [Chen and Allgöwer 1998; Jadbabaie et al. 2001; Mayne et al. 2000]. Determining these functions is especially difficult for nonlinear time-varying systems. Consequently, only a few results—compared to the large number of publications on NMPC for autonomous systems—explicitly consider predictive control for time-varying systems, e.g. [Fontes 2001; Gondhalekar and Jones 2011; Kern et al. 2009].[1]

## 3.3 NMPC Schemes for Output Trajectory Tracking

Often tracking problems are solved based on the definition of the error variable

$$e(t) := h(x(t)) - y_r(t). \tag{3.2}$$

We make the following standing assumption to avoid problems of existence of solutions. It is valid throughout the remainder of this chapter.

**Assumption 3.1** (Smoothness of reference trajectory)**.**
*The reference $y_r : [0, \infty) \to \mathbb{R}^{n_y}$ is a priori known and $y_r(t) \in \mathcal{C}^1$.*

Relying on this assumption the tracking problem can be reformulated as an output stabilization problem for the augmented dynamics

$$\dot{x}(t) = f(x(t), u(t)) \tag{3.3a}$$

$$\dot{e}(t) = \frac{\partial h}{\partial x} \cdot f(x(t), u(t)) - \dot{y}_r(t) \tag{3.3b}$$

$$\tilde{y}(t) = e(t) \tag{3.3c}$$

where $\tilde{y}$ is the output corresponding to the tracking error (3.2). These augmented dynamics are time-varying for time-varying $y_r(t)$. In this general version the trajectory problem is challenging even without constraints. The challenges stem from the fact that in the problem statement non-square input-output structures and constraints are allowed. As we will see, additional NMPC specific difficulties arise from the fact that an output reference trajectory should be tracked.

[1] Note that if the reference is generated by an exo system, the error dynamics are not necessarily time-varying. However, the exo system can be regared as an uncontrollable part of the error dynamics, cf. [Isidori 1995].

In order to solve the output tracking problem we propose an NMPC scheme based on the error variable $e$ defined in (3.2). The main idea is to use the knowledge about the reference $y_r$ in an NMPC scheme to predict the error dynamics (3.3), and to stabilize $e$ at 0. To distinguish between the predicted controller variables and the real system variables we denote the predicted inputs, states, and outputs with $\bar{u}, \bar{x}, \bar{y}$, respectively. To find suitable inputs, as commonly done in NMPC, at each sampling instant $t_k = k\delta, \quad k \in \mathbb{N}, \delta > 0$ an optimal control problem (OCP) is solved. The cost functional to be minimized is

$$J\left(t_k, x(t_k), \bar{e}(\cdot), \bar{u}(\cdot)\right) = \int_{t_k}^{t_k+T_p} F(\tau, \bar{e}(\tau), \bar{u}(\tau))\, d\tau + E(t, \bar{x}(t))|_{t_k+T_p}. \tag{3.4}$$

The OCP is

$$\underset{\bar{u}(\cdot)\in\mathcal{PC}(\mathcal{U})}{\text{minimize}}\; J\left(t_k, x(t_k), \bar{e}(\cdot), \bar{u}(\cdot)\right) \tag{3.5a}$$

subject to

$$\forall \tau \in [t_k, t_k + T_p]: \;\; \dot{\bar{x}}(\tau) = f(\bar{x}(\tau), \bar{u}(\tau)), \quad \bar{x}(t_k) = x(t_k) \tag{3.5b}$$

$$\bar{e}(\tau) = h(\bar{x}(\tau)) - y_r(\tau) \tag{3.5c}$$

$$\bar{x}(\tau) \in \mathcal{X} \tag{3.5d}$$

$$\bar{u}(\tau) \in \mathcal{U} \tag{3.5e}$$

$$\bar{x}(t_k + T_p) \in \mathcal{E}_{t_k+T_p}. \tag{3.5f}$$

For simplicity we assume that the problem data fulfill our standard assumptions from Chapter 2. The differences to these assumptions are as follows. Now, the stage cost $F : \mathbb{R} \times \mathbb{R}^{n_y} \times \mathcal{U} \to \mathbb{R}_0^+$ penalizes the error $e$ and $F(t, 0, 0) = 0$. Similar to Assumption 2.5 we assume that $F$ is lower bounded by a class $\mathcal{K}$ function $\underline{\psi}(\|e\|)$. The function $E : \mathbb{R} \times \mathbb{R}^{n_x} \to \mathbb{R}_0^+$ is the end penalty. As in Chapter 2 the optimal solution is denoted as $\bar{u}_k^\star(\cdot)$, and its first part is applied to the system

$$\forall t \in [t_k, t_k + \delta): \quad u(t) = \bar{u}_k^\star(t).$$

Equation (3.5f) requires that at the end of each prediction the predicted state $\bar{x}(t_k+T_p)$ has to be inside a terminal region in the state space. One should also note that in the cost functional (3.4) the end penalty $E(t, \bar{x})$ is defined as a function of the time and the predicted state $\bar{x}$. The reason for this is that the end penalty is used to bound from above the cost-to-go of the NMPC scheme for any solution which starts inside the terminal region $\mathcal{E}_t \subseteq \mathcal{X}$. This region, however, is defined in the state space. And thus we use a state-dependent end penalty. Since $E(t, x)$ is required to be positive semi-definite, this choice captures the case where one penalizes the output tracking error $e$ via an end penalty $E(t, e)$. Furthermore, we advocate the use of time-varying terminal regions, which we denote as $\mathcal{E}_{t_k+T_p}$. We assume that the time-varying sets are such that their boundary set evolves without sharp kinks in time, and for fixed $t$ the set $\mathcal{E}_t$ is closed. For details on time-varying sets and their properties we refer to

Appendix C. Clearly, it has to hold that $\mathcal{E}_{t_k+T_p} \subseteq \mathcal{X}$. At this point we do not specify how to obtain suitable time-varying terminal regions. In Section 3.3.2 we discuss the computation of suitable sets. Note that the length of the prediction horizon $T_p$ has to be chosen such that the OCP (3.5) is feasible.

The question arises of under which conditions the proposed control scheme guarantees convergence of the tracking error. We have to take into account that the trajectory-tracking problem is inherently time-varying. The next result is mainly an adaption of Theorem 2.1.

**Theorem 3.1** (Convergence of NMPC for trajectory tracking).
*Given Problem 3.1, the tracking error $e(t) = h(x(t)) - y_r(t)$, and its dynamics* (3.3). *Suppose that an end penalty $E(t, x(t))$, and a time-varying terminal region $\mathcal{E}_t \subseteq \mathcal{X}$ exist such that the following holds:*

*i) $E(t, x(t)) \in \mathcal{C}^1$ is positive semi-definite. And for all $t \geq 0$ the sets $\mathcal{E}_t \subseteq \mathcal{X}$ are closed.*

*ii) For all $x_t \in \mathcal{E}_t$ and all $t \in [0, \infty)$ there exists a scalar $\epsilon \geq \delta > 0$, and a control $u_{\mathcal{E}}(\cdot) \in \mathcal{PC}(\mathcal{U})$ such that for all $\tau \in [t, t+\delta]$*

$$x(\tau, t, x_t | u_{\mathcal{E}}(\cdot)) \;\in\; \mathcal{E}_\tau \tag{3.6a}$$

*holds.*

*iii) For all $\tau \in [t, t+\delta]$ the solutions $x(\tau, t, x_t | u_{\mathcal{E}}(\cdot)) \in \mathcal{E}_\tau$ satisfy*

$$\frac{\partial E}{\partial \tau} + \frac{\partial E}{\partial x} f(\tau, x(\tau, t, x_t | u_{\mathcal{E}}(\cdot)), u_{\mathcal{E}}(\tau)) + F(\tau, e(\tau), u_{\mathcal{E}}(\tau)) \leq 0, \tag{3.6b}$$

*where $e(\tau) = h(x(\tau, t, x_t | u_{\mathcal{E}}(\cdot))) - y_r(\tau)$.*

*iv) The optimal control problem* (3.5) *has a feasible solution for $t = 0$ and $x(0)$.*

*Then the closed loop defined by* (3.1) *and* (3.5) *guarantees convergence of the tracking error in the sense that*

$$\lim_{t\to\infty} \|e(t)\| = \lim_{t\to\infty} \|h(x(t)) - y_r(t)\| = 0$$

*and satisfaction of the constraints for all $t \geq 0:\; x(t) \in \mathcal{X},\; u(t) \in \mathcal{U}$.*

*Proof.* In essence this result is an adaption of the stability result on NMPC for time-varying systems as presented in Theorem 2.1. We briefly sketch the main differences to the proof of Theorem 2.1 as given in Appendix A. Firstly, note that part ii) is simply a version of positive invariance, where the invariant set $\mathcal{E}_t$ is allowed to change with time. If the positive invariance of $\mathcal{E}_t$ is guaranteed this causes no further difficulties.[2]

[2] Verifying the invariance of general time-varying sets can be complicated. A useful property which simplifies these investigations is Property P which is introduced in the Appendix C. This property ensures that one can check positive invariance of candidates $\mathcal{E}_t$ by evaluation of $f(x, u_{\mathcal{E}})$ on the boundary $\partial\mathcal{E}_t$. In detail these issues are discussed in Appendix C.

Secondly, recursive feasibility can easily be shown by concatenating an optimal input with the terminal control $u_{\mathcal{E}}(\cdot)$. Thirdly, condition (3.6b) requires a cost decrease for all $x(t) \in \mathcal{E}_t$, which is necessary in order to conclude from Barbalat's Lemma that $\lim_{t\to\infty} \|e(t)\| = 0$, see Appendix A. The crucial difference to Theorem 2.1 is that $F$ is lower bounded by a class $\mathcal{K}$ function $\underline{\psi}(\|e\|)$. Thus $F$ is only positive semi-definite with respect to $x$. Consequently, we merely establish convergence of the output to the reference. □

## 3.3.1 Challenges of Predictive Output Tracking

The convergence conditions of Theorem 3.1 are in general difficult to verify. Two main causes for these difficulties can be identified. Firstly, for general nonlinear systems it is hard to check whether for a given time-varying reference there exists an admissible input $u(\cdot) \in \mathcal{U}$ such that the corresponding state evolution $x(t, t_0, x_0|u(\cdot))$ fulfills $h(x(t, t_0, x_0|u(\cdot)) = y_r(t)$ for all times $t$. Secondly, the derivation of a suitable terminal region $\mathcal{E}_t$ depends on $y_r(\cdot)$ since the reference is defined in terms of the output $y = h(x)$.

To illustrate these issues we consider the set of all points in the output space which lie on the reference trajectory $y_r(\cdot)$, and denote this set as

$$\mathcal{R} := \{r \in \mathbb{R}^{n_y} \mid t \in [0, \infty) \mapsto y_r(t)\}. \tag{3.7}$$

If one asks for conditions ensuring trackability of reference trajectories, it is clear that the pointwise image of the state constraints $h(\mathcal{X}) := \{y \in \mathbb{R}^{n_y} \mid x \in \mathcal{X} \mapsto h(x)\}$ has to be a superset of the reference $\mathcal{R}$, cf. Figure 3.1. Hence a basic necessary condition for trackability of reference trajectories in the presence of constraints is

$$\mathcal{R} \subset h(\mathcal{X}). \tag{3.8}$$

If this relation does not hold, parts of the output reference $\mathcal{R}$ are not feasible under the given state constraints $\mathcal{X}$. Usually, the output space has a smaller dimension than the state space $n_y < n_x$, and hence it is not easy to characterize the pointwise preimage of the reference $h^{-1}(\mathcal{R})$. For general continuous output maps $h : \mathbb{R}^{n_x} \to \mathbb{R}^{n_y}$ with $n_x > n_y$ the preimage of a compact set $\mathcal{R}$ might neither be simply connected nor compact, cf. Figure 3.1. Formally, one can require that at the end of each prediction $\bar{x}(t_k + T_p, t_k, x(t_k)|\bar{u}(\cdot))$ lies in some neighborhood of a set $\Gamma \subseteq \{h^{-1}(\mathcal{R}) \cap \mathcal{X}\}$. Here $\Gamma$ is the set of all constraint consistent state space trajectories which correspond to an output identical to the reference trajectory $y_r(\cdot)$. However, for general systems it is difficult to characterize $\Gamma$, and to determine such terminal constraints solely in terms of the output $y = h(x)$.

Subsequently, we discuss two possibilities to overcome these problems. Either one postulates rather restrictive *observability* conditions on the output space and relies on

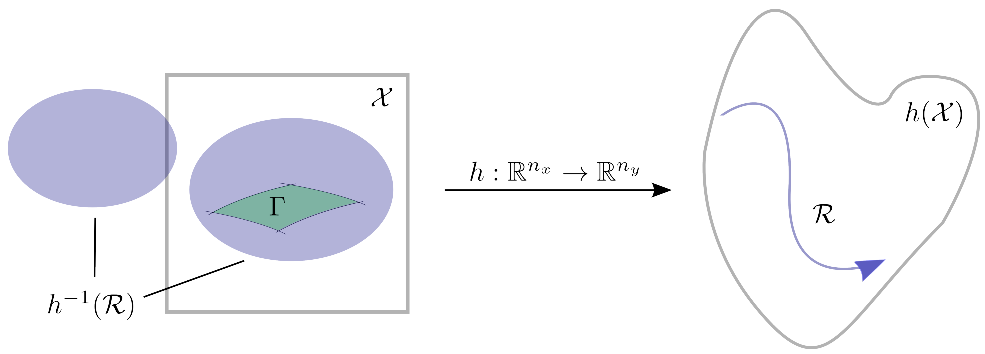


**Figure 3.1:** Relations between constraints $\mathcal{X}$, reference $\mathcal{R}$, and preimage $h^{-1}(\mathcal{R})$.

zero terminal constraints. Or one restricts the consideration to reference trajectories which are initially defined in the state space. The former is discussed next while the latter is elaborated in Section 3.4.

### 3.3.2 Output Tracking via Zero Terminal Constraints

One way to circumvent the aforementioned difficulties is to rely on the concept of output trackability as used in [Michalska 1996].

**Definition 3.1** (Output trackability).
*The system* (3.1) *is said to be completely output trackable with respect to a reference* $y_r(\cdot)$, *if for all* $t_0 \geq 0$, *and all* $x$ *with* $h(x_0) = y_r(t_0)$, *there exists an admissible input* $u(\cdot) \in \mathcal{PC}(\mathcal{U})$ *such that for all* $t \geq t_0$ *it holds* $h(x(t, t_0, x_0|u(\cdot))) = y_r(t)$.

Relying on an output trackability assumption it is rather easy to state stabilizing terminal regions and end penalties. The main idea is to enforce that the predicted outputs reach the reference trajectory.

**Corollary 3.1** (Convergence of output tracking via zero terminal constraints).
*Consider the output tracking problem for system* (3.1) *as defined in Problem 3.1. The time-varying terminal region is given by* $\mathcal{E}_{t_k+T_p} = \{x \in \mathbb{R}^{n_x} \mid h(x(t_k+T_p)) = y_r(t_k+T_p)\}$ *and* $E(t,x) = 0$, *and the following conditions hold:*

*i) The system is output trackable with respect to the reference* $y_r(\cdot)$, *i.e., for all* $t \geq 0$, *and all* $x_t \in \mathcal{E}_t$ *there exists an input* $u_r(\cdot) \in \mathcal{PC}(\mathcal{U})$ *such that* $h(x_t) = y_r(t)$ *implies* $h(x(\tau, t, x_t|u_r(\tau)) = y_r(\tau)$ *for all* $\tau \in [t, \infty)$.

*ii) The cost function is such that for all* $\tau \geq t :\quad F(\tau, 0, u_r(\tau)) = 0$.

*iii) The optimal control problem* (3.5) *has a feasible solution for* $t = 0$ *and* $x(0)$.

*Then the closed loop defined by* (3.1) *and* (3.5) *guarantees convergence of the tracking error*

$$\lim_{t\to\infty} \|e(t)\| = \lim_{t\to\infty} \|h(x(t)) - y_r(t)\| = 0,$$

*and satisfaction of the constraints for all* $t \geq 0 :\ x(t) \in \mathcal{X},\ u(t) \in \mathcal{U}$.

Mainly, the corollary expresses the idea of using a time-varying zero terminal constraint as stabilizing terminal region. The proof follows directly from Theorem 3.1 and is omitted here. The result has two main pitfalls. Firstly, the zero terminal constraint $h(x(t_k + T_p)) = y_r(t_k + T_p)$ is a strict finite time controllability requirement. It causes numerical difficulties and usually shrinks the region of attraction, cf. Section 2.2. Secondly, except for cases of explicitly invertible output maps $h : \mathbb{R}^{n_x} \to \mathbb{R}^{n_y}$ with $n_x = n_y$, it is hard to verify the output trackability assumption. Often even academic example systems turn out to be not output trackable.

**Example 3.1** (Output trackability).
*Consider the double integrator*

$$\dot{x} = \begin{pmatrix} 0 & 1 \\ 0 & 0 \end{pmatrix} x + \begin{pmatrix} 0 \\ 1 \end{pmatrix} u, \quad x(0) = x_0 \tag{3.9a}$$

$$y = \begin{pmatrix} 1 & 0 \end{pmatrix} x, \tag{3.9b}$$

*where no constraints except* $\forall t : \|u(t)\| < \infty$ *are present. The reference to be tracked is* $y_r(t) = t$. *Assume that at* $t = 1$ *the system state is* $x(1) = (1, 0)$. *Clearly* $y(1) = y_r(1)$. *In order to derive an input* $u(t)$ *at time* $t = 1$*, which keeps the output on the reference, we determine* $\dot{y} = C^T(Ax + Bu)$ *and check whether there exists an* $u(t)$ *such that* $\dot{y}(t) = \dot{y}_r(t)$. *It is easy to see that* $\dot{x}(t) = (x_2(t), u(t))^T$*, and therefore one yields* $\dot{y}(1) = 0$. *Consequently, at* $t = 1$ *there exists no finite* $u(t)$ *to keep the output on the reference. And hence the double integrator is not output trackable with respect to the considered reference.*

Note this small example system has rather strong control properties. It is minimum phase, controllable, and furthermore the considered output is a differentially flat output, cf. Section 4.4 and the references therein for details on flatness. Thus one can conclude that even in the case of unconstrained linear controllable systems output trackability assumptions are very restrictive.

**Remark 3.1** (Output trackability of differentially flat systems).
*If the reference is defined in a flat output space things simplify. If the output map* $y = h(x)$ *defines a differentially flat output, this implies (among other properties) that the state evolution can be locally completely parametrized by a map*

$$x = \Phi\left(y_1, \dot{y}_1, \ldots, y_1^{(l_1)}, \ldots, y_{n_y}, \ldots, y_{n_y}^{(l_{n_y})}\right), \tag{3.10}$$

*where* $y_i^{(j)}$ *is the* $j$*-th time derivative of the* $i$*-th output component, cf. [Fliess et al. 1995b] and Section 4.4. In this case, and under suitable technical assumptions, one may equivalently reformulate any reference* $y_r(t) \in \mathcal{C}^{\hat{l}}$*, where* $\hat{l}$ *is highest derivative appearing in* (3.10)*, as a state space trajectory given by* (3.10).

These insights—and the fact that zero terminal constraints impose strict controllability requirements and are numerically not desireable—motivate to focus the further considerations on state space trajectory-tracking problems.

## 3.4 Trajectory Tracking in the State Space

In the following we focus on trajectory-tracking problems, where the reference is defined directly in the state space of the considered system. Thus instead of (3.1) we consider

$$\dot{x}(t) = f(x(t), u(t)), \quad x(0) = x_0, \tag{3.11}$$

where $x \in \mathcal{X} \subseteq \mathbb{R}^{n_x}$, $u \in \mathcal{U} \subset \mathbb{R}^{n_u}$ are as before. Suppose that the system and the constraints fulfill our standard assumptions from Chapter 2. We want to solve the following state space trajectory-tracking problem.

**Problem 3.2** (Constrained state space trajectory tracking)**.**
*Given system* (3.11) *and an a priori known reference trajectory* $x_r : [0, \infty) \to \mathbb{R}^{n_x}$ *where for all* $t \geq 0$ *it holds* $x_r(t) \in \mathcal{C}^1$*. Design a controller such that:*

*i)* ***Reference Convergence:*** *The system state* $x$ *converges to the reference* $\lim_{t\to\infty} \|x(t) - x_r(t)\| = 0$.
*ii)* ***Constraint Satisfaction:*** *The state and input constraints are satisfied for all* $t \geq 0 : x(t) \in \mathcal{X}, u(t) \in \mathcal{U}$.

Trajectory tracking in state space is relevant and important for many applications. Often the desired state trajectories are computed offline by means of dynamic optimization based on system models. Typical examples from chemical and biochemical engineering are the startup and set point changes of processes like batch crystallization or batch fermentation, see [Constantinides et al. 1970; Kravaris et al. 1989; Nagy et al. 2007; Soroush and Kravaris 1992]. In these cases *state* trajectories are computed offline such that the process performance is optimized with respect to yield, energy consumption or time duration. The optimal trajectories are often tracked by means of a two-degrees-of-freedom control structure, where a nominal feedforward input is combined with a feedback controller, e.g. [Anderson and Moore 1990; Hagenmeyer and Delaleau 2003; Hagenmeyer and Zeitz 2004].[3] However, this makes it challenging to consider constraints.

As for the output tracking case, the solution is based on the error variable

$$e(t) := x(t) - x_r(t). \tag{3.12}$$

We rely on Assumption 3.1, i.e., the reference is a priori known and continuously differentiable. Thus the tracking problem can be reformulated as a set point stabilization

[3] Note that two-degrees-of-freedom control structures are also used to track references defined in an output space. Hence the feedback part can be state or output feedback.

problem for the error dynamics

$$\dot{e} = \tilde{f}(t, e, u) := f(e + x_r(t), u) - \dot{x}_r(t), \tag{3.13}$$

which are inherently time-varying for varying $x_r(t)$.
Similar to the one for output tracking (3.5) the NMPC scheme for tracking of state space trajectories reads as follows. The cost functional to be minimized is

$$J\left(t_k, x(t_k), \bar{e}(\cdot), \bar{u}(\cdot)\right) = \int_{t_k}^{t_k+T_p} F(\tau, \bar{e}(\tau), \bar{u}(\tau))\ d\tau + E(t, \bar{e}(t))|_{t_k+T_p}, \tag{3.14}$$

where $F : \mathbb{R} \times \mathcal{X} \times \mathcal{U} \to \mathbb{R}_0^+$ is the stage cost and fulfills Assumption 2.5. And $E : \mathbb{R} \times \mathbb{R}^{n_x} \to \mathbb{R}_0^+$ is the positive semi-definite end penalty, which is now defined in terms of the state space tracking error. The OCP to be solved repetitively is

$$\underset{\bar{u}(\cdot)\in\mathcal{PC}(\mathcal{U})}{\text{minimize}}\ J\left(t_k, x(t_k), \bar{e}(\cdot), \bar{u}(\cdot)\right). \tag{3.15a}$$

subject to

$$\forall\tau \in [t_k, t_k + T_p] :\ \dot{\bar{e}}(\tau) = \tilde{f}(\tau, \bar{e}(\tau), \bar{u}(\tau)), \quad \bar{e}(t_k) = x(t_k) - x_r(t_k) \tag{3.15b}$$

$$\bar{e}(\tau) + x_r(\tau) \in \mathcal{X} \tag{3.15c}$$

$$\bar{u}(\tau) \in \mathcal{U} \tag{3.15d}$$

$$\bar{e}(t_k + T_p) \in \mathcal{E}_{t_k+T_p}. \tag{3.15e}$$

The main difference of this scheme compared to (3.5) is the fact that the reference is defined in the state space. The next result is a corollary to Theorem 3.1.

**Corollary 3.2** (Convergence of NMPC for state space trajectory tracking)**.**
*Consider Problem 3.2, the tracking error* $e(t) = x(t) - x_r(t)$*, and its dynamics* (3.13)*. Suppose that an end penalty* $E(t, e(t)) \in \mathcal{C}^1$ *and a time-varying terminal region* $\mathcal{E}_{t_k+T_p}$ *exist, such that for all* $t \geq 0$ *the set* $\mathcal{E}_t$ *is closed, and a feedback* $k(t, e) \in \mathcal{C}^0$ *guarantees the following:*

*i) For all* $e_t \in \mathcal{E}_t$ *and all* $\tau \in [t, \infty)$ *it holds that*

$$\begin{aligned} e(\tau, t, e_t|k(\tau, e)) &\in \mathcal{E}_\tau \\ x_r(\tau) + e(\tau, t, e_t|k(\tau, e)) &\in \mathcal{X}. \end{aligned} \tag{3.16a}$$

*ii) For all solutions* $e(\tau,\ t, e_t|k(\tau, e)) \in \mathcal{E}_\tau$ *it holds that*

$$\frac{\partial E(\tau, e)}{\partial \tau} + \frac{\partial E(\tau, e)}{\partial e}\dot{e} + F(\tau, e(\tau), k(\tau, e)) \leq 0. \tag{3.16b}$$

*iii) The optimal control problem* (3.15) *has a feasible solution for* $t = 0$*.*

*Then the closed loop defined by* (3.11) *and* (3.15) *guarantees convergence of the error*

$$\lim_{t\to\infty} \|e(t)\| = \lim_{t\to\infty} \|x(t) - x_r(t)\| = 0,$$

*and satisfaction of the constraints for all* $t \geq 0 :\ e(t) + x_r(t) \in \mathcal{X},\ u(t) \in \mathcal{U}$*.*

The proof follows mutatis mutandis the previous considerations and is thus omitted. However, one difference should be observed. Instead of a control signal $u_{\mathcal{E}}(\cdot)$ we require the existence of a continuous time-varying feedback $k(t,e)$, which is admissible on the terminal region $\mathcal{E}_t$. This result is the basis for our further developments.

## 3.5 Tracking of Asymptotically Constant References

Subsequently, we focus on a special case which is of interest in many applications. In order to derive a terminal region and an end penalty which fulfill the suppositions of Corollary 3.2 we restrict our investigations to reference trajectories which are asymptotically constant. We make the following standing assumptions.

**Assumption 3.2** (Asymptotically constant reference)**.**

*i) The asymptotically constant reference trajectory is a priori known such that for all* $t \geq 0: \; x_r(t) \in \operatorname{int}\mathcal{X} \subseteq \mathbb{R}^{n_x}$*, and* $x_r(t) \in \mathcal{C}^1$*. Furthermore,* $\lim_{t\to\infty} x_r(t) = x_r(T)$ *with* $T < \infty$*.*

*ii) An admissible reference input* $u_r : [0,\infty) \to \operatorname{int}\mathcal{U} \subset \mathbb{R}^{n_u}, u_r(t) \in \mathcal{C}^0$ *with* $\dot{x}_r = f(x_r, u_r)$ *is known.*

*iii) The reference trajectory* $x_r(\cdot)$ *ends at* $t = T$ *in a stabilizable set point of* (3.11)*, i.e.* $f(x,u)|_{x_r(T),u_r(T)} = 0$ *and the matrix pair* $A(T), B(T)$

$$A(T) := \left.\frac{\partial f}{\partial x}\right|_{x_r(T),u_r(T)} \in \mathbb{R}^{n_x \times n_x}, \qquad B(T) := \left.\frac{\partial f}{\partial u}\right|_{x_r(T),u_r(T)} \in \mathbb{R}^{n_x \times n_u} \tag{3.17}$$

*is stabilizable.*

**Assumption 3.3** (Quadratic cost function and box constraints)**.**

*i) The constraint sets* $\mathcal{X}$,$\mathcal{U}$ *of the original system* (3.11) *are box constraints*

$$\begin{aligned} \forall i \in \{1,\dots,n_x\}: &\quad x_{min,i} \;\leq x_i \;\leq\; x_{max,i} \\ \forall i \in \{1,\dots,n_u\}: &\quad u_{min,i} \;\leq u_i \;\leq\; u_{max,i}. \end{aligned}$$

*ii) The stage cost* $F$ *in* (3.14) *is given by*

$$F(t,e,u) := e^T Q_F e + (u - u_r(t))^T R_F (u - u_r(t))$$

*with* $Q_F, R_F > 0$*.*

We proceed as follows: Firstly, we consider the linearization of the error dynamics (3.13) along the reference $x_r(\cdot)$. Assumption 3.2 enables the derivation of a suitable feedback law as well as a Lyapunov function for the contolled linear time-varying (LTV) error system. This feedback law serves as terminal control law $k(t,e)$ in (3.16). Secondly, we introduce the concept of time-varying level sets of Lyapunov functions to derive candidate terminal regions for the LTV error system. We formulate an optimal control problem to compute the time-varying level sets via an approximation to a convex optimization problem. Based on the linearization we derive a suitable time-varying terminal region also for the nonlinear error dynamics. Finally, we clarify how the suppositions of Corollary 3.2 can be verified.

### 3.5.1 Stabilization of the Linearized Error System

Consider the error dynamics (3.13) and Assumptions 3.2–3.3. The Jacobian linearization of the error system along the reference trajectory $x_r(\cdot)$ and reference input $u_r(\cdot)$ expressed in the coordinates $e = x - x_r$, $w = u - u_r$ is

$$\dot{e} = A(t)e + B(t)w. \tag{3.18}$$

From Assumption 3.2 it follows that the time-varying matrices $A(t)$, $B(t)$ are bounded and continuous in their elements, which is briefly written as $A(t) \in \mathcal{BC}(\mathbb{R}^{n_x \times n_x})$ and $B(t) \in \mathcal{BC}(\mathbb{R}^{n_x \times n_u})$. Our goal is to derive a time-varying feedback which exponentially stabilizes the LTV system (3.18). We rely on a solution to a time-varying Riccati differential equation (RDE) to construct such a feedback. To this end we recall the following definition and a helpful result.

**Definition 3.2** ($Q$-stabilizability, [Phat and Jeyakumar 2010]).
*Consider the LTV system* (3.18) *and a matrix* $Q(t) \in \mathcal{BC}_0^+(\mathbb{R}^{n_x \times n_x})$. *System* (3.18) *is denoted as $Q$-stabilizable, if for any initial condition $e_0$ there exists a control $w(\cdot) \in \mathcal{L}^2$ such that the functional*

$$J_Q(e_0, w(\cdot)) = \int_0^\infty \|w\|^2 + e^T Q(\tau) e \; d\tau, \tag{3.19}$$

*is bounded.*

**Lemma 3.1** (Existence of semi-definite RDE solutions, [Phat and Jeyakumar 2010]).
*If the LTV system* (3.18) *is $Q$-stabilizable for some $Q(t) \in \mathcal{BC}_0^+(\mathbb{R}^{n_x \times n_x})$, then for all $t \geq 0$ the Riccati differential equation*

$$\dot{P}(t) = P(t)B(t)B^T(t)P(t) - Q(t) - P(t)A(t) - A^T(t)P(t), \quad P(T) = P_T \tag{3.20}$$

*has a positive semi-definite solution $P(t) \in \mathcal{BC}_0^+(\mathbb{R}^{n_x \times n_x})$.*

Now we are ready to state sufficient conditions for exponential stabilizability of the LTV system (3.18).

**Lemma 3.2** (Exponential stabilizability of LTV error system).
*If Assumption 3.2 holds, then the LTV error system* (3.18) *is exponentially stabilizable.*

*Proof.* We give a constructive proof. We explicitly derive a suitable feedback and a Lyapunov function for (3.18) subject to this feedback. Firstly, we verify that the error system (3.18) is $Q$-stabilizable for any $Q(t) \in \mathcal{BC}_0^+(\mathbb{R}^{n_x \times n_x})$. Secondly, we construct a feedback via Lemma 3.1 and a suitably chosen RDE. Finally, we derive a Lyapunov function for the controlled system.

**Step 1:** To show that (3.18) is $Q$-stabilizable we have to verify the boundedness of (3.19). Recall that due to Assumption 3.2 iii) for any $t \geq T$ the pair $(A(t), B(t))|_{t \geq T}$ is constant and stabilizable. Pick any constant feedback $w = Ke$, $K \in \mathbb{R}^{n_x \times n_u}$ such that for fixed $t = T$ the matrix $A(T) + B(T)K$ is asymptotically stable. Split (3.19) into two parts

$$J_Q(e_0, Ke) = \int_0^T \|Ke\|^2 + e^T Q(t) e \; d\tau + \int_T^\infty \|Ke\|^2 + e^T Q(t) e \; d\tau,$$

where $Q(t)$ is any matrix from $\mathcal{BC}_0^+(\mathbb{R}^{n_x \times n_x})$. Obviously, the first integral is bounded. The second integral is also bounded, since for all $t \geq T$ the closed loop behaves like a stable LTI-system. Hence (3.18) is $Q$-stabilizable for any $Q(t) \in \mathcal{BC}_0^+(\mathbb{R}^{n_x \times n_x})$.

**Step 2:** Consider another RDE

$$\dot{P}(t) = P(t)B(t)R^{-1}(t)B^T(t)P(t) - Q(t) - P(t)A(t) - A^T(t)P(t), \quad P(T) = P_T \quad (3.21)$$

where the boundary condition $P(T) = P_T$ solves

$$0 = P_T B(T) R_T^{-1} B(T) P_T - Q_T - P_T A(T) - A^T(T) P_T. \quad (3.22)$$

If we rely on an input transformation $\tilde{w} = \sqrt{R(t)^{-1}} w$ and take Step 1 into account, we can conclude that for any $Q(t) \in \mathcal{BC}_0^+(\mathbb{R}^{n_x \times n_x})$ and $R(t) \in \mathcal{BC}^+(\mathbb{R}^{n_u \times n_u})$ the RDE (3.21) has a positive semi-definite solution $P(t) \in \mathcal{BC}_0^+(\mathbb{R}^{n_x \times n_x})$.

W.l.o.g. assume that two positive definite and symmetric matrices $Q(t) \in \mathcal{BC}^+(\mathbb{R}^{n_x \times n_x})$ and $R(t) \in \mathcal{BC}^+(\mathbb{R}^{n_u \times n_u})$ are chosen such that for all $t \in [0, T]$

$$Q(t) - \left(A(t) + A^T(t) + B(t)R^{-1}(t)B^T(t)\right) \geq \tilde{q} I \quad (3.23)$$

holds for some $\tilde{q} > 0$, and for $t \geq T$ $Q(t) = Q_T, R(t) = R_T$ are constant. Subsequently, we use $P(t) \in \mathcal{BC}_0^+(\mathbb{R}^{n_x \times n_x})$ to verify that the time-varying feedback given by

$$\omega = K(t)e = -\frac{1}{2} R^{-1}(t) B^T(t) \left(P(t) - I\right) e \quad (3.24)$$

stabilizes the LTV error system (3.18) exponentially.

**Step 3:** We restrict ourselves to the case that $Q(t), R(t)$ have been chosen according to (3.23). $\tilde{A}(t) := A(t) + B(t)K(t)$ is the closed loop system matrix of (3.18) under (3.24). Consider the candidate Lyapunov function

$$V(t, e) = e^T \left(P(t) + I\right) e \quad (3.25)$$

where $P(t) + I \in \mathcal{BC}^+(\mathbb{R}^{n_x \times n_x})$. Its time derivative along the solution trajectories of (3.18) under the feedback (3.24) is

$$\frac{\partial V(t,e)}{\partial t} + \frac{\partial V(t,e)}{\partial e}\dot{e} = e^T \left(\tilde{A}^T(t)\tilde{P}(t) + \tilde{P}(t)\tilde{A}(t) + \dot{P}(t)\right) e \tag{3.26}$$

where $\tilde{P}(t) = P(t) + I$. Since

$$\dot{P}(t) + \tilde{A}^T(t)\tilde{P}(t) + \tilde{P}(t)\tilde{A}(t) = -Q(t) + \left(A(t) + A^T(t) + B(t)R^{-1}(t)B^T(t)\right) \tag{3.27}$$

it follows from (3.23) that $\dot{V}(t,e) \leq -\tilde{q}\|e\|^2$. Hence $V(t,e) = e^T\left(P(t) + I\right)e$ is a Lyapunov function for (3.18) under the feedback (3.24). Recall $P(t) \in \mathcal{BC}_0^+(\mathbb{R}^{n_x \times n_x})$, and for all $t \geq T:\ P(t) = P_T$. We can assume w.l.o.g. that $\overline{p} := \sup_{t\in[0,T]} \|P(t)\|$ with $\overline{p} \geq 0$ exists. Thus quadratic bounds for the Lyapunov function are given by

$$c_1\|e\|^2 \leq V(t,e) \leq \quad c_2\|e\|^2 \tag{3.28a}$$

$$\frac{\partial V}{\partial t} + \frac{\partial V}{\partial e}\dot{e} \leq -c_3\|e\|^2 \tag{3.28b}$$

$$\left\|\frac{\partial V}{\partial e}\right\| \leq \quad c_4\|e\| \tag{3.28c}$$

where $c_1 = 1$, $c_2 = \overline{p} + 1$, and $c_4 = 2(\overline{p} + 1)$. The constant $c_3 = \tilde{q}$ follows directly from (3.27) combined with (3.23). Using Lemma B.3 from Appendix B it follows that the LTV error system (3.18) is exponentially stabilized by (3.24). □

In principle, the core statement of the last lemma can be proven more briefly than done here. Firstly, construct a simple time-invariant feedback and an exponential bound on the controlled solutions of (3.18) $t \geq T : \|e(t)\| \leq \alpha e^{-\beta t}, \quad \alpha, \beta > 0$. Secondly, choose $\alpha$ sufficiently large, such that the exponential bound also captures the solutions on the finite time interval $[0, T)$. In contrast to that, we have chosen a constructive approach, which leads to a time-varying Lyapunov function for the LTV error system (3.18) under the control (3.24). Explicit knowledge of this Lyapunov function is crucial for the later developments. We also mention that the finite-time convergence stated in Assumption 3.2 is important for the construction of the Lyapunov function. If we allow $T = \infty$—i.e., the reference trajetory converges only in the limit to a set point—it is much more difficult to establish exponential stabilizability of (3.18).
Recall that in order to compute $P(t)$ we have to choose $Q(t)$ and $R(t)$ such that (3.23) is satisfied. At first glance this seems to be hard to verify. However, for a constant $R(t) = R > 0$ one can set

$$Q(t) = \tilde{Q} + A(t) + A^T(t) + B(t)R^{-1}B^T(t) > 0, \quad \tilde{Q} > 0 \tag{3.29}$$

which—for sufficiently large matrices $\tilde{Q} > 0$—fulfills (3.23). A suitable $\tilde{Q} > \tilde{q}I$ can be determined via a time-discretized approximation of (3.29). In that case the decay

(3.26) of $V(t,e)$ is $\dot{V} = -e^T\tilde{Q}e$, and for all $t \geq T$ the RDE (3.21) is time-invariant. To simplify the later considerations we make the assumption.

**Assumption 3.4** (Choice of $Q$ and $R$ in the RDE).
*The solution $P(t) \in \mathcal{BC}_0^+$ to the RDE* (3.21) *is obtained for a constant matrix $R(t) = R > 0$ and a time-varying matrix $Q(t)$ satisfying* (3.29)*.*

**Remark 3.2** (Uniformly controllable LTV error systems).
*If the matrix pair $(A(t), B(t))$ from* (3.17) *is uniformly controllable, the existence of a symmetric strictly positive definite solution $P(t)$ to* (3.21) *is guaranteed, see Lemma D.2 from Appendix D. Moreover, the altered version of the stabilizing feedback* (3.24) *is $w = -\frac{1}{2}R^{-1}(t)B^T(t)P(t)e$. Using this feedback $V(t,e) = e^TP(t)e$ being a suitable Lyapunov function is easily verified. For this case all of the subsequent considerations apply similarly.*

### 3.5.2 Positive Invariant Time-varying Level Sets

So far we have shown how to construct a Lyapunov function for the controlled LTV error system. Now we want to use this Lyapunov function to compute a terminal region. In a standard NMPC approach a terminal region would be obtained as a level set $\mathcal{E}_t = \{e \mid V(t,e) \leq c^2\}$ such that for all $e \in \mathcal{E}_t$ and all $t \geq 0$ the constraints $e + x_r(t) \in \mathcal{X}, K(t)e + u_r(t) \in \mathcal{U}$ and $\frac{\partial V}{\partial e}\tilde{f}(\cdot) + F(\cdot) \leq 0$ are satisfied, see [Chen and Allgöwer 1998]. Indeed such a terminal region would be already time-varying, since $V(t,e)$ depends explicitly on $t$. However, it is a restrictive choice. For a given $V(t,e)$ the set is defined by a constant $c > 0$, i.e., the time instant $t \geq 0$ where the constraints are most restrictive determines the value of $c$. Subsequently, we want to relax this conservatism by using a time-varying function $\pi : \mathbb{R}_0^+ \to \mathbb{R}^+$ on the right hand side of the inequality, and thus we work with $V(t,e) \leq \pi^2(t)$. To this end we formulate the notion of a positive invariant time-varying level set of a Lyapunov function.[4]

Consider the Lyapunov function (3.25) for the controlled LTV system and a function $\pi : \mathbb{R}_0^+ \to \mathbb{R}^+, \pi \in \mathcal{C}^1$. In order to handle the time-varying right hand side in $V(t,e) \leq \pi^2(t)$ we consider the closed set

$$\Lambda := \left\{(t,e) \mid V(t,e) \leq \pi^2(t)\right\} \subset \mathbb{R}_0^+ \times \mathbb{R}^{n_x}, \tag{3.30}$$

in the extended space $\mathbb{R}_0^+ \times \mathbb{R}^{n_x}$. It is helpful to work with a subset of $\Lambda$ where the coordinate $t$ is fixed

$$\Lambda_t := \Lambda \cap \{\{t\} \times \mathbb{R}^{n_x}\} \subset \mathbb{R}_0^+ \times \mathbb{R}^{n_x}. \tag{3.31}$$

[4] A related approach to periodic Lyapunov functions for periodic discrete-time systems was presented in [Böhm 2010; Böhm et al. 2010a,b]. There periodic Lyapunov functions which decrease only from period to period and not monotonously are considered. In [Böhm 2010] the use of inequalities with time-varying levels $\pi(t)$ is hinted. However, this issue is not fully elaborated.

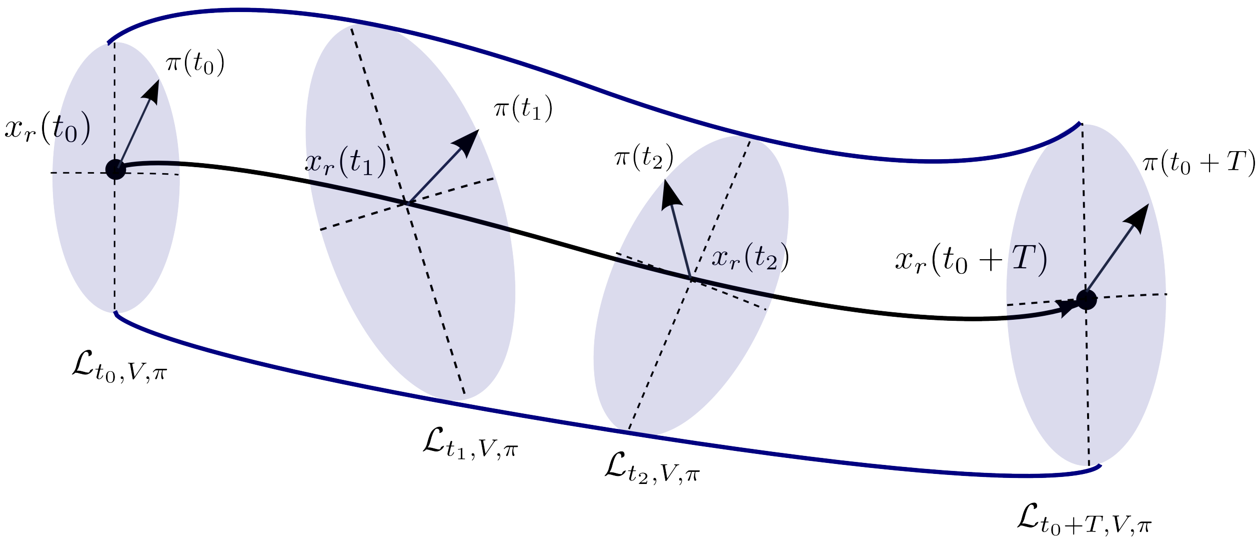


**Figure 3.2:** Time-varying level set of the LTV error system.

We define the map $\Pi : \mathbb{R}_0^+ \times \mathbb{R}^{n_x} \to \mathbb{R}^{n_x}$

$$\Pi : (t, e) \mapsto e \tag{3.32}$$

which projects any extended state $(t, e)$ onto $e \in \mathbb{R}^{n_x}$. Relying on $\Pi$ we define time-varying level sets of $V(t, e)$ as the images $t \mapsto \Pi(\Lambda_t)$.

**Definition 3.3** (Time-varying level sets).
*For all $t \in [0, \infty)$ we call the family of sets*

$$\mathcal{L}_{t,V,\pi} := \{\Pi(\Lambda_t) \mid t \in [0, \infty)\} \tag{3.33a}$$

*a time-varying level set of the Lyapunov function $V(t, e)$ from* (3.25)*. Accordingly, we define the boundary of $\mathcal{L}_{t,V,\pi}$ point-wise in time as*

$$\partial\mathcal{L}_{t,V,\pi} := \{\partial\Pi(\Lambda_t) \mid t \in [0, \infty)\}\,. \tag{3.33b}$$

For the LTV error system of the trajectory-tracking task the time-varying level set can be understood as ellipsoids $\{x \in \mathbb{R}^{n_x} \mid (x - x_r(t))^T(P(t) + I)(x - x_r(t)) \le \pi^2(t)\}$ which are centered along the reference, see Figure 3.2. Note that the shape $P(t) + I$ and the diameter $\pi(t)$ of the ellipsoids vary with time.
For level sets of Lyapunov functions defined by constants $\{V(t, e) \le c^2\}$ it is straightforward to show positive invariance with respect to (3.18) subject to (3.24). In the case of time-varying level sets as defined above we need an additional property to guarantee this. The next result is directly formulated for the LTV error system (3.18) and the Lyapunov function from Lemma 3.2. Sufficient and necessary conditions for positive invariance of these sets are as follows.

**Theorem 3.2** (Positive invariance of time-varying level sets).
*Consider system* (3.18) *under the feedback* (3.24) *and the time-varying level sets* $\mathcal{L}_{t,V,\pi}$. *All solutions* $e(t, t_0, e_0 \mid K(t)e)$ *with* $e_0 \in \mathcal{L}_{t_0,V,\pi}$ *stay inside* $\mathcal{L}_{t,V,\pi}$ *for all* $t \geq t_0 \geq 0$ *if and only if*

$$\forall t \geq t_0, \ \forall e \in \partial\mathcal{L}_{t,V,\pi} : \quad \dot{V}(t,e) \leq 2\pi(t)\dot{\pi}(t). \tag{3.34}$$

*Proof.* Consider the function $s(t) = V(t, e(t)) - \pi^2(t)$. Since $\pi(t) \in \mathcal{C}^1$ the time derivative of $s(t)$

$$\dot{s}(t) = \dot{V}(t, e(t)) - 2\pi(t)\dot{\pi}(t)$$

is continuous. If at some time $t_0$ the error state $e_0 \in \partial\mathcal{L}_{t_0,V,\pi}$ we have $s(t_0) = 0$. Assume (3.34) holds at $t_0$, then a $\tau > 0$ exists such that $s(t_0 + \tau) = \int_{t_0}^{t_0+\tau} \dot{s}\, dt \leq 0$. Hence $e(t_0 + \tau, t_0, e_0 \mid K(t)e) \in \mathcal{L}_{t_0+\tau,V,\pi}$. Thus (3.34) is sufficient.
The necessity of condition (3.34) is shown via contradiction. Assume that at some time $t_0$ we have $s(t_0) = 0, \dot{s}(t_0) > 0$. Then for some $\tau > 0$ we have that $s(t + \tau) = s(t_0) + \int_{t_0}^{t_0+\tau} \dot{s}\, dt > 0$. Which implies $V(t_0+\tau, e(t_0+\tau)) > \pi^2(t_0+\tau)$, and consequently $e(t_0 + \tau, t_0, e_0 \mid K(t)e) \notin \mathcal{L}_{t_0+\tau,V,\pi}$. □

An intuitive explanation of the invariance condition (3.34) is as follows: the decay of $\pi^2(t)$ may not be faster than the decay of the Lyapunov function $V(t, e)$ along solutions of (3.18) controlled via (3.24). One should note that by Assumption 3.2 the reference is constant for $t \geq T$. Moreover, the Lyapunov function $V(t, e)$ (3.25) of the LTV error system (3.18) is explicitly time-varying only for $t \in [0, T]$. Thus if $\dot{\pi}(t) = 0$ for $t \geq T$, then the sets $\mathcal{L}_{t,V,\pi}$ are time-invariant for $t \geq T$.

**Remark 3.3** (Time-varying level sets for nonlinear systems).
*Two issues concerning time-varying level sets should be noted. Firstly, at no point in the preceding proof we use the fact that the LTV error system is linear. The concept of positive invariant time-varying level sets of Lyapunov functions is applicable to nonlinear globally asymptotically stable systems as well. Secondly, it is not required that the function* $\pi : \mathbb{R} \to \mathbb{R}^+$, *which defines the time-varying level set in* (3.30), *is monotonously decreasing. An increasing function* $\pi(t)$ *always fulfills the conditions of Theorem 3.2. However, constraints on states and inputs usually limit the maximum size of the time-varying level set and thereby imply a bound on* $\pi(t)$.

**Remark 3.4** (Extension to $\pi(t) \in \mathcal{C}^0$).
*To simplify the computation of* $\pi(t)$ *one may wish to extend the time-varying level sets to functions* $\pi(t)$ *which are not* $\mathcal{C}^1$. *If one requires that* $\pi(t)$ *is absolutely continuous, one can reformulate the invariance condition* (3.34) *as follows*

$$\forall t \geq t_0, \forall e \in \partial\mathcal{L}_{t,V,\pi} : \quad \dot{V}(t,e) \leq 2\pi(t)D^+\pi(t).$$

*Here* $D^+\pi(t)$ *is the upper right hand derivative of* $\pi(t)$. *The sufficiency of this condition is shown in Lemma C.3 in Apppendix C. There we also show that* $V(t,e)$ *does not need to be a Lyapunov function.*

### 3.5.3 Approximative Computation of Time-varying Level Sets

The consideration of invariant sets becomes more complicated if constraints on states and inputs are present. The LTV error system (3.18) is subject to the constraints $\forall t \geq 0 : \; e(t) + x_r(t) \in \mathcal{X}$ and $K(t)e(t) + u_r(t) \in \mathcal{U}$. Subsequently, we want to determine $\pi(t)$ such that $\mathcal{L}_{t,V,\pi}$ is as large as possible, consistent with the constraints, and positive invariant with respect to the flow of (3.18). To achieve this one can state the problem of finding the maximum integral volume time-varying level set as follows. Determine

$$\sup_{w_\pi(\cdot)\in\mathcal{C}^0,\; \pi_0} \int_0^T \mathrm{vol}\left(\mathcal{L}_{\tau,V,\pi}\right)\; d\tau \tag{3.35a}$$

subject to the scalar ODE

$$\dot{\pi}(t) = w_\pi(t), \quad \pi(0) = \pi_0,\; \dot{\pi}(T) = 0 \tag{3.35b}$$

and

$$\forall t \in [0,T] : \qquad \pi(t) \geq 0 \tag{3.35c}$$

$$\forall t \in [0,T],\; \forall e \in \partial\mathcal{L}_{t,V,\pi} : \qquad \dot{V}(t,e) \leq 2\pi(t)w_\pi(t) \tag{3.35d}$$

$$\forall t \in [0,T],\; \forall e \in \mathcal{L}_{t,V,\pi} : K(t)e + u_r(t) \in \mathcal{U} \subset \mathbb{R}^{n_u} \tag{3.35e}$$

$$\forall t \in [0,T],\; \forall e \in \mathcal{L}_{t,V,\pi} : \qquad e + x_r(t) \in \mathcal{X} \subseteq \mathbb{R}^{n_x}. \tag{3.35f}$$

The main idea behind this OCP is to maximize the volume of the corresponding projections $\mathcal{L}_{t,V,\pi} = \Pi\left(\Lambda_t\right)$ over the time span $[0,T]$ by influencing the evolution of the function $\pi(t)$. We work here with sup instead of max, since for general compact constraints $\mathcal{X},\mathcal{U}$ the existence of an optimal solution $\pi(t) \in \mathcal{C}^1$ is difficult to verify. Note the time span $[0,T]$ is induced by the time length of the asymptotically constant reference trajectory, cf. Assumption 3.2. We describe the time evolution of $\pi(t)$ by the scalar ODE (3.35b), where $w_\pi : [0,T] \to \mathbb{R}$ is the input and consequently a decision variable of the OCP (3.35). Since $\pi(t) \in \mathcal{C}^1$ we have to require that $w_\pi(t) \in \mathcal{C}^0$. At the end of the reference trajectory the time-varying level set should not change anymore, thus for $t = T$ we enforce $w_\pi(T) = 0$. The initial condition $\pi(0) = \pi_0$ is also a decision variable. Due to the construction of the time-varying level sets $\pi(t)$ has to be non-negative (3.35c). The positive invariance property from (3.34) is expressed in (3.35d). Additionally, we want to achieve that the constraints on states and input are respected, hence (3.35e-f). One could also ask for the maximal averaged volume. If this is desired, then one has to modify (3.35a) to

$$\sup_{w_\pi(\cdot)\in\mathcal{C}^0,\; \pi_0} \frac{1}{T}\int_0^T \mathrm{vol}\left(\mathcal{L}_{\tau,V,\pi}\right)\; d\tau. \tag{3.36}$$

In principle, one could not only optimize the right hand side of the inequality $e^T(P(t)+I)e \leq \pi^2(t)$ but also the shape of the ellipsoids $\mathcal{L}_{t,V,\pi}$ by changing $P(t)$. More precisely,

one could add the RDE (3.21) as a dynamic constraint to (3.35) and regard $Q(t), R(t)$ as decision variables. However, we are interested in obtaining a computationally less demanding approach. Thus we do not optimize the shape matrix $P(t)$.
It is easy to see that the OCP (3.35) has the trivial feasible solution $\pi(t) = 0$. The question arises of whether the OCP (3.35) admits feasible and strictly positive solutions $\pi(t) > 0$. The next lemma answers this question.

**Lemma 3.3** (Existence of non-zero time-varying level sets)**.**
*If Assumption 3.2 holds, then OCP* (3.35) *has at least one strictly positive feasible solution, such that for all* $t \in [0, T] : \pi(t) > 0$.

*Proof.* The proof is done by construction of an admissible solution $\pi(t) > 0$. Due to Assumption 3.2 part i) the reference is contained in the interior of the state constraints for all $t \in [0,T] : x_r(t) \in \operatorname{int} \mathcal{X}$. Hence an $\epsilon_{\mathcal{X}} > 0$ exists, such that for all $e \in \{\|e\|^2 \leq \epsilon_{\mathcal{X}}\}$ and all $t \in [0,T]$ one has $e + x_r(t) \in \mathcal{X}$. Due to Assumption 3.2 part ii) also a constant $\epsilon_{\mathcal{U}} > 0$ with $e \in \{\|e\|^2 \leq \epsilon_{\mathcal{U}}\}$ exists, such that for all $t \in [0,T]$ one has that $K(t)e + u_r(t) \in \mathcal{U}$. Denote with $\bar{\epsilon}$ the minimum of these constants $\bar{\epsilon} = \min\{\epsilon_{\mathcal{X}}, \epsilon_{\mathcal{U}}\}$.
W.l.o.g. we restrict ourselves to the set $\{\|e\|^2 \leq \bar{\epsilon}\}$ and choose $\pi(0) = \frac{\bar{\epsilon}}{2}$. For all $t \in [0, T)$ an admissible input driving the evolution of $\pi(t)$ is $w_\pi(t) = \bar{\epsilon}/T^2 \cdot (T - t)$. For $t = T$ we have $w_\pi(T) = 0$. Since $\pi(0) = \frac{\bar{\epsilon}}{2} > 0$ and $w_\pi \geq 0$ the invariance condition (3.35d) is satisfied for all $t \in [0,T]$. Consequently, one obtains a feasible solution $0 < \pi(t) \leq \bar{\epsilon}$, $\pi(t) \in \mathcal{C}^1$ to OCP (3.35). □

The numerical solution to the OCP (3.35) is not straightforward. Even if (3.35) is discretized in time, the constraints (3.35d-g) have to be evaluated over compact sets of real vectors. Subsequently, we rely on concepts for computation of maximum volume ellipsoids to reformulate (3.35) in a more convenient way. Mainly, we use the fact that the Lyapunov function (3.25) is quadratic.
Consider the change of coordinates

$$\xi = \frac{1}{\pi(t)} S(t)e, \quad S(t) = \sqrt{(P(t) + I)}. \tag{3.37}$$

Note that due to $P(t) + I \in \mathcal{BC}^+(\mathbb{R}^{n_x \times n_x})$ it follows that $S(t) \in \mathcal{BC}^+(\mathbb{R}^{n_x \times n_x})$ with $S(t) = S^T(t)$ and $S(t)S(t) = P(t) + I$ exists. We reformulate $\mathcal{L}_{t,V,\pi}$ in $\xi$ coordinates

$$\mathcal{L}_{t,V,\pi} = \left\{ e \in \mathbb{R}^{n_x} \mid \xi \mapsto \pi(t) S^{-1}(t)\xi,\ \|\xi\|^2 \leq 1 \right\}. \tag{3.38}$$

Using similar ideas as in [Boyd and Vandenberghe 2004, Chap. 8] the objective (3.35a) can be rewritten as

$$\sup \int_0^T \log\det\left(S^{-1}(\tau)\pi(\tau)\right) d\tau.$$

Since $P(t)$ and $S(t)$ are not effected by the choice of $\pi(t)$, we could consider the objective $\sup \int_0^T \log(\pi(\tau)) d\tau$. Due to the strict monotonicity of the log function this is equivalent to

$$\sup \int_0^T \pi(\tau)\, d\tau.$$

We now reformulate the invariance constraint (3.35d). Recall that the weight matrix $Q(t)$ is chosen according to Assumption 3.4. From (3.23) and (3.27) we know $\dot{V}(t,e) \leq -e^T\tilde{Q}e$. Rewriting (3.35d) in $\xi$ coordinates we obtain

$$\dot{V}(t,e) \leq -\pi^2(t) \cdot \xi^T S^{-T}(t)\tilde{Q}S^{-1}(t)\xi \leq -\underline{q}(t)\pi^2(t)$$

where

$$\underline{q}(t) = \lambda_{min}\left(S^{-T}(t)\tilde{Q}S^{-1}(t)\right) > 0.$$

Since $\pi(t) > 0,\ \dot{\pi} = w_\pi$ we require $-\underline{q}(t)\pi(t) \leq 2w_\pi(t)$ instead of (3.35d). This leads to an inner approximation of (3.35d). It remains to reformulate (3.35e-f). The input and state constraints (3.35e-f) of the error system are affine in $e$, and the set $\mathcal{L}_{t,V,\pi}$ is compact. We express these constraints in $\xi$ coordinates by

$$\begin{aligned} x_{min} - x_r(t) &\preceq \pi(t)S^{-1}(t)\xi \preceq x_{max} - x_r(t) \\ u_{min} - u_r(t) &\preceq \pi(t)K(t)S^{-1}(t)\xi \preceq u_{max} - u_r(t). \end{aligned}$$

Note that $\preceq$ denotes component-wise inequality. We rewrite the matrices $S^{-1}(t)$ and $K(t)S^{-1}(t)$ in terms of their rows as

$$\begin{aligned} S^{-1}(t) &= (\sigma_1^T(t), \sigma_2^T(t), \ldots, \sigma_{n_x}^T(t))^T \\ K(t)S^{-1}(t) &= (\kappa_1^T(t), \kappa_2^T(t), \ldots, \kappa_{n_u}^T(t))^T. \end{aligned}$$

and use

$$\forall \|\xi\|^2 \leq 1: \quad -\|\sigma_i^T(t)\| \leq \sigma_i^T(t)\xi \leq \|\sigma_i^T(t)\|.$$

This yields an inner approximation of the state constraints (3.35f)

$$\begin{aligned} \forall i \in \{1,\ldots,n_x\}: &\quad \|x_{min,i} - x_{r,i}(t)\| \geq \pi(t)\|\sigma_i^T(t)\| \\ \forall i \in \{1,\ldots,n_x\}: &\quad \|x_{max,i} - x_{r,i}(t)\| \geq \pi(t)\|\sigma_i^T(t)\|. \end{aligned}$$

The input constraints (3.35e) can be rewritten in a similar fashion. The reformulation of (3.35) can now be stated as follows:

$$\sup_{w_\pi(\cdot)\in\mathcal{C}^0,\ \pi_0} \int_0^T \pi(\tau)\, d\tau \tag{3.39a}$$

subject to

$$\forall t \in [0,T]: \quad \dot{\pi}(t) = w_\pi(t), \quad \pi(0) = \pi_0,\ \dot{\pi}(T) = 0 \tag{3.39b}$$

$$\forall t \in [0,T]: \quad \pi(t) \geq 0 \tag{3.39c}$$

$$\forall t \in [0,T]: \ 2w_\pi(t) \geq -\underline{q}(t)\pi(t) \tag{3.39d}$$

and

$$\forall i \in \{1, \ldots, n_x\}: \quad \|x_{max,i} - x_{r,i}(t)\| \geq \|\sigma_i^T(t)\|\pi(t) \tag{3.39e}$$
$$\forall i \in \{1, \ldots, n_x\}: \quad \|x_{min,i} - x_{r,i}(t)\| \geq \|\sigma_i^T(t)\|\pi(t) \tag{3.39f}$$
$$\forall i \in \{1, \ldots, n_u\}: \quad \|u_{max,i} - u_{r,i}(t)\| \geq \|\kappa_i^T(t)\|\pi(t) \tag{3.39g}$$
$$\forall i \in \{1, \ldots, n_u\}: \quad \|u_{min,i} - u_{r,i}(t)\| \geq \|\kappa_i^T(t)\|\pi(t). \tag{3.39h}$$

OCP (3.39) is an infinite dimensional *linear program* (LP). It is straightforward to approximate its solution by a finite dimensional LP. To this end one discretizes the ODE $\dot{\pi} = w_\pi$, and uses the fact that the cost and all constraints are affine in $\pi(t)$. Clearly, one has to be careful to use a sufficiently accurate time discretization. Taking Lemma 3.3 into account it is also clear that a time discretization of the reformulated problem is an LP with at least one feasible and hence also an optimal solution. The price for this reformulation of (3.35) as an LP is that the invariance and input/state constraints (3.35d-f) are only inner approximated by (3.39d-h). Note that the assumption of box constraints—Assumption 3.3 part i)—can be relaxed to polytopic constraints.

### 3.5.4 Terminal Regions and End Penalties

So far the conceptual idea of time-varying level sets allows us to compute constraint consistent positive invariant time-varying terminal regions at least for trajectory-tracking of LTV systems. Here, we aim at a control scheme applicable to trajectory-tracking problems of constrained nonlinear systems. Thus we need to guarantee that the time-varying set $\mathcal{L}_{t,V,\pi}$ is positive invariant with respect to the nonlinear error dynamics (3.13) subject to the two-degrees-of-freedom control $u = K(t)e + u_r(t)$. In general this is not the case and difficult to enforce. As we will show, the existence of a function $\tilde{\pi} \in \mathcal{C}^1$ with $\forall t \in [0, T] : \tilde{\pi}(t) \leq \pi(t)$, which describes a sufficiently smaller time-varying level set valid for the nonlinear system, can be guaranteed.
We rewrite the nonlinear error dynamics (3.13) under the linear feedback (3.24) as

$$\dot{e} = \tilde{A}(t)e + \Phi(t, e). \tag{3.40}$$

$\tilde{A}(t) = A(t) + B(t)K(t)$ is the closed loop system matrix of the LTV error system and $\Phi(t, e) = \tilde{f}\,(t, e, K(t)e + u_r(t)) - \tilde{A}(t)e$. For sake of simplicity we denote the solutions of (3.40) as $e(t, t_0, e_0)$.

**Lemma 3.4** (Existence of time-varying level sets for nonlinear error dynamics)**.**
*Given the LTV error system* (3.18)*, and assume that Assumptions 3.2–3.3 hold. Suppose that a time-varying level set* $\mathcal{L}_{t,V,\pi}$ *based on* $V(t, e)$ *from* (3.25) *has been obtained via* (3.35)*.*
*Then a function* $\tilde{\pi}(t)$*, which for all* $t \in [0, T]$ *satisfies* $0 < \tilde{\pi}(t) \leq \pi(t)$, $\dot{\tilde{\pi}}(T) = 0$, *exists such that for all* $e \in \tilde{\mathcal{L}}_{t,V,\tilde{\pi}} = \{e \in \mathbb{R}^{n_x} \mid V(t, e) \leq \tilde{\pi}(t)\}$ *the following holds:*

*i) All solutions* $e(t, t_0, e_0)$ *of* (3.40) *starting at* $t_0 \in [0, T]$ *and* $e_0 \in \tilde{\mathcal{L}}_{t_0,V,\tilde{\pi}}$ *converge to* $e = 0$ *exponentially fast, and* $\tilde{\mathcal{L}}_{t,V,\tilde{\pi}}$ *is positively invariant with respect to* (3.40).

*ii) Along the solutions* $e(t, t_0, e_0)$ *starting at* $t_0 \in [0, T]$ *and* $e_0 \in \tilde{\mathcal{L}}_{t_0,V,\tilde{\pi}}$ *the constraints are satisfied* $\forall t \geq t_0 : u(t) = K(t)e(t) + u_r(t) \in \mathcal{U}$ *and* $e(t) + x_r(t) \in \mathcal{X}$.

*Proof.* Recall that for $t \geq T$ the set $\tilde{\mathcal{L}}_{t,V,\tilde{\pi}}$ and the error dynamics (3.40) are time invariant. Due to Assumption 3.2 and the assumptions on the original system dynamics (3.11) the nonlinear error dynamics are locally Lipschitz for all $t \geq 0$ and all $e+x_r(t) \in \mathcal{X}$. Moreover, the closed loop system matrix $A(t)+B(t)K(t)$ of the LTV system (3.18) is bounded for all $t \geq 0$ and its closed loop solutions are exponentially stable. Thus one can apply results on Lyapunov's indirect method for non-autonomous systems and conclude that $e = 0$ is a locally exponentially stable equilibrium also for the nonlinear error system (3.40), see [Khalil 2002, Thm. 4.13]. Consequently, a set $\{e \mid \|e\|^2 \leq \rho^2\}, \rho > 0$ exists such that all solutions of the controlled nonlinear error dynamics starting in this set stay inside the set and converge to $e = 0$ exponentially fast. If we choose $\bar{\pi} = \min_{t\in[0,T]}\{\sqrt{c_2}\rho,\ \pi(t)\}$, with $c_2 > 0$ from (3.28), it follows

$$\forall t \in [0, \infty): \quad \left\{e \in \mathbb{R}^{n_x} \mid V(t, e) \leq \bar{\pi}^2\right\} \subseteq \{e \mid \|e\|^2 \leq \rho^2\}.$$

With the same arguments as in the proof of Lemma 3.3 one can construct an increasing function $\tilde{\pi}(t)$ such that $0 < \tilde{\pi}(t) \leq \bar{\pi} \leq \pi(t)$ and $\dot{\tilde{\pi}}(t) \geq 0$. Moreover, $\dot{\tilde{\pi}}(t) \geq 0$ ensures that $\tilde{\mathcal{L}}_{t,V,\tilde{\pi}}$ is positively invariant with respect to (3.40). This proves part i). Part ii) follows direct from $\tilde{\pi}(t) \leq \pi(t)$ and the positive invariance of $\tilde{\mathcal{L}}_{t,V,\tilde{\pi}}$ with respect to (3.40). □

From Lemma 3.4 we know that if we shrink the level set of the LTV error system $\mathcal{L}_{t,V,\pi}$ sufficiently, we obtain a time-varying set $\tilde{\mathcal{L}}_{t,V,\tilde{\pi}}$ for the nonlinear system (3.40). And inside this shrunken set $V(t, e)$ is a local Lyapunov function also for the nonlinear error dynamics subject to $u = K(t)e+u_r(t)$. Unfortunately, the time-varying set $\tilde{\mathcal{L}}_{t,V,\tilde{\pi}}$ is often very small and a conservative approximation of the true region of attraction. To relax this conservatism we propose to compute $\tilde{\pi}(t)$ such that only for $t \geq T$ the function $V(t, e)$ is a local Lyapunov function. In other words, for $t \in [0, T)$ the linear feedback law $u = K(t)e + u_r$ shall ensure positive invariance of $\tilde{\mathcal{L}}_{t,V,\tilde{\pi}}$ for solutions of the nonlinear error dynamics (3.13) controlled via $u = K(t)e + u_r$. Stabilization is merely enforced for $t \geq T$ and all $e \in \tilde{\mathcal{L}}_{T,V,\tilde{\pi}}$.
To compute a time-varying $\tilde{\pi}(t)$ we apply a similar reasoning as for usual time-invariant level sets, cf. [Chen and Allgöwer 1998; Michalska and Mayne 1993]. We distinguish two cases: $t \geq T$ and $t \in [0, T)$.
**Case 1** $t \geq T$: We derive an upper bound on $\dot{V}(t, e)$ along the trajectories of the nonlinear error dynamics (3.40). Recall Assumption 3.4. Hence we have $\dot{V}(t, e) = -e^T\tilde{Q}e$ for the decay of $V(t, e)$ along the solutions of (3.18). The decay of $V(t, e)$

along the solutions of the nonlinear system (3.40) is

$$\forall t \geq T: \quad \dot{V}_{\tilde{f}}(t,e) = 2e^T \tilde{P}(T)\Phi(T,e) - e^T \tilde{Q} e. \tag{3.41}$$

where $\tilde{P}(T) = P(T) + I$. It holds that

$$2e^T \tilde{P}(T)\Phi(T,e) - e^T \tilde{Q} e \leq 2\|e\|^2 \|\tilde{P}(T)\| \frac{\|\Phi(T,e)\|}{\|e\|} - e^T \tilde{Q} e. \tag{3.42}$$

For $\|e\| \to 0$ we have $\frac{\|\Phi(T,e)\|}{\|e\|} \to 0$, and thus there exist constants $0 < \epsilon, \tilde{\pi}(T) < \infty$ such that

$$\forall e \in \tilde{\mathcal{L}}_{T,V,\tilde{\pi}}: \quad 2e^T \tilde{P}(T)\Phi(T,e) - e^T \tilde{Q} e + \epsilon \cdot e^T \tilde{P}(t) e \leq 0. \tag{3.43}$$

W.l.o.g. we choose $\epsilon = \lambda_{min}\left(S(T)^{-1}\tilde{Q}S(T)^{-1}\right)$ with $S(t)$ from (3.37). We denote the function on the left hand side of the last inequality as

$$\phi_T(e) = 2e^T \tilde{P}(T)\Phi(T,e) - e^T \tilde{Q} e + \epsilon \cdot e^T \tilde{P}(T) e.$$

Now, we are ready to shrink $\pi(T)$ down to $\tilde{\pi}(T) \leq \pi(T)$ by solving the semi-infinite program

$$\underset{\tilde{\pi}(T) \leq \pi(T)}{\text{maximize}}\ \tilde{\pi}(T) \tag{3.44a}$$

subject to

$$\forall e \in \tilde{\mathcal{L}}_{T,V,\tilde{\pi}}: \quad \phi_T(e) \leq 0. \tag{3.44b}$$

The solution to this problem can be approximated by a sequence of global optimization problems. Start with $\tilde{\pi}(T) = \pi(T)$ and compute $\phi_T^\star = \max \phi_T(e)$. If $\phi_T^\star > 0$, halve $\tilde{\pi}(T)$, and solve (3.44a) again. Repeat until $\phi_T^\star \leq 0$. Note that for small values of $\tilde{\pi}(T)$ the function $\phi_T$ is concave, cf. [Michalska and Mayne 1993]. Moreover, we have

$$\forall e \in \tilde{\mathcal{L}}_{T,V,\tilde{\pi}}: \quad \dot{V}_{\tilde{f}}(T,e) \leq -\epsilon \cdot e^T \tilde{P}(T) e \leq -\epsilon \cdot \|e\|^2$$

which ensures that $V(T,e)$ is a local Lyapunov function of (3.40) on $\tilde{\mathcal{L}}_{T,V,\tilde{\pi}}$.

**Case 2** $t \in [0,T)$: For the remaining time points $0 \leq t < T$ we only enforce that $\tilde{\mathcal{L}}_{T,V,\tilde{\pi}}$ is positively invariant. We do not require that $V(t,e)$ is a local Lyapunov function for the nonlinear system (3.40). The derivative of $V(t,e) - \tilde{\pi}(t)^2$ along solutions of (3.40) is

$$\dot{V}_{\tilde{f}}(t,e) - 2\tilde{\pi}(t)\dot{\tilde{\pi}}(t) = 2e^T \tilde{P}(t)\Phi(t,e) - e^T \tilde{Q} e - 2\tilde{\pi}(t)\dot{\tilde{\pi}}(t) =: \phi_t(e).$$

For $0 \leq t < T$ we solve in a similar fashion as before the slightly easier problem

$$\underset{\tilde{\pi}(t) \leq \pi(t)}{\text{maximize}}\ \tilde{\pi}(t) \tag{3.44c}$$

subject to

$$\forall e \in \partial\tilde{\mathcal{L}}_{T,V,\tilde{\pi}}: \quad \phi_t(e) \leq 0. \tag{3.44d}$$

The main idea is to check the invariance condition (3.34) for the time-varying level set only on its boundary $\partial\tilde{\mathcal{L}}_{t,V,\tilde{\pi}}$. From Lemma C.3, Appendix C it follows that (3.44d) ensures positive invariance of $\tilde{\mathcal{L}}_{T,V,\tilde{\pi}}$ with respect to (3.40). Obviously, we cannot solve this problem for all $t \in [0,T)$. If one applies a time discretization on the ODE $\dot{\tilde{\pi}}(t) = w_{\tilde{\pi}}$, a sequence of nonlinear optimization problems is obtained, which can be solved recursively backwards in time. We point out that one needs to ensure a sufficiently fine time discretization in order to keep the error sufficiently small.
It remains to show that the time-varying level sets $\tilde{\mathcal{L}}_{t,V,\tilde{\pi}}$ and a suitably defined end penalty fulfill the suppositions of Corollary 3.2. This is done in the next lemma.

**Lemma 3.5** (Time dependent end penalties)**.**
*Consider Problem 3.2 under Assumptions 3.2-3.4, and assume further that* $\tilde{\pi} : [0,T] \to (0,\infty)$ *has been obtained via* (3.44).
*Suppose that the terminal region is* $\mathcal{E}_{t_k+T_p} = \tilde{\mathcal{L}}_{t_k+T_p,V,\tilde{\pi}}$*, then the time-varying set* $\tilde{\mathcal{L}}_{t,V,\tilde{\pi}}$ *and the end penalty*

$$E(t) = \begin{cases} \int_t^T \alpha(\tau)\beta \; d\tau + \frac{\alpha(T)\beta}{2\gamma} & t \in [0,T) \\ \frac{\alpha(T)\beta}{2\gamma} e^{-2\gamma(t-T)} & t \geq T \end{cases} \tag{3.45a}$$

*where* $\alpha(t), \beta, \gamma$ *are*

$$\alpha(t) = \tilde{\pi}^2(t) \left\| S^{-1}(t) \right\|^2 \cdot \| Q_F + K(t)^T R_F K(t) \| + \hat{\alpha}, \quad \hat{\alpha} \in [0,\infty) \tag{3.45b}$$

$$\beta = \overline{p} + 1, \qquad \overline{p} = \sup_{t\in[0,T]} \|P(t)\| \tag{3.45c}$$

$$\gamma = \tfrac{1}{2(\overline{p}+1)} \lambda_{min} \left( S^{-1}(T) \tilde{Q} S^{-1}(T) \right), \tag{3.45d}$$

*fulfill the suppositions* (3.16) *of Corollary 3.2.*

*Proof.* The end penalty (3.45a) is obtained as an approximation of the worst case cost inside $\tilde{\mathcal{L}}_{t,V,\tilde{\pi}}$ which consists of two parts, see Figure 3.3. The first part is the cost associated to a solution which travels through the boundary of the terminal region $\partial\tilde{\mathcal{L}}_{t,V,\tilde{\pi}}$ for all $t \in [0,T)$. The second part uses the fact that inside $\tilde{\mathcal{L}}_{T,V,\tilde{\pi}}$ the terminal control law guarantees exponential cost decrease. By construction the time-varying sets $\tilde{\mathcal{L}}_{t,V,\tilde{\pi}}$ are positive invariant with respect to (3.40). That is $\tilde{\mathcal{L}}_{t,V,\tilde{\pi}}$ is a positive invariant time-varying set of (3.13) under the terminal control law $u = K(t)e + u_r(t)$. Note that state and input constraints are fulfilled for any solution $e(t, t_0, e_0|u)$ with $e_0 \in \tilde{\mathcal{L}}_{t_0,V,\tilde{\pi}}$. Hence the terminal region is set as $\mathcal{E}_{t_k+T_p} = \tilde{\mathcal{L}}_{t_k+T_p,V,\tilde{\pi}}$. Furthermore, it is straightforward to check that the proposed terminal penalty (3.45a) is mapping $E : \mathbb{R}_0^+ \to \mathbb{R}_0^+$ and $E(t) \in \mathcal{C}^1$.
As a preparation step of the proof we show that inside $\tilde{\mathcal{L}}_{t,V,\tilde{\pi}}$ the function $\alpha(t)$ from (3.45b) is an upper bound for the cost $F(t, e, K(t)e + u_r(t))$. Due to Assumption 3.3

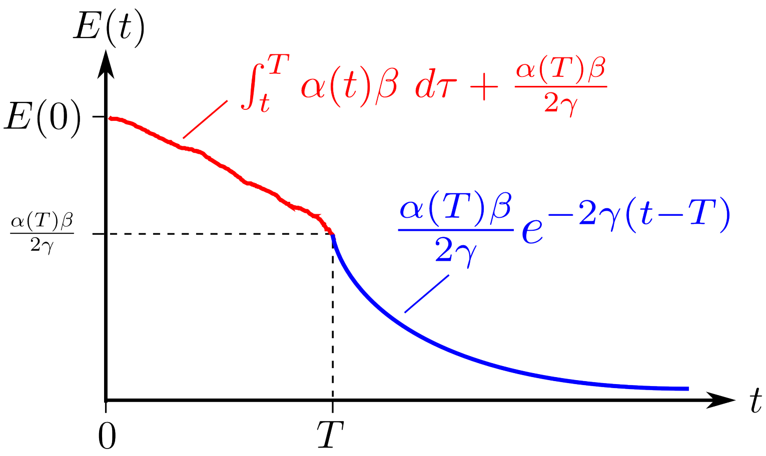


**Figure 3.3:** Schematic sketch of the end penalty $E(t)$ from (3.45).

part ii) it holds for all $e \in \mathbb{R}^{n_x}$

$$F(t, e, K(t)e + u_r(t)) \leq \|e\|^2 \cdot \left\| Q_F + K^T(t) R_F K(t) \right\|.$$

Using the coordinate transformation $e = \tilde{\pi}(t) S^{-1}(t)\xi$ from (3.37), the set $\tilde{\mathcal{L}}_{t,V,\tilde{\pi}}$ is described by $\|\xi\| \leq 1$. Hence we obtain

$$\forall e \in \tilde{\mathcal{L}}_{t,V,\tilde{\pi}} : \quad F(\cdot) \leq \tilde{\pi}^2(t) \left\| S^{-1}(t) \right\|^2 \cdot \left\| Q_F + K^T(t) R_F K(t) \right\|.$$

Referring to $\alpha(t)$ from (3.45b) the right hand side of this inequality is exactly $\alpha(t) - \hat{\alpha}$, where $\hat{\alpha} \in [0, \infty)$. Recalling from (3.45c) that $\beta \geq 1$ it follows

$$\forall t \in [0, T), \; \forall e \in \tilde{\mathcal{L}}_{t,V,\tilde{\pi}} : \quad F(\cdot) \leq \alpha(t) - \hat{\alpha} \leq (\alpha(t) - \hat{\alpha})\, \beta. \tag{3.46}$$

It remains to verifiy that $E(t)$ from (3.45) fulfills (3.16b) of Corollary 3.2. The time derivative of $E(t)$ is

$$\dot{E}(t) = \begin{cases} -\alpha(t)\beta & t \in [0, T) \\ -\alpha(T)\beta e^{-2\gamma(t-T)} & t \geq T \end{cases}. \tag{3.47}$$

Thus we proceed with a case distinction for $t < T$ and $t \geq T$.
**Case 1** $t \in [0, T)$**:** Using the approximation (3.46) to check supposition (3.16b) of Corollary 3.2 for all $t \in [0, T)$ yields

$$\dot{E}(t) + F(t, e, K(t)e + u_r(t)) \leq -\alpha(t)\beta + (\alpha(t) - \hat{\alpha})\, \beta \tag{3.48}$$

where $\beta \geq 1$ and $\hat{\alpha} \in [0, \infty)$. Hence $E(t)$ from (3.45) fufills (3.16b) for all $t \in [0, T)$.
**Case 2** $t \geq T$**:** Recall that for $t \geq T : \tilde{\pi}(t) = \tilde{\pi}(T)$. And $\tilde{\pi}(T)$ is determined via the optimization problem (3.44a) such that inside $\tilde{\mathcal{L}}_{T,V,\tilde{\pi}}$ the exponential stability of $e = 0$ with respect to (3.40) is guaranteed. Hence one can use [Khalil 2002, Thm. 4.10] to

derive a bound on the solutions of (3.40) which start inside $\tilde{\mathcal{L}}_{T,V,\tilde{\pi}}$. We obtain

$$\forall t \geq T,\ \forall e_T \in \tilde{\mathcal{L}}_{T,V,\tilde{\pi}} : \quad \|e\left(t,T,e_T\right)\| \leq \sqrt{\bar{p}+1} \cdot \|e_T\| \cdot e^{-\dfrac{\epsilon(t-T)}{2(\bar{p}+1)}},$$

where $\bar{p} = \sup_t \|P(t)\|$, and as before $\epsilon = \lambda_{min}\left(S^{-1}(T)\tilde{Q}S^{-1}(T)\right) > 0$. Using $\beta$ from (3.45c) and $\gamma$ from (3.45c) the last equation can be written as

$$\forall e_T \in \tilde{\mathcal{L}}_{T,V,\tilde{\pi}} : \quad \|e(t,T,e_T)\| \leq \sqrt{\beta} \cdot \|e_T\| \cdot e^{-\gamma(t-T)}. \tag{3.49}$$

We use this bound on $\|e\left(t,T,e(T)\right)\|$—which are the solutions to the nonlinear error dynamics (3.13) under the terminal control (3.24)—to estimate from above the decay of $F(t,e,K(t)e+u_r(t))$ along these solutions. This yields

$$\forall t \geq T : \quad F(t,e,K(t)e+u_r(t)) \leq \beta e^{-2\gamma(t-T)} \cdot \|e(T)\|^2 \cdot \left\|Q_F + K^T(t)R_F K(t)\right\|.$$

Note that for $t \geq T$ the feedback gain and the coordinate transformation (3.37) are constant $K(t) = K(T), S(t) = S(T)$. We rely on (3.37) and obtain for all $e_T \in \tilde{\mathcal{L}}_{T,V,\tilde{\pi}}$

$$\|e_T\|^2 \cdot \left\|Q_F + K^T(T)R_F K(T)\right\| \leq \tilde{\pi}^2(T)\left\|S^{-1}(T)\right\|^2 \cdot \left\|Q_F + K^T(T)R_F K(T)\right\|.$$

If we combine the last two equations to evaluate (3.16b) for $t \geq T$, it follows

$$\dot{E} + F(\cdot) \leq \beta e^{-2\gamma(t-T)}\left(-\alpha(T) + \tilde{\pi}^2(T)\left\|S^{-1}(T)\right\|^2 \cdot \left\|Q_F + K^T(T)R_F K(T)\right\|\right).$$

Due to (3.45b) we have that

$$\alpha(T) = \tilde{\pi}^2(T)\left\|S^{-1}(T)\right\|^2 \cdot \left\|Q_F + K^T(T)R_F K(T)\right\| + \hat{\alpha}, \quad \hat{\alpha} \geq 0.$$

Hence

$$\forall t \geq T : \quad \dot{E} + F(\cdot) \leq -\hat{\alpha}\beta e^{-2\gamma(t-T)} \leq 0,$$

and therefore the end penalty $E(t)$ from (3.45) fulfills (3.16b) for all $t \geq T$. □

A surprising consequence of Lemma 3.5 is that we can use $E(t) = 0$ in conjunction with the terminal region $\tilde{\mathcal{L}}_{t_k+T_p,V,\tilde{\pi}}$ to guarantee convergence of the proposed NMPC scheme. This can be explained as follows: The end penalty $E(t)$ from (3.45a) is purely time-dependent. However, a purely time-dependent end penalty is not effected by the inputs computed via the NMPC scheme (3.15). This implies that $E(t)$ can be dropped during the optimization.

**Remark 3.5** (Purely time dependent end penalties for set point stabilization).
*It is easy to see that purely time-dependent end penalties can also be used for set point stabilization problems. Whenever a terminal feedback $u_{\mathcal{E}} = k(x)$ ensures exponential set point convergence for solutions starting at $x_0 \in \mathcal{E}$, we have a bound*

$\|x(t)\| \le \alpha(x_0)e^{-\beta t}$. *If additionally* $\lim_{t\to\infty}\|x\| = 0$ *implies that* $u_{\mathcal{E}} \to 0$, *and technical integrability conditions hold, then we can estimate from above the cost-to-go inside the terminal region by a purely time-dependent function. In other words, if the terminal feedback ensures good convergence, then we can drop the terminal penalty.*

One might want to consider a terminal penalty, which also penalizes the tracking error at the end of each prediction. The next result shows that this is also possible.

**Lemma 3.6** (State dependent end penalties)**.**
*Consider Problem 3.2 under Assumptions 3.2–3.4. Suppose that a time-varying terminal region* $\mathcal{E}_{t_k+T_p} = \tilde{\mathcal{L}}_{t_k+T_p,V,\tilde{\pi}}$ *based on* $\tilde{\pi}(t) \in (0,\infty)$ *from* (3.44) *is used in the NMPC scheme* (3.15)*, then any end penalty of the form*

$$\tilde{E}(t,e) = \eta \cdot e^T(P(t)+I)e, \quad \eta \in [0,\infty), \tag{3.50}$$

*guarantees convergence of the tracking error*

$$\lim_{t\to\infty}\|e(t)\| = \lim_{t\to\infty}\|x(t) - x_r(t)\| = 0.$$

*Proof.* Our proof consists of two parts. Firstly, we show that a modified NMPC scheme based on the time-varying terminal region and a preliminary end penalty $E_1(t,e)$ fulfills the conditions of Corollary 3.2. This part follows along the lines of the proof of Lemma 3.5. The main idea is to use the free parameter $\hat{\alpha}$ in the definition of $E(t)$ in (3.45) to compensate $\eta e^T(P(t)+I)e$ not being a Lyapunov function for $t \in [0,T)$. Secondly, we show the equivalence in terms of generated inputs using either (3.50) or $E_1(t,e)$ in the NMPC scheme (3.15).
Consider the NMPC scheme (3.15) with $\mathcal{E}_{t_k+T_p} = \tilde{\mathcal{L}}_{t_k+T_p,V,\tilde{\pi}}$ and the preliminary choice of an end penalty

$$E_1(t,e) = E(t) + \eta e^T(P(t)+I)e, \tag{3.51}$$

where $E(t)$ is from (3.45) and $\eta \in [0,\infty)$. Due to $0 < \tilde{\pi}(t) < \infty$ for $t \in [0,\infty)$ the sets $\tilde{\mathcal{L}}_{t_k+T_p,V,\tilde{\pi}}$ are compact. Note that $\tilde{f}$ from (3.13) is locally Lipschitz. Hence we can assume w.l.o.g. that the free parameter $\hat{\alpha} \in [0,\infty)$ of $E(t)$ appearing in (3.45b) is such that

$$\forall t \in [0,T]: \quad \hat{\alpha} \ge \eta \cdot \max_{e \in \tilde{\mathcal{L}}_{t,V,\tilde{\pi}}} e^T\dot{P}(t)e + 2e^T(P(t)+I)\tilde{f}(t,e,K(t)e+u_r(t)). \tag{3.52}$$

**Case 1** $t \in [0,T)$**:** Considering this case as in the preceding proof yields

$$\forall t \in [0,T): \quad \dot{E}_1(t,e(t)) + F(\cdot) = -\hat{\alpha}\beta + \eta\left(e^T\dot{P}(t)e + 2e^T(P(t)+I)\tilde{f}(\cdot)\right).$$

Since $\hat{\alpha}$ satisfies (3.52) and $\beta \ge 1$ it follows

$$\forall t \in [0,T): \quad \dot{E}_1(t,e(t)) + F(\cdot) \le 0.$$

**Case 2 $t \geq T$:** The same steps as in the proof of Lemma 3.5 yield

$$\forall t \geq 0 : \quad \dot{E}_1(t, e(t)) + F(\cdot) \leq -\hat{\alpha}\beta e^{-2\gamma(t-T)} + \eta \left( e^T \dot{P}(t) e + 2e^T (P(t) + I) \tilde{f}(\cdot) \right).$$

Clearly, the first term on the right hand side of the inequality is negative. Due to the construction of $\tilde{\mathcal{L}}_{T,V,\tilde{\pi}}$ via (3.44) it holds that

$$\forall t \geq T, \ \forall e \in \tilde{\mathcal{L}}_{T,V,\tilde{\pi}}, \ \forall \eta \geq 0 : \quad \eta \left( e^T \dot{P}(t) e + 2e^T (P(t) + I) \tilde{f}(\cdot) \right) \leq 0.$$

Hence we have shown that an NMPC scheme with $\mathcal{E}_{t_k+T_p} = \tilde{\mathcal{L}}_{t_k+T_p,V,\tilde{\pi}}$, and the preliminary end penalty (3.51) guarantees reference convergence.

As last step consider two versions of the OCP (3.15) with two different objective functionals

$$J_1(t_k, x(t_k), e(\cdot), u(\cdot)) = \int_{t_k}^{t_k+T_p} F(\cdot) d\tau + \eta e(t)^T (P(t) + I) e(t)\Big|_{t_k+T_p} + E(t)\Big|_{t_k+T_p}$$
$$J_2(t_k, x(t_k), e(\cdot), u(\cdot)) = \int_{t_k}^{t_k+T_p} F(\cdot) d\tau + \eta e(t)^T (P(t) + I) e(t)\Big|_{t_k+T_p}$$

where $E(t)$ is from (3.45). The value of $E(t_k + T_p)$ is not effected by the choice of $u(\cdot)$, i.e., an input that minimizes $J_1(\cdot)$ is also a minimizing input for $J_2(\cdot)$. Hence one obtains the same sequence of input signals via optimization of $J_1$ or $J_2$. And thus the NMPC scheme (3.15) with terminal region $\mathcal{E}_{t_k+T_p} = \tilde{\mathcal{L}}_{t_k+T_p,V,\tilde{\pi}}$ and end penalty $\eta \cdot e^T (P(t) + I) e$ is stabilizing in the sense of Corollary 3.2. □

Let us briefly summarize what we have shown in the last two sections of this chapter: From Section 3.5.3 we learned how to compute candidate time-varying terminal regions as time-varying level sets of Lyapunov functions. From the Lemmas 3.5 and 3.6 we know how to choose suitable end penalties.

An important point to recognize is that the length of the prediction horizon $T_p$ in the OCP (3.15) is not directly related to the *finite* length of the reference trajectory $T < \infty$. The prediction horizon $T_p$ has to be chosen sufficiently long, such that for a given initial condition $x_0$ and a start time $t_0$ the terminal constraint (3.15e) is satisfied. Often one can work with $T_p \ll T$, which is desireable from the computations as well as from the robustness point of view.

### 3.5.5 Example: Trajectory Tracking of a Chemical Reactor

To illustrate the concept of time-varying terminal regions we consider a set point change of a continuously stirred tank reactor (CSTR) along an a priori given reference trajectory. In the reactor an exothermic, irreversible reaction $A \rightarrow B$ takes place. The dynamics of the CSTR are as follows

$$\dot{c}_A = \frac{q}{V}(c_{Af} - c_A) - k(c_A, T) \tag{3.53a}$$

$$\dot{T} = \frac{q}{V}(T_f - T) + \tfrac{-\triangle H}{\rho C_p} k(c_A, T) + \tfrac{UA}{V\rho C_p}(T_C - T) \tag{3.53b}$$

where

$$k(c_A, T) = k_0 e^{\frac{-E}{RT}} c_A.$$

Details on the model can be found in [Henson and Seborg 1997], the model parameters are listed in Table 3.1. The states $c_A$ and $T$ describe the educt concentration and the reactor temperature, respectively. The coolant stream temperature $T_C$ is the input variable. The objective is to design an NMPC controller which stabilizes the CSTR around a previously computed reference trajectory which drives the system in 18 minutes from the set point $c_{A1} = 0.6$mol/, $T_1 = 344.4$K to $c_{A2} = 0.45$mol/l, $T_2 = 352.8$K. The coolant stream temperature is subject to the input constraint 270K $\leq T_C \leq$ 350K, the state constraints are 0.1mol/l$\leq c_A \leq 0.9\text{mol/l}, 300\text{K} \leq T \leq 400$K. Reference trajectory and input are precomputed via system inversion and depicted in Figure 3.4.

The weight matrices for the cost function $F$ are

$$R_F = 10^{-3}, \quad Q_F = \begin{pmatrix} 60.7 & -6.5 \\ -6.5 & 2.5 \end{pmatrix}$$

where $Q_F$ satisfies (3.29). The boundary condition $P(T)$ and the time-varying $Q(t)$ for the RDE (3.21) are chosen according to Assumption 3.4 with $\tilde{Q} = Q_F$ and $R = R_F$. The terminal control law is computed according to Lemma 3.2 based on the solution $P(t)$ to the RDE. The diameter function $\pi(t)$ is obtained via (3.39) and $\tilde{\pi}(t)$ via (3.44), both on a time grid with $\delta t = 10^{-3}$min.

The results are illustrated in Figure 3.5 left part. The red curve shows $\pi(t)$ which defines the positively invariant time-varying level set $\mathcal{L}_{t,V,\pi}$ from (3.33). The blue curve depicts $\tilde{\pi}(t)$, which is obtained via successive shrinking of $\pi(t)$ point-wise in time until (3.44) is satisfied. The peaks at $t = 4$min and $t = 5$min in the blue curve are caused by changes in the set of active constraints. It should be noted that the

**Table 3.1:** Parameters for CSTR model (3.53).

| | | | | | |
|---|---|---|---|---|---|
| $q$ | 100 | [l/min] | $c_{Af}$ | 1 | [mol/l] |
| $T_f$ | 350 | [K] | $V$ | 100 | [l] |
| $\rho$ | 1000 | [ g/l] | $C_p$ | 0.239 | [J/g·K] |
| $-\triangle H$ | $5 \cdot 10^4$ | [ J/mol] | $\frac{E}{R}$ | 8750 | [K] |
| $k_0$ | $7.2 \cdot 10^{10}$ | [ min$^{-1}$] | $UA$ | $5 \cdot 10^4$ | [J/min K] |

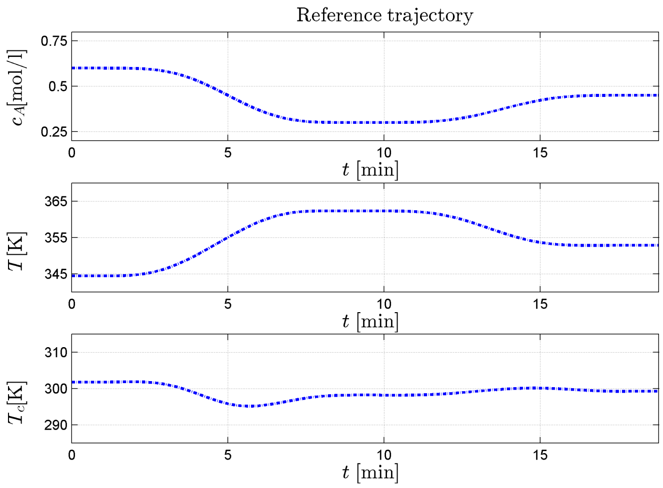


**Figure 3.4:** Reference trajectory and reference input.

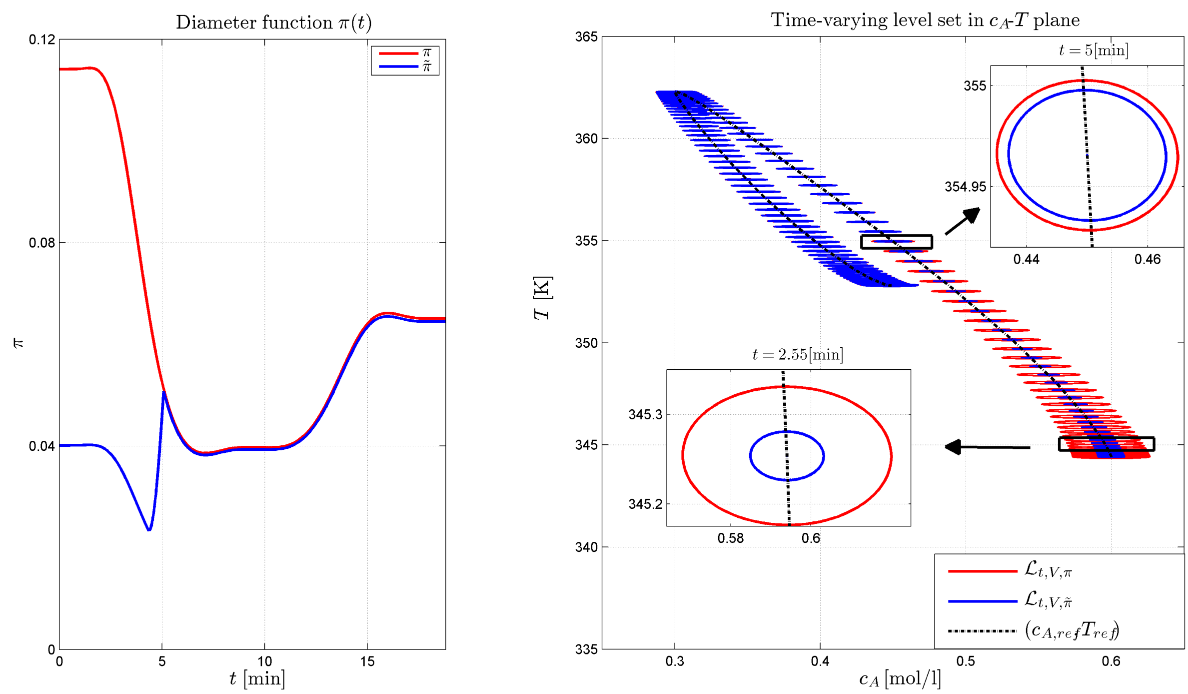


**Figure 3.5:** Diameter function $\pi(t)$ and visualization of time-varying level sets $\tilde{\mathcal{L}}_{t,V,\tilde{\pi}}$.

time-varying level sets are of varying size. This can be observed in Figure 3.5 left part. The diameter $\tilde{\pi}(t)$ is increasing along several parts of the reference trajectory. The varying size can also be seen in the visualization of the time-varying level set $\tilde{\mathcal{L}}_{t,V,\tilde{\pi}}$ in Figure 3.5, right part. The black curve depicts the reference trajectory in the $c_A - T$ plane. The red ellipsoids are a selection from the time-varying level set for the LTV error system. The blue ellipsoids are samples from the terminal region $\tilde{\mathcal{L}}_{t,V,\tilde{\pi}}$ obtained via (3.44). We plot only a few of the numerous ellipsoids computed on the time grid with $\delta t = 10^{-3}$min.

At this point one can ask, whether the efforts to work with time-varying terminal regions pay off. One could compute a constraint-consistent level set $\{e|V(t,e) \leq c^2\}$ with constant $c$ for (3.53). However, the following issues should be noted: A constant level $c$ is always upper bounded by $c \leq \min_{t\in[0,T]} \tilde{\pi}(t)$. Furthermore, we only enforce positive invariance of the terminal region $\tilde{\mathcal{L}}_{t,V,\tilde{\pi}}$ with respect to the nonlinear error dynamics (3.13) for $t \in [0,T)$. In other words, for $t \in [0,T)$ $V(t,e)$ is not necessarily a local Lyapunov function on $\tilde{\mathcal{L}}_{t,V,\tilde{\pi}}$. Moreover, positive invariance on $\tilde{\mathcal{L}}_{t,V,\tilde{\pi}}$ is a much weaker property than local Lyapunov stability. Hence a constant level $c$ is in many cases much smaller than $\tilde{\pi}(t)$. Taking these issues and Figure 3.5 into account we conclude that working with time-varying level sets increases the terminal region as well as the region of attraction of the NMPC schemes (3.15).

To assess the performance of the proposed NMPC scheme with time-varying terminal region we compare it to the local controller derived for the LTV error system along the reference trajectory. The structure of this controller (3.24) is

$$u_{2DoF}(t) = K(t)e + u_r(t), \quad K(t) = -\frac{1}{2}R^{-1}B^T(t)\left(P(t) + I\right).$$

Basically, it is a two-degrees-of-freedom (2-DoF) scheme, where the nominal input $u_r(t)$ is used as feedforward control. The solution $P(t) \in BC^+(\mathbb{R}^{n_x\times n_x})$ of the RDE (3.21) is used to obtain the feedback part. The input $u_{2DoF}(t)$ is clipped whenever the constraints are violated

$$u(t) = \begin{cases} u_{min} & u_{2DoF}(t) < u_{min} \\ u_{2DoF}(t) & u_{2DoF}(t) \in [u_{min}, u_{max}] \\ u_{max} & u_{2DoF}(t) > u_{max}. \end{cases}$$

In Figure 3.6 the behaviors of the closed loop under this 2-DoF controller and the proposed NMPC scheme are illustrated on the left and right side, respectively. In all pictures the blue-colored areas visualize the constraints on states and inputs. We plot the behavior of the closed loops for several initial conditions. Clearly, the convergence of the solutions to the reference using the 2-DoF controller depends on the initial conditions. For some initial conditions very slow transient behavior can be observed in the reactor temperature $T$ (middle left side) and the product concentration $c_A$ (upper left side). The corresponding input signals $u(t) = T_C(t)$—i.e., the cooling stream temperature—are depicted on the lower left side. Also note that for one of the solutions starting at $t = 0$min the state constraints on $c_A$ and $T$ are violated.

Figure 3.6 right shows the closed-loop behavior of the proposed NMPC scheme. The same initial conditions as for the 2-DoF controller are used. The prediction horizon is

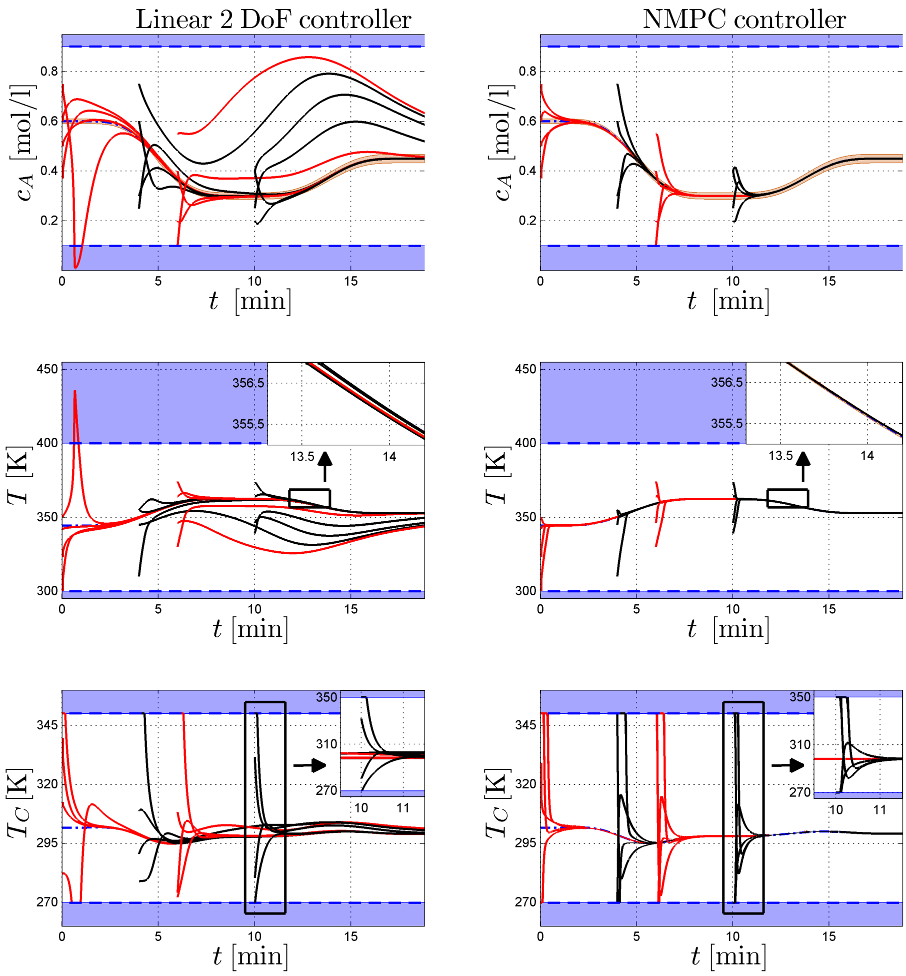


**Figure 3.6:** Simluation results for 2-DoF controller and NMPC scheme.

set to $T_p = 1.0$min and much shorter than the length of the reference trajectory 18min. The time dependent terminal penalty $E(t)$ is skipped during the optimization. The resampling time is $\delta = 0.01$min. The solutions have been computed with the ACADO Toolkit [Houska et al. 2011]. All solutions converge rapidly to the reference.

In the lower part of the Figure 3.6 the input signals for the 2-DoF and the NMPC controller are depicted. One can see that the NMPC controller is slightly more aggressive. The orange tubes around the reference trajectories in the upper and middle plots on both sides are an outer-bounding projection of the time-varying terminal region to the time domain. Obviously, the time-varying terminal constraint allows only small temperature and larger concentration deviations. Comparing the zoomed plots in the middle part, we see that even close to the reference trajectory the 2-DoF controller results in much slower convergence than the NMPC scheme.

## 3.6 Summary

In this chapter we discussed predictive control approaches to trajectory-tracking problems. We derived convergence conditions based on time-varying terminal regions for general constrained output trajectory-tracking problems. These conditions are a reformulation of the usual ones for set point stabilization of time-varying systems. The new feature is the use of time-varying terminal regions in the context of NMPC for trajectory tracking. We focussed on the special case of asymptotically constant references to show how time-varying terminal regions can be obtained as time-varying level sets of Lyapunov functions. In essence, these time-varying level sets are an approximation of the domain of attraction of a two-degrees-of-freedom control scheme along a reference trajectory. For systems with a quadratic Lyapunov function these sets are efficiently computable via an optimal control problem, which can be easily approximated by a linear program. Besides this, the application of the proposed NMPC scheme requires solving a Riccati differential equation offline and storing the solution in order to define the terminal regions online. The sequence of global optimization problems to be solved offline in case of time-varying level sets for nonlinear systems limits our scheme to small scale nonlinear systems. For linear systems these problems are avoided. As we have seen from the CSTR example allowing time-varying right hand sides in the inequality $V(t, e) \leq \pi(t)^2$ can increase the size of the terminal region significantly.

The main challenge of NMPC for trajectory-tracking problems—even if autonomous systems are considered—is the inherent time-varying nature. As we see in the next chapters, this is not the case if path following of autonomous systems is considered.

# Part III

# Predictive Path Following

# 4 Path Following and Path Followability

In this chapter we shift the focus to path-following problems. Subsequently, the reference to be followed is not a time-varying trajectory but rather a geometric curve without any preassigned timing information. We begin with a statement of the path-following problem in Section 4.1. A brief overview of existing control approaches is given in Section 4.2. In Section 4.3 we investigate the question of under which conditions a given path in the output space of a nonlinear system is exactly followable. In order to also consider state and input constraints we focus on differentially flat systems in Section 4.4. The results presented in this section have appeared in [Faulwasser et al. 2011]. Finally, this chapter ends with a summary in Section 4.5.

## 4.1 The Constrained Output Path-following Problem

We consider nonlinear systems

$$\dot{x}(t) = f(x(t), u(t)), \quad x(t_0) = x_0, \tag{4.1a}$$

$$y(t) = h(x(t)), \tag{4.1b}$$

where $x \in \mathcal{X} \subseteq \mathbb{R}^{n_x}$, $u \in \mathcal{U} \subset \mathbb{R}^{n_u}$ are state and input constraints. The map $h : \mathbb{R}^{n_x} \to \mathbb{R}^{n_y}$ (4.1b) defines the output $y \in \mathbb{R}^{n_y}$. We assume that the maps $f, h$ are sufficiently often continuously differentiable and that the system as well as the constraints fulfill our standard assumptions from Chapter 2.

In contrast to set point stabilization and trajectory tracking we aim at driving the system along a geometric reference. This reference is denoted as path $\mathcal{P}$ and given as a parametrized regular curve in the output space

$$\mathcal{P} = \{y \in \mathbb{R}^{n_y} \mid \theta \in [\theta_0, \theta_1] \mapsto p(\theta)\}. \tag{4.2}$$

The scalar variable $\theta$ is called the path parameter. Note that the regularity of a geometric curve implies the local bijectivity of the parametrization $p(\theta)$, cf. [Topogonov 2006]. The domain $[\theta_0, \theta_1]$ of the path parameter is a closed but might be unbounded, i.e., $\theta_1 = \infty$ is possible. The map $p$ is sufficiently often continuously differentiable. In general, the path parameter $\theta$ is time dependent but its time evolution $t \mapsto \theta(t)$ is not known a priori. Subsequently, we investigate the problem of steering the output (4.1b) to the path $\mathcal{P}$ and following it along in direction of increasing values. In other words, we consider the following problem.

**Problem 4.1** (Constrained output path following)**.**
*Given the system* (4.1) *and the reference path* $\mathcal{P}$ (4.2) *design a controller that achieves:*

*i)* ***Path Convergence****: The system output* $y = h(x)$ *converges to the set* $\mathcal{P}$ *s.t.:*

$$\lim_{t\to\infty} \|h(x(t)) - p(\theta(t))\| = 0.$$

*ii)* ***Strict Forward Motion****: The system moves along* $\mathcal{P}$ *in the direction of increasing values of* $\theta$ *s.t.* $\dot{\theta}(t) > 0$ *holds for almost all* $\theta \in [\theta_0, \theta_1)$*.*

*iii)* ***Constraint Satisfaction****: The constraints on states* $x \in \mathcal{X}$ *and inputs* $u \in \mathcal{U}$ *are satisfied for all times.*

Whenever no confusion can arise we may simply speak of constrained path-following problems and drop the reference to the output. If no constraints are present—cf. part iii) of the problem statement—we say it is an unconstrained path-following problem. Part ii) requires that the system should not stop along the path unless $\theta = \theta_1$.

Referring to the path-following problem two issues arise immediately:

- Given a system (4.1), possibly subject to input and state constraints, and a path $\mathcal{P}$. Under which conditions is the path $\mathcal{P}$ exactly followable such that for all $t \geq t_0$ it holds $\|h(x(t)) - p(\theta(t))\| = 0$?
- How can a controller fulfilling the requirements of the problem statement be designed?

The former question requires a system theoretic analysis. It is considered in this chapter. The latter question refers to the controller design. The conceptual idea of controller design for path-following problems is to obtain the system inputs $u : t \mapsto u(t)$ as well as the reference timing $t \mapsto \theta(t)$ in the controller. The path parameter is regarded as a virtual state, whose evolution is determined through a *timing law*

$$g\left(\theta^{(k)}, \theta^{(k-1)}, \ldots, \dot{\theta}, \theta, v\right) = 0, \quad \forall i \in \{1, \ldots, k\} : \theta^{(i)}(t_0) = \theta_0^{(i)},\ \theta(t_0) = \theta_0. \tag{4.3}$$

The timing law $g$ is an additional degree of freedom during the controller design. It is important to note that the time evolution of $\theta$ can be influenced by the virtual input $v \in \mathcal{V} \subset \mathbb{R}$. At this point it remains open how to choose the timing law $g$. Usually, one restricts the choices for the timing law $g$ such that it can be written as an explicit ODE, which is controllable through $v$. Furthermore, it is convenient to require that equivalent properties as assumed for $f$ from (4.1a) hold. We will discuss the choice of suitable timing laws in detail in Section 4.3.1. The design of predictive controllers solving Problem 4.1 is postponed to Chapter 5.

## 4.2 Existing Approaches to Path-following Problems

Before we start the further investigations, existing approaches to the path-following problem are briefly reviewed. Besides the different scopes—controller synthesis and problem analysis—the available results differ in terms of methods used. Figure 4.1 depicts a schematic overview of results on path following. As shown, mainly two different approaches focus on the analysis of the problem while many more methods are used to solve the controller synthesis problem.

### 4.2.1 Problem Analysis and Path Followability

Referring to the problem analysis two main questions have been examined: performance comparisons to trajectory-tracking problems and geometric approaches.

#### $\mathcal{L}^2$ Performance Limits

Several works focus on fundamental performance limits of trajectory-tracking and path-following problems in terms of $\mathcal{L}^2$ error norms. It is well-known that the non-minimum phase nature of a system implies fundamental performance limits not only to cheap control problems [Kwakernaak and Sivan 1972b; Seron et al. 1999] but also to general tracking or servomechanism problems [Qui and Davison 1993; Su et al. 2003]. However, the situation is different for path-following problems. It can be shown that for linear non-minimum phase systems and certain classes of paths such fundamental limits of path-following performance are not present [Aguiar et al. 2004, 2005; Dacic and Kokotovic 2006; Miller and Middleton 2008]. Even in the case of nonlinear non-minimum phase systems in strict-feedback form no fundamental performance limits exist for path-following problems, see [Aguiar et al. 2008]. Also note that the problems of constrained and unconstrained exact path followability, which we discuss in Sections 4.3–4.4, refer to cases where the $\mathcal{L}^2$ norm of the path-following error can be kept identically zero along the path.

#### Geometric Analysis of Path Following

Another branch of the analysis refers to the geometric properties of the problem. The conceptual idea of the works [Banaszuk and Hauser 1994, 1995; Nielsen and Maggiore 2004, 2006, 2008] is to consider path following as a problem, where the output path implicitly defines a manifold in the state space. This *zero-path-error manifold* or shortly *path manifold* has to be stabilized and rendered positively invariant via an appropriate feedback. In order to achieve such a stabilization with feedback linearization techniques, the first step is to map the nonlinear output path-following problem into new coordinates via a diffeomorphism. In these coordinates the dynamics are splitted into a part transverse to the zero-path-error manifold and the dynamics on that manifold. The second step is to decouple the transverse part of the dynamics from the part on the zero-path-error manifold by means of feedback linearization. The works of [Banaszuk and Hauser 1995; Nielsen and Maggiore 2006, 2008] derive necessary and

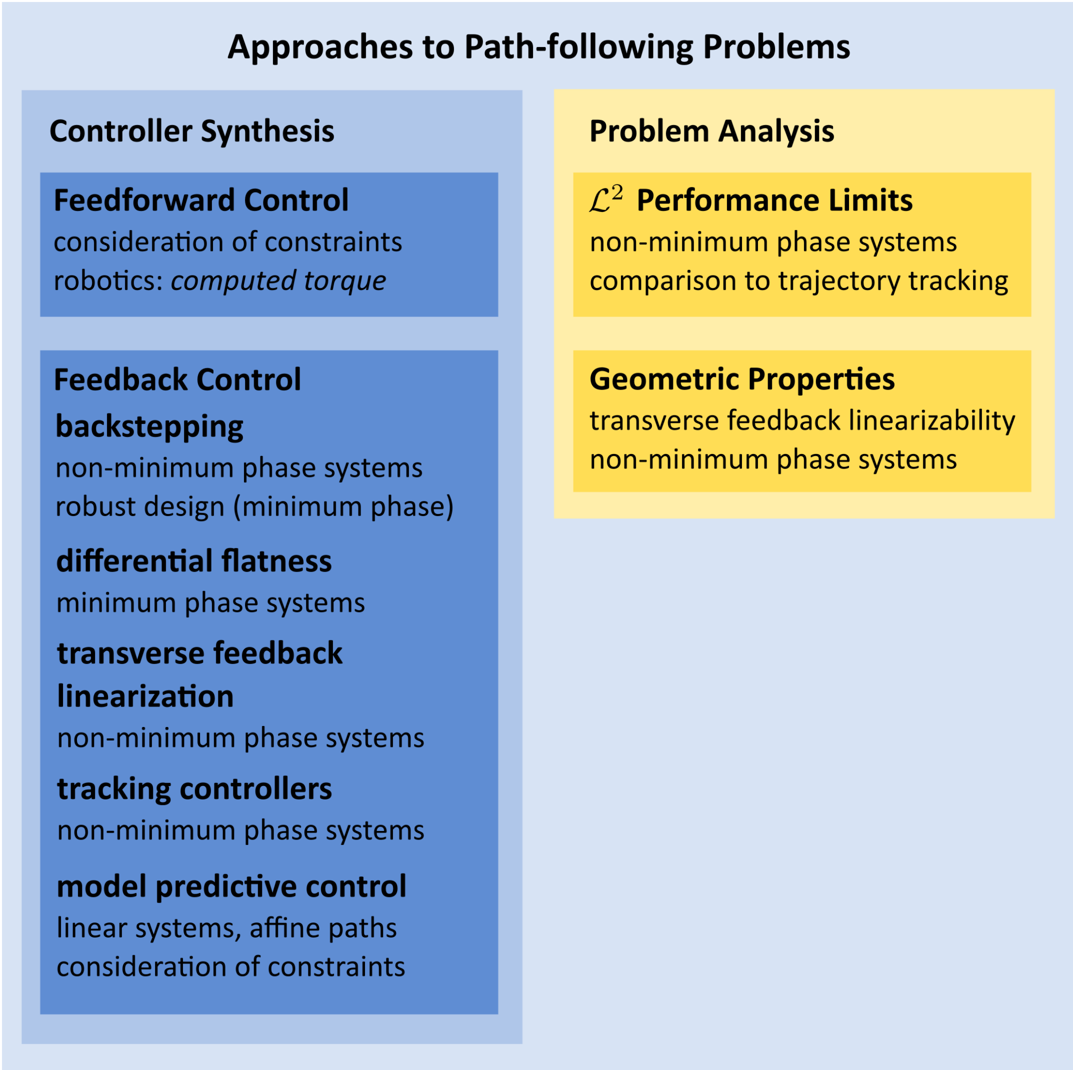


**Figure 4.1:** Schematic overview of existing results for path following.

sufficient conditions for the existence of a nonlinear coordinate transformation and a transversely linearizing feedback. The early works [Banaszuk and Hauser 1994, 1995] coined the term *transverse feedback linearization* for these approaches. They consider periodic state space paths of single-input systems. The extension to non-periodic paths can be found in [Nielsen and Maggiore 2006]. The case of nonlinear MIMO systems is presented in [Nielsen and Maggiore 2008].

In Section 4.3 we present conditions closely related to the ones provided in [Nielsen and Maggiore 2008]. While these results use a description of the zero-path-error manifold, we rely later on a known path parametrization $p(\theta)$ from (4.2) and on an augmented system. Note that the works mentioned so far do not consider constraints on states nor inputs. In Section 4.4 we tackle the problem of constrained path-followability with a combined geometric and optimization-based ansatz for the special case of differentially flat systems.

### 4.2.2 Controller Synthesis

Referring to Figure 4.1 several methods are used for the design of path-following controllers one can distinguish two main directions: feedforward and feedback control.

#### Feedforward Control Approaches

In robotic applications often a robotic manipulator has to be steered precisely and fast along a given geometric reference curve. An early optimization-based approach to the problem of computing suitable feedforward controls in the presence of input constraints is proposed in [Shin and McKay 1985]. From the systems theory point of view this approach mainly uses the fact that the considered robots are fully acutated and hence the dynamic models are invertible. More precisely, they are differentially flat, see i.a. [Fliess et al. 1995a; Lévine 2009; Sira-Ramírez and Agrawal 2004] and Section 4.4. Follow-up works improve the numerical efficiency and incorporate effects as viscous friction [Slotine and Yang 1989]. In [Boe and Hannaford 1998] it is suggested to iteratively perform a time-rescaling of the reference trajectories in order to reduce the path-following error.

Recently, a convex reformulation of the involved optimization problems was proposed, see [Verscheure 2009; Verscheure et al. 2009]. However, all these approaches rely on the differentially flatness of the system model and exploit special structures arising in flat mechanical systems. Thus their applicability is limited. Input constraints (precisely torque constraints) are frequently considered. A closely related approach—relying on a differentially flat system and a path specified in a flat output space—is presented in [Raczy and Jacob 1999] for the problem of designing time-optimal feedforward controls for an overhead crane. There constraints on states and inputs are considered.

#### Feedback Control Approaches

Compared to the existing results mentioned so far the area of feedback control approaches is rather rich in terms of methods used, cf. Figure 4.1.

**Backstepping/Lyapunov Approaches:** Frequently, path-folllowing problems are solved by classic backstepping techniques, cf. [Krstic et al. 1995] for details on backsteppping. The main idea as presented in [Aguiar et al. 2004] is to use the path evolution $\theta(t)$ or more precisely a virtual input $v$ influencing $\theta(t)$ through the so-called *timing law* $g(\theta^{(k)}, \dots, \theta, v) = 0$ to stabilize the unstable zero dynamics of non-minimum phase systems via recursive backstepping. This approach is further elaborated in [Encarnaçao and Pascoal 2001; Skjetne and Fossen 2001], where a similar approach is taken towards path following for ships. In [Dacic and Kokotovic 2006] the path-following problem is solved for linear systems via a time discretization. Note that [Aguiar et al. 2004; Dacic and Kokotovic 2006] work with non-minimum phase systems while [Encarnaçao and Pascoal 2001; Skjetne and Fossen 2001] consider minimum phase systems. Specific path following tasks with an additional requirement that the time-derivative of the path parameter converges to a prespecified reference $\dot{\theta}(t)$ are frequently discussed in context of vehicle-like systems. These tasks are also called *maneuver regulation problems*, see [Skjetne 2005]. An optimization-based approach for the case of maneuvering problems defined directly in the state space is presented in [Skjetne et al. 2002]. The constructive design of Lyapunov functions is also employed in [Astolfi et al. 2004] in order to tackle path following of the frequently discussed car with n-trailers. A special feature of this last work is the fact that input saturation is explicitly considered.

Backstepping is a control design technique which also allows to consider parameter uncertainties. Thus it is not surprising that [Do and Pan 2006; Do et al. 2004; Skjetne et al. 2004, 2005] rely on backstepping in order to derive results on adaptive control of path-following problems. While [Skjetne et al. 2004] focus on robust output feedback for a class of minimum phase nonlinear systems, [Do and Pan 2006; Do et al. 2004; Skjetne et al. 2005] design adaptive controllers for specific ship models.

A similar approach to path following for the uni-cycle under parametric uncertainties is suggested in [Lapierre et al. 2006]. As a variant the combination of backstepping and logic-based switching is proposed in [Aguiar and Hespanha 2004, 2007]. Hybrid control approaches to path-following problems are considered in [Balluchi et al. 2005; Dacic et al. 2007; Hamel et al. 2001; Soueres et al. 2001]. Results on passivity-based path following are given in [El-Hawwary and Maggiore 2008; Ihle et al. 2007]. Synchronized or formation-based path following is discussed in [Ghabcheloo et al. 2005; Ihle et al. 2007].

**Transverse Feedback Linearizaton:** Another route to path-following problems is to map the associated dynamics of the system and the path parameter via a diffeomorphism—and a suitably chosen state feedback—into new coordinates of a *transverse normal form*. As mentioned before, these new coordinates consist of an integrator chain of finite length for each output and the partially decoupled, possibly unstable, zero dynamics with respect to the zero-path-error manifold. Such control approaches are presented in [Banaszuk and Hauser 1994, 1995; Nielsen and Maggiore 2004, 2006, 2008]. One should note that the crucial step is the derivation of the diffeomorphism and the input-output linearizing state feedback. If this is achieved, the task of ensuring path convergence and boundedness of the zero dynamics is signifcantly simplified. In essence these approaches solve the path-following problem by breaking it down into two subproblems. In suitable coordinates, the dynamics transversal to zero-path-error manifold are decoupled from the dynamics in the manifold by input-output feedback linearization. Based on this decoupling two controllers are designed, one to stabilize the transversal dynamics, and another one to stabilize the internal dynamics. In [Hladio et al. 2011] this is tailored to mechanical systems. The application to a magnetic levitation system is considered in [Nielsen et al. 2010].

An alternative but related approach via input-output feedback linearization for a general car with n-trailers and off-axle hitching is considered in [Altafini 2002]. The last results pay attention to the question of existence of the transformation and the state feedback, which yield the transversely feedback linearized system. Variants of these approaches suppose that a transverse normal form is given and focus on the controller design, for example, in [Al-Hiddabi and McClamroch 2002] constant LQR feedback gains are used. In [Dacic et al. 2011] an input-to-state stability assumption is employed.

**Differential Flatness:** If the mapping to the transverse coordinates can be achieved such that the mapped system does not have any internal dynamics, the problem is simplified. For example, this is the case for statically feedback linearizable systems and also for differentially flat systems, cf. to [Fliess et al. 1995b; Lévine 2009; Rothfuß 1997; Sira-Ramírez and Agrawal 2004] and the references therein for details on flatness. Flatness is exploited in the early work [Hauser and Hindman 1997]. How to obtain a controller for maneuver regulation of a flat system from an available trajectory-tracking controller is discussed in [Hauser and Hindman 1996]. A related inversion based approach for a kinematic model of an object moving in 3 dimensions in the presence of disturbances on states and outputs is presented in [Consolini and Tosques 2005]. A different route which directly relies on the flatness of the system to be controlled is taken by [Samson 1995]. There a controller for path following of a car with n-trailers and on-axle hitching is derived. Online time scaling of reference trajectories for differentially flat models of robots, which can be regarded as a path-following approach, is presented in [Dahl and Nielsen 1990]. Therein the authors propose a closed-loop scheme to scale the reference trajectories in time.

**Tracking Controllers:** Often path-following problems are solved as tracking problems or via the application of tracking controllers. These approaches are based on a simple reasoning: if one tracks the trajectory resulting from an a priori choice of the path parameter evolution one follows the underlying geometric path. In [Frezza 1999; Notarstefano et al. 2005] receding horizon control approaches are presented, which are based on the combination of a backstepping tracking controller with suitable reference trajectories. The references are computed in a receding horizon fashion in order to approximate the path reasonably well. A similar idea is used in [Frezza et al. 2004; Saccon et al. 2012] to explore the set of feasible trajectories approximating a given path well for a motorcycle. In [Wahl and Gilles 2003] a similar idea is used to design controllers for ships following rivers or canals. Also predictive controllers have been proposed to solve the resulting trajectory-tracking problem, however, the stability issues are not investigated [Kanjanawanishkul and Zell 2009]. Application-related approaches are considered in [Kehl et al. 2005], where a path-following problem for a single-track model of a car is solved via trajectory tracking, and in [Nakamura et al. 2001], where trailers with extra steering are considered.

**Model Predictive Control:** It is also to possible to design predictive path-following controllers. In Chapter 5 we present NMPC schemes for path-following problems in the presence of constraints. These results have partially appeared in [Faulwasser and Findeisen 2009a,b, 2010; Faulwasser et al. 2009a].
Besides the results of Chapter 5, MPC is also used to solve path-following problems in a few other works. In [Ghaemi et al. 2010; Li et al. 2009] the path-following problem for a simplified nonlinear model of a ship is considered. Although constraints on inputs and states are considered these results are of limited applicability to general path-following problems. Due to the problem setup only paths consisting of straight lines are considered, and the proposed MPC algorithm is based on linearization and time discretization of the error dynamics. Furthermore, the stability of the proposed control approach is not investigated. An extension with a local linear approximation of the optimization problem and explicit stability conditions for the linearized MPC scheme are provided in [Lam et al. 2010], whereby the higher order nonlinear terms are neglected, and the nominal stability of the MPC scheme is enforced by contraction constraints. The pitfall is that recursive feasibility of the optimal control problems to be solved is lost, cf. [de Oliveira Kothare and Morari 2000]. An application of the ideas from [Lam et al. 2010] to a contouring task in a 2-dimensional output space is presented in [Lam et al. 2011]. The advantages of our NMPC schemes presented in Chapter 5 are: We avoid linearization and derive rigorous stability conditions, which ensure recursive feasibility. Moreover, we consider constraints on states and inputs.

Two general conclusions can be drawn from this overview. A variety of control methods are applied to path-following problems. However, only a few results explicitly consider constraints on states or inputs.

## 4.3 Path Followability

Referring to Problem 4.1 one can ask for sufficient conditions ensuring that a given path $\mathcal{P}$ is exactly followable by a system (4.1). To this end we define path followability as follows.

**Definition 4.1** (Exact path followability).
*A path $\mathcal{P}$ is called exactly followable by the system* (4.1)*, if there exists at least one continuous solution trajectory $x(t, t_0, x_0|u(\cdot))$ driven by an input $u : t \mapsto u(t)$, such that for all $t \geq t_0$ the error variable*

$$e(t) = h(x(t, t_0, x_0|u(\cdot))) - p(\theta(t)) \tag{4.4}$$

*is zero, while the path parameter $\theta(t)$ evolves continuously with time, and $\dot{\theta} > 0$ holds almost everywhere in $[\theta_0, \theta_1)$.*

The question arises of how to verifiy if a path $\mathcal{P}$ is exactly followable by a system. To this end assume temporarily that $e(t) \in \mathcal{C}^1$. Differentiating the error variable (4.4) with respect to time we obtain

$$\dot{e}(t) = \frac{\partial h}{\partial x} \cdot f(x,u) - \frac{\partial p}{\partial \theta} \cdot \dot{\theta}. \tag{4.5}$$

Clearly, if we want to ensure that a path is exactly followable by a system, we have to investigate whether it is possible to keep the error dynamics (4.5) at zero while $\dot{\theta} \geq 0$ holds. This naive approach reveals two interesting aspects of path-following problems: Firstly, if the system to be controlled (4.1) is time-invariant, then also the error dynamics (4.5) are time-invariant. Secondly, since $\dot{\theta}$ appears on the right side of (4.5) the degree of freedom to choose $\theta(t)$ can be understood as the possibility to scale the length but not the direction of $\dot{p}(\theta(t))$. We illustrate these considerations by an example.

**Example 4.1** (Ship course control).
*We consider a simple model of a ship [Wahl and Gilles 2003]*

$$\begin{pmatrix} \dot{x}_1 \\ \dot{x}_2 \\ \dot{x}_3 \\ \dot{x}_4 \end{pmatrix} = \begin{pmatrix} w\cos x_3 - Lwx_4 \sin x_3 \\ w \sin x_3 + Lwx_4 \cos x_3 \\ x_4 \\ \frac{1}{\tau}(-x_4 + Ku) \end{pmatrix}. \tag{4.6}$$

*Here, $x_1, x_2$ is the position in the plane, $x_3$ is the yaw angle of the ship, and $x_4$ is the velocity of the yaw angle. The model parameter $w > 0$ refers to the forward velocity of the ship. The input $u$ is the rudder angle. The considered output is the position in the $x_1 - x_2$ plane*

$$y = \begin{pmatrix} x_1, & x_2 \end{pmatrix}^T.$$

*The path to be followed is a regular curve $\mathcal{P}$*

$$\mathcal{P} := \left\{ y \in \mathbb{R}^2 \mid \theta \in \mathbb{R} \mapsto (p_1(\theta), p_2(\theta))^T \right\}.$$

*Definition 4.1 implies that a path is exactly followable, if the time derivatives of output and reference are the same. Hence we have to check whether there exist inputs such that*

$$\dot{y}_i = \frac{\partial p_i}{\partial \theta}\dot{\theta}, \qquad i = 1, 2$$

*holds. Evaluating these conditions we obtain*

$$\begin{pmatrix} \dot{\theta}\frac{\partial p_1}{\partial \theta} \\ \dot{\theta}\frac{\partial p_2}{\partial \theta} \end{pmatrix} = \begin{pmatrix} w\cos x_3 - Lwx_4 \sin x_3 \\ w \sin x_3 + Lwx_4 \cos x_3 \end{pmatrix}.$$

*From the dynamics* (4.6) *it follows that $x_4 = \dot{x}_3$. Thus the last equations can be written* *as a system of two implicit nonlinear ODEs*

$$\begin{pmatrix} \dot\theta \frac{\partial p_1}{\partial\theta} \\ \dot\theta \frac{\partial p_2}{\partial\theta} \end{pmatrix} = \begin{pmatrix} w\cos x_3 - Lw\dot x_3 \sin x_3 \\ w\sin x_3 + Lw\dot x_3 \cos x_3 \end{pmatrix}.$$

*These equations are affine in* $\dot\theta$ *and* $\dot x_3$*, and thus they can be solved for these variables*

$$\dot\theta = \frac{w}{\cos x_3 \cdot \frac{\partial p_1}{\partial\theta} + \sin x_3 \cdot \frac{\partial p_2}{\partial\theta}} \tag{4.7a}$$

$$\dot x_3 = \frac{\cos x_3 \cdot \frac{\partial p_2}{\partial\theta} - \sin x_3 \cdot \frac{\partial p_1}{\partial\theta}}{L\left(\cos x_3 \cdot \frac{\partial p_1}{\partial\theta} + \sin x_3 \cdot \frac{\partial p_2}{\partial\theta}\right)}. \tag{4.7b}$$

*If these ODEs have a solution such that*

$$\forall t \geq t_0: \quad \cos x_3 \cdot \frac{\partial p_1}{\partial\theta} + \sin x_3 \cdot \frac{\partial p_2}{\partial\theta} > 0, \tag{4.8}$$

*and additionally* $w > 0$*, then* $\dot\theta > 0$ *holds for all* $t \geq t_0$*. Based on a solution* $x_3(t)$ *to* (4.7) *it is straightforward to obtain a suitable* $u(t)$ *via inversion of the linear part* $\dot x_3, \dot x_4$ *of the dynamics* (4.6)*. Hence the path is exactly followable by* (4.6)*. Additionally, for this particular example, we have that the existence of a unique solution to* (4.7) *implies that the veloctiy to follow the path exactly is not free. The speed is determined by the path geometry and the parameter* $w > 0$ *which is the forward speed of the ship.*

### 4.3.1 Geometric Approach to Unconstrained Path Followability

In the last example we used very specific properties of the model (4.6) to derive (4.8) from the first time derivative of the error (4.4). One can ask how to generalize this approach in order to state sufficient conditions for path followability. One possibility to derive such conditions is to not only consider the first time derivative of the error (4.4) but also higher derivatives obtaining a set of suitable equations. As we show subsequently, this leads to a setting which relates path followability to the question of existence of a specific nonlinear Byrnes-Isidori normal form. To proceed we make the following assumption which is valid for the remainder of this section.

**Assumption 4.1** (Square input-output structure)**.**
*System* (4.1) *has a square input-output structure, i.e.,* $n_y = n_u$*. The vector fields* $f, h$ *are smooth* ($f, h \in \mathcal{C}^\infty$)*.*

Further, we use the notion of a vector relative degree of a system.

**Definition 4.2** (Vector relative degree)**.**
*The nonlinear MIMO system* (4.1) *is said to have vector relative degree* $r = (r_1, r_2, \ldots, r_{n_y})$ *at a point* $x = x_0 \in \mathbb{R}^{n_x}$ *if the following two conditions hold:*

*i)*
$$\forall j,k \in \{1,\dots,n_y\},\ i = 1,\dots,r_{k-1}: \quad \frac{\partial}{\partial u_j} \mathrm{L}_f^i\, h_k(x) = 0 \tag{4.9a}$$
$$\textit{For at least one } j \in \{1,\dots,n_y\} \quad : \quad \frac{\partial}{\partial u_j} \mathrm{L}_f^{r_k}\, h_k(x) \neq 0 \tag{4.9b}$$

*for all admissible $u$ and all $x$ in a neighborhood $\mathcal{N}_{x_0}$ of $x_0$.*

*ii) The $n_y \times n_y$ decoupling matrix*

$$\mathbf{A}(x) := \begin{pmatrix} \frac{\partial}{\partial u_1} \mathrm{L}_f^{r_1}\, h_1(x) & \dots & \frac{\partial}{\partial u_{n_y}} \mathrm{L}_f^{r_1}\, h_1(x) \\ \vdots & & \vdots \\ \frac{\partial}{\partial u_1} \mathrm{L}_f^{r_{n_y}}\, h_{n_y}(x) & \dots & \frac{\partial}{\partial u_{n_y}} \mathrm{L}_f^{r_{n_y}}\, h_{n_y}(x) \end{pmatrix} \tag{4.9c}$$

*is non-singular at $x = x_0$.*

In this definition $\mathrm{L}_f$ denotes the Lie derivative along the vector field $f$. Note that the above definition is a slight modification of the standard definition provided in [Isidori 1995]. As in [Nijmeijer and van der Schaft 1990, Chap. 13] we consider $\dot{x} = f(x,u)$ (4.1) instead of an input affine MIMO system $\dot{x} = f(x) + g(x)u$.
If a system has a well-defined vector relative degree at $x_0$, this implies its static input-output feedback linearizability for all $x$ neighborhood of $x_0$, cf. [Isidori 1995; Nijmeijer and van der Schaft 1990]. Based on this definition we make the following assumptions which ensure that we can map the path-following problem into suitable coordinates.

**Assumption 4.2** (Well-defined vector relative degree)**.**
*At a point $x_0 \in \mathbb{R}^{n_x}$ system* (4.1) *has a well-defined vector relative degree*

$$r = (r_1,\dots,r_{n_y}), \quad \hat{r} = \max\{r_1,\dots,r_{n_y}\}, \quad \rho = \sum_{i=1}^{n_y} r_i \leq n_x. \tag{4.10}$$

As mentioned at the beginning of this chapter a common ansatz to solve path-following problems is to describe the time evolution of the path parameter $\theta$ via an additional ODE. This additional ODE is called *timing law*. It is controlled via a virtual path parameter input $v$, cf. (4.3). To simplify the later developments we assume that the timing law is a sufficiently long integrator chain.

**Assumption 4.3** (Timing law and path parametrization)**.**

*i) The timing law $g$ from* (4.3) *is chosen as*

$$\theta^{(\hat{r}+1)} = v, \quad \theta(t_0) = \theta_0,\ \forall j \in 1,\dots,\hat{r} : \theta^{(j)}(t_0) = 0, \tag{4.11}$$

*with $\hat{r}$ from* (4.10)*.*

*ii) The path parametrization $p(\theta)$ from* (4.2) *is $\hat{r}$-times continuously differentiable with $\hat{r}$ from* (4.10)*.*

This assumption has technical reasons. If the timing law is chosen as an integrator chain of length $\hat{r}+1$, the influence of $v$ to the solution $\theta(t,\theta_0|v)$ can be described by a state space model that simplifies the notation. In other words, it is written as

$$\dot{z} = l(z,v) = Az + Bv, \quad z(t_0) = (\theta_0, 0, \ldots, 0) \in \mathbb{R}^{\hat{r}+1} \tag{4.12a}$$

$$\theta = Cz \quad = z_1 \tag{4.12b}$$

where $C = (1, 0, \ldots, 0) \in \mathbb{R}^{1\times n_x}$, and

$$A := \left(\begin{array}{c|c} \mathbf{0}^{\hat{r}\times 1} & \mathbf{I}^{\hat{r}\times\hat{r}} \\ \hline 0 & \mathbf{0}^{1\times\hat{r}} \end{array}\right) \in \mathbb{R}^{(\hat{r}+1)\times(\hat{r}+1)}, \quad B := \Big(0, \ldots, 0, 1\Big)^T \in \mathbb{R}^{\hat{r}+1}. \tag{4.12c}$$

The idea is that $\theta(t)$ and the first $\hat{r}$ time derivatives of $\theta(t)$ are the states $z = (\theta, \dot{\theta}, \ldots, \theta^{(\hat{r})})^T$. We are only interested in solutions of (4.12) with $z_1(t) \in [\theta_1, \theta_2]$ and $z_2(t) = \dot{\theta} \geq 0$. Therefore we define

$$\mathcal{Z} := \Big\{[\theta_0, \theta_1] \times [0, \infty) \times \mathbb{R}^{\hat{r}-1}\Big\} \subset \mathbb{R}^{\hat{r}+1}, \tag{4.13}$$

which is the set of all states $z$ of (4.12) consistent with the forward motion requirement $\dot{\theta} \geq 0$ of the path-following problem. Using this description of the path parameter dynamics we introduce an augmented system

$$\begin{pmatrix} \dot{x} \\ \dot{z} \end{pmatrix} = \begin{pmatrix} f(x,u) \\ l(z,v) \end{pmatrix} \tag{4.14a}$$

$$\begin{pmatrix} e \\ \theta \end{pmatrix} = \begin{pmatrix} h(x) - p(z_1) \\ z_1 \end{pmatrix} \tag{4.14b}$$

where $(x,z)^T \in \mathbb{R}^{n_x+\hat{r}+1}$ and $(e, z_1) \in \mathbb{R}^{n_y+1}$. We show subsequently that this augmented system description allows analyzing path followability. The next result is a technical Lemma which prepares the ground for local geometric conditions on path followability.

**Lemma 4.1** (Existence of a local transverse normal form)**.**
*Consider the augmented system* (4.14) *and Assumptions 4.1–4.3 then the following statements hold:*

*i) For all* $(x,z)^T \in \mathcal{N}_{x_0} \times \mathcal{Z}$ *system* (4.14) *has a well-defined vector relative degree* $\tilde{r} = (r_1, \ldots, r_{n_y}, \hat{r}+1)$*, where* $r_1, \ldots, r_{n_y}$ *and* $\hat{r}$ *are from* (4.10)*.*

*ii) For all* $(x,z)^T \in \mathcal{N}_{x_0} \times \mathcal{Z}$ *there exists a local diffeomorphism* $(\xi, \eta) = \Phi(x,z)$ *s.t.* (4.14) *is equivalent to a transverse normal form*

$$\dot{\xi}_i = \left(\begin{array}{c|c} \mathbf{0}^{r_i-1\times 1} & \mathbf{I}^{r_i-1\times r_i-1} \\ \hline 0 & \mathbf{0}^{1\times r_i-1} \end{array}\right) \xi_i + \begin{pmatrix} \mathbf{0}^{r_i-1\times 1} \\ \alpha_i(\xi_1, \ldots, \xi_{n_y}, \eta_1, \eta_2, u) \end{pmatrix} \tag{4.15a}$$

$$\dot{\eta} = \beta(\xi, \eta, u, v) \tag{4.15b}$$

*where*

$$\xi = \Big(\underbrace{e_1, \dot{e}_1, \dots, e_1^{(r_1-1)}}_{\xi_1},\ \underbrace{e_2, \dots, e_2^{(r_2-1)}}_{\xi_2},\ \underbrace{\dots,}_{\dots}\ \underbrace{e_{n_y}, \dots, e_{n_y}^{(r_{n_y}-1)}}_{\xi_{n_y}}\Big)^T \in \mathbb{R}^\rho$$

*with* $\rho = \sum_{i=1}^{n_y} r_i$ *and* $\eta \in \mathbb{R}^{n_x+\hat{r}+1-\rho}$.

*Proof.* The proof mainly exploits the fact that the dynamics of $x$ and $z$ are only coupled via the output of (4.14). We proceed in two steps. Firstly, we show how the Lie derivatives of the output of the augmented system (4.14) can be obtained, and thereby we proof part i) of the Lemma. Secondly, we rely on results given in [Nijmeijer and van der Schaft 1990]. We use the Lie derivatives of (4.14b) to obtain a suitable diffeomorphism and to prove part ii).
**Step 1:** Using the simple change of coordinates $\chi = (x, z)^T$, $\nu = (u, v)$, $\mu = (e, \theta)$ system (4.14) can be written as

$$\dot{\chi} = \phi(\chi, \nu) \tag{4.16a}$$
$$\mu = \psi(\chi) \tag{4.16b}$$

where the vector fields $\phi : \mathbb{R}^{n_x+\hat{r}+1} \times \mathbb{R}^{n_y+1} \to \mathbb{R}^{n_x+\hat{r}+1}, \psi : \mathbb{R}^{n_x+\hat{r}+1} \to \mathbb{R}^{n_y+1}$ follow directly from (4.14). Next, we apply condition (4.9a) from Definition 4.2 to this system. For all $k \in \{1, \dots, n_y\}$ the first Lie derivative of the $k$-th component of $\mu$ is

$$\mathrm{L}_\phi\, \psi_k(\chi) = \frac{\partial \psi_k(\chi)}{\partial \chi}\phi = \begin{pmatrix} \frac{\partial h_k}{\partial x}, & -\frac{\partial p_k}{\partial z} \end{pmatrix} \begin{pmatrix} f(x,u) \\ l(z,v) \end{pmatrix}.$$

For the $i$-th Lie derivative of the $k$-th component of $\mu$ with $k \in \{1, \dots, n_y\}$ it follows that

$$\mathrm{L}_\phi^i\, \psi_k(\chi) = \mathrm{L}_f^i\, h_k(x) - \mathrm{L}_l^i\, p_k(z).$$

Now, consider the partial derivatives with respect to the inputs of (4.16)

$$\forall k \in \{1, \dots, n_y\} : \quad \frac{\partial}{\partial \nu_j}\mathrm{L}_\phi^i\, \psi_k(\chi) = \begin{cases} \frac{\partial}{\partial u_j}\mathrm{L}_f^i\, h_k(x) & j \in \{1, \dots, n_u\} \\ -\frac{\partial}{\partial v}\ \mathrm{L}_l^i\, p_k(z) & j = n_u + 1 \end{cases}. \tag{4.17}$$

Using this and Assumption 4.2 we yield for all $j \in \{1, \dots, n_u\}$ and all $k \in \{1, \dots, n_y\}$

$$\forall i \in \{1, \dots, r_{k-1}\} : \quad \frac{\partial}{\partial \nu_j}\mathrm{L}_\phi^i\, \psi_k(\chi) = \frac{\partial}{\partial u_j}\mathrm{L}_f^i\, h_k(x) = 0 \tag{4.18a}$$
$$i = r_k : \quad \frac{\partial}{\partial \nu_j}\mathrm{L}_\phi^i\, \psi_k(\chi) = \frac{\partial}{\partial u_j}\mathrm{L}_f^i\, h_k(x) \neq 0. \tag{4.18b}$$

And for $j = n_u + 1$ and all $k \in \{1, \dots, n_y\}$ it follows

$$\forall i = \{1, \dots, \hat{r}\} : \quad \frac{\partial}{\partial \nu_j} \mathrm{L}_\phi^i \psi_k(\chi) = -\frac{\partial}{\partial v} \mathrm{L}_l^i p_k(z) = 0, \tag{4.18c}$$

i.e., the first $\hat{r}$ time derivatives of $p(\theta(t))$ do not depend on the input $v = \nu_{n_y+1}$.
It remains to consider the Lie derivatives of the $n_y + 1$-th output of (4.16). From (4.17), and the timing law being an integrator chain of length $\hat{r} + 1$, we obtain

$$\frac{\partial}{\partial \nu_j} \mathrm{L}_\phi^i \psi_{n_y+1}(\chi) = \begin{cases} 0 & j \in \{1, \dots, n_u\}, \; i \in \{1, \dots, \hat{r}\} \\ 1 & j = n_u + 1, \qquad i = \hat{r} + 1 \end{cases} . \tag{4.18d}$$

Bascially, (4.18a-d) state that condition i) of Definition 4.2 is fulfilled. Recall that we consider systems with a square input-output structure ($n_u = n_y$). Thus the $(n_y + 1) \times (n_y + 1)$ decoupling matrix of (4.16) is

$$\mathbf{A}(\chi) = \begin{pmatrix} \frac{\partial}{\partial \nu_1} \mathrm{L}_\phi^{\tilde{r}_1} \psi_1(\chi) & \dots & \frac{\partial}{\partial \nu_{n_y+1}} \mathrm{L}_\phi^{\tilde{r}_1} \psi_1(\chi) \\ \vdots & & \vdots \\ \frac{\partial}{\partial \nu_1} \mathrm{L}_\phi^{\tilde{r}_{n_y+1}} \psi_{n_y+1}(\chi) & \dots & \frac{\partial}{\partial \nu_{n_y+1}} \mathrm{L}_\phi^{\tilde{r}_{n_y+1}} \psi_{n_y+1}(\chi) \end{pmatrix}.$$

Using (4.18a-d) and $\chi = (x, z)$ we rewrite $\mathbf{A}(\chi)$ in $(x, z)$ coordinates

$$\mathbf{A}(x, z) = \left(\begin{array}{ccc|c} \frac{\partial}{\partial u_1} \mathrm{L}_f^{r_1} h_1(x) & \dots & \frac{\partial}{\partial u_{n_y}} \mathrm{L}_f^{r_1} h_1(x) & 0 \\ \vdots & & \vdots & \vdots \\ \frac{\partial}{\partial u_1} \mathrm{L}_f^{r_{n_y}} h_{n_y}(x) & \dots & \frac{\partial}{\partial u_{n_y}} \mathrm{L}_f^{r_{n_y}} h_{n_y}(x) & 0 \\ \hline 0 & \dots & 0 & 1 \end{array}\right) = \left(\begin{array}{c|c} \mathbf{A}(x) & \mathbf{0}^{n_y \times 1} \\ \hline \mathbf{0}^{1 \times n_y} & 1 \end{array}\right). \tag{4.19}$$

The upper left part of this matrix is the decoupling matrix $\mathbf{A}(x)$ of the original system (4.1). Clearly, for all $(x, z) \in \mathcal{N}_{x_0} \times \mathcal{Z}$ the matrix $\mathbf{A}(\chi)$ is non-singular if and only if the decoupling matrix $\mathbf{A}(x)$ of the original system (4.1) is non-singular for all $x \in \mathcal{N}_{x_0}$. Hence Assumptions 4.2 and 4.3 guarantee that the augmented system (4.14) has a well-defined vector relative degree $\tilde{r} = (r_1, \dots, r_{n_y}, \hat{r} + 1)$.

**Step 2:** So far we have shown that the augmented system (4.14) has a well-defined vector relative degree. In order to obtain the transverse normal form (4.15) we follow along the lines of [Nijmeijer and van der Schaft 1990]. Consider a change of coordinates $\Phi : \mathbb{R}^{n_x} \times \mathbb{R}^{\hat{r}+1} \to \mathbb{R}^{n_x} \times \mathbb{R}^{\hat{r}+1}$. The first $\rho$-components where $\rho = \sum_{i=1}^{n_y} r_i$ of $\Phi$ are chosen as the components of the error output $e = h(x) - p(\theta)$ and their time derivatives

$$\begin{aligned} \Phi_\xi(x, z) = & \left(\psi_1, \mathrm{L}_\phi \psi_1(\chi), \dots, \mathrm{L}_\phi^{r_1 - 1} \psi_1(\chi), \psi_2, \dots, \psi_{n_y}, \dots, \mathrm{L}_\phi^{r_{n_y} - 1} \psi_{n_y}(\chi)\right)^T \\ = & \Big(\underbrace{e_1, \dot{e}_1, \dots, e_1^{(r_1 - 1)}}_{\xi_1}, \underbrace{e_2, \dots, e_2^{(r_2 - 1)}}_{\xi_2}, \underset{\dots}{\dots}, \underbrace{e_{n_y}, \dots, e_{n_y}^{(r_{n_y} - 1)}}_{\xi_{n_y}}\Big)^T . \end{aligned} \tag{4.20a}$$

This yields $\Phi_\xi(x,z) = \xi \in \mathbb{R}^\rho$. And for all $j \in \{n_x+1,\dots,n_x+\hat{r}+1\}$ we choose

$$\Phi_{\eta_2,j}(x,z) = z_{j-n_x} \tag{4.20b}$$

and obtain

$$\Phi_{\eta_2}(x,z) = \eta_2 = (z_1,\dots,z_{\hat{r}+1})^T \in \mathbb{R}^{\hat{r}+1}.$$

The remaining $n_x - \rho$ components of $\Phi$ have to be chosen such that

$$\Phi_{\eta_1}(x,z) = \eta_1 \in \mathbb{R}^{n_x-\rho} \tag{4.20c}$$

holds. Furthermore, we have to ensure that $\Phi = (\Phi_\xi, \Phi_{\eta_1}, \Phi_{\eta_2})^T$ is a diffeomorphism. The independence of $\Phi_\xi, \Phi_{\eta_2}$ as well as the existence of the supplementary independent functions $\Phi_{\eta_1}(x,z)$ is guaranteed since the augmented system (4.14) is smooth and has a well-defined vector relative degree for $(x,z) \in \mathcal{N}_{x_0} \times \mathcal{Z}$, cf. [Nijmeijer and van der Schaft 1990, Thm. 13.24, p. 418]. Using $\xi = (\xi_1,\dots,\xi_{n_y})^T$ from (4.20a) one obtains a transverse normal form in the proposed structure (4.15)

$$\dot{\xi}_i = \left(\begin{array}{c|c} \mathbf{0}^{r_i-1\times 1} & \mathbf{I}^{r_i-1\times r_i-1} \\ \hline 0 & \mathbf{0}^{1\times r_i-1} \end{array}\right)\xi_i + \begin{pmatrix} \mathbf{0}^{r_i-1\times 1} \\ \alpha_i(\xi_1,\dots,\xi_{n_y},\eta_1,\eta_2,u) \end{pmatrix} \tag{4.21a}$$

$$\dot{\eta}_1 = \beta_1(\xi_1,\dots,\xi_{n_y},\eta_1,\eta_2,u,v) \tag{4.21b}$$

$$\dot{\eta}_2 = \beta_2(\eta_2,v) \tag{4.21c}$$

where $i \in \{1,\dots,n_y\}$. The functions $\alpha_i : \mathbb{R}^{n_x+\hat{r}+1} \times \mathbb{R}^{n_y} \to \mathbb{R}$ in the nonlinear part of (4.21a) are

$$\alpha_i(\xi_1,\dots,\xi_{n_y},\eta_1,\eta_2,u) = \left(\mathrm{L}_f^{r_i} h_i(x) - \mathrm{L}_l^{r_i} p_i(z)\right) \circ \Phi^{-1}(x,z). \tag{4.22}$$

Recalling (4.18c) it is clear that $\alpha_i$ do not depend on the path parameter input $v$.[1] Due to the fact that the $\Phi_j$ from (4.20b) simply map $z$ onto $\eta_2$ the vector field in (4.21b) is $\beta_2(\eta_2,v) = A\eta_2 + Bv$, where the matrices $A, B$ are from the path parameter dynamics (4.12). This finishes the proof. □

We have shown that for $(x,z) \in \mathcal{N}_{x_0} \times \mathcal{Z}$ we can map (4.14) into new coordinates (4.21). In general, these coordinates are valid only locally on $\mathcal{N}_{x_0} \times \mathcal{Z}$, since we have assumed that (4.1) has a well-defined vector relative degree at $x_0$.

For the further developments it is helpful to interpret the local coordinates (4.21) geometrically. To this end we define a projection $\Pi : \mathbb{R}^{n_x} \times \mathbb{R}^{\hat{r}+1} \to \mathbb{R}^{n_x}$

$$\Pi : \quad (x,z)^T \mapsto x. \tag{4.23}$$

Basically, this projection maps from the augmented system description (4.14) back to

[1] If one would choose the *timing law* in Assumption (4.3) as $\theta^{(\hat{r})} = v$, then the functions $\alpha_i$ depend explicitly on $v$ for all $i : r_i = \hat{r}$.

the original system (4.1). To locally describe the set of all points $x$ which map to the path $\mathcal{P}$—i.e., the path pre-image $h^{-1}(\mathcal{P}) = \{x \in \mathbb{R}^{n_x} \mid h(x) \in \mathcal{P}\}$—we consider the following subset of $\mathbb{R}^{n_x+\hat{r}+1}$

$$\hat{\Xi} = \left\{(\xi, \eta) \in \mathbb{R}^{n_x+\hat{r}+1} \mid (\xi_{1,1}, \xi_{2,1} \ldots, \xi_{n_y,1})^T = 0\right\}, \tag{4.24}$$

where $\xi_{i,1} = e_i(x, z), i \in \{1, \ldots, n_y\}$ as in (4.20a). The set $\hat{\Xi}$ is characterized in $(\xi, \eta)$ coordinates by $\xi_i = 0$ and $\xi_i = e_i = h_i(x) - p_i(\theta)$. We rely on the diffeomorphism (4.20) and on the map $\Pi$ to project $\hat{\Xi}$ to $x$ coordinates. This way we obtain the path pre-image with respect to the output map $h$ of the original description (4.1)

$$h^{-1}(\mathcal{P}) = \Pi\left(\Phi^{-1}\left(\hat{\Xi}\right)\right). \tag{4.25}$$

Additionally, we can use the coordinates (4.21) to locally describe the set of solutions to (4.1) which are such that the output (4.1b) travels along the path $\mathcal{P}$. Consider a subset of $\hat{\Xi}$ which is defined as follows

$$\Xi = \left\{(\xi, \eta) \in \mathbb{R}^{n_x+\hat{r}+1} \mid \xi = 0\right\} \subset \hat{\Xi}. \tag{4.26}$$

Literally speaking, $\Xi$ is the subset of $\mathbb{R}^{n_x+\hat{r}+1}$ where the time derivatives of the path error (4.4) are exactly zero. A local description of the manifold of solutions to (4.1) which travel exactly along the path $\mathcal{P}$— the *zero-path-error manifold*—is obtained by projecting $\Xi$ to $x$ coordinates

$$\mathcal{I}_{\mathcal{P}} = \Pi\left(\Phi^{-1}(\Xi)\right). \tag{4.27}$$

Using this notation we can interpret the local transverse normal form (4.21) geometrically, see Figure 4.2. The coordinates $\xi = (\xi_1, \ldots, \xi_{n_y})^T$ locally describe the dynamics transversal to the zero-path-error manifold $\mathcal{I}_{\mathcal{P}}$. In other words, these directions point away from $\mathcal{I}_{\mathcal{P}}$.

As illustrated in Figure 4.2, the first set of internal states $\eta_1$ describes the dynamics on $\mathcal{I}_{\mathcal{P}}$. That is (4.21b) corresponds to the internal dynamics of (4.1) with respect to the error output $e = h(x) - p(\theta)$ from (4.4). Finally, $\eta_2$ lives in $\mathcal{Z} \subset \mathbb{R}^{\hat{r}+1}$ from (4.13). The state $\eta_2 = z$ is merely a virtual one and not directly influenced by $\eta_1$ or $\xi$. It describes the dynamics of the reference $p(\theta(t))$ which can be controlled via the virtual input $v$, cf. (4.21c).

The decomposition into transversal states and states in the zero-path-error manifold is the reason to call (4.15) and (4.21) *transverse normal forms*, cf. [Banaszuk and Hauser 1995; Nielsen and Maggiore 2006, 2008].

We show subsequently that the introduction of the augmented dynamics (4.14) and their local description via (4.21) simplifies the analysis path-following problems. Based on Lemma 4.1 we can state a local result for unconstrained path followability.

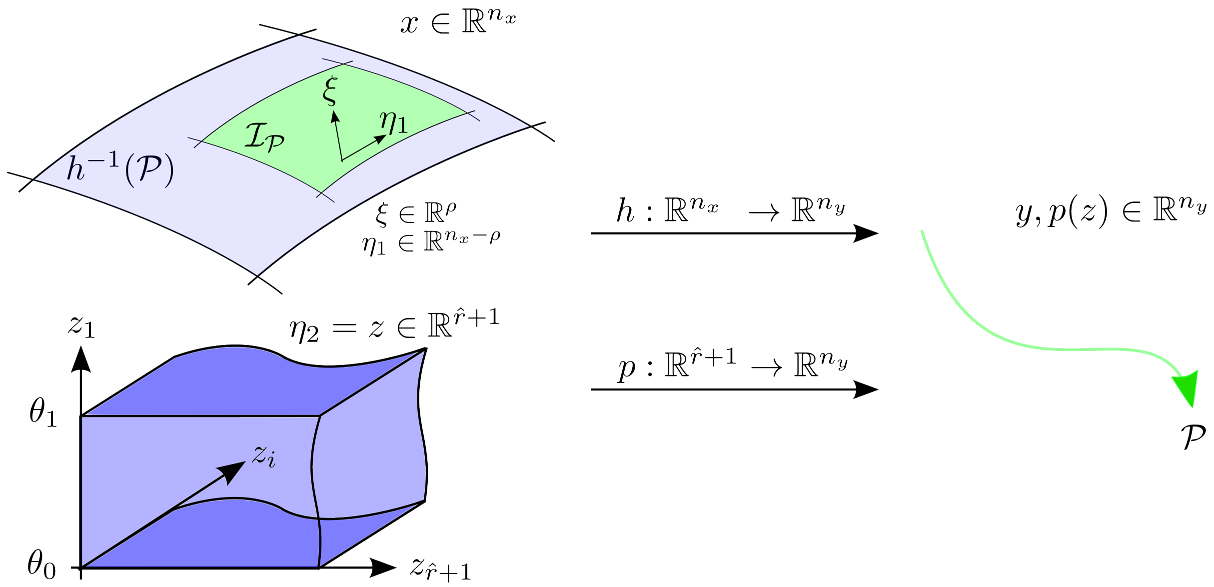


**Figure 4.2:** Geometric interpretation of the transverse normal form (4.21).

**Theorem 4.1** (Sufficient conditions for local path followability)**.**
*Consider system* (4.1)*, a path* $\mathcal{P}$ *as defined in* (4.2) *and Assumptions 4.1–4.3 hold. Suppose* $\Phi : \mathcal{N}_{x_0} \times \mathcal{Z} \mapsto \mathbb{R}^{n_x} \times \mathbb{R}^{\hat{r}+1}$ *is a local diffeomorphism mapping to a transverse normal formal, and* $\Xi$*,* $\mathcal{Z}$ *are as defined in* (4.26) *and* (4.13)*.*
*Then for any* $(x_0, z_0) \in \mathcal{N}_{x_0} \times \mathcal{Z}$ *with*

$$\Phi(x_0, z_0) \in \Xi \quad \textit{and} \quad z_0 \in \operatorname{int} \mathcal{Z}, \tag{4.28}$$

*the path* $\mathcal{P}$ *is locally exactly followable by system* (4.1) *s.t.* $\dot{\theta} > 0$ *holds.*

*Proof.* Assumptions 4.1–4.2 ensure that for any point $(x_0, z_0)$, we can find a local diffeomorphism $\Phi$ to map the system into a transversal normal from. Rewriting the exact path-following problem in the local coordinates (4.21) yields

$$\begin{aligned}
\dot{\xi}_i &= \left(\begin{array}{c|c} \mathbf{0}^{r_i-1\times 1} & \mathbf{I}^{r_i-1\times r_i-1} \\ \hline 0 & \mathbf{0}^{1\times r_i-1} \end{array}\right) \xi_i + \begin{pmatrix} \mathbf{0}^{r_i-1\times 1} \\ \alpha_i(\xi_1, \dots, \xi_{n_y}, \eta_1, \eta_2, u) \end{pmatrix} \\
\dot{\eta}_1 &= \beta_1(\xi_1, \dots, \xi_{n_y}, \eta_1, \eta_2, u, v) \\
\dot{\eta}_2 &= A\eta_2 + Bv.
\end{aligned}$$

In these coordinates we can check whether the initial condition satisfies (4.28). The condition (4.28) implies that $\xi(t_0) = 0$. Additionally, we need to ensure that we can move forward along the path. $z_0 \in \operatorname{int} \mathcal{Z}$ is required, since it implies that $\dot{\theta}_0 > 0$. The input $u_\mathcal{P}$ to the transverse part of the dynamics is chosen such that

$$\forall i \in \{1, \dots, n_y\} : \quad \alpha_i(0, \dots, 0, \eta_1, \eta_2, u_\mathcal{P}) = 0. \tag{4.29}$$

Due to the implicit function theorem and the rank condition (4.9c) $u_{\mathcal{P}}$ can be calculated at least locally from the last equation as a function of the current values of $\eta_1, \eta_2$. Hence the zero dynamics of (4.21) can be written as

$$\dot{\eta}_1 = \beta_1(0, \dots, 0, \eta_1, \eta_2, u_{\mathcal{P}}, v) \tag{4.30a}$$

$$\dot{\eta}_2 = A\eta_2 + Bv. \tag{4.30b}$$

Provided the original system (4.1) is locally Lipschitz these dynamics are locally Lipschitz. Denote $\eta_2(0) = \Phi_{\eta_2}(z_0)$. In (4.30) the virtual input $v$ is a degree of freedom. It can be chosen such that the solution $\eta_2(t, \eta_2(0)|v)$ stays inside the interior of $\mathcal{Z}$ from (4.13), the solutions $x(t, x_0|u_{\mathcal{P}})$ to the original system (4.1) exist locally, and they fulfill $h(x(t, x_0|u_{\mathcal{P}})) = p(\theta(t|v))$ with $\dot{\theta} > 0$. □

One should note that the conditions of the theorem can easiliy be modified to guarantee path followability with non-increasing timings $\dot{\theta} \lesseqgtr 0$. One simply needs to modify or drop the condition $z_0 \in \operatorname{int} \mathcal{Z}$ from (4.28). Note that for any path parameter evolution, and thus for any $\eta_2 \in \mathcal{Z}$, we can use (4.29) to obtain the inputs $u_{\mathcal{P}}$. In other words, this implies that the square input-output structure (Assumption 4.1) ensures that the speed to move along the path is a degree of freedom.

**Remark 4.1** (Local nature of Theorem 4.1)**.**
*The last result is of local nature only. Firstly, in many cases only local diffeomorphisms $\Phi$ to map into the transverse normal can be found. Secondly, only local existence of the solutions to the zero dynamics* (4.30) *is guaranteed. Furthermore, the result does not imply stability in the sense of boundedness of solutions to the zero dynamics* (4.30)*. A stability statement can be obtained, for example, if either the zero dynamics $\dot{\eta}_1$ are minimum phase, or if input-to-state stability properties of $\dot{\eta}_1$ can be verified. In the latter case one needs to design a suitable control to ensure $\dot{\theta} \geq 0$ and stability or boundedness of $\dot{\eta}_1 = \beta_1(\xi, \eta_1, \eta_2, u, v)$, see [Dacic et al. 2011]. However, the design of suitable feedback strategies is beyond the scope of this chapter. For an overview on existing methods we refer the reader to Section 4.2.*

One might ask how one can check unconstrained exact path followability for a given application. One way to do this is as follows:

1. Start with a point $x \in h^{-1}(\mathcal{P})$ which has a well defined vector relativ degree with respect to (4.1) in a neighborhood of $x$, cf. Definition 4.2.
2. Define a suitable augmented system as in (4.14).
3. Calculate a local diffeomorphism $\Phi$ around $x$. Map the augmented system to a transverse normal form as described in the proof of Lemma 4.1.
4. Evaluate the set of all $x \in \mathcal{I}_{\mathcal{P}}$ for which $\Phi$ is defined, and compute the corresponding values of $z_1 = \theta$.
5. The transverse normal description obtained via $\Phi$ is valid for the parts of the path identified in the last step.

For the parts of the path where $\Phi$ is not a diffeomorphism one has to adjust the free components of the diffeomorphism, which are related to the internal dynamics on the zero-path-error manifold (4.21b) and for the path parameter dynamics (4.21c). From the procedure described above one obtains a transverse normal form description which is valid at least for a part of the path. If one fails to find one diffeomorphism to cover the whole path, one can still try to cover the path with several local diffeomorphisms.[2]

**Example 4.2** (Planar 2-DOF robot)**.**
*To illustrate the last developments we consider a fully-actuated planar robot with two degrees of freedom as an example. Without friction and external contact forces the dynamics of such a robot are*

$$\begin{pmatrix} \dot{x}_1 \\ \dot{x}_2 \end{pmatrix} = \begin{pmatrix} x_2 \\ B^{-1}(x_1)\left(u - C(x_1, x_2)x_2 - g(x_1)\right) \end{pmatrix} \tag{4.31a}$$

$$y = x_1. \tag{4.31b}$$

*Here* $x_1 = (q_1, q_2) \in \mathbb{R}^2$ *is the vector of joint angles,* $x_2 = (\dot{q}_1, \dot{q}_2) \in \mathbb{R}^2$ *is the vector of joint velocities.* $B : \mathbb{R}^2 \to \mathbb{R}^{2\times 2}$*,* $C : \mathbb{R}^4 \to \mathbb{R}^{2\times 2}$ *describe the dependence of the inertias on the joint angles and dependence of centrifugal and coriolis forces on joint angles and velocities, respectively.* $g : \mathbb{R}^2 \to \mathbb{R}^2$ *models the effect of gravity. The output* $y = x_1$ *denotes the space of joint angles. The matrix* $B$ *is vertible for all* $x_1 \in \mathbb{R}^2$ *and* $C$ *and* $g$ *are bounded. The considered path-following task is described in the joint space. The path is assumed to be a regular curve*

$$\mathcal{P} = \left\{ y \in \mathbb{R}^2 \mid \theta \mapsto \begin{pmatrix} p_1(\theta) \\ p_2(\theta) \end{pmatrix} \right\}$$

*with* $p(\theta) \in \mathcal{C}^2$*. Here, we aim at the construction of a transverse normal form for this path-following problem.*
*It is easy to see that* (4.31) *has a global vector relative degree* $r = (2, 2)^T$ *with respect to the output* $y = x_1$*. As in Assumption 4.3 we use as path parameter dynamics an integrator chain of length* 3*. Thus we obtain an augmented system description* (4.14)

$$\begin{pmatrix} \dot{x}_1 \\ \dot{x}_2 \end{pmatrix} = \begin{pmatrix} x_2 \\ B^{-1}(x_1)\left(u - C(x_1, x_2)x_2 - g(x_1)\right) \end{pmatrix} \tag{4.32a}$$

$$\dot{z} = \left(\begin{array}{c|c} \mathbf{0}^{2\times 1} & \mathbf{I}^{2\times 2} \\ \hline 0 & \mathbf{0}^{1\times 2} \end{array}\right) z + \begin{pmatrix} 0, & 0, & 1 \end{pmatrix}^T v \tag{4.32b}$$

[2] Basically, such an approach can be seen as obtaining an atlas of maps to cover the whole zero-path-error manifold. For details on the connection between differentiable manifolds and nonlinear normal forms we refer the reader to [Bullo and Lewis 2004; Isidori 1995; Nijmeijer and van der Schaft 1990] and the references therein.

$$e = x_1 - p(z_1) \tag{4.32c}$$

$$\theta = z_1. \tag{4.32d}$$

*We want to map these augmented dynamics into a transverse normal form. Following along the lines of the proof of Lemma 4.1 we obtain a coordinate transformation* $\Phi : \mathbb{R}^4 \times \mathbb{R}^3 \to \mathbb{R}^4 \times \mathbb{R}^3$ *and its inverse* $\Phi^{-1}$

$$\Phi : \begin{pmatrix} \xi_1 \\ \xi_2 \\ \eta \end{pmatrix} = \begin{pmatrix} x_1 - p(z_1) \\ x_2 - \frac{\partial p}{\partial z_1} z_2 \\ z \end{pmatrix}, \qquad \Phi^{-1} : \begin{pmatrix} x_1 \\ x_2 \\ z \end{pmatrix} = \begin{pmatrix} \xi_1 - p(\eta_1) \\ \xi_2 - \frac{\partial p}{\partial \eta_1} \eta_2 \\ \eta \end{pmatrix}.$$

*Compared to* (4.21) *we have chosen a different ordering of the* $\xi$*-variables. Furthermore, note that only the virtual states* $z$ *appear in* $\eta$*. This can be explained as follows: The robot dynamics have a state dimension of* $n_x = 4$ *and a vector relative degree of* (4.31) *of* $r = (2, 2)^T$ *with respect to the output* $y = x_1$*. Thus by calculation of the time derivatives of* $e$ *we obtain four new coordinates* $\xi \in \mathbb{R}^4$*.*
*Due to its simple structure and the global vector relative degree* $(2, 2)^T$ *it is easy to see that* $\Phi$ *is a global diffeomorphism. Using* $\Phi$ *it is straightforward to rewrite the augmented robot dynamics* (4.32) *into a transversal normal form. We obtain*

$$\begin{pmatrix} \dot{\xi}_1 \\ \dot{\xi}_2 \end{pmatrix} = \begin{pmatrix} \xi_2 \\ \alpha(\xi, \eta, u) \end{pmatrix} \tag{4.33a}$$

$$\dot{\eta} = \left( \begin{array}{c|c} \mathbf{0}^{2\times 1} & \mathbf{I}^{2\times 2} \\ \hline 0 & \mathbf{0}^{1\times 2} \end{array} \right) \eta + \begin{pmatrix} 0, & 0, & 1 \end{pmatrix}^T v \tag{4.33b}$$

$$e = \xi_1 - p(\eta_1) \tag{4.33c}$$

$$\theta = \eta_1 \tag{4.33d}$$

*and the vector field* $\alpha : \mathbb{R}^4 \times \mathbb{R}^3 \times \mathbb{R}^2 \to \mathbb{R}^2$ *is*

$$\alpha(\xi, \eta, u) = B^{-1}(\xi_1, \eta_1) \left( u - C(\xi, \eta) \left( \xi_2 - \frac{\partial p}{\partial \eta_1} \eta_2 \right) - g(\xi_1, \eta_1) \right) - \frac{\partial^2 p}{\partial \eta_1^2} (\eta_2)^2 - \frac{\partial p}{\partial \eta_1} \eta_3.$$

*Based on this problem description path following for the robot can be achieved by breaking the problem down into two parts: Firstly, we feedback linearize the transversal part of* (4.33)*. And secondly, we assign a timing to the path via the virtual input* $v$*. In other words, one can use the feedback*

$$u_{\mathcal{P}}(\xi, \eta) = C(\xi, \eta) \left( \xi_2 - \frac{\partial p}{\partial \eta_1} \eta_2 \right) + g(\xi_1, \eta_1) + B(\xi_1, \eta_1) \left( \frac{\partial^2 p}{\partial \eta_1^2} (\eta_2)^2 + \frac{\partial p}{\partial \eta_1} \eta_3 \right) \tag{4.34}$$

*to achieve exact path following for any initial condition with* $\Phi_\xi(x_0, z_0) = \xi_0 = 0$*. Note we have not assigned* $v$*, and thus the speed to follow the path exactly is free. We conclude that the 2-DOF robot* (4.31) *can follow paths with* $p(\theta) \in \mathcal{C}^2$ *exactly.*

The ansatz to use the augmented system description (4.14) to describe path-following problems has further degrees of freedom which have not been mentioned so far. It also offers insights on the connection between path following and other problems. We briefly comment on these issues in the next remarks.

**Remark 4.2** (Non-uniqueness of transverse normal forms)**.**
*In general the transverse normal form* (4.21) *is not unique. Due to* (4.20) *we have*

$$\Phi(x,z) = \begin{pmatrix} \Phi_\xi(x,z) \\ \Phi_{\eta_1}(z) \\ \Phi_{\eta_2}(x,z) \end{pmatrix} = \begin{pmatrix} \Phi_\xi(x,z) \\ \Phi_{\eta_1}(x,z) \\ z \end{pmatrix}. \tag{4.35}$$

*If one changes the last two components of* $\Phi$ (4.35) *such that the resulting map is still a (local) diffeomorphism, the obtained (local) system description is another transverse normal form. This means that we have degrees of freedom not only in the choice of* $\Phi_{\eta_1}$ *but also in the choice of* $\Phi_{\eta_2}$ *in* (4.35)*. One does not necessarily need to set* $\Phi_{\eta_2} : \eta_2 = z$*. The derivatives* $\theta^{(i)} = z_{i+1}$ *appear affinely in the i-th derivative of the path-following error* $e = h(x) - p(\theta)$*. More precisely we have for all* $j \in \{1, \ldots, n_y\}$ *and all* $i \in \{1, \ldots, r_j\}$

$$e_j^{(i)} = \mathrm{L}_f^i\, h_j(x) - \mathrm{L}_l^i\, p_j(z) = \mathrm{L}_f^i\, h_j(x) - \left( \frac{\partial^i p_j}{\partial z_1^i} z_2^i + \cdots + \frac{\partial p_j}{\partial z_1} z_{i+1} \right).$$

*The structure of these equations can be used to calculate* $z_i$ *from* $e_j^{(i)}$*. Clearly, singularities should be avoided in the definition of the map* $\Phi$*. It is also useful, if the inverse map* $\Phi^{-1}$ *does not have singularities, since* $\Phi^{-1}$ *directly enters the transverse normal form through* $\alpha_i(\cdot)$ *in* (4.21a)*. As we see later in Section 4.3.2 one can use this freedom in the choice of* $\Phi_{\eta_1,\eta_2}$ *to influence the structure of the transverse normal form.*

**Remark 4.3** (Choice of suitable timing laws)**.**
*The statements of Lemma 4.1 and Theorem 4.1 rely on the timing law* $\theta^{(\hat{r}+1)} = v$ *from Assumption 4.3. Thus they offer some insight, how to choose timing laws in a suitbale way. Due to Assumption 4.2 it is reasonable to choose the timing law such that, given a class of path parameter inputs* $v \in \mathcal{V}$*, the parameter evolution* $\theta(t, \theta_0|v)$ *is sufficiently often continuously differentiable. So, either one restricts the admissible inputs* $v$*, or one ensures that even discontinuous inputs* $v$ *result in* $\theta(t, \theta_0|v) \in \mathcal{C}^{\hat{r}}$*, where* $\hat{r}$ *is largest element of the vector relative degree. In Section 4.4 we present an optimal control scheme to compute suitable feedforward controls for exact path following. Our ansatz to rely on sufficiently long integrator chains as timing laws is directly motivated by this optimization-based approach. Due to this choice we can use piecewise constant path parameter inputs* $v$*. In applications—for example, if continuous feedbacks or a sufficiently fine input discretization are used—one might also rely on* $\theta^{(\hat{r})} = v$*.*

**Remark 4.4** (Path followability and DAEs).
*The augmented system* (4.14) *provides also some insight on the connection between the question of path-followability and differential algebraic equations (DAEs). Recalling the structure of* (4.14) *it is clear that exact path followability in the sense of Definition 4.1 requires keeping* $e = h(x) - p(\theta) = 0$ *while the* $\dot{\theta} \geq 0$ *holds. Thus* $h(x) - p(\theta) = 0$ *can be understood as an algebraic constraint. One can regard the path-followability problem as the question of existence of solutions to the DAE*

$$\begin{pmatrix} \dot{x} \\ \dot{z} \end{pmatrix} = \begin{pmatrix} f(x,u) \\ Az + Bv \end{pmatrix} \tag{4.36a}$$

$$\theta = z_1 \tag{4.36b}$$

$$0 = h_i(x) - p_i(z_1), \quad i \in \{1, \ldots, n_u\} \tag{4.36c}$$

*subject to the additional state constraint* $\dot{\theta} = z_2 \geq 0$*. In the proof of Lemma 4.1 we verified that one needs to differentiate the i-th components of the constraint* $h_i(x) - p_i(\theta) = 0$ $r_i$*-times in order to obtain the description in the transverse normal form* (4.21)*. And in the proof of Theorem 4.1 we have shown how to obtain an input which renders the zero-path-error manifold* $\mathcal{I}_{\mathcal{P}}$ *from* (4.26) *positively invariant, and how to characterize all solutions of* (4.36) *consistent with* $h(x) - p(\theta) = 0$ *via* (4.30)*. Thus one can conclude that the differential index of the DAE* (4.36) *is* $\hat{r}$, $\quad \hat{r} = \max\{r_1, \ldots, r_{n_y}\}$, *cf. [Brenan et al. 1996].*
*A similar approach in context of general DAEs is considered in [McClamroch 1990]. There the vector relative degree of an algebraic constraint is used to make statements about the existence of solutions to DAEs.*[3]

**Remark 4.5** (Non-square input-output structures).
*In our previous consideration we require that the number of inputs* $n_u$ *is identical to the number of outputs* $n_y$*, cf. Assumption 4.1. The path followability results as presented are thus restricted to the case of square input-output structures. However, often one has to deal with non-square input-output structures.*
*If the number of outputs* $n_y$ *is less than the number of inputs* $n_u$*, no problems arise as long as decoupling matrix* $\mathbf{A}(x)$ *appearing in Definition 4.2 has full column rank, cf. [Isidori 1995]. The main idea is to reduce the number of inputs needed to obtain a transverse normal form. The contrary case* $n_y > n_u$ *is much more sophisticated. The easiest version of this case is* $n_y - 1 = n_u$*. One can try to tackle this case via variant*

[3] So far we have not commented on the connection between holonomic and non-holonomic constraints—as they are often present in mechanical systems—and the path-followability problem we are discussing here. For example, the question of whether the 2-DoF robot from Example 4.2 can follow a joint space path is in essence equivalent to the introduction of *virtual* holonomic constraints. However, our approach, which is basically the classification of the vector relative degree of the algebraic constraints, is more general and applicable to holonomic as well as to non-holonomic constraints, see also [McClamroch 1990].

*of the augmented system* (4.14) *where the output* $\theta = z_1$ *is neglected*

$$\begin{pmatrix} \dot{x} \\ \dot{z} \end{pmatrix} = \begin{pmatrix} f(x,u) \\ Az + Bv \end{pmatrix}$$
$$e = h(x) - p(z_1).$$

*Relying on this formulation, one can attempt to check whether this system has a well-defined vector relative degree with respect to the square input-output structure* $(u, v) \in \mathbb{R}^{n_u} \times \mathbb{R}$ *and* $e = h(x) - p(z_1) \in \mathbb{R}^{n_y}$*. Even if the DAE given by* $e = 0$ *has a unique solution, it is often not possible to ensure forward motion* $\dot{\theta} = z_2 \geq 0$ *and exact path followability at the same time. In Section 4.3.2 we use this ansatz to derive a transverse normal form for the non-square ship dynamics from Example 4.1.*
*A different possibility of dealing with the case* $n_y > n_u$ *is to adapt the problem formulation. Instead of a* 1*-dimensional path* $\mathcal{P}$ *from* (4.2) *one can consider generalized* $k$*-dimensional geometric reference descriptions. The intuitive idea is to add spatial degrees of freedom to the geometric reference description and derive a generalized problem setting. First steps in this direction have been proposed in [Faulwasser and Findeisen 2009a; Faulwasser et al. 2009a].*

### 4.3.2 Example: Geometric Ship Course Control

So far we have proposed to analyze path-following problems with the help of an augmented system (4.14). We have seen that this description allows a local analysis of the problems. To illustrate our augmented system approach further we reconsider the ship course control problem from Example 4.1. Our goal is to obtain a transverse normal form description of the path-following problem for the ship model (4.6). Recall that the ship dynamics (4.6) are non-square with $\dim u = 1$ and $\dim y = 2$. To handle this, we use the ideas presented in Remarks 4.2 and 4.5.
We rewrite the path-following task for (4.6) in the augmented system description (4.14)

$$\begin{pmatrix} \dot{x}_1 \\ \dot{x}_2 \\ \dot{x}_3 \\ \dot{x}_4 \\ \dot{z}_1 \\ \dot{z}_2 \end{pmatrix} = \begin{pmatrix} w\cos x_3 - Lwx_4 \sin x_3 \\ w \sin x_3 + Lwx_4 \cos x_3 \\ x_4 \\ \frac{1}{\tau}(-x_4 + Ku) \\ z_2 \\ v \end{pmatrix}. \tag{4.37a}$$

The considered output becomes

$$e = \begin{pmatrix} x_1 - p_1(z_1) \\ x_2 - p_2(z_1) \end{pmatrix}, \tag{4.37b}$$

where the path parametrization $p(\theta) = (p_1(\theta), p_2(\theta))^T$ from (4.2) is used, and the $z$-states describe the path parameter $\theta$ and its time derivative $\dot{\theta}$. This augmented system has a square input-output structure. The virtual dynamics for $z$ are chosen as an integrator chain of length two due to two reasons: the system input $u$ appears in $\ddot{e}_{1,2}$

$$\ddot{e}_1 = -Lw\left(\dot{x}_4 \sin x_3 - x_4^2 \cos x_3\right) - wx_4 \sin x_3 - \left(\tfrac{\partial^2 p_1}{\partial z_1^2} z_2^2 + \tfrac{\partial p_1}{\partial z_1} v\right) \tag{4.38a}$$

$$\ddot{e}_2 = \quad Lw\left(\dot{x}_4 \cos x_3 - x_4^2 \sin x_3\right) + wx_4 \cos x_3 - \left(\tfrac{\partial^2 p_2}{\partial z_1^2} z_2^2 + \tfrac{\partial p_2}{\partial z_1} v\right) \tag{4.38b}$$

and we want to avoid the appearance of derivatives of the input $u$. Checking the definition of the vector relative degree (4.9) for the augmented system (4.37) leads to the decoupling matrix

$$\mathbf{A}(x, z) = \begin{pmatrix} -\gamma \sin x_3 & -\frac{\partial p_1}{\partial z_1} \\ \gamma \cos x_3 & -\frac{\partial p_2}{\partial z_1} \end{pmatrix}, \quad \gamma = \tfrac{LwK}{\tau} \neq 0. \tag{4.39}$$

$\mathbf{A}(x, z)$ has full rank if and only if

$$\delta(x_3, z_1) := \left(\tfrac{\partial p_2}{\partial z_1} \sin x_3 + \tfrac{\partial p_1}{\partial z_1} \cos x_3\right) \neq 0. \tag{4.40}$$

This is always the case if the exact path-following condition obtained in (4.8) in Example 4.1 holds. From (4.8) it can be also deduced that if the ship follows the path exactly and $w > 0$, then forward motion is equivalent to

$$\dot{\theta} > 0 \quad \Leftrightarrow \quad \delta(x_3, z_1) > 0.$$

Consequently, the augmented dynamics (4.37) locally have a vector relative degree of $r = (2,\ 2)^T$. Next, we map (4.37) to a transverse normal form. Since $r = (2,\ 2)^T$, and recalling the structure of $\Phi$ from (4.35), it is clear that

$$\begin{pmatrix} \xi_1 \\ \xi_2 \\ \xi_3 \\ \xi_4 \end{pmatrix} = \Phi_\xi(x, z) = \begin{pmatrix} x_1 - p_1(z_1) \\ w \cos x_3 - Lwx_4 \sin x_3 - \frac{\partial p_1}{\partial z_1} z_2 \\ x_2 - p_2(z_1) \\ w \sin x_3 + Lwx_4 \cos x_3 - \frac{\partial p_2}{\partial z_1} z_2 \end{pmatrix} = \begin{pmatrix} e_1 \\ \dot{e}_1 \\ e_2 \\ \dot{e}_2 \end{pmatrix}. \tag{4.41}$$

Hence we only need to find two more elements of $\Phi$. If one follows directly the approach used in the proof of Lemma 4.1, and in Example 4.2, the choice would be

$$\eta = \Phi_\eta(x, z) = \begin{pmatrix} z_1 \\ z_2 \end{pmatrix} = \begin{pmatrix} \theta \\ \dot{\theta} \end{pmatrix}. \tag{4.42}$$

Provided that the Jacobian of $\Phi$ has full rank, which is equivalent to the condition

$$\left| \left( \frac{\partial \Phi}{\partial x}, \frac{\partial \Phi}{\partial z} \right) \right| = L^2 w^2 \ x_4 \neq 0,$$

this choice of coordinates defines a (local) diffeomorphism. The inverse map $\Phi^{-1}$ is, however, complicated, since for given $\xi_{2,4}$ and $\eta_{1,2}$ one needs to solve

$$\begin{aligned} \xi_2 &= w\cos x_3 - Lwx_4\sin x_3 - \tfrac{\partial p_1}{\partial \eta_1}\eta_2 \\ \xi_4 &= w\sin x_3 + Lwx_4\cos x_3 - \tfrac{\partial p_2}{\partial \eta_1}\eta_2 \end{aligned}$$

for $x_3$ and $x_4$. Furthermore, a complicated inverse $\Phi^{-1}$ often leads to complicated expressions in the transverse normal from, cf. Remark 4.2. Hence we discard $\Phi_\eta$ from (4.42). As pointed out in Remark 4.2, we are free to modify $\Phi_\eta$ from (4.42) to obtain more convienient expressions. Therefore we consider the alternative map $\tilde{\Phi} = (\Phi_\xi,\ \tilde{\Phi}_\eta)^T$, where

$$\eta = \tilde{\Phi}_\eta(x,z) = \begin{pmatrix} z_1 \\ x_3 \end{pmatrix} = \begin{pmatrix} \theta \\ x_3 \end{pmatrix}. \tag{4.43}$$

This choice is motivated by the fact that the remaining coordinates $\dot{\theta} = z_2$ and $x_4$ appear affinely in the equations for $\xi_2, \xi_4$ in (4.41). The Jacobian of $\tilde{\Phi}$ has full rank if and only if

$$\left| \left( \frac{\partial \tilde{\Phi}}{\partial x}, \frac{\partial \tilde{\Phi}}{\partial z} \right) \right| = -Lw \cdot \delta(x_3, z_1) \neq 0,$$

where $\delta(x_3,\theta)$ is as defined in (4.40). Note that this is equivalent to the condition ensuring a well-defined relative degree (4.40) of the augmented system (4.37). The full rank of the Jacobian of $\tilde{\Phi}$ is also implied by the exact path followability condition (4.8) given in Example 4.1. The inverse of $\tilde{\Phi}$ is

$$\begin{pmatrix} x \\ z \end{pmatrix} = \tilde{\Phi}^{-1}(\xi,\eta) = \begin{pmatrix} \xi_1 + p_1(\eta_1) \\ \xi_3 + p_2(\eta_1) \\ \eta_2 \\ \dfrac{1}{Lw\delta(\eta)} \left( \frac{\partial p_1}{\partial \eta_1}(\xi_4 - w\sin\eta_2) + \frac{\partial p_2}{\partial \eta_1}(w\cos\eta_2 - \xi_2) \right) \\ \eta_1 \\ \dfrac{1}{\delta(\eta)} \left( w - \xi_2\cos\eta_2 - \xi_4\sin\eta_2 \right), \end{pmatrix}, \tag{4.44}$$

where $\delta(\eta) = \delta(x_3, z_1)$ as in (4.40). Obviously, $\tilde{\Phi}^{-1}$ is defined for all $\eta \in \{\eta \in \mathbb{R}^2 \mid \delta(\eta) \neq 0\}$. The internal dynamics of the transverse normal form description of (4.37) are

$$\begin{pmatrix} \dot{\eta}_1 \\ \dot{\eta}_2 \end{pmatrix} = \frac{1}{Lw\delta(\eta)} \begin{pmatrix} Lw\left(w - \xi_2\cos\eta_2 - \xi_4\sin\eta_2\right) \\ \frac{\partial p_1}{\partial \eta_1}(\xi_4 - w\sin\eta_2) + \frac{\partial p_2}{\partial \eta_1}(w\cos\eta_2 - \xi_2) \end{pmatrix} = \begin{pmatrix} \beta_1(\xi,\eta) \\ \beta_2(\xi,\eta) \end{pmatrix}. \tag{4.45a}$$

The transverse dynamics of (4.37) are obtained using (4.38) and the fact that $\dot{x}_3 = x_4$

implies $\dot{\eta}_2 = \beta_2(\cdot) = x_4$. This leads to

$$\begin{pmatrix}\dot{\xi}_1\\ \dot{\xi}_2\\ \dot{\xi}_3\\ \dot{\xi}_4\end{pmatrix} = \begin{pmatrix} \xi_2 \\ -a_1\left((\beta_2(\cdot)+a_2u)\sin\eta_2 + a_3(\beta_2(\cdot))^2\cos\eta_2\right) - \frac{\partial^2 p_1}{\partial\eta_1^2}(\beta_1(\cdot))^2 - \frac{\partial p_1}{\partial\eta_1}v \\ \xi_4 \\ a_1\left((\beta_2(\cdot)+a_2u)\cos\eta_2 - a_3(\beta_2(\cdot))^2\sin\eta_2\right) - \frac{\partial^2 p_2}{\partial\eta_1^2}(\beta_1(\cdot))^2 - \frac{\partial p_2}{\partial\eta_1}v \end{pmatrix}, \tag{4.45b}$$

where the terms $\beta_{1,2}(\cdot) = \beta_{1,2}(\xi,\eta)$ are from (4.45a), and the constants $a_i, i = 1,\ldots,3$ are

$$a_1 = \frac{w(\tau - L)}{\tau}, \quad a_2 = \frac{KL}{\tau - L}, \quad a_3 = \frac{L\tau}{\tau - L}. \tag{4.46}$$

Finally, (4.45) states a transverse normal form description of the path-following problem for the ship dynamics (4.6). Note that forward motion on the path ($\dot{\xi}_{1,\ldots,4} = 0$) as well as existence and invertibility of $\tilde{\Phi}$ are guaranteed by the constraint $\delta(\eta) \geq 0$.
From (4.45) we can also calculate inputs $u_{\mathcal{P}}$ and $v_{\mathcal{P}}$ which render the zero-path-error manifold positively invariant. Rendering the zero-path-error manifold positively invariant implies application of inputs to the transversal dynamics (4.45b) such that $\xi = \dot{\xi} = 0$ holds. In other words, one needs to calculate output-zeroing inputs for (4.45). Setting $\xi_{1,\ldots,4} = 0$ this is achieved by solving $\dot{\xi}_{2,4} = 0$ for $u$ and $v$. Since the inputs appear affinely in (4.45b) we obtain without difficulty the exact path-following inputs $u_{\mathcal{P}}, v_{\mathcal{P}}$

$$\left(u_{\mathcal{P}},\ v_{\mathcal{P}}\right)^T = \mathbf{A}^{-1}(\eta)\cdot k_{\mathcal{P}}(\xi,\eta)|_{\xi=0}, \tag{4.47}$$

where

$$k_{\mathcal{P}}(\xi,\eta) = \begin{pmatrix} a_1\left(\beta_2(\xi,\eta)\sin\eta_2 + a_3(\beta_2(\xi,\eta))^2\cos\eta_2\right) + \frac{\partial^2 p_1}{\partial\eta_1^2}(\beta_1(\xi,\eta))^2 \\ -a_1\left(\beta_2(\xi,\eta)\cos\eta_2 - a_3(\beta_2(\xi,\eta))^2\sin\eta_2\right) + \frac{\partial^2 p_2}{\partial\eta_1^2}(\beta_1(\xi,\eta))^2 \end{pmatrix}.$$

The matrix $\mathbf{A}^{-1}(\eta)$ is directly the inverse of the decoupling matrix (4.39) expressed in $\xi,\eta$ coordinates. Again $\delta(\eta) > 0$ is sufficient to guarantee the existence of $\mathbf{A}^{-1}(\eta)$. The exact path-following inputs are unique and depend on the zero dynamics $\dot{\eta} = \beta(0,\eta)$. This implies that the speed to follow the path along exactly is not free. Note that the internal dynamics (4.45a) for $\xi = 0$ are directly the equations (4.7) obtained in the previous consideration of the ship example.
Now, consider the following parameter values for the ship (4.37) $w = 10$m/s, $L = 3.92$, $K = -0.036$ and $\tau = 22.32$s. The path to be followed is given by the regular curve

$$p(\theta) = \begin{pmatrix}\theta \\ c_1\sin(c_2\theta)\end{pmatrix}^T. \tag{4.48}$$

The path constants are $c_1 = -10^3$ and $c_2 = -1.5 \cdot 10^{-3}$. For this particular path and the given parameters we solve the internal dynamics (4.45a) under the condition $\xi = 0$. The phase portrait of the zero dynamics is depicted in Figure 4.3. For any initial condition with $\delta(\eta(0)) > 0$ the path parameter $\eta_1(t) = z_1(t)$ grows unboundedly. For $\delta(\eta(0)) > 0$ the solutions converge to a stable oscillation in the phase plane which is depicted as a continuous blue curve $(\eta_{1,\mathcal{P}}, \eta_{2,\mathcal{P}})$ in Figure 4.3. For initial conditions with $\delta(\eta(0)) < 0$ we have $\dot{\eta}_1 = \dot{z}_1(t) < 0$ and $\eta_1(t) \to -\infty$. The red curves illustrate the convergence of solutions $\eta(t)$ for different initial conditions with $\delta(\eta(0)) < 0$. Again the solutions converge—now to the blue dash-dot curve $(\eta_{1,\mathcal{P}}, \eta_{2,\mathcal{P}})$ in Figure 4.3. This curve refers to the zero-dynamics (4.45a) for a backward motion with $\eta_1 < 0$ along $\mathcal{P}$. The behavior of $\eta_{1,\mathcal{P}}(t)$ and $\eta_{2,\mathcal{P}}(t)$ in the time domain for $\delta(\eta) > 0$ is shown in Figure 4.4 left. The exact path-following inputs $u_{\mathcal{P}}(t), v_{\mathcal{P}}(t)$ are depicted in Figure 4.4 right. One can also construct a nonlinear controller to stabilize the path. The exact path-following inputs $u_{\mathcal{P}}, v_{\mathcal{P}}$ (4.47) are obtained via static input-output linearization of (4.37). Hence the feedback

$$\left(u_{\mathcal{P}},\ v_{\mathcal{P}}\right)^T = \mathbf{A}^{-1}(\eta)\left(k_{\mathcal{P}}(\xi,\eta) + K\xi\right)$$

leads to linear input-output dynamics and nonlinear internal dynamics

$$\begin{aligned}\dot{\xi} &= (A + BK)\xi \\ \dot{\eta} &= \beta(\xi,\eta).\end{aligned}$$

Obviously, $K$ has to be chosen such that the transversal part of the dynamics is stabilized. Such an approach suffers from the general drawbacks of input-output linearization. The linearizing part of the feedback $\mathbf{A}^{-1}(\eta)k_{\mathcal{P}}(\xi,\eta)$ can be very large. Especially, if the initial condition is close to $\delta(\eta) = 0$. For $\delta(\eta) = 0$ the matrix $\mathbf{A}(\eta)$ is singular. The initial condition determines, if the path is transversed with $\dot{\theta} > 0$ or $\dot{\theta} < 0$. In general, one needs to check whether the internal dynamics are stable or not.

Our approach via the augmented dynamics (4.37) allows deriving a transverse normal form for this example. Comparing Example 4.2 on robot path following with this example several issues can be noted: Since the original ship model (4.6) has only one input and two outputs we have no input left to stabilize the internal dynamics. However, for general systems with square input-output structures—and fulfilling Assumptions 4.1–4.3—the path parameter input $v$ appears in the internal dynamics of the augmented system, cf. Example 4.2. Thus this virtual input might be used to stabilize the internal dynamics. Finally, the conclusion from this example is that the price for allowing a non-square input-output structure are uncontrolled internal dynamics. Moreover, we have seen that the derivation of a transverse normal form can be difficult. Yet, the approach allows a structured assessment of path followability.

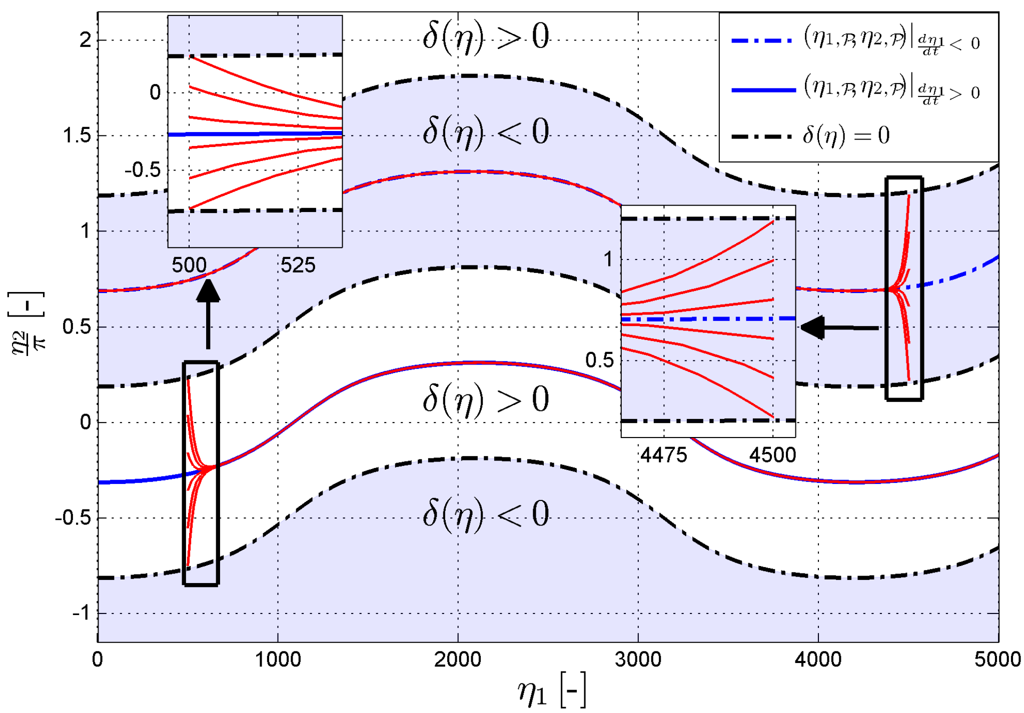


**Figure 4.3:** Phase portrait of the zero dynamics of (4.45).

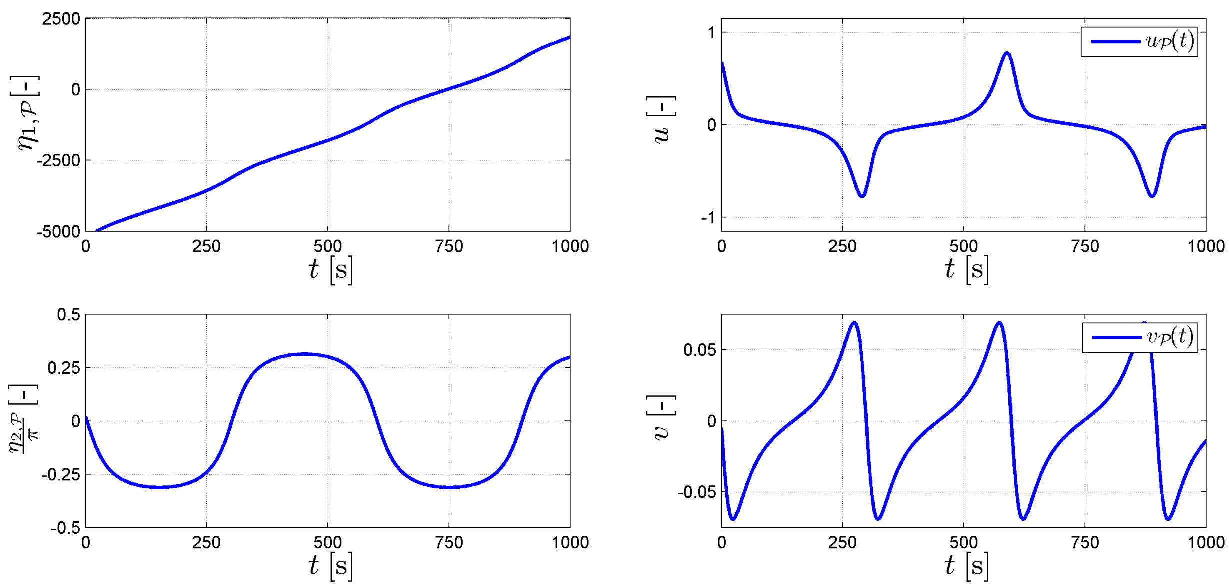


**Figure 4.4:** Nominal solution to (4.45a) and exact path-following inputs for $\delta(\eta) > 0$.

## 4.4 Constrained Path Followability of Flat Systems

So far our results do not allow to assess path followability in the presence of constraints directly. We know, however, that the dynamics on the zero-path-error manifold are governed by the internal dynamics of the augmented system (4.14) with respect to the error output $e = h(x) - p(\theta)$. If we rely on assumptions on the structure of the augmented system (4.14) and its internal dynamics, it is easier to answer the question of path followability in presence of constraints. In other words, we change the class of considered systems such that in the transverse normal form description (4.21) no internal dynamics of the original system (4.1) are present.

One way to ensure this is as follows: As before consider the nonlinear system (4.1). Temporarily suppose that locally the vector relative degree $r = (r_1, \ldots, r_{n_y})^T$ of (4.1) is such that $\rho = \sum_{i=1}^{n_y} r_i = n_x$. This implies that (locally) the dimension of the internal dynamics is $\dim \eta_1 = n_x - \rho = 0, \dim \eta_2 = \hat{r} + 1$. The requirement $\rho = n_x$ is equivalent to the requirement that the orignal system (4.1) is statically feedback linearizable. Here, we do not use this assumption but a more general one.

Subsequently, we assume that the considered system (4.1) is *differentially flat*. For MIMO systems static feedback linearizability is a sufficient condition for flatness [Fliess et al. 1995b; Lévine 2009; Martin et al. 1997; Rothfuß 1997; Sira-Ramírez and Agrawal 2004].[4] Moreover, also systems which are linearizable by endogenous dynamic feedbacks are differentially flat. Thus flatness of (4.1) is more general than static feedback linearizablility. The focus on flat systems enables us to state sufficient conditions for exact path followability in the presence of constraints on states and inputs. Formally flatness can be defined as follows, cf. [Fliess et al. 1995b; Lévine 2009; Rothfuß 1997].

**Definition 4.3** (Differential flatness).
*Consider the system* (4.1). *If there exists a variable* $\zeta = (\zeta_1, \ldots, \zeta_{n_u})^T$ *with* $\dim \zeta = \dim u$ *such that the following statements hold at least locally:*

*i) The variable $\zeta$ can be written as a function of the state variables $x = (x_1, \ldots, x_{n_x})^T$, the input variables $u = (u_1, \ldots, u_{n_u})^T$, and a finite number of time derivatives of the input variables*

$$\zeta = k\left(x, u_1, \ldots, u_1^{(l_1)}, \ldots, u_{n_u}, \ldots, u_{n_u}^{(l_{n_u})}\right). \tag{4.49a}$$

*ii) The system variables $x$ and $u$ can be expressed as functions of the variable $\zeta = [\zeta_1, \ldots, \zeta_{n_u}]^T$ and a finite number of time-derivatives of $\zeta$. Hence*

$$x = \Phi\left(\zeta_1, \ldots, \zeta_1^{(k_1-1)}, \ldots, \zeta_{n_u}, \ldots, \zeta^{(k_{n_u}-1)}\right), \tag{4.49b}$$

$$u = \Psi\left(\zeta_1, \ldots, \zeta_1^{(k_1)}, \ldots, \zeta_{n_u}, \ldots, \zeta_{n_u}^{(k_{n_u})}\right). \tag{4.49c}$$

[4]For SISO systems differential flatness is equivalent to static feedback linearizability [Charlet et al. 1989, 1991].

*A variable $\zeta$ satisfying i)–ii) is called a* flat output *of* (4.1)*. And* (4.1) *is called a (differentially) flat system.*

Note that if a system is flat, the flat output is not unique. For example, consider a system with two inputs. If $y = (y_1,\ y_2)^T$ is a flat output, then $z = (y_1 + \dot{y}_2,\ y_2)^T$ is also a flat output, since $y = (z_1 - \dot{z}_2,\ z_2)^T$, cf. [Lévine 2009].
Flatness can, simplistically, be interpreted as follows: The map $\Phi$ (4.49b) parametrizes the state $x(t)$ in terms of a flat output $\zeta(t)$ and its time derivatives. This can be understood as an observability property of a flat output $\zeta$. Additionally, the map $\Psi$ (4.49c) parametrizes the input $u(t)$ in terms of the flat output. This implies that if we want to steer a flat system from $x_0(t_0)$ to $x_1(t_1)$, it suffices to compute an output trajectory $\zeta(t) \in \mathcal{C}^{(\hat{k})}$ such that $x_0 = \Phi(\zeta_1(t_0), \ldots, \zeta^{(k_{n_u}-1)}(t_0)$ and $x_1 = \Phi(\zeta_1(t_1), \ldots, \zeta^{(k_{n_u}-1)}(t_1)$. Hence flatness implies a (local) nonlinear reachability property. For details on flatness and its implications for controller design we refer to [Fliess et al. 1995b; Hagenmeyer 2003; Lévine 2009; Martin et al. 1997; Rothfuß 1997; Sira-Ramírez and Agrawal 2004] and the references therein.
A consequence of the previous definition is that flat systems have a square input-output structure. Thus Assumption 4.1 remains valid. We replace the relative degree Assumption 4.2 by an assumption that the path is defined in a flat output space of the system. Additionally, Assumption 4.3 needs to be modified. The required degree of continuous differentiability is now defined via the derivatives of the flat output appearing in (4.49c). This leads to the following assumptions.

**Assumption 4.4** (Differentially flat system)**.**
*System* (4.1) *is differentially flat. The output* (4.1b) *is a flat output of* (4.1)*.*

**Assumption 4.5** (Timing law and path parametrization)**.**
*i) The timing law $g$ from* (4.3) *is chosen as*

$$\theta^{(\hat{k}+1)} = v, \quad \theta(t_0) = \theta_0,\ \forall j \in 1, \ldots, \hat{k} : \theta^{(j)}(t_0) = 0,$$

*with $\hat{k} = \max\{1, \ldots, k_{n_u}\}$ from* (4.49c)*.*
*ii) The path parametrization $p(\theta)$ from* (4.2) *is $\hat{k}$-times continuously differentiable with $\hat{k} = \max\{1, \ldots, k_{n_u}\}$ from* (4.49c)*.*

**Assumption 4.6** (Input and state constraints)**.**
*The input and state constraints of* (4.1) *are described by continuous functions $c_x^i : \mathbb{R}^{n_x} \to \mathbb{R}$ and $c_u^i : \mathbb{R}^{n_u} \to \mathbb{R}$ as $c_x^i(x) \leq 0$ and $c_u^i(u) \leq 0$.*

The last assumption is purely technical and will be used in the proof of Theorem 4.3 later on. For convenient notation we write the evaluation of $\Phi$ (4.49b) along an output trajectory $\zeta(t)$ as $x(t) = \Phi(\cdot)|_{\zeta(t)}$. If we refer to a single point rather than a trajectory we write $x(t_0) = \Phi(\cdot)|_{\zeta(t=t_0)}$. The evaluation of $\Psi$ from (4.49c) is denoted in the same fashion.

Subsequently, we derive sufficient conditions for exact path followability of flat systems in the presence of constraints. Moreover, we propose an optimal control problem subject to a small dimensional linear single input system, which allows to compute admissible feedforward controls that nominally guarantee exact path-following. The consideration of constraints is simplified due to the fact that property (4.49b) implies that (4.1) has no internal dynamics. In order to be precise about our later results we reformulate the path followability problem implicity stated in Definition 4.1 as follows.

**Problem 4.2** (Optimal exact path following).
*Given the constrained system* (4.1)*, and a path* $\mathcal{P}$ (4.2) *to be followed. Find a transition time* $T > 0$ *and an input signal* $u : [0, T] \to \mathcal{U}$ *such that the following conditions are satisfied:*

*i)* ***Exact Path-following:*** *The system output* (4.1b) *moves from a consistent initial condition* $h(x_0) = p(\theta_0)$ *in forward direction exactly along the path* $\mathcal{P}$*. Hence for all* $t \in [0, T]$ *it holds that* $\dot{\theta}(t) \geq 0$ *and* $h(x(t, x_0|u(\cdot))) \in \mathcal{P}$*.*

*ii)* ***Constraint Satisfaction:*** *For all* $t \in [0, T]$ *the feedforward signal* $u(\cdot)$ *satisfies the input constraints* $u(t) \in \mathcal{U}$*, and the corresponding system trajectory satisfies the state constraints* $x(t, x_0|u(\cdot)) \in \mathcal{X}$*.*

*iii)* ***Cost Minimization:*** *The feedforward input signal is designed such that the cost functional*

$$J(u(\cdot), x(\cdot)) = \int_0^T 1 + F(x(\tau), u(\tau)) \, d\tau, \tag{4.50}$$

*with* $F : \mathcal{X} \times \mathcal{U} \to \mathbb{R}_0^+$ *and* $F(x, u) \in \mathcal{C}^1$*, is minimized.*

It is well-known that trajectory tracking or set point changes can be achieved easily for flat systems, cf. [Fliess et al. 1995b; Lévine 2009; Sira-Ramírez and Agrawal 2004]. If a sufficiently smooth reference trajectory is known a priori, one basically exploits (4.49c) and obtains a suitable feedforward control. Consequently, it is rather easy to state sufficient conditions for *unconstrained* exact path followability of flat systems.

**Lemma 4.2** (Unconstrained path followability of flat systems).
*Given an unconstrained nonlinear flat system* (4.1) *and any regular path* $\mathcal{P}$ *specified by an a priori known parametrization* $p(\theta)$ *in a flat output space* (4.1b)*.*
*Suppose that*

*i) the parametrization* $p(\theta) \in \mathcal{C}^{\hat{k}}$*, where* $\hat{k} = \max\{k_i\}$ *and the constants* $k_i \in \mathbb{N}$ *are defined by* (4.49c)*;*

*ii) the initial condition* $x_0$ *of* (4.1) *is consistent with* $\mathcal{P}$ *and* $\theta(t) \in \mathcal{C}^{\hat{k}}$*, i.e.*

$$x_0 = \Phi\left(\cdot\right)|_{p(\theta(t=0))}, \tag{4.51}$$

*where* $\dot{\theta}(t) \geq 0$*, and* $\theta(0) = \theta_0$*,* $\theta(T) = \theta_1$*.*

*Then the feedforward input*

$$u(t) = \Psi\left(p_1(\theta(t)), \dots, \frac{d^{k_1} p_1(\theta(t))}{dt^{k_1}}, \dots, p_{n_y}(\theta(t)), \dots, \frac{d^{k_{n_y}} p_{n_y}(\theta(t))}{dt^{k_{n_y}}}\right) \tag{4.52}$$

*guarantees that the system* (4.1)*, starting from* $x_0$*, follows the path* $\mathcal{P}$ *exactly in forward direction.*

*Proof.* The proof of this lemma follows directly by calculation of the time derivatives of $p(\theta(t))$, use of (4.49c) and the ideas, e.g. presented in [Hagenmeyer and Delaleau 2003; Lévine 2009; Sira-Ramírez and Agrawal 2004]. The path $\mathcal{P}$ and its parametrization $p(\theta)$ are given a priori. Thus $p(t) := p(\theta(t))$ is the reference to be followed. The time derivatives of all components $p_i(\theta)$, $i = 1, \dots, n_y$ of this reference are

$$\dot{p}_i(\theta(t)) = \partial_\theta p_i(\theta) \cdot \dot{\theta} \tag{4.53a}$$

$$\ddot{p}_i(\theta(t)) = \partial_\theta^2 p_i(\theta) \cdot \dot{\theta}^2 + \partial_\theta p_i(\theta) \cdot \ddot{\theta} \tag{4.53b}$$

$$\vdots \qquad \vdots$$

$$\frac{d^{k_i} p_i(\theta(t))}{dt^{k_i}} = \partial_\theta^{k_i} p_i(\theta) \cdot \dot{\theta}^{k_i} + \dots + \partial_\theta p_i(\theta) \cdot \theta^{(k_i)}. \tag{4.53c}$$

Since $\theta(t) \in \mathcal{C}^{\hat{k}}$ and $\hat{k}$ as in condition i), each component of $p(\theta)$ satisfies $p_i(\theta(t)) \in \mathcal{C}^{\hat{k}}$. Hence we substitute these derivatives into the flat input parametrization given by (4.49c). This yields (4.52). Condition ii) of the lemma ensures that the initial condition of the system (4.1) is consistent with the path $\mathcal{P}$ and a timing $\theta(t)$. Due to the flatness of (4.1) it follows, that any non-decreasing timing $\theta(t)$ specifies an input $u = \Psi(\cdot)|_{p(\theta(t))}$ which follows the path $\mathcal{P}$ exactly in forward direction. □

The challenging part is to extend Lemma 4.2 such that constraints on inputs and states can be considered. We start with a technical lemma. It is subsequently used to project the feedforward controlled nonlinear MIMO dynamics (4.1) along the path $\mathcal{P}$ to a linear single-input system in Brunovský normal form. Finally, the projection is used to obtain a small dimensional optimal control problem and sufficient conditions for exact path followability.

**Lemma 4.3.**
*Given a regular path* $\mathcal{P} \subset \mathbb{R}^{n_y}$ *from* (4.2) *and its* $k$*-times continuously differentiable parametrization* $\theta \mapsto p(\theta)$*. Suppose that the time evolution* $t \mapsto \theta(t)$ *is also* $k$*-times continuously differentiable. Then the map* $\Delta : \mathbb{R}^{k+1} \to \mathbb{R}^{n_y \times (k+1)}$

$$\Delta : \left(\theta, \dot{\theta}, \dots, \theta^{(k)}\right)^T \mapsto \left(p, \dot{p}, \dots, p^{(k)}\right)$$

*given by* $p(\theta(t))$ *and its time derivatives is locally invertible for all values of* $\left(p, \dot{p}, \dots, p^{(k)}\right)^T$ *which are contained in the image of* $\Delta$*.*

*Proof.* The regularity of $\mathcal{P}$ implies the local bijectivity of $\theta \mapsto p(\theta)$ and $rank\,(\partial_\theta p(\theta)) = 1$ for all $\theta$, cf. [Topogonov 2006]. Therefore, given the parametrization $p(\theta)$ and a specific point $y \in \mathcal{P}$, the equation $y = p(\theta)$ can be locally solved for the unique value of $\theta$. Due to the rank condition, it follows that at least one component of $\partial_\theta p(\theta) = (\partial_\theta p_1(\theta), \dots, \partial_\theta p_i(\theta), \dots, \partial_\theta p_{n_y}(\theta))^T$ is not equal to zero. Hence one can solve $\dot{p}_i = \partial_\theta p_i(\theta) \cdot \dot{\theta}$ for $\dot{\theta}$. Using the equation for $\ddot{p}(\theta)$, and the previously calculated values of $\theta$ and $\dot{\theta}$, one can determine $\ddot{\theta}$ from $\ddot{p}_i - \partial_\theta^2 p_i(\theta) \cdot \dot{\theta}^2 = \partial_\theta p_i(\theta) \cdot \ddot{\theta}$. Following this procedure for the remaining time derivatives of $p(\theta)$ one obtains the unique values of $\dddot{\theta}, \dots, \theta^{(k)}$. □

The following result sets the conceptual basis for the further considerations.

**Theorem 4.2** (Equivalence to single input system)**.**
*Given a nonlinear flat system* (4.1) *and a regular path* $\mathcal{P}$ *specified by an a priori known parametrization* $p(\theta)$ *in a flat output space of* (4.1). *Suppose that conditions i) and ii) of Lemma 4.2 are satisfied.*
*Then the dynamics of the nonlinear MIMO system* (4.1) *under the feedforward control* $u = \Psi(\cdot)|_{p(\theta(t))}$ *given by* (4.52), *where* $\theta(t)$ *is of class* $\mathcal{C}^{\hat{k}}$, *are equivalent to a linear, single input system in Brunovský normal form.*

*Proof.* Provided that condition i) of Lemma 4.2 is satisfied, any choice of a class $\mathcal{C}^{\hat{k}}$ timing $\theta(t)$ specifies a sufficiently often continuously differentiable output reference trajectory for the flat system (4.1). It follows that system (4.1) under the feedforward control (4.52) is equivalent to a linear MIMO system in Brunovský normal form such that for all $i = 1, \dots, n_y$

$$\dot{\chi}_i = \left(\begin{array}{c|c} \mathbf{0}^{k_i-1\times 1} & \mathbf{I}^{k_i-1\times k_i-1} \\ \hline 0 & \mathbf{0}^{1\times k_i-1} \end{array}\right) \chi_i + \begin{pmatrix} \mathbf{0}^{k_i-1\times 1} \\ 1 \end{pmatrix} \frac{d^{k_i} p_i(\theta(t))}{dt^{k_i}} \tag{4.54}$$

where the time derivatives $\frac{d^{k_i} p_i(\theta(t))}{dt^{k_i}}$ are the inputs, see [Hagenmeyer and Delaleau 2003]. On the one hand, the input and state parametrizations (4.49b-c) reveal that any choice of $\theta(t) \in \mathcal{C}^{\hat{k}}$ leads to a unique state evolution of (4.1). On the other hand, Lemma 4.3 states that from the knowledge of the parametrization $p(\theta)$ and the values $p, \dot{p}, \dots, p^{(\hat{k})}$ the values of $\theta, \dot{\theta}, \dots, \theta^{(\hat{k})}$ can be uniquely determined. Thus the dynamics of the system (4.1) along a given regular path $\mathcal{P}$ are uniquely described by the choice of a class $\mathcal{C}^{\hat{k}}$ timing $\theta(t)$. Therefore the MIMO Brunovský normal form reduces to the following single input Brunovský normal form

$$\begin{aligned} \dot{z}_1 &= z_2 \\ \dot{z}_2 &= z_3 \\ &\vdots \\ \dot{z}_{\hat{k}+1} &= \theta^{(\hat{k}+1)}(t), \end{aligned} \tag{4.55}$$

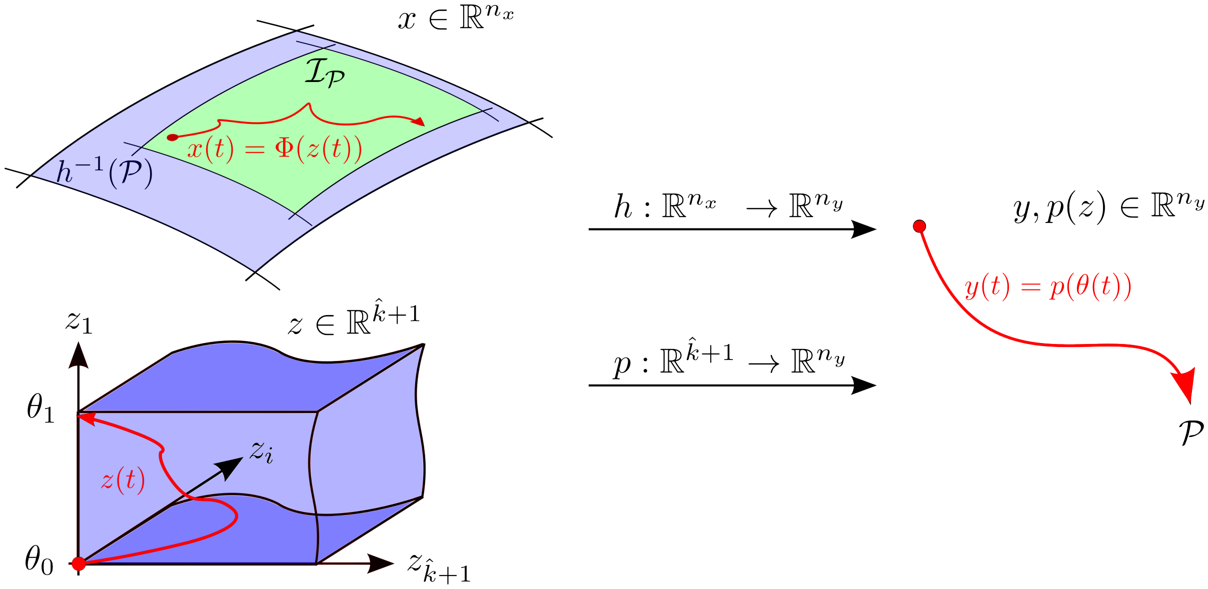


**Figure 4.5:** Geometric interpretation of Theorem 4.2.

where the $\hat{k}+1$-th time derivative of $\theta(t)$ can be regarded as free input variable. Since system (4.1) under the feedforward control $u = \Psi(\cdot)|_{p(\theta(t))}$ is equivalent to (4.54), and the latter is equivalent to (4.55), it follows that (4.1) is also equivalent to (4.55). □

The core statement of the last theorem is illustrated in Figure 4.5. The motion along the path using the feedforward input (4.52) is completely parametrized by the states $z_1, \ldots, z_{\hat{k}+1}$ of (4.55). This implies that the dimension of the zero-path-error manifold $\mathcal{I}_\mathcal{P}$ is zero, since the transversal directions as introduced in Section 4.3.1 have dimension $n_x$. Comparing this to the result on the transversal normal form reveals an essential difference: no internal dynamics related to the state $x$ are present, cf. Figure 4.2 in Section 4.3.1.

### 4.4.1 Optimal Exact Feedforward Path Following

The previous considerations show that the feedforward input $u = \Psi(\cdot)|_{p(\theta(t))}$ can be reformulated as a function of $\theta(t)$ and its first $\hat{k}$ time derivatives. Equivalently, one may use the representation via the single input system (4.55). Recall the path parameter dynamics (4.12), where the $\hat{k}+1$-th time derivative of $\theta(t)$ is the path parameter input $v$. Similar to (4.12) we use the substitution

$$z := (z_1, z_2, \ldots, z_{\hat{k}+1})^T = \left(\theta, \dot{\theta}, \ldots, \theta^{(\hat{k})}\right)^T.$$

We rewrite (4.52) and (4.49b) as

$$u = \Psi\left(\theta, \dot{\theta}, \ldots, \theta^{(\hat{k})}\right) =: \Psi(z) \tag{4.56a}$$

$$x = \Phi\left(\theta, \dot{\theta}, \ldots, \theta^{(\hat{k}-1)}\right) =: \Phi(z). \tag{4.56b}$$

Consider the feedforward path-following task stated in Problem 4.2 for (4.1). A feedforward input signal, which respects the constraints $(x, u) \in \mathcal{X} \times \mathcal{U}$, is given by the solution of the following optimal control problem

$$\underset{v(\cdot),T}{\text{minimize}} \int_0^T 1 + F(x(\tau), u(\tau))\, d\tau \tag{4.57a}$$

subject to the dynamics

$$\dot{z} = Az + Bv, \tag{4.57b}$$

the (convex) state constraints

$$z(0) = [\theta_0, 0, \ldots, 0]^T, \tag{4.57c}$$

$$z(T) = [\theta_1, 0, \ldots, 0]^T, \tag{4.57d}$$

$$\forall t \in [0, T]: \quad z_2 \geq 0, \tag{4.57e}$$

and the additional constraints

$$\forall t \in [0, T]: \quad u(t) = \Psi(z(t)) \in \mathcal{U}, \tag{4.57f}$$

$$\forall t \in [0, T]: \quad x(t) = \Phi(z(t)) \in \mathcal{X}, \tag{4.57g}$$

$$\forall t \in [0, T]: \quad v(t) \in \mathcal{V}. \tag{4.57h}$$

Note that the proposed optimal control problem has a small number of linearly coupled dynamic states. Scalar input $v(\cdot)$ and free end time $T$ are decision variables. The class of considered virtual inputs $v(\cdot)$ are scalar measurable functions taking values in a sufficiently large closed interval $\mathcal{V} \subset \mathbb{R}$. The cost functional (4.57a) directly expresses the requirement from part ii) of Problem 4.2. The dynamics (4.57b) are the path parameter dynamics as defined in (4.12). Note that due to Assumption 4.5 we have an integrator chain of length $\hat{k} + 1$ as timing law. The constraints (4.57c-d) state that the initial path point is $p(\theta_0)$, and the final path point is $p(\theta_1)$. Equation (4.57e) expresses the condition on forward movement along the path. The constraints on states and inputs of the flat system (4.1) $u = \Psi(z) \in \mathcal{U}, x = \Phi(z) \in \mathcal{X}$ are considered via (4.57f,g), cf. part ii) of Problem 4.2. Note that the optimal solution $v^\star(\cdot)$ is the input to the virtual system (4.57b). Finally, the input applied to the nonlinear differentially flat system (4.1) is calculated from the optimal evolution of $z(t, z_0|v^\star(\cdot))$ via the input parametrization $u(t) = \Psi(z(t, z_0|v^\star(\cdot)))$ from (4.56). In order to achieve that the original system (4.1) follows the path $\mathcal{P}$ exactly, it suffices to compute any admissible solution $v$ to (4.57) and the corresponding evolution of $z(t, z_0|v(\cdot))$.

**Remark 4.6** (Bang-bang solutions).
*If the cost function is $F(x,u) = 0$, the condition (4.57h) is necessary in order to avoid impulsive solutions, which typically arise in minimum-time or cheap optimal control problems. In general, the OCP (4.57) might have* bang-bang *solutions for $v(\cdot)$. The virtual input $v$ acts on the derivative of $z_{\hat{k}+1} = \theta^{(\hat{k})}$. Thus the restriction of $v$ to a compact set $\mathcal{V}$ and $\Psi \in \mathcal{C}^0$ ensure that the input applied to the original system $u = \Psi(z_1, \dots, z_{\hat{k}+1})$ is continuous.*

For general flat systems and arbitrary paths $\mathcal{P}$ the constraints of the proposed optimal control problem will usually be non-convex due to the nonlinear maps $\Psi$ and $\Phi$ from (4.57f–g). Nevertheless, under fairly mild assumptions, the existence of optimal solutions to (4.57) in the presence of constraints on states and inputs of the original system (4.1) can be guaranteed. To this end we investigate the relation between a path $\mathcal{P}$, the set of steady states, and the constraints of (4.1).

**Definition 4.4** (Steady state consistent path).
*We call a path $\mathcal{P}$ from (4.2) weakly steady state consistent with respect to system (4.1) and its constraints $\mathcal{X}$ and $\mathcal{U}$, if for all $\theta \in [\theta_0, \theta_1]$ exist $(x_s, u_s)^T \in \operatorname{int}(\mathcal{X} \times \mathcal{U})$ s.t.*

$$0 = f(x_s, u_s), \tag{4.58a}$$

$$p(\theta) = h(x_s, u_s, 0, \dots, 0) \tag{4.58b}$$

*hold.*
*If additionally for all $\theta \in [\theta_0, \theta_1]$ we have that $(x_s, u_s) \in \operatorname{int}(\mathcal{X} \times \mathcal{U})$ then we call $\mathcal{P}$ strongly steady state consistent.*

Let $\mathcal{Z} \subset \mathbb{R}^{\hat{k}+1}$ be the set of all states $z$ which satisfy the constraints (4.57c-e). This is equivalent to our previous introduction of $\mathcal{Z}$ in (4.13). For steady state consistent paths the following result holds.

**Theorem 4.3** (Constrained path followability of flat systems).
*Given a flat system (4.1), a path $\mathcal{P}$ (4.2), Assumptions 4.4–4.6, and the corresponding optimal control problem (4.57).*
*Suppose that conditions i) and ii) of Lemma 4.2 are satisfied, and $[\theta_0, \theta_1]$ is compact. Moreover, assume that*

*i) the maps $\Psi : z \in \mathbb{R}^{\hat{k}+1} \mapsto u \in \mathbb{R}^{n_u}$ and $\Phi : z \in \mathbb{R}^{\hat{k}+1} \mapsto x \in \mathbb{R}^{n_x}$ from (4.56) are continuous in a neighborhood of the set $\{[\theta_0, \theta_1] \times 0 \times \dots \times 0\} \subset \mathcal{Z}$;*
*ii) the path $\mathcal{P}$ is strongly steady state consistent with respect to (4.1) and the constraint sets $\mathcal{X}$,$\mathcal{U}$.*

*Then*

a) *$\mathcal{P}$ is exactly followable by system* (4.1) *s.t. the constraints $x \in \mathcal{X}$ and $u \in \mathcal{U}$ are satisfied;*

b) *and if condition i) holds for all $z \in \mathcal{Z}$, then OCP* (4.57) *has an optimal solution. Moreover, if the minimum-time case ($F(x, u) = 0$) is considered, then the minimal transition time $T^\star$ is finite.*

*Proof.* Our proof is based on the construction of an admissible solution to (4.57). We proceeds in four steps. Firstly, we express the supposition of strongly path consistency in terms of the flat state and input parametrizations. Secondly, we split the integrator chain (4.57b) into two parts, consider the last integrator as a flat system, and use that $[\theta_0, \theta_1]$ is compact. We construct an admissible reference signal for $z_2(t) = \dot{\theta}$ which guarantees that $\theta_1 < \infty$ is reached in finite time. In the third step, we consider the remaining $\hat{k}$ integrators again as a flat system, and design an admissible $v$ such that the desired $z_2(t)$ trajectory is perfectly tracked. This leads to part a). Finally, we conclude from the existence of an admissible input $v : [0, T] \to \mathcal{V}$ to the existence of an optimal finite-time solution to (4.57) (part b)).

**Step 1**: In terms of the flat input and state parametrization a strongly steady state consistent path implies that for all $z_1 \in [\theta_0, \theta_1]$

$$\Phi(z_1, 0, \ldots, 0) \in \operatorname{int} \mathcal{X}, \tag{4.59a}$$

$$\Psi(z_1, 0, \ldots, 0) \in \operatorname{int} \mathcal{U}. \tag{4.59b}$$

In the following we focus solely on the constraint $\Psi(\cdot) \in \mathcal{U}$ since the consideration of $\Phi(\cdot) \in \mathcal{X}$ relies on the same concept. Consider the set $\tilde{\mathcal{Z}} := [\theta_0, \theta_1] \times [0, c_2] \times [-c_3, c_3] \times \cdots \times [-c_{\hat{k}+1}, c_{\hat{k}+1}]$. Due to the continuity of $\Psi(\cdot)$ on a neighborhood of $\{[\theta_0, \theta_1] \times 0 \times \cdots \times 0\} \subset \mathcal{Z}$ there exists constants $c_i$ such that the image of $\tilde{\mathcal{Z}}$ under $\Psi$ is completely contained in the interior of $\mathcal{U}$. The main idea is to rely on the tightened constraint set $\tilde{\mathcal{Z}}$ since keeping $z(t)$ in $\tilde{\mathcal{Z}}$ suffices to satisfy (4.57f). Thus we restrict the considerations to $\tilde{\mathcal{Z}}$ with $\Psi(\tilde{\mathcal{Z}}) \in \operatorname{int} \mathcal{U}$.

W.l.o.g. assume that there exists a function $\gamma(t) \in \mathbb{R}$, defined on $t \in [0, s], 0 < s < \infty$, which is monotonously increasing $\dot{\gamma}(t) \geq 0$ and $\gamma(t) \in \mathcal{C}^{\hat{k}}$. Moreover, this function can be chosen such that $\gamma(0) = 0$, $\gamma(s) = c_2$, $\gamma^{(i)}(t)|_0 = \gamma^{(i)}(t)|_s = 0$ for $i = 1, \ldots, \hat{k}$. And $\gamma^{(i)} \in [-c_{i+1}, c_{i+1}]$ for all $i = 1, \ldots, \hat{k}$ holds. Basically, $\gamma(t)$ is a sufficiently smooth signal which increases from 0 to $c_2$ during some finite time $s$, while its time derivatives remain bounded. Using $\gamma(t)$ we can construct a reference motion for $z_2(t)$.

**Step 2**: Consider the last part of the integrator chain (4.57b) and denote $z_2$ as $w$, hence $\dot{z}_1 = w$. Next, we design a signal $w \in [0, c_2]$ which is sufficiently often continuously differentiable ($w \in \mathcal{C}^{\hat{k}}$) and ensures for some $T < \infty$ that $z_1(T, \theta_0|w) = \theta_1$. Using the function $\gamma(t)$ introduced before we choose $w$ as

$$w(t,T) = \begin{cases} \gamma(t), & t \in [0, s] \\ c_2, & t \in (s, s+T) \\ c_2 - \gamma(t), & t \in [s+T, 2s+T]. \end{cases}$$

Due to the properties of $\gamma(t)$ the signal $w(t,T)$ is in $\mathcal{C}^{\hat{k}}$. Furthermore, $w(t,T) \geq 0$ for all $t \in [0, 2s+T]$, and $w^{(i)}(t,T)|_0 = w^{(i)}(t,T)|_{2s+T} = 0$ for $i = 1, \ldots, \hat{k}$. For any $\infty > T \geq \frac{\theta_1 - \theta_0}{c_2}$ it follows that

$$z_1(2s+T, \theta_0 | w(t,T)) = \theta_0 + \int_0^{2s+T} w(\tau, T) d\tau > \theta_1.$$

The inequality follows directly from the construction of $w(t,T)$. Furthermore, $s$ and $T$ are finite, and so is $2s+T$. We know from the mean value theorem that for some finite $T^\circ :\ 0 \leq T^\circ < T$ the value $z_1(2s+T^\circ, \theta_0 | w(t, T^\circ)) = \theta_1$. It is clear that $w(t,T^\circ) \in \mathcal{C}^{\hat{k}}$ and $w(t,T^\circ) \geq 0$.

**Step 3**: Note that the complete integrator chain (4.57b) is linear controllable, and thus it is a flat system, cf. [Fliess et al. 1995b]. A flat output of (4.57b) is given by $z_1$. Indeed also the $\hat{k}$ last parts of the integrator chain $z_2^{(\hat{k})}(t) = v$ can be regarded as a flat system, where $z_2$ is the considered flat output. In order to design the desired input we set $v^\circ(t) = w^{(\hat{k})}(t, T^\circ)$. Since $w(t,T^\circ) \in \mathcal{C}^{\hat{k}}$ it follows that $w^{(\hat{k})}(t,T^\circ) \in \mathcal{V}$, where $\mathcal{V}$ is some closed interval of $\mathbb{R}$. So far we have shown that an admissible input $v^\circ(t)$ to (4.57) exists. This proves part a).

**Step 4**: To derive the existence of an optimal solution to (4.57) we apply Theorem E.1 from Appendix E. By assumption the maps $\Psi : z \in \mathbb{R}^{\hat{k}+1} \mapsto u \in \mathbb{R}^{n_u}$ and $\Phi : z \in \mathbb{R}^{\hat{k}+1}$ from (4.56) are now continuous for all $z \in \mathcal{Z}$. Combining this with Assumption 4.6 we obtain that the constraints on the states $z$ (4.57f-g) are given by continuous functions $c_{x_i}(\Phi(z)) = x$ and $c_{u_i}(\Psi(z)) = u$. Thus the existence of an optimal solution to (4.57) can be deduced from two properties: the existence of at least one admissible solution to the problem and the convexity and compactness of the extended velocity set

$$\mathcal{S} := \left\{ s \in \mathbb{R}^{\hat{k}+2} \mid v \in \mathcal{V} \mapsto (Az + Bv, F(\Phi(z), \Psi(z))^T \right\}$$

for all fixed $z$. Linearity of (4.57b) and compactness of $\mathcal{V} \subset \mathbb{R}$ imply compactness and convexity of $\mathcal{S}$.

In the preceding steps we have constructed an admissible input $v^\circ(\cdot)$ for (4.57) which guarantees that the solution $z(t, z_0 | v^\circ)$ satisfies the tightened constraints $\tilde{\mathcal{Z}}$, therefore $u = \Psi\left(z(t, z_0|v^\circ)\right) \in \mathrm{int}\,\mathcal{U}$ satisfies the constraint (4.57f). Hence we conclude from the existence of an admissible solution that an optimal solution to OCP (4.57) exists.

Moreover, if the minimum time case ($F(\cdot) = 0$) is considered, then $v^\circ$ guarantees that for some finite $T^\circ :\ z_1(2s+T^\circ, \theta_0|v^\circ) = \theta_1$. It follows that $0 \leq T^\star < 2s + T^\circ < \infty$. Hence the minimal transition time $T^\star$ is finite. This proves part b). □

Note that strong steady state consistency of a path $\mathcal{P}$ combined with local continuity of input and state parametrizations of a flat system is merely a sufficient condition. However, if $\mathcal{P}$ is only weakly steady state consistent, then it is in general difficult to guarantee constraint satisfaction. In that case even a slow motion along the path might cause violation of the constraints.

Moreover, the existence of an admissible solution to (4.57) can also be shown for the case of infinitely long paths, i.e., the path parameter interval $[\theta_0, \theta_1]$ is not bounded. This means that also for infinitely long paths strong steady state consistency implies exact path followability. One should also note that we required continuity of the maps $\Psi, \Phi$ in part b) to derive existence of optimal controllers via Theorem E.1. In applications the continuity of the flat state and input parametrization might hold only locally. Nevertheless, one can compute admissible—not necessarily optimal—path evolutions via OCP (4.57).

**Remark 4.7** (Path followability and constrained reachability).
*In essence, the last result implies a reachability property of flat systems in presence of constraints: Given two constraint consistent steady states. The transition between these set points can be achieved in finite time, if the set points are connected by strongly steady state consistent paths.*

The result of Theorem 4.3 simplifies, if no state constraints are present.

**Corollary 4.1** (Path followability and input constraints).
*Given the optimal control problem* (4.57) *in which the state constraint* (4.57g) *is not present. Suppose that for all* $z \in \mathcal{Z} \subset \mathbb{R}^{\hat{k}+1}$

*i)* $\Psi(z) : z \in \mathbb{R}^{\hat{k}+1} \mapsto u \in \mathbb{R}^{n_u}$ *is continuous;*

*ii) and additionally*

$$\lim_{z_2 \downarrow 0} \|\Psi(z_1, z_2, \ldots, z_{\hat{k}+1})\| = 0. \tag{4.60}$$

*Then for any compact constraint set* $\mathcal{U} \subset \mathbb{R}^{n_u}$*, that contains* $0 \in \mathbb{R}^{n_u}$ *in its interior, OCP* (4.57) *has an optimal solution. Moreover, if the minimum-time case* ($F(x,u) = 0$) *is considered, the optimal transition time* $T^\star$ *is finite.*

*Proof.* The proof follows along the same ideas as the preceding proof of Theorem 4.3 and is hence only briefly sketched here. Continuity of $\Psi$ combined with the input scaling property expressed in (4.60) guarantees that $u = \Psi(z)$ can be kept in a sufficiently small neighborhood of the origin. Basically, (4.60) means that by *driving* slower along the path the inputs can be made arbitrarily small.

Consider the set $\tilde{\mathcal{Z}} := \{z \in \mathcal{Z}, \|\Psi(z)\| \leq \delta\}$. Due to continuity of $\Psi(z)$ a constant $\delta > 0$ exists, s.t. for all $z \in \tilde{\mathcal{Z}}$ and any compact set $\mathcal{U} \subset \mathbb{R}^{n_u}$ with $0 \in \operatorname{int}\mathcal{U}$ we have $z \in \tilde{\mathcal{Z}} \Rightarrow \Psi(z) \in \mathcal{U}$. Now, proceed with similar constructive steps as in the proof of Theorem 4.3 to construct a signal $v(t)$ which keeps $z \in \tilde{\mathcal{Z}}$ and drives the system exactly along the path. □

At first glance the conditions of Corollary 4.1 seem to be restrictive. However, for certain paths the kinematic unicycle or car-trailer systems with on-axle-hitching partially fulfill the input scaling property expressed in (4.60), e.g. [Rouchon et al. 1993].

**Example 4.3** (Path followability of an autonomous robot).
*As an example of a flat system partially fulfilling the suppositions of Corollary 4.1 consider the model of mobile robot in a fixed coordinate frame*

$$\begin{pmatrix} \dot{x}_1 \\ \dot{x}_2 \\ \dot{x}_3 \end{pmatrix} = \begin{pmatrix} u_1 \cos(x_3) \\ u_1 \sin(x_3) \\ u_1 \tan(u_2) \end{pmatrix}. \tag{4.61}$$

*The states $x_1$ and $x_2$ describe the position in the $x_1$–$x_2$ plane. $x_3$ is the yaw angle. $u_1$ refers to the speed of the vehicle, and $u_2$ is the steering angle. The system inputs are subject to constraints $u_1 \in [0, \hat{u}_1]$ and $u_2 \in [-\tilde{u}_2, \tilde{u}_2]$. The considered flat output of system* (4.61) *is*

$$y = (x_1,\ x_2)^T.$$

*The flat parametrizations of state and input variables (4.49b-c) are*

$$\begin{aligned} x &= \Phi(y_1, \dot{y}_1, y_2, \dot{y}_2) &&= \left(y_1,\ \ y_2,\ \ \arctan\tfrac{\dot{y}_2}{\dot{y}_1}\right) \\ u_1 &= \Psi_1(\dot{y}_1, \dot{y}_2) &&= \dot{y}_1\sqrt{1 + \left(\tfrac{\dot{y}_2}{\dot{y}_1}\right)^2} \\ u_2 &= \Psi_2(\dot{y}_1, \ddot{y}_1, \dot{y}_2, \ddot{y}_2) &&= \arctan\left(\left(1 + \left(\tfrac{\dot{y}_2}{\dot{y}_1}\right)^2\right)^{-\frac{3}{2}} \cdot \frac{\ddot{y}_2\dot{y}_1 - \dot{y}_2\ddot{y}_1}{(\dot{y}_1)^3}\right). \end{aligned}$$

*The maps $\Phi, \Psi$ are valid only locally. Specifically, one has to restrict the yaw angle $x_3 \in (-\frac{\pi}{2}, \frac{\pi}{2})$. Under this restriction it holds that $-\infty < \frac{\dot{y}_2}{\dot{y}_1} < \infty$. The path $\mathcal{P}$ to be followed is an explicitly parametrized curve*

$$\mathcal{P} = \left\{ y \in \mathbb{R}^2 \mid [\theta_0, \theta_1] \mapsto p(\theta) = \left(\theta,\ \rho(\theta)\right)^T \right\},$$

*where $\rho : \mathbb{R} \to \mathbb{R}$ is a twice continuously differentiable function. Substitution of the path parametrization $p(\theta)$ into $u = \Psi(\cdot)$ yields*

$$\begin{aligned} u_1 &= \dot{\theta} \cdot \sqrt{1 + \left(\tfrac{\partial\rho}{\partial\theta}\right)^2} \\ u_2 &= \arctan\left(\left(1 + \left(\tfrac{\partial\rho}{\partial\theta}\right)^2\right)^{-\frac{3}{2}} \cdot \frac{\partial^2\rho}{\partial\theta^2}\right). \end{aligned}$$

*Recall $z = (\theta, \dot{\theta}, \ldots, \theta^{(\hat{k})})^T$. Thus the input parametrization for the speed of the vehicle $u_1 = \Psi_1(\cdot)$ fulfills the scaling property* (4.60) *of Corollary 4.1. The steering input $u_2 = \Psi_2(\cdot)$ depends solely on the geometry of the reference path. From the flat state parametrization $x = \Phi(\cdot)$ one can also infer that a consistent initial condition $x(0) = x_0$*

*for exact path-following—see also condition ii) of Lemma 4.2—has to fulfill*

$$x_0 = \left(\theta_0,\ \rho(\theta_0),\ \arctan\left(\tfrac{\partial\rho}{\partial\theta}\right)\Big|_{\theta_0}\right)^T .$$

*Additionally, one should note that for this example the higher time derivatives of the path parameter $\theta$ do not appear in the path specific input maps. Thus it suffices to choose a timing law $\dot\theta = v$ to obtain inputs $u(t) \in \mathcal{C}^1$ via OCP* (4.57) *under the restriction $v(t) \in \mathcal{C}^0$. In case of piecewise constant $v(\cdot)$ the timing law should be chosen as $\ddot\theta = v$.*

Let us briefly summarize the main points of this section: For flat systems we can project the feedforward controlled MIMO dynamics onto linear single input dynamics which describe the motion along the path. Using this description we obtain an optimal control problem with small dimensional linear dynamic constraints. Furthermore, the projection enables us to state sufficient conditions for exact path followability as conditions guaranteeing the existence of admissible solutions to (4.57). The bottleneck of this OCP is that the constraints (4.57f-g)—i.e., the constraints that parametrize the states and inputs of the original system (4.1)—are usually non-convex.

### 4.4.2 Example: Feedforward Path Following for a Chemical Reactor

To illustrate the previous investigations we consider a *Van der Vusse* CSTR reactor described by the dynamics

$$\dot c_A = r_A(c_A, T) + (c_{In} - c_A)u_1 \tag{4.62a}$$

$$\dot c_B = r_B(c_A, c_B, T) - c_B u_1 \tag{4.62b}$$

$$\dot T = h(c_A, c_B, T) + \alpha(u_2 - T) + (T_{In} - T)u_1, \tag{4.62c}$$

where

$$\begin{aligned} r_A(c_A, T) &= -k_1(T)c_A - k_2(T)c_A^2 \\ r_B(c_A, c_B, T) &= \quad k_1(T)(c_A - c_B) \\ h(c_A, c_B, T) &= -\delta\left(k_1(T)\left(c_A H_{AB} + c_B H_{BC}\right) + k_2(T)c_A^2 H_{AD}\right)\right), \end{aligned}$$

and the reactions kinetics are of Arrhenius type $k_i(T) = k_{i0}e^{\frac{-E_i}{T+T_0}}, \quad i = 1, 2$. The system states $c_A$ and $c_B$ refer to the educt and product concentration in the CSTR. $T$ is the reactor temperature. The educt concentration is subject to the constraint 2mol/l$\leq c_A \leq$ 10mol/l. The input $u_1 \geq$ 01/h is the normalized flow rate through the reactor and $u_2 \in$ [106.2°C, 115°C] refers to the temperature in the cooling jacket. The system parameters are listed in Table 4.1. In [Rothfuß 1997; Rothfuß et al. 1996] it is shown that

$$y = \left(T,\ \ \tfrac{c_{In} - c_A}{c_B}\right)^T \tag{4.63}$$

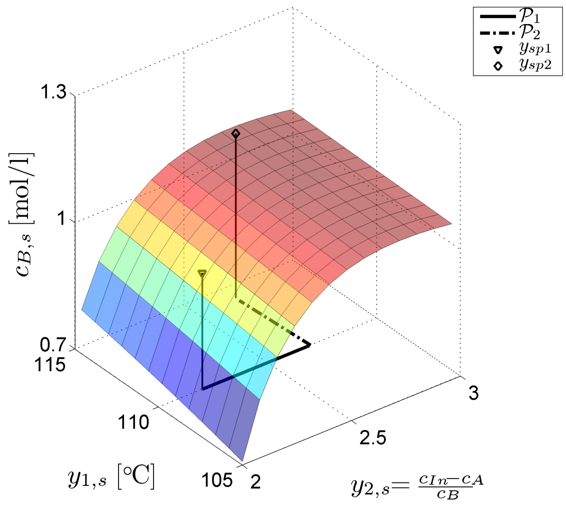


**Figure 4.6:** Paths $\mathcal{P}_{1,2}$ and surface of stationary product concentration.

is a flat output of (4.62). There an extended version of the model (4.62) is considered: the temperature dynamics of the cooling jacket are described by an additional scalar linear ODE, and the cooling rate instead ot the jacket temperature is an input variable. Nevertheless, one can rely on these results in order to show that the reduced system (4.62) admits (4.63) as a flat output. Since the calculation of the flat state and input parametrizations (4.49b,c) leads to vast and complex expressions, we give here only functional dependencies. The detailed derivation can be found in [Rothfuß 1997; Rothfuß et al. 1996]. Considering the flat output (4.63) the states of (4.62) can be expressed as

$$c_B = \Phi_1(y_1, y_2, \dot{y}_2) \tag{4.64a}$$
$$c_A = c_{In} - y_2\Phi_1(y_1, y_2, \dot{y}_2) \tag{4.64b}$$
$$T = y_1. \tag{4.64c}$$

**Table 4.1:** Parameters for system (4.62), [Rothfuß et al. 1996].

| | | | | | |
|---|---|---|---|---|---|
| $\alpha$ | 30.828 | [h$^{-1}$] | $k_{20}$ | $9.043 \cdot 10^6$ | [m$^3$/(mol h)] |
| $\delta$ | $3.522 \cdot 10^{-4}$ | [m$^{-3}$ K kJ ] | $E_1$ | 9578.3 | |
| $T_{In}$ | 104.9 | [°C] | $E_2$ | 8560.0 | |
| $T_0$ | 273.15 | [°C] | $H_{AB}$ | 4.2 | [kJ/mol] |
| $c_{In}$ | $5.1 \cdot 10^3$ | [mol/m$^3$] | $H_{BC}$ | $-11.0$ | [kJ/mol] |
| $k_{10}$ | $1.287 \cdot 10^{12}$ | [h$^{-1}$] | $H_{AB}$ | $-41.85$ | [kJ/mol] |

The inputs are parametrized via

$$u_1 = \Psi_1 (y_1, y_2, \dot{y}_1, \dot{y}_2, \ddot{y}_2) \tag{4.64d}$$

$$u_2 = \Psi_2 (y_1, y_2, \dot{y}_1, \dot{y}_2, \ddot{y}_2) \,. \tag{4.64e}$$

The considered path-following problem was proposed in [Rothfuß 1997; Rothfuß et al. 1996]. The task is to perform a *fast* set point change in two steps, see Figure 4.6. The first step leads from the set point $y_{SP1} = (110°\text{C}, 2.2)^T$ along the path $\mathcal{P}_1$ defined by the affine parametrization

$$\mathcal{P}_1 : \theta \in [2.2, 2.69] \mapsto p(\theta) = \Big(110°\text{C}, \;\; \theta\Big)^T .$$

The second step is to move along the path of maximal steady state product concentration given by the nonlinear parametrization

$$\mathcal{P}_2 : \theta \in [110°\text{C}, 114.21°\text{C}] \mapsto p(\theta) = \left(\theta, \;\; 2\sqrt{\tfrac{k_1(\theta)+c_{In}k_2(\theta)}{k_1(\theta)}}\right)^T$$

to the final set point $y_{SP2} = (114.21°\text{C}, 2.69)^T$.

Relying on the input parametrization (4.64) and the path descriptions for $\mathcal{P}_{1,2}$, it is easy to check numerically that the considered path is strongly steady state consistent with respect to the considered input and state constraints. In Figure 4.7 the black continuous and dash-dot lines show the steady states along to the paths $\mathcal{P}_{1,2}$ and the corresponding stationary input values. Clearly, the paths $\mathcal{P}_{1,2}$ are steady state consistent in the sense of Definition 4.4. Since the flat parametrization from (4.64) depends on $\ddot{y}_2$ as highest output derivative, the virtual dynamics (4.57b) are an integrator chain of length three. The set point change should be achieved reasonably fast, therefore the cost $F(x, u) = 0$ is used in (4.57a). In order to compute feedforward controls which nominally move the system (4.62) from one set point to the other we apply the proposed approach for both paths separately.

The simulations are carried out with Matlab and a multiple-shooting implementation available in the ACADO Toolkit [Houska et al. 2011]. Problem (4.57) is solved separately for both paths $\mathcal{P}_{1,2}$. How the solution in the state space differs from the steady state solutions is depicted in Figure 4.7. The red continuous curves show the trajectories as computed via (4.57). The behavior in the time domain is illustrated in Figure 4.8. The left hand side shows the state evolutions of the original system (4.62), the right hand side presents the corresponding input signals. $\mathcal{P}_1$ is accomplished in less then 0.2h while steering the system along $\mathcal{P}_2$ needs about 0.06h. The simulation results show that the obtained solution respects the considered constraints. Additionally, the overall transition time $\approx$ 0.26h is much shorter than the heuristic solution of 1.0h presented in [Rothfuß 1997; Rothfuß et al. 1996]. Note that if the obtained inputs are applied to a real system, one needs to combine them with a suitable feedback controller in a two-degrees-of-freedom structure, cf. [Hagenmeyer and Delaleau 2003].

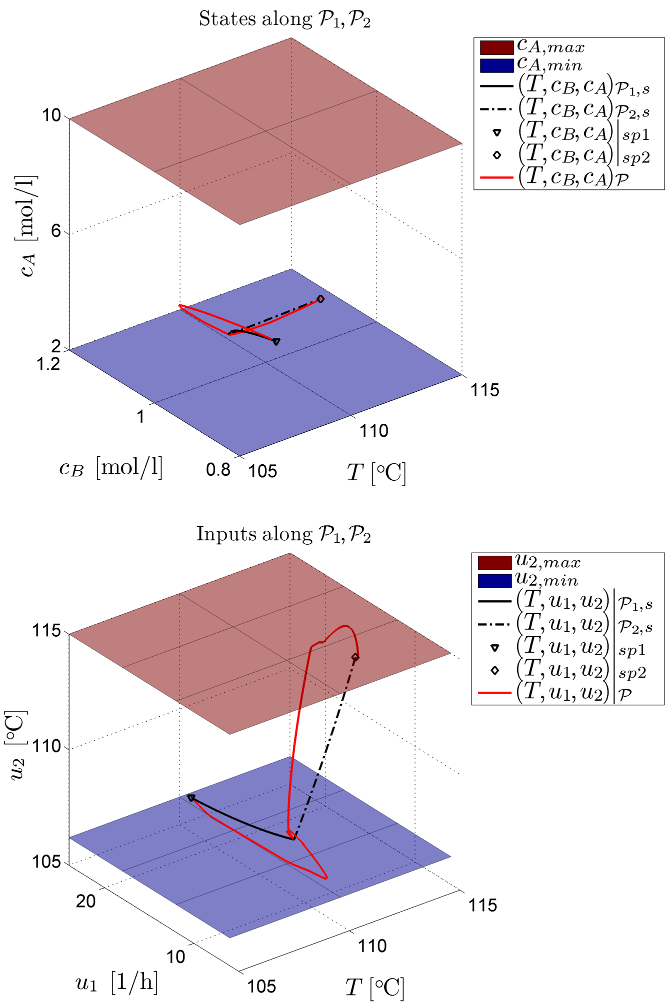


**Figure 4.7:** Steady state consistency of $\mathcal{P}_1, \mathcal{P}_2$ and optimized $x(t), u(t)$.

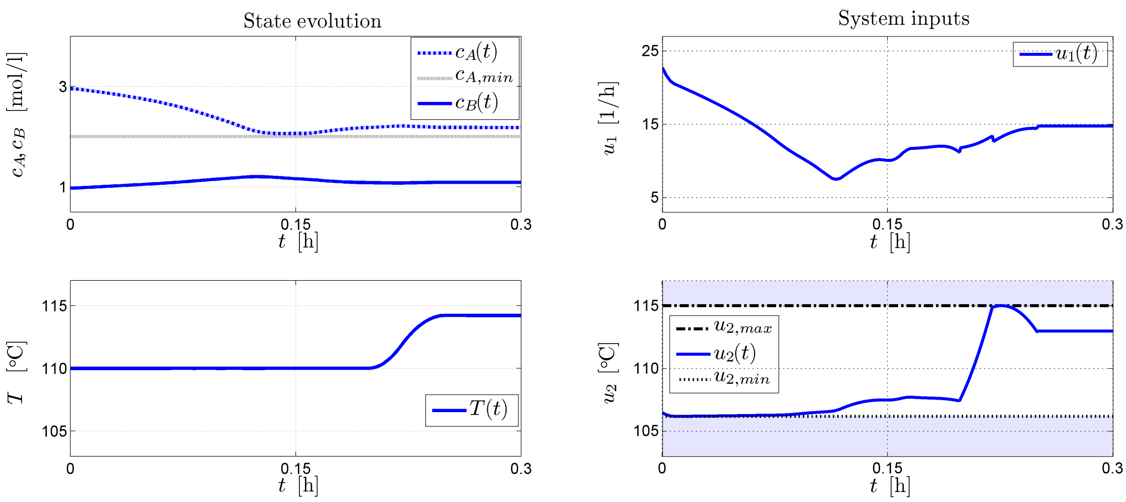


**Figure 4.8:** Optimized state evolution and inputs.

## 4.5 Summary

In this chapter we gave an introduction on path following for nonlinear systems and investigated the question of path followability. Firstly, we provided an extensive overview of existing results on path following. Secondly, we introduced an augmented system description of these problems. Under mild assumptions this description allows local transformation of the problem into suitable coordinates, which allow to analyze path-followability problems. In accordance with [Banaszuk and Hauser 1995; Nielsen and Maggiore 2006] we call this description a transverse normal form. In essence it is a Byrnes-Isidori normal form which is tailored to path-following problems. This description allows investigation of the question of (unconstrained) path followability.

Finally, we investigated path followability in the presence of constraints on states and inputs for the special case of flat systems. We have shown that along a path a feedforward controlled nonlinear flat MIMO system can be projected onto a linear single-input system. Based on this projection we proposed a small dimensional optimal control problem, which can be efficiently solved in order to compute optimal feedforward control signals for exact path following. Additionally, we presented sufficient conditions for path followability of flat systems in the presence of constraints on states and inputs.

So far we have not discussed the question of designing path-following controllers in the presence of constraints. In the next chapter we shift the focus to the design of tailored predictive controllers.

# 5 Predictive Path-following Control

In this chapter we discuss tailored predictive control schemes for path-following problems. We start with a simplified problem, where the reference path is directly defined in the state space to line out the conceptual ideas. These results have appeared in [Faulwasser and Findeisen 2009a,b; Faulwasser et al. 2009a]. In Section 5.2 we consider the general and application-relevant case of reference paths defined in an output space. These results have been partially presented in [Faulwasser and Findeisen 2010]. To illustrate our results we discuss examples in Sections 5.2.2 and 5.2.3. Specifically, we consider an example from robot control and a ship course control problem.

## 5.1 Predictive Path Following in the State Space

We consider nonlinear systems

$$\dot{x}(t) = f(x(t), u(t)), \quad x(t_0) = x_0, \tag{5.1}$$

where $x \in \mathcal{X} \subseteq \mathbb{R}^{n_x}$, $u \in \mathcal{U} \subset \mathbb{R}^{n_u}$ are state and input constraints. To outline the main ideas we do not consider an output map. Rather we focus on problems, where the path is directly defined in the state space. Let us suppose that the system and the constraints fulfill our standard assumptions from Chapter 2. Moreover, we require $f(0, 0) = 0$. The path to be followed is a regular curve defined in the state space

$$\mathcal{P} = \{x \in \mathbb{R}^{n_x} \mid \theta \in [\theta_0, 0] \mapsto p(\theta)\}. \tag{5.2}$$

To simplify the exposition we require $-\infty < \theta_0 \leq 0$, and that the path ends in the origin $p(0) = 0$. Additionally, we assume the parametrization $p$ to be sufficiently often continuously differentiable. We aim at solving a modified version of the general path-following problem introduced in Section 4.1 which reads as follows.

**Problem 5.1** (State space path-following).
*Given system* (5.1) *design a controller that achieves:*

*i)* ***Path Convergence:*** *The path-following error converges asymptotically*

$$\lim_{t\to\infty} \|x(t) - p(\theta(t))\| = 0.$$

*ii)* ***Strict Forward Motion:*** *The system moves along $\mathcal{P}$ in the direction of increasing values of $\theta$ s.t. $\dot{\theta}(t) > 0$ holds for almost all $\theta \in [\theta_0, 0)$.*

*iii)* ***Constraint Satisfaction**: The constraints on states $x \in \mathcal{X}$ and inputs $u \in \mathcal{U}$ are satisfied for all times.*

Note that we require in ii) that $\dot{\theta} > 0$ holds only for the open interval $[\theta_0, 0)$. This, combined with $f(0,0) = 0$, allows to consider cases where the system should stop at a final path point $p(0) = 0$.
The time evolution of the path parameter is not given a priori, it has to be obtained by the controller. We rely on a *timing law*

$$\dot{\theta} = g(\theta, v), \quad \theta(t_0) = \theta_0 \tag{5.3}$$

which allows controlling the evolution along the path via the virtual input $v$. Here, we assume a first-order timing law. The motivation for this choice is similar to the previous considerations on output paths: the order of the timing law corresponds to the lowest time derivative of the path-following error in which the input $u$ appears. Consider a non-pathological system (5.1) where for all $x \in \mathcal{X} : rank\left(\frac{\partial f}{\partial u}\right) > 0$. Similar to the geometric considerations from Section 4.3 the first time derivative of the error $e = x - p(\theta)$ is

$$\dot{e} = f(x,u) - \left(\frac{\partial p_1}{\partial \theta}, \ldots, \frac{\partial p_{n_x}}{\partial \theta}\right)^T \cdot g(\theta, v). \tag{5.4}$$

Clearly, $\dot{e}$ depends on $u$. Thus a first-order timing law is a reasonable choice for path-following problems in the state space.

### 5.1.1 Model Predictive Path Following

We propose a continuous time sampled-data NMPC scheme, denoted as *model predictive path-following control* (MPFC), to tackle this problem. Our main idea is to treat the path parameter as an additional state variable which can be controlled via the virtual path parameter input $v$. We propose an expanded predictive setup to obtain the path parameter input $v$ and the real system input $u$ by solving repetitively an optimal control problem. Predicted system states and inputs are denoted by $\bar{x}$ and $\bar{u}$. In contrast to standard NMPC approaches—cf. Chapter 2—the cost functional to be minimized at the sampling instances $t_k = k\delta, k \in \mathbb{N}$ is

$$J\left(x(t_k), \bar{x}(\cdot), \bar{\theta}(\cdot), \bar{u}(\cdot), \bar{v}(\cdot)\right) = \int_{t_k}^{t_k+T_p} F\left(\bar{x}(\tau), \bar{\theta}(\tau), \bar{u}(\tau), \bar{v}(\tau)\right) d\tau \\ + E\left(\bar{x}(t_k + T_p), \bar{\theta}(t_k + T_p)\right). \tag{5.5}$$

Here, $F : \mathcal{X} \times [\theta_0, 0] \times \mathcal{U} \times \mathbb{R} \to \mathbb{R}_0^+$ denotes the cost function, and $E : \mathcal{X} \times [\theta_0, 0] \to \mathbb{R}_0^+$ is the end penalty. $F$ is assumed to be lower bounded by a class $\mathcal{K}$ function $\underline{\psi}(\|x - p(\theta)\|)$, i.e., $F$ penalizes the deviation from the path. Besides $\bar{x}$ and $\bar{u}$, the cost functional depends on the path parameter $\bar{\theta}$ and the path parameter input $\bar{v}$. The proposed control strategy is based on the repeated solution of the following optimal control problem:

$$\underset{(\bar{u}(\cdot),\bar{v}(\cdot))\in\mathcal{PC}(\mathcal{U}\times\mathcal{V})}{\text{minimize}} \quad J\left(x(t_k),\bar{x}(\cdot),\bar{\theta}(\cdot),\bar{u}(\cdot),\bar{v}(\cdot)\right) \tag{5.6a}$$

subject to

$$\forall\tau\in[t_k,t_k+T_p]:\ \dot{\bar{x}}(\tau)=f(\bar{x}(\tau),\bar{u}(\tau)),\quad \bar{x}(t_k)=x(t_k) \tag{5.6b}$$
$$\bar{x}(\tau)\in\mathcal{X} \tag{5.6c}$$
$$\bar{u}(\tau)\in\mathcal{U} \tag{5.6d}$$
$$\bar{x}(t_k+T_p)\in\mathcal{E}\subseteq\mathcal{X}\subseteq\mathbb{R}^{n_x} \tag{5.6e}$$

and the additional path-following constraints

$$\forall\tau\in[t_k,t_k+T_p]:\ \dot{\bar{\theta}}(\tau)=g\left(\bar{\theta}(\tau),\bar{v}(\tau)\right),\quad \bar{\theta}(t_k)=\theta\left(t_k\right) \tag{5.6f}$$
$$\bar{\theta}(\tau)\in[\theta_0,0] \tag{5.6g}$$
$$\bar{v}(\tau)\in\mathcal{V}. \tag{5.6h}$$

As common in NMPC the system dynamics appear as constraints (5.6b). Equations (5.6c-d) are the state and input constraints. The terminal constraint (5.6e) restricts the predicted state $\bar{x}(t_k+T_p)$ to a specific region at the end of each prediction, i.e., at time $t_k+T_p$ the predicted state needs to be in the closed set $\mathcal{E}$. The extra constraints (5.6f-h) describe the evolution of the path, which is specified by the timing law $\dot{\bar{\theta}}=g(\bar{\theta},\bar{v})$. The virtual input $v$ controls the evolution of $\theta$. Note that the timing law $g:[\theta_0,0]\times\mathcal{V}\to\mathbb{R}_0^+$ is an additional degree of freedom in the controller design. To solve the (5.6f) an initial condition $\theta(t_k)$ is necessary at every sampling instance $t_k$. If an initial path point $p_0=p(\theta_0)$ is given a priori, then the corresponding value of the path parameter $\theta_0$ serves as an initial condition for $\bar{\theta}(t_0)$ at the first sampling instant. If no initial path point is given, we have to choose a suitable initial condition $\bar{\theta}(t_0)$. For example, a path point close to $x_0$ can be obtained by (locally) solving the minimum distance problem

$$\bar{\theta}(t_0)=\underset{\theta\in[\theta_0,0]}{\text{argmin}}\ \|x_0-p(\theta)\|. \tag{5.7}$$

This problem might have several optimal solutions, and we have to pick one of them. At all subsequent sampling instances $k\geq 1$ the corresponding value of the previous prediction can be used

$$\theta(t_k)=\bar{\theta}\left(t_k,t_{k-1},\bar{\theta}(t_{k-1})|\bar{v}\right).$$

The solution of (5.6) leads to the optimal input trajectory $u_k^\star(\cdot)$ which is applied for all $t\in[t_k,t_k+\delta):\ u(t)=u_k^\star(t)$.

The proposed MPFC scheme (5.6) is an extended NMPC scheme. The open-loop optimal control problem is augmented by the virtual state $\theta$ and by the virtual input $v$. Essentially, $v$ controls the path parameter evolution $t\mapsto\theta(t)$. The main idea of this scheme is to obtain the real system inputs $u(\cdot)$ as well as the virtual input $v(\cdot)$ via repeated solutions of the optimal control problem (5.6). Thus it tackles two issues at once: the planning of suitable trajectories $t \mapsto p(\theta(t))$ inside $\mathcal{P}$, and the computation of inputs $u(\cdot)$ to track the resulting trajectories. We do not aim at a time-optimal motion along the path as it is often considered in robotics [Raczy and Jacob 1999; Shin and McKay 1985; Verscheure et al. 2009]. Instead we aim at stabilization of the zero-path-error manifold. We want to achieve that the system state converges to the path and moves along it as close as possible. Referring to the MPFC scheme (5.6) *path convergence is more important than speed.*

### 5.1.2 Stability of Predictive Path Following

To ensure stability of the proposed MPFC scheme we suppose that our standard NMPC specific assumptions from Chapter 2 hold. Additionally, we assume the following.

**Assumption 5.1** (Constraint consistent path).
*The path* (5.2) *is contained in the interior of the state constraints* $\mathcal{P} \subset \operatorname{int} \mathcal{X}$ *and* $p(0) = 0$ *holds.*

**Assumption 5.2** (Monotonous solutions to timing law).
*The timing law is chosen such that* $g(\theta, v)$ *has equivalent properties as required for* $f(x, u)$ *in Chapter 2. Furthermore, for all* $v \in \mathcal{V}$ *and all* $\theta \in [\theta_0, 0)$ *it holds that* $\dot{\theta} = g(\theta, v) > 0$.

The first assumption ensures that the path $\mathcal{P}$ is consistent with the state constraints $\mathcal{X}$. The second assumption is technical. It is introduced to avoid cases where the system stops on the path before the end point 0 is reached or moves backward on the path. For example, a suitable choice is $g(\theta, v) = -\lambda \cdot \theta + v,\ \lambda > 0$ and $v \in [0, v_{max}]$. Given the MPFC scheme (5.6) the following result holds.

**Theorem 5.1** (Convergence of MPFC for state space paths).
*Consider the path-following problem as defined in Problem 5.1 and Assumptions 5.1–5.2. Suppose that a terminal region* $\mathcal{E} \subseteq \mathcal{X}$ *and a terminal penalty* $E(x, \theta)$ *exist such that the following holds:*

*i)* $\mathcal{E}$ *is closed.* $E(x, \theta)$ *is positive semi-definite,* $\mathcal{C}^1$ *in* $(x, \theta)$, *and* $E(0, 0) = 0$.

*ii) For all* $(\tilde{x}, \tilde{\theta}) \in \mathcal{E} \times [\theta_0,\ 0]$ *there exists a scalar* $\epsilon \geq \delta > 0$ *and a pair of admissible inputs* $(u_{\mathcal{E}}(\cdot), v_{\mathcal{E}}(\cdot)) \in \mathcal{PC}(\mathcal{U} \times \mathcal{V})$ *such that for all* $\tau \in [0, \delta]$

$$\left(\frac{\partial E}{\partial x}, \frac{\partial E}{\partial \theta}\right) \cdot \begin{pmatrix} f(x(\tau), u_{\mathcal{E}}(\tau)) \\ g(\theta(\tau), v_{\mathcal{E}}(\tau)) \end{pmatrix} + F\Big(x(\tau), \theta(\tau), u_{\mathcal{E}}(\tau), v_{\mathcal{E}}(\tau)\Big) \leq 0, \tag{5.8}$$

*and the solutions* $x(\tau) = x(\tau, \tilde{x} | u_{\mathcal{E}}(\cdot)),\ \theta(\tau) = \theta(\tau, \tilde{\theta} | v_{\mathcal{E}}(\cdot))$, *starting at* $(\tilde{x}, \tilde{\theta}) \in \mathcal{E} \times [\theta_0, 0]$, *stay in* $\mathcal{E} \times [\theta_0, 0]$ *for* $\tau \in [0, \delta]$.

*iii) The OCP* (5.6) *is feasible for* $t_0$.

*Then the MPFC scheme based on* (5.6) *solves Problem 5.1.*

*Proof.* The proof consists of two steps. Firstly, we show that the proposed MPFC scheme is equivalent to a set point stabilization in different coordinates. In these coordinates one can apply Theorem 2.1 from Chapter 2. Secondly, we demonstrate how the stability conditions map back to the original coordinates.
**Step 1:** Consider the change of coordinates

$$y = \Big(x - p(\theta), \;\; \theta\Big)^T, \quad w = \Big(u, \;\; v\Big)^T. \tag{5.9}$$

In the new coordinates $y, w$ the control scheme is equivalent to a set point stabilization in $\mathbb{R}^{n_x+1}$, thus we can apply the NMPC stability conditions directly, see e.g. Chapter 2. In fact, conditions i) and iii) of the theorem are special cases of conditions i) and iii) of Theorem 2.1 from Chapter 2.
In $y, w$ coordinates the augmented system dynamics are given by

$$\dot{y} = \tilde{f}(y, w) = \begin{pmatrix} f_1(x,u) - \dfrac{\partial p_1}{\partial \theta} g(\theta, v) \\ \vdots \\ f_{n_x}(x,u) - \dfrac{\partial p_{n_x}}{\partial \theta} g(\theta, v) \\ g(\theta, v) \end{pmatrix}.$$

The terminal region in $y, w$ coordinates is the image of $\mathcal{E} \times [\theta_0, 0]$ under (5.9). For $w_{\mathcal{E}} = (u_{\mathcal{E}}, v_{\mathcal{E}})^T$ the cost-decrease condition inside the terminal region is given by

$$\frac{\partial \tilde{E}(y)}{\partial y} \cdot \tilde{f}(y, w_{\mathcal{E}}) + \tilde{F}(y, w_{\mathcal{E}}) \leq 0. \tag{5.10}$$

**Step 2:** To map this condition back to the original coordinates $x, \theta, u, v$ we use

$$\frac{\partial \tilde{E}(y)}{\partial y} = \left(\frac{\partial E}{\partial x}, \frac{\partial E}{\partial \theta}\right) \cdot \left(\begin{array}{c|c} \mathbf{I}^{n_x \times n_x} & \frac{\partial p}{\partial \theta} \\ \hline \mathbf{0}^{\,1 \times n_x} & 1 \end{array}\right).$$

If we apply this relation to (5.10), condition (5.8) follows immediately. Since convergence of $y$ to 0 implies $\lim_{t\to\infty} \|x - p(\theta)\| = 0$ we conclude that the main parts of the state space path-following problem—path convergence i) and constraint satisfaction ii)—are fulfilled. Furthermore, Assumption 5.2 requires the timing law $\dot{\theta} = g(\theta, v)$ to be chosen such that $\dot{\theta}$ is positive for all admissible $v \in \mathcal{V}$ and all $\theta \in [\theta_0, 0)$. Hence the forward motion requirement ii) of the system along the path is also satisfied. □

Note that the last theorem also ensures recursive feasibility of the MPFC scheme (5.6). This can easily be shown along the lines of the proof of Theorem 2.1 in Appendix A.

**Remark 5.1** (Ensuring forward motion).
*In the design of the cost function $F$ and the timing law $g$ the forward motion requirement of Problem 5.1 has to be taken into account. Mainly, one has to prevent cases*

*where the system stops on the path without reaching the final point $\theta = 0$. Either Assumption 5.2 has to hold, which restricts the choice of suitable timing laws. Or one ensures that the cost function $F$ is lower bounded by a class $\mathcal{K}$ function $\underline{\psi}(\|(x - p(\theta), \theta)\|)$, i.e., the cost penalizes $\theta \neq 0$. In the latter case it is tricky to ensure strict forward motion $\dot{\theta} > 0$. Nevertheless, one can use a path-followability argument to show that optimal solutions move the system forward along the path such that $\dot{\theta} \geq 0$ and $\lim_{t\to\infty} \theta = 0$ hold.*
*In some cases no (controlled) equilibria lie on the path $\mathcal{P}$, and additionally staying inside $\mathcal{P}$ implies that $\dot{\theta} > 0$ holds. In such a situation one can drop Assumption 5.2, and it is also not necessary to require penalization of $\|\theta\|$ in $F$.*

### 5.1.3 Stabilizing Terminal Path Constraints

As we have already seen in Chapter 3 the calculation of suitable end penalties $E$ and terminal regions $\mathcal{E}$ for NMPC schemes is challenging, see also [Chen and Allgöwer 1998; Findeisen 2006; Mayne et al. 2000; Yu et al. 2009]. This raises the question of whether suitable $E$ and $\mathcal{E}$ can be found for path following. For the proposed scheme (5.6) we basically need to derive a local controller which stabilizes the path $\mathcal{P}$ and renders it positively invariant. Subsequently, we use the fact that $f$ and $g$ appear decoupled in (5.8) to find suitable terminal regions and penalties for the proposed MPFC scheme. The main idea is to employ the path $\mathcal{P}$ as terminal region.
The considerations are simplified if the cost function is restricted to be quadratic in the path error $e = x - p(\theta)$ as well as in the path parameter $\theta$ and the inputs $u, v$.

**Assumption 5.3** (Quadratic cost function).
*The cost function $F : \mathcal{X} \times \mathcal{U} \times [\theta_0, 0] \times \mathbb{R} \to \mathbb{R}_0^+$ for the MPFC scheme (5.6) is*

$$F(x, \theta, u, v) = \left\| \begin{matrix} x - p(\theta) \\ \theta \end{matrix} \right\|_{\hat{Q}}^2 + \left\| \begin{matrix} u \\ v \end{matrix} \right\|_R^2, \tag{5.11}$$

*where*

$$\hat{Q} = \left( \begin{array}{c|c} Q & \mathbf{0}^{n_x \times 1} \\ \hline \mathbf{0}^{1 \times n_x} & \hat{q} \end{array} \right) > 0, \quad Q \in \mathbb{R}^{n_x \times n_x}$$

*and $R \geq 0$.*

We use the fact that $f(x, u)$ and $g(\theta, v)$ appear decoupled in (5.8) to derive the following corollary to Theorem 5.1.

**Corollary 5.1** (Stabilizing zero path constraint for MPFC).
*Consider Problem 5.1 and Assumptions 5.1–5.3. Suppose that the terminal region is $\mathcal{E} = \mathcal{P}$ and the following holds:*

*i) For all* $\theta \in [\theta_0, 0]$ *there exists a pair of admissible input signals* $(u_{\mathcal{E}}(\cdot), v_{\mathcal{E}}(\cdot)) \in \mathcal{PC}(\mathcal{U} \times \mathcal{V})$*, which guarantee that the system follows the path* $\mathcal{P}$ *exactly, and* $\dot{\theta} = g(\theta, v_{\mathcal{E}}) > 0$ *holds on* $[\theta_0, 0)$*.*

*ii) Along the path parameter evolution* $\theta(t, \theta_0|v_{\mathcal{E}})$ *it holds for all* $t \geq 0$

$$\infty > \eta > -\frac{\hat{q} \cdot (\theta(t))^2 + \left\| \begin{matrix} u_{\mathcal{E}}(t) \\ v_{\mathcal{E}}(t) \end{matrix} \right\|_R^2}{g(\theta(t), v_{\mathcal{E}}(t)) \cdot (-1)^k (\theta(t))^{k-1}} \geq 0, \quad k \geq 1. \tag{5.12a}$$

*iii) The optimal control problem* (5.6) *has a feasible solution for* $t_0$*.*

*Then the end penalty*

$$E_k(\theta) = \eta \frac{(-1)^k}{k} \theta^k \tag{5.12b}$$

*guarantees that the MPFC scheme* (5.6) *solves Problem 5.1.*

*Proof.* The corollary is built upon two ideas. Firstly, we use the path parameter $\theta$ as alternative time coordinate along the path. Secondly, we eliminate the state $x$ from the cost-decrease condition (5.8) of Theorem 5.1, and we derive a bound on the cost-to-go which solely depends on the path parameter $\theta$. Our proof directly follows these ideas.

Start at a point $p(\theta_0)$ on the path $\mathcal{P}$ and apply the admissible inputs $u_{\mathcal{E}}(\cdot)$ and $v_{\mathcal{E}}(\cdot)$. These inputs are designed such that the system follows the trajectory $p(\theta(t, \theta_0|v_{\mathcal{E}}))$, where $\dot{\theta} = g(\theta, v_{\mathcal{E}})$. Due to i) $\dot{\theta} > 0$ holds on $[\theta_0, 0)$. Thus one can invert the map $t \mapsto \theta(t, \theta_0|v_{\mathcal{E}})$ also on $[\theta_0, 0]$. Consequently, for all $\theta \in [\theta_0, 0]$ one writes $t = t(\theta)$, and hence $u_{\mathcal{E}}(t) = u_{\mathcal{E}}(\theta)$ and $v_{\mathcal{E}}(t) = v_{\mathcal{E}}(\theta)$.
Using this substitution the cost function $F(\cdot)$ from (5.11) depends only on the arguments $\theta, u_{\mathcal{E}}, v_{\mathcal{E}}$ since on $\mathcal{P}$ it holds that $x = p(\theta)$. This leads to a simplified version of (5.8) in $\mathcal{E} = \mathcal{P}$

$$\frac{\partial E_k(\theta)}{\partial \theta} \cdot g(\theta, v_{\mathcal{E}}) + \hat{q}\theta^2 + \left\| \begin{matrix} u_{\mathcal{E}}(\theta) \\ v_{\mathcal{E}}(\theta) \end{matrix} \right\|_R^2 \leq 0.$$

Using $E_k(\theta) = \eta \frac{(-1)^k}{k} \theta^k$ yields

$$\eta (-1)^k \theta^{k-1} \cdot g(\theta, v_{\mathcal{E}}) + \hat{q}\theta^2 + \left\| \begin{matrix} u_{\mathcal{E}}(\theta) \\ v_{\mathcal{E}}(\theta)) \end{matrix} \right\|_R^2 \leq 0.$$

Solving this equation for $\eta$ directly leads to (5.12a). □

The conceptual idea is to project the cost-decrease condition (5.8) onto the virtual state $\theta$. If some known inputs $u_{\mathcal{E}}(\cdot)$ and $v_{\mathcal{E}}(\cdot)$ guarantee that the system follows the path exactly, the costs of driving the system along the path solely depends on $\theta$. We only need to check that for all $\theta \in [\theta_0, 0]$ the costs of following the path along converge to zero and are upper bounded along $\theta$. Consider the special case of a linear timing

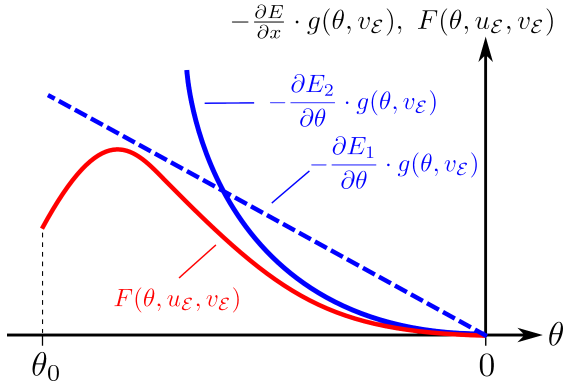


**Figure 5.1:** Bounding the costs along the path by $E_k(\theta)$.

law $g(\theta, 0) = -\lambda\theta$. In that case the decay of $E_k(\theta)$, $k = 1, 2$ along the path—i.e., $\frac{\partial E_1}{\partial \theta} g(\theta, 0)$ and $\frac{\partial E_2}{\partial \theta} g(\theta, 0)$—are a linear function and a quadratic function, respectively. The graphical interpretation of this situtation for $k = 1, 2$ is provided in Figure 5.1. Basically, the corollary suggests to use a polynomial function in $\theta$ to upper bound the costs along the path. Moreover, one can also construct other end penalties by superposition of two end penalties $E_k(\theta)$.

**Lemma 5.1** (Superposition of end penalties)**.**
*Consider two end penalties $E_{k_1}(\theta)$ and $E_{k_2}(\theta)$, which fulfill the conditions of Corollary 5.1, and $k_1, k_2 \geq 1$ holds. Then for positive scalars $\alpha_1, \alpha_2 \geq 0$ with $\alpha_1 + \alpha_2 \geq 1$ the end penalty*

$$E_{k_1,k_2}(\theta) = \alpha_1 E_{k_1}(\theta) + \alpha_2 E_{k_2}(\theta)$$

*fulfills the cost-decrease property* (5.8)*.*

*Proof.* Checking (5.8) along the path $\mathcal{P}$ for $E_{k_1,k_2}(\theta)$ yields

$$\frac{\partial E_{k_1,k_2}}{\partial \theta} g(\theta, v_{\mathcal{E}}) + F(0, \theta, u_{\mathcal{E}}, v_{\mathcal{E}}) = \left(\alpha_1 \frac{\partial E_{k_1}}{\partial \theta} + \alpha_2 \frac{\partial E_{k_2}}{\partial \theta}\right) g(\theta, v_{\mathcal{E}}) + F(0, \theta, u_{\mathcal{E}}, v_{\mathcal{E}}).$$

If $\alpha_1 \geq 1$ or $\alpha_2 \geq 1$, then verifcation of (5.8) is straightforward. It remains to deal with $\alpha_1, \alpha_2 < 1$. Using $\alpha_2 = (\alpha_2 - 1 + \alpha_1) + (1 - \alpha_1)$ we rearrange terms and obtain

$$\begin{aligned}\frac{\partial E_{k_1,k_2}}{\partial \theta} g(\theta, v_{\mathcal{E}}) + F(0, \theta, u_{\mathcal{E}}, v_{\mathcal{E}}) &= \alpha_1 \left(\frac{\partial E_{k_1}}{\partial \theta} g(\theta, v_{\mathcal{E}}) + F(0, \theta, u_{\mathcal{E}}, v_{\mathcal{E}})\right) \\ &+ (1 - \alpha_1) \left(\frac{\partial E_{k_2}}{\partial \theta} g(\theta, v_{\mathcal{E}}) + F(0, \theta, u_{\mathcal{E}}, v_{\mathcal{E}})\right) + (\alpha_2 - 1 + \alpha_1) \frac{\partial E_{k_2}}{\partial \theta} g(\theta, v_{\mathcal{E}}).\end{aligned}$$

Clearly, $\frac{\partial E_{k_1}}{\partial \theta} g + F \leq 0$ and $\frac{\partial E_{k_2}}{\partial \theta} g + F \leq 0$, and thus the first two terms are negative. Furthermore, $(\alpha_2 - 1 + \alpha_1) > 0$ and $\frac{\partial E_{k_2}}{\partial \theta} g \leq 0$. It follows that $\frac{\partial E_{k_1,k_2}}{\partial \theta} g + F \leq 0$. □

As we will see later, the freedom to choose $k$ in $E_k(\theta)$, and the possibility to construct combined end penalties $E_{k_1,k_2}(\theta)$ allow tuning of the MPFC scheme with respect to the trade-off between path convergence and speed.

In contrast to common zero terminal or terminal equality constraints, the zero path constraint is less demanding from the computations point of view: For set point stabilization problems terminal equality constraints require $\bar{x}(t_k+T_p) = 0$, i.e., the predicted state trajectory has to reach the set point. In contrast to that, the zero path constraint enforces $\bar{x}(t_k + T_p) = p(\bar{\theta}(t_k + T_p))$. In other words, the predicted trajectories have to reach the 1-dimensional path manifold $\mathcal{P}$, but it is not exactly determine where.

### 5.1.4 Example: Path Following for an Autonomous Robot

To illustrate the proposed MPFC scheme we reconsider the autonomous robot from Example 4.3. In a fixed coordinate frame the dynamics of the robot are

$$\begin{pmatrix} \dot{x}_1 \\ \dot{x}_2 \\ \dot{x}_3 \end{pmatrix} = \begin{pmatrix} u_1 \cos(x_3) \\ u_1 \sin(x_3) \\ u_1 \tan(u_2) \end{pmatrix}, \quad x(0) = x_0. \tag{5.13}$$

As before the states $x_1$ and $x_2$ describe the position in the $x_1$–$x_2$ plane, $x_3$ is the yaw angle, cf. Figure 5.2 left part. $u_1$ refers to the speed of the vehicle, and $u_2$ is the steering angle. The system inputs are subject to the constraints $u_1 \in [0, 6]$ and $u_2 \in [-0.63, 0.63]$. The path $\mathcal{P}$ to be followed is

$$\mathcal{P} = \left\{ x \in \mathbb{R}^3 \mid [\theta_0, 0] \mapsto p(\theta) = \begin{pmatrix} \theta \\ \rho(\theta) \\ \arctan\left(\frac{\partial\rho}{\partial\theta}\right) \end{pmatrix} \right\}, \tag{5.14}$$

where

$$\rho(\theta) = -\alpha \log(\gamma/(\beta + |\theta|)) \cdot \sin(\omega\theta)$$

and $\theta_0 = -30$. The coefficients of $\rho(\theta)$ are given by $\alpha = 6,\ \beta = 5,\ \gamma = 20,\ \omega = 0.35$. The path is depicted in the $x_1$–$x_2$ plane in Figure 5.2 right part. From (5.14) it can be deduced that the vehicle should always follow the curve $(\theta, \rho(\theta))^T$ along a tangential direction.

The considered cost function is (5.11), the weight matrices are

$$\hat{Q} = 8 \cdot \operatorname{diag}\left(10^4,\ 10^5,\ 10^4,\ \frac{1}{16}\right), \qquad R = \operatorname{diag}(10,\ 10,\ 1).$$

As mentioned, the timing law is a degree of freedom in the controller design. Here we choose a simple timing law of the form

$$\dot{\theta} = g(\theta, v) = -\lambda\theta + v,$$

where $\lambda = -10^{-3}$ and $v \in [0, 6]$. The initial condition is $\theta_0 = -30$. Note that the chosen timing law satisfies Assumption 5.2. Since we want to apply Corollary 5.1 the path $\mathcal{P}$ is chosen as terminal region $\mathcal{E} = \mathcal{P}$.

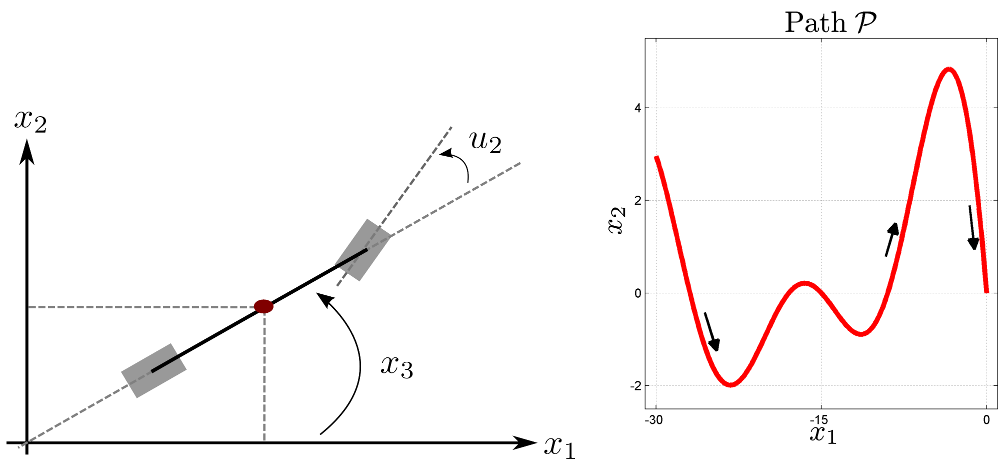


**Figure 5.2:** Sketch of the autonomous robot (5.13) and the path from (5.14).

To apply Corollary 5.1 we need to know inputs signals $u_{\mathcal{E}}(\cdot)$ and $v_{\mathcal{E}}(\cdot)$ which render $\mathcal{P}$ positively invariant and ensure $\dot{\theta} \geq 0$. In Example 4.3 we derived inputs which guarantee exact path following:

$$u_{1,\mathcal{E}} = \dot{\theta} \cdot \sqrt{1 + \left(\frac{\partial \rho}{\partial \theta}\right)^2}$$
$$u_{2,\mathcal{E}} = \arctan\left(\left(1 + \left(\frac{\partial \rho}{\partial \theta}\right)^2\right)^{-\frac{3}{2}} \cdot \frac{\partial^2 \rho}{\partial \theta^2}\right).$$

The inputs depend on the path parametrization $p(\theta)$ and the parameter evolution specified by $\dot{\theta} = g(\theta, v)$. In Figure 5.3 these inputs are plotted for $\forall t \geq 0 : v_{\mathcal{E}}(t) = 0$. Clearly, this virtual input leads to admissible inputs $u_{1,2,\mathcal{E}}(\cdot)$. Also note that for $v_{\mathcal{E}}(\cdot) = 0$ the second input $u_{2,\mathcal{E}}$ does not vanish at the end of the path, cf. zoomed plot in Figure 5.3 right side. Thus we penalize $u - \tilde{u}$ in $F$. The reference values $\tilde{u}$ are set to $\tilde{u}_2 = u_{2,\mathcal{E}}|_{\theta=0}$ and $\tilde{u}_1 = 0$.
Investigation of the simplified condition (5.12a) for different values of $\epsilon > 0$ and $k = 1, 2$ yields that the end penalties

$$E_1(\theta) = -1900 \cdot \theta, \qquad E_2(\theta) = \frac{450}{2} \cdot \theta^2$$

fulfill the conditions of Corollary 5.1. The time derivatives $\frac{\partial E_k}{\partial \theta} g(\theta, 0),\ k = 1, 2$ along the path are depicted in Figure 5.4. While the quadratic $E_2(\theta)$ end penalty is a tighter bound for the cost-to-go in the neighborhood of $\theta = 0$ the linear end penalty $E_1(\theta)$ is significantly less conservative for $\theta \ll 0$. In Figure 5.5 the simulation results for two different MPFC schemes are shown. Both schemes use the same prediction horizon of $T_p = 1$ and the sampling time $\delta = 0.05$. Only the end penalties are different, i.e., $E_1(\theta), E_2(\theta)$ from above are used. For both control schemes the system initial condition is $x(0) = (-30,\ 1,\ 0)^T$. The upper part of Figure 5.5 illustrates the movement of the

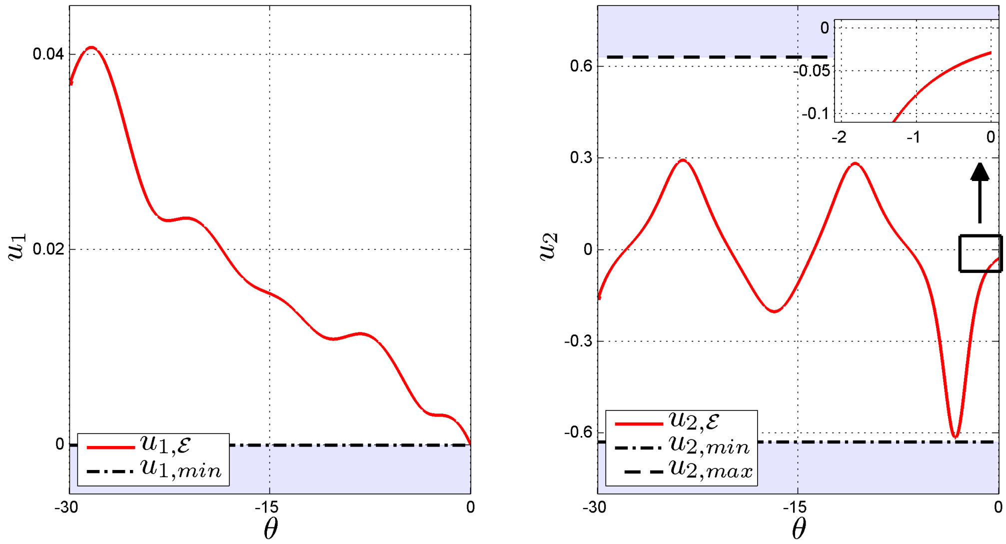


**Figure 5.3:** Inputs $u_{1,\mathcal{E}}$ and $u_{2,\mathcal{E}}$ for $v_{\mathcal{E}} = 0$.

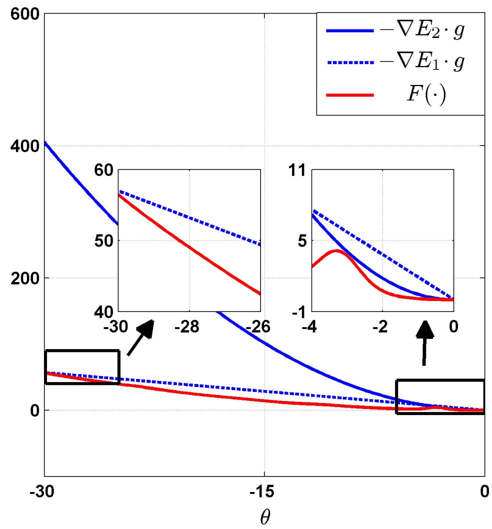


**Figure 5.4:** Cost function $F$ and derivatives of $E_k(\theta),\ k = 1, 2$ along $\mathcal{P}$.

autonomous robot in the $x_1$–$x_2$ plane. The black arrows indicate the direction of movement. Both schemes converge to the path rapidly such that in the $x_1$–$x_2$ plane no difference can be observed. However, in the time domain the performance of the MPFC scheme with linear end penalty $E_1(\theta)$ differs from the one with quadratic end penalty $E_2(\theta)$. The lower part of Figure 5.5 depicts the time evolution of the path parameter $\theta$, the path parameter input $v$ and the inputs applied to the autonomous robot $u_1, u_2$. Dashed blue lines correspond to the scheme with $E_1(\theta)$, continuous blue lines to the scheme with $E_2(\theta)$. Clearly, the scheme with $E_2(\theta)$ is more aggressive in

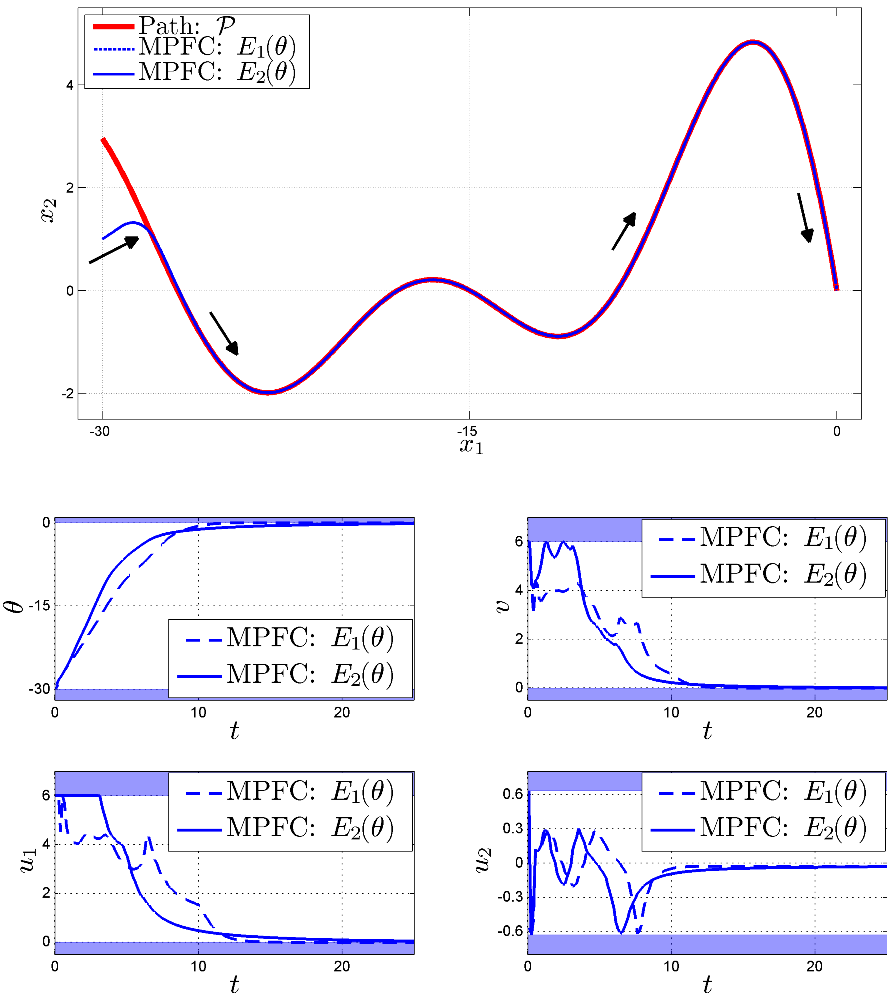


**Figure 5.5:** Simulation results for MPFC schemes with $E_k(\theta),\ k = 1, 2$.

terms of advancing along the path during the first part of the path. As soon as $\theta$ is close to 0 this scheme converges only very slowly to $\theta = 0$. This means that the vehicle is moving very slow along the last part of the path $\mathcal{P}$. In contrast to that the scheme with $E_1(\theta)$ is less aggressive during the first part of the path and much more aggressive for small $\theta$. To understand this behavior in detail reconsider Figure 5.4. We know that $E_1(\theta)$ induces comparably high costs for $\theta$ close to 0 and rather low costs for $\theta \ll 0$. Vice versa $E_2(\theta)$ penalizes $\theta \ll 0$ heavily. Hence the choice of the end penalty $E_k(\theta)$ has to be made carefully, since it directly influences the trade-off between the speed to follow along the path and the accuracy. As shown in Lemma 5.1 one can rely on the superposition of end penalties $E_{1,2}(\theta) = \alpha_1 E_1(\theta) + \alpha_2 E_2(\theta),\ \alpha_1 + \alpha_2 \geq 1$, if one wants to achieve rapid movement along the complete path.

## 5.2 Predictive Output Path Following

So far we have introduced an NMPC scheme to solve path-following problems in the state space. The conceptual idea is to treat the path parameter $\theta$ as an additional state, which can be controlled by means of the virtual path parameter input $v$. Next we shift to the more general and application relevant problem of following paths in output spaces. We transfer the conceptual ideas from the last section to output path following as introduced in Chapter 4.

We consider nonlinear systems of the form

$$\dot{x}(t) = f(x(t), u(t)), \quad x(t_0) = x_0 \tag{5.15a}$$

$$y(t) = h(x(t)). \tag{5.15b}$$

Here, $x \in \mathcal{X} \subset \mathbb{R}^{n_x}$ and $u \in \mathcal{U} \subseteq \mathbb{R}^{n_u}$ denote the state and input constraints. The sufficiently often continuously differentiable map $h : \mathbb{R}^{n_x} \to \mathbb{R}^{n_y}$ defines the output $y$. We suppose that the system and the constraints fulfill our standard assumptions from Chapter 2. The path is a regular curve in the output space $\mathbb{R}^{n_y}$

$$\mathcal{P} = \left\{ y \in \mathbb{R}^{n_y} \mid \theta \in [\theta_0, 0] \mapsto p(\theta) \right\}. \tag{5.16}$$

We assume that the parametrization $p$ is sufficiently often continuously differentiable. In constrast to Chapter 4 we require $-\infty < \theta_0 \leq 0$. As in (4.12) from Chapter 4 the dynamics of the path parameter are an integrator chain $\theta^{(\hat{r}+1)} = v$ and are written as

$$\begin{aligned} \dot{z} &= l(z, v) = Az + Bv, \quad z(t_0) = z_0 \in \mathbb{R}^{\hat{r}+1}, \ \hat{r} < \infty \\ \theta &= Cz \qquad\quad = z_1. \end{aligned}$$

As in (4.14) we use the augmented system

$$\begin{pmatrix} \dot{x} \\ \dot{z} \end{pmatrix} = \begin{pmatrix} f(x, u) \\ l(z, v) \end{pmatrix} \tag{5.17a}$$

$$\begin{pmatrix} e \\ \theta \end{pmatrix} = \begin{pmatrix} h(x) - p(z_1) \\ z_1 \end{pmatrix} \tag{5.17b}$$

to describe the path-following problem to be solved.

**Problem 5.2** (Output path following with monotonous forward motion)**.**
*Given system* (5.17) *and the reference path* $\mathcal{P}$ (5.16) *design a controller that achieves:*

*i)* ***Path Convergence****: The error* $e = h(x) - p(\theta)$ *converges s.t.* $\lim_{t\to\infty} \|e(t)\| = 0$.

*ii)* ***Forward Motion****: The system moves along* $\mathcal{P}$ *in the direction of increasing values of* $\theta$ *s.t.* $\lim_{t\to\infty} \theta = 0$ *and* $\dot{\theta} = \dot{z}_1(t) \geq 0$.

*iii)* ***Constraint Satisfaction****: The constraints on states* $(x, z) \in \mathcal{X} \times \mathcal{Z}$ *and inputs* $(u, v) \in \mathcal{U} \times \mathcal{V}$ *are satisfied for all times.*

Note that this problem description is a slightly modified version of Problem 4.1. The major difference is that the forward motion requirement is relaxed, we have to reach the final path point $\theta = 0$. However, we allow $\dot{\theta} = 0$ for finite time spans. Moreover, the formulation directly relies on the augmented system description (5.17). Subsequently, we formulate the predictive path-following control scheme as well as the convergence results directly in terms of the augmented system (5.17) in usual coordinates. We rely on these coordinates to avoid an assumption on existence of a transverse normal form.

Similar to the case of state space paths we propose a predictive control scheme to tackle the problem. The scheme is based on the repeated solution of an OCP. The cost functional to be minimized at each sampling instance $t_k = t_0 + k\delta, k \in \mathbb{N}$ is

$$J\left(x(t_k), \bar{e}(\cdot), \bar{\theta}(\cdot), \bar{u}(\cdot), \bar{v}(\cdot)\right) = \int_{t_k}^{t_k+T_p} F\left(\bar{e}(\tau), \bar{\theta}(\tau), \bar{u}(\tau), \bar{v}(\tau)\right) d\tau + E\left(\bar{x}(t_k+T_p), \bar{z}(t_k+T_p)\right). \quad (5.18)$$

As before $F : \mathbb{R}^{n_y} \times [\theta_0, 0] \times \mathcal{U} \times \mathcal{V} \to \mathbb{R}_0^+$ is denoted as cost function, and $E : \mathbb{R}^{n_x} \times \mathbb{R}^{\hat{r}+1} \to \mathbb{R}_0^+$ is termed end penalty. The OCP to be solved repetitively becomes:

$$\underset{(\bar{u}(\cdot),\bar{v}(\cdot))\in\mathcal{PC}(\mathcal{U}\times\mathcal{V})}{\text{minimize}} \; J\left(x(t_k), \bar{e}(\cdot), \bar{\theta}(\cdot), \bar{u}(\cdot), \bar{v}(\cdot)\right) \quad (5.19a)$$

subject to

$$\begin{aligned}
\forall \tau \in [t_k, t_k+T_p]: \quad & \dot{\bar{x}}(\tau) = f(\bar{x}(\tau), \bar{u}(\tau)), \quad \bar{x}(t_k) = x(t_k) && (5.19b)\\
& \dot{\bar{z}}(\tau) = l(\bar{z}(\tau), \bar{v}(\tau)), \quad \bar{z}(t_k) = \bar{z}(t_k, t_{k-1}, \bar{z}(t_{k-1})|\bar{v})) && (5.19c)\\
& \bar{e}(\tau) = h(\bar{x}(\tau)) - p(\bar{z}_1(\tau)) && (5.19d)\\
& \bar{\theta}(\tau) = \bar{z}_1(\tau) && (5.19e)\\
& \bar{x}(\tau) \in \mathcal{X}, \; \bar{u}(\tau) \in \mathcal{U} && (5.19f)\\
& \bar{z}(\tau) \in \mathcal{Z}, \; \bar{v}(\tau) \in \mathcal{V} && (5.19g)\\
(\bar{x}(t_k+T_p), \bar{z}(t_k+T_p))^T \in \mathcal{E} \subset \mathcal{X} \times \mathcal{Z}. & && (5.19h)
\end{aligned}$$

The equations (5.19c) and (5.19e) state that the path parameter $\bar{\theta}$ is regarded as the output of the (virtual) path parameter dynamics. These dynamics are described through the higher order timing law $l$ and can be influenced by the virtual input $\bar{v}$. As before $\bar{v}$ is an additional decision variable of the minimization. Since we want to minimize the deviation from the path, the error output is stated in (5.19d).

Furthermore, the path parameter dynamics (5.19c) are subject to the state and input constraints (5.19g). The state constraint $\mathcal{Z}$ is defined as in (4.13)

$$\mathcal{Z} := \left\{[\theta_0, 0] \times [0, \infty) \times \mathbb{R}^{\hat{r}-1}\right\} \subset \mathbb{R}^{\hat{r}+1}.$$

This constraint ensures that $\bar{\theta} = \bar{z}_1 \in [\theta_0, 0]$ and $\dot{\bar{\theta}} \geq 0$. In order to avoid impulsive

solutions to the path parameter dynamics $\dot{\bar{z}} = l(\bar{z}, \bar{v})$ the admissible path parameter inputs $\bar{v}$ are restricted to a compact set $\mathcal{V} \subset \mathbb{R}$ containing 0 in its interior.
While at each sampling instance the measured state information $x(t_k)$ serves as initial condition for (5.19b) the initial conditions for the timing law (5.19c) is the last predicted trajectory $\bar{z}(t, t_{k-1}, \bar{z}(t_{k-1})|\bar{v})$ evaluated at time $t_k$. If no initial condition for the first sampling instance $k = 0$ is given, we obtain $z(t_0)$ similarly to (5.7)

$$\bar{z}(t_0) = (\theta(t_0), 0, \ldots, 0)^T$$
$$\theta(t_0) = \underset{\theta \in [\theta_0, 0]}{\operatorname{argmin}} \ \|h(x_0) - p(\theta)\|.$$

To initialize the scheme a value $\theta(t_0)$ which (at least locally) minimizes the distance $\|h(x_0) - p(\theta)\|$ has to be obtained. The optimal solution of problem (5.19) is denoted as $J^\star(\cdot)$ and leads to optimal input trajectories $\bar{u}_k^\star(\cdot)$ and $\bar{v}_k^\star(\cdot)$. Finally, $\bar{u}_k^\star(\cdot)$ is applied to system (5.15) such that for all $t \in [t_k, t_k + \delta)$: $u(t) = \bar{u}_k^\star(t)$.
It is important to note that (5.19h) requires that at the end of each prediction the predicted augmented state $(\bar{x}(t_k + T_p), \bar{z}(t_k + T_p))$ is inside a terminal region $\mathcal{E}$. Although only outputs and inputs are penalized in the cost function $F$, the terminal constraint is stated in the state space. We want to ensure recursive feasibility of the OCPs (5.19) arising from our MPFC scheme as well as convergence to the output path. Therefore arguments similar to those used in Section 3.3.1 for the output trajectory-tracking problem lead to the conclusion that this can be guaranteed via terminal regions in the state space. And since the end penalty $E(x, z)$ is used to bound from above the cost-to-go for all solutions starting in the terminal region, it is stated as a state-dependent function, i.e., a positive semi-definite function of the predicted augmented state $(x, z)$. Similar to Section 3.3 this allows to include cases where error-dependent end penalties $E(e, \theta)$ are used.
This MPFC scheme to follow paths in output spaces is built upon the same conceptual ideas as the previous one for state space paths. Relying on (5.19) we compute the reference motion $t \mapsto p(\theta(t))$ together with the real system inputs $u(t)$ to track this motion.

## 5.2.1 Sufficient Convergence Conditions

We are interested in conditions ensuring that the MPFC scheme (5.19) solves Problem 5.2. Next we present sufficient conditions which ensure that the repetitive solution of (5.19) leads to convergence of path-following error $e = h(x) - p(\theta)$, forward motion $\dot{\theta} \geq 0$, and satisfaction of constraints. To this end we adjust our assumptions.

**Assumption 5.4** (Consistency of path and state constraints).
*The path $\mathcal{P}$ from* (5.16) *is contained in the interior of the pointwise image of the state constraints $\mathcal{X}$ under the output map $h : \mathbb{R}^{n_x} \to \mathbb{R}^{n_y}$ from* (5.17b)

$$\mathcal{P} \subset \operatorname{int} h(\mathcal{X}).$$

If $\mathcal{P} \not\subset h(\mathcal{X})$, then parts of the path are not consistent with the state constraints. Additionally, we require that the cost function fits to the considered path-following problem such that $F(e, \theta, u, v) \to 0 \Rightarrow \|e\| \to 0$.

**Assumption 5.5** (Lower bounded cost function $F$)**.**
*The cost function $F(e, \theta, u, v)$ from (5.18) is lower bounded by a class $\mathcal{K}$ function $\underline{\psi}(\|(e, \theta)\|)$.*

Under these assumptions the following result can be obtained.

**Theorem 5.2** (Convergence of MPFC for constrained output path following)**.**
*Consider Problem 5.2 and Assumptions 5.4–5.5. Suppose that a terminal region $\mathcal{E} \subset \mathcal{X} \times \mathcal{Z}$, and a terminal penalty $E(x, z)$ exist such that the following holds:*

*i) The set $\mathcal{E}$ is closed. $E(x, z) \in \mathcal{C}^1$ is positive semidefinite.*

*ii) For all $(\tilde{x}, \tilde{z}) \in \mathcal{E}$ there exists a scalar $\epsilon \geq \delta > 0$ and admissible inputs $(u_\mathcal{E}(\cdot), v_\mathcal{E}(\cdot)) \in \mathcal{PC}(\mathcal{U} \times \mathcal{V})$ such that for all $\tau \in [0, \delta]$*

$$\left(\frac{\partial E(x,z)}{\partial x}, \frac{\partial E(x,z)}{\partial z}\right) \cdot \begin{pmatrix} f(x(\tau), u_\mathcal{E}(\tau)) \\ l(z(\tau), v_\mathcal{E}(\tau)) \end{pmatrix} + F\Big(e(\tau), \theta(\tau), u_\mathcal{E}(\tau), v_\mathcal{E}(\tau)\Big) \leq 0, \quad (5.20)$$

*and the solutions $x(\tau) = x(\tau, \tilde{x}|u_\mathcal{E}(\cdot))$, $z(\tau) = z(\tau, \tilde{z}|v_\mathcal{E}(\cdot))$, starting at $(\tilde{x}, \tilde{z}) \in \mathcal{E}$, stay in $\mathcal{E}$ for all $\tau \in [0, \delta]$.*

*iii) The OCP (5.19) is feasible for $t_0$.*

*Then the MPFC scheme based on (5.19) solves Problem 5.2.*

*Proof.* In essence this result is a time-invariant reformulation of the results of Theorem 2.1. The main difference is that the cost function $F$ is lower bounded by class $\mathcal{K}$ functions of the outputs $(e, \theta)$ of (5.17). Recursive feasibility is shown using the same concatenation of optimal inputs $(u_k^\star(\cdot), v_k^\star(\cdot))$ with $(u_\mathcal{E}(\cdot), v_\mathcal{E}(\cdot))$ as in Appendix A. All the remaining steps of the proof of Theorem 2.1 apply mutatis mutandis. Merely the last steps which rely on Barbalat's Lemma lead to a different conclusion. Due to Assumption 5.5 we can only conclude that the error $e = h(x) - p(\theta)$ and the path parameter $\theta$ converge to 0. Additionally, we know that the virtual states $z$ inside $\mathcal{E}$ are restricted to $\mathcal{Z}$, which implies that the forward motion requirement $\dot{\theta} = z_2 \geq 0$ holds. □

Note that the proposed control scheme aims at convergence of the output $y = h(x)$ to the path and not at *Lyapunov*-like state stability. In other words, Theorem 5.2 allows cases where the output converges to the path while the states might move through $\mathcal{E}$. We also allow cases where the zero dynamics of (5.17) with respect to the outputs $e, \theta$ are not stable.

**Remark 5.2** (Design of suitable cost functions).
*So far we have not said anything about the cost function $F$ appearing in the OCP* (5.19) *except the assumption that $F(e, \theta, u, v)$ should be bounded from below by class a $\mathcal{K}$ function. Often one chooses quadratic path error and input penalties for $F$ as in the case of state space paths in Assumption 5.3. Due to the penalization of $e = h(x) - p(\theta)$ such a choice ensures that deviations of the system output from the pre-image of the path $h^{-1}(\mathcal{P})$ are penalized. However, we know from the geometric problem analysis (Chap. 4) that the zero-path-error manifold is specified by the time-derivatives of the path-following error $\frac{d^k e}{dt^k} = 0$. Thus it is reasonable to penalize $e = h(x) - p(\theta)$ as well as its time derivative $\dot{e}$, i.e., one can use cost functions such as*

$$F(e, \dot{e}, \theta, u, v) = \|(e, \dot{e}, \theta)\|_Q^2 + \|(u, v)\|_R^2.$$

*With straightforward modifications the result of Theorem 5.2 remains valid for this choice of cost functions.*

The question arises of how to verify the conditions Theorem 5.2. In other words, how to compute suitable end penalties, terminal regions, and local controllers inside the terminal regions. In general this is difficult. Mainly, two challenges appear. Firstly, we need to check if the path is exactly followable. This means we have to pinpoint the zero-path-error manifold. For square MIMO systems this can be done in a structured way via a transformation to a local transverse normal form, cf. Section 4.3. If constraints (on state and inputs) are present one needs to identify a sufficiently large constraint consistent subset of the zero-path-error manifold. For general systems this step is complicated and one usually needs to take the structure of the nonlinearities into account. Secondly, we have to verify the existence of local controls $u_{\mathcal{E}}(\cdot), v_{\mathcal{E}}(\cdot)$. Actually, designing a local controller for the augmented system (5.17) means to design a controller which stabilizes the zero-path-error manifold while satisfying constraints on states and inputs.

Similar to NMPC for set point stabilitzation one could circumvent these problems with an engineering approach: neglect the terminal constraints and use a sufficiently long prediction horizon. However, in this case it is in general difficult to ensure recursive feasibility of the OCP (5.19). Furthermore, boundedness of the internal dynamics of the augmented system (5.17) is not guaranteed since these states are not penalized in the cost function.

Yet, if a terminal constraint $(\bar{x}(t_k+T_p), \bar{z}(t_k+T_p))^T \in \mathcal{E}$ is employed, the corresponding solutions are required to reach a closed or compact set $\mathcal{E} \subseteq \mathcal{X} \times \mathcal{Z}$, and recursive feasibility is guaranteed. This means that suitable compact state constraints and terminal regions ensure the boundedness of the closed-loop trajectories.

To illustrate the properties of the MPFC scheme for output path following we consider two examples: Firstly, we deal with a path-following task for a robot in Section 5.2.2. We design an MPFC scheme with terminal region and end penalty. Secondly, we discuss a ship course control problem with a non-square input-output structure in Section 5.2.3. There we show that stabilizing a path in an output space can lead to situations where the internal dynamics of the augmented system (5.17) are unstable.

### 5.2.2 Example: Predictive Robot Control

As an example we reconsider the fully-actuated robot with two degrees of freedom from Example 4.2. Without friction and external contact forces the dynamics of such a robot are

$$\begin{pmatrix} \dot{x}_1 \\ \dot{x}_2 \end{pmatrix} = \begin{pmatrix} x_2 \\ B^{-1}(x_1)\left(u - C(x_1, x_2)x_2 - g(x_1)\right) \end{pmatrix} \tag{5.21a}$$

$$y \quad = x_1 \tag{5.21b}$$

$$y_{ca} \quad = h_{ca}(x_1). \tag{5.21c}$$

$x_1 = (q_1, q_2) \in \mathbb{R}^2$ is the vector of joint angles, $x_2 = (\dot{q}_1, \dot{q}_2) \in \mathbb{R}^2$ is the vector of joint velocities. $B : \mathbb{R}^2 \to \mathbb{R}^{2\times 2}$, $C : \mathbb{R}^4 \to \mathbb{R}^{2\times 2}$ describe the dependence of the inertias on the joint angles and dependence of centrifugal and coriolis forces on joint angles and velocities, respectively. $g : \mathbb{R}^2 \to \mathbb{R}^2$ models the effect of gravity. The output $y = x_1$ denotes the space of joint angles, the output $y_{ca}$ is the position of the robot tool in cartesian coordinates. A sketch of the robot is shown in Figure 5.6. The terms $B, C, g, h_{ca}$ are as follows

$$B(q) \quad = \begin{pmatrix} b_1 + b_2\cos(q_2) & b_3 + b_4 cos(q_2) \\ b_3 + b_4 cos(q_2) & b_5 \end{pmatrix} \tag{5.21d}$$

$$C(q, \dot{q}) = -c_1 \sin(q_2) \begin{pmatrix} \dot{q}_1 & \dot{q}_1 + \dot{q}_2 \\ -\dot{q}_1 & 0 \end{pmatrix} \tag{5.21e}$$

$$g(q) \quad = \left(g_1\cos(q_1) + g_2\cos(q_1 + q_2), \quad g_2\cos(q_1 + q_2)\right)^T \tag{5.21f}$$

$$h_{ca}(q) = \begin{pmatrix} l_1\cos(q_1) + l_2\cos(q_1 + q_2) \\ l_1\sin(q_1) + l_2\sin(q_1 + q_2) \end{pmatrix}. \tag{5.21g}$$

The system parameters are listed in Table 5.1. For details on the modelling we refer to [Siciliano et al. 2009]. The inputs $u = (u_1, u_2)^T$ are the torques applied to each joint. We consider box constraints on states and inputs

$$\mathcal{U} = \left\{u \in \mathbb{R}^2 \mid \|u\|_\infty \leq \bar{u}\right\} \tag{5.22a}$$

$$\mathcal{X} = \left\{x = (x_1, x_2) \in \mathbb{R}^4 \mid \|x_2\|_\infty = \|(\dot{q}_1, \dot{q}_2)\|_\infty \leq \bar{\dot{q}}\right\} \tag{5.22b}$$

whereby $\bar{u} = 4000\text{Nm}$ and $\bar{\dot{q}} = \frac{3}{2}\pi\text{rad/s}$.

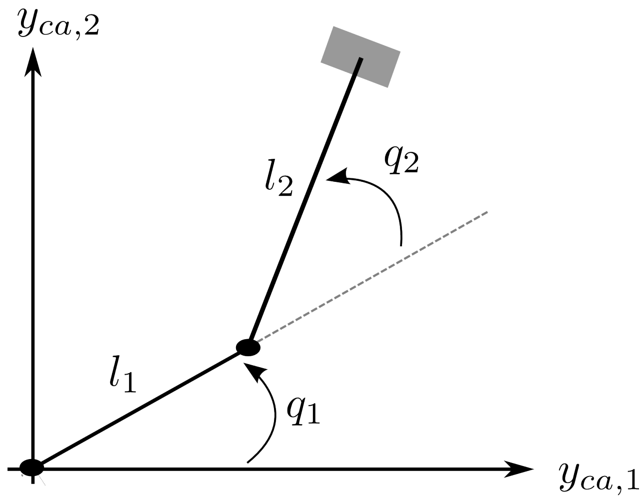


**Figure 5.6:** Schematic sketch of a 2-DoF robot.

The considered path-following task is stated in the joint space. The path is given as

$$\mathcal{P} = \left\{ y \in \mathbb{R}^2 \mid [\theta_0, 0] \mapsto p(\theta) = \begin{pmatrix} \theta - \frac{\pi}{3} \\ \omega_1 \cos(\omega_2(\theta - \frac{\pi}{3})) \end{pmatrix} \right\}, \tag{5.23}$$

and the constants are $\theta_0 = -5.3, \omega_1 = 5, \omega_2 = 0.6$. We describe the path-following task via the augmented system

$$\dot{x} = \begin{pmatrix} x_2 \\ B^{-1}(x_1)\left(u - C(x_1, x_2)x_2 - g(x_1)\right) \end{pmatrix} \tag{5.24a}$$

$$\dot{z} = \begin{pmatrix} 0 & 1 \\ 0 & 0 \end{pmatrix} z + \begin{pmatrix} 0 \\ 1 \end{pmatrix} v \tag{5.24b}$$

$$e = x_1 - p(z_1) \tag{5.24c}$$

$$\theta = z_1. \tag{5.24d}$$

Since we will apply a very fine input discretization, we use here an integrator chain of length two as path parameter dynamics, cf. Remark 4.3.

**Table 5.1:** Parameters for system (5.21), [Siciliano et al. 2009].

| | | | | | |
|---|---|---|---|---|---|
| $b_1$ | 200.0 | [kg m$^2$/rad] | $b_2$ | 50.0 | [kg m$^2$/rad] |
| $b_3$ | 23.5 | [kg m$^2$/rad] | $b_4$ | 25.0 | [kg m$^2$/rad] |
| $b_5$ | 122.5 | [kg m$^2$/rad] | $c_1$ | −25.0 | [Nms$^{-2}$] |
| $g_1$ | 784.8 | [Nm] | $g_2$ | 245.3 | [Nm] |
| $l_1$ | 0.5 | [m] | $l_2$ | 0.5 | [m] |

The cost function for the MPFC scheme is chosen according to Remark 5.2

$$\begin{aligned} F(e,\dot{e},\theta,u,v) &= \|(e,\ \dot{e},\ \theta)\|_Q^2 + \|(u-\tilde{u},\ v)\|_R^2 \\ Q &= \operatorname{diag}(10^5,\ 10^5,\ 10,\ 10,\ 5) \\ R &= \operatorname{diag}(10^{-6},\ 10^{-6},\ 10^{-4}). \end{aligned}$$

In Appendix F we derive a terminal region for the augmented system (5.24). Mainly, we use the exact feedback linearizability of (5.21) to compute an end penalty, which is of the form

$$\mathcal{E} \ = \left\{(x,z) \in \mathbb{R}^6 \mid (e,\dot{e})^T P_\xi (e,\dot{e}) \le 2.53),\ z \in \mathcal{E}_z\right\}, \tag{5.25a}$$

$$\mathcal{E}_z = \left\{z \in \mathbb{R}^2 \mid z_1 \in [-5.3, 0],\ z_2 \in [0, 0.4],\ (-0.78,\ -0.63)(z_1, z_2)^T \ge 0\right\}. \tag{5.25b}$$

In (5.25a) the virtual states $z$ are restricted to a polyhedral terminal region $\mathcal{E}_z$. The path error and its derivative are restricted to an ellipsoidal terminal region (5.25b) with

$$P_\xi = \begin{pmatrix} 1.73 & 0 & 1 & 0 \\ 0 & 1.73 & 0 & 1 \\ 1 & 0 & 1.73 & 0 \\ 0 & 1 & 0 & 1.73 \end{pmatrix}.$$

In Appendix F we show that the terminal penalty $E(x,z) = 0$ combined with $\mathcal{E}$ leads to path convergence in the sense of Theorem 5.2.

The simulations are performed with the following parameters: The virtual input $v$ is restricted to $\mathcal{V} = [-50, 50]$. The prediction horizon is $T_p = 0.75$s, the sampling time is $\delta = 0.005$s, and the OCP is solved with the ACADO Toolkit [Houska et al. 2011]. The terminal region (5.25) and no terminal penalty are used.

Figure 5.7 presents simulations results for an initial condition with $x(0) = (-5.86, 2.43, 0, 0)^T$ and $\theta(0) = -5.3$. The upper right side shows the time evolution of the joints $x_1 = (q_1, q_2)$ in blue color and the reference $p(z_1(t))$ in red color. The joint positions converge rapidly to the reference. The upper left side depicts the corresponding joint velocities and their constraints. In the lower left side the virtual states $z_1 = \eta_1, z_2 = \eta_2$ and the virtual input $v$ are plotted. One can observe that the path parameter moves forward to the end of the path at $\theta = z_1 = 0$.

The input torques are shown in the lower right side. Both inputs satisfy the constraints. The proposed controller also works for a wide range of initial conditions. In Figure 5.8 the path convergence for several initial conditions is depicted. On the left side the plane of joint angles $x_1 = (q_1, q_2)$ is plotted. The black arrows indicate the direction of movement of the robot. On the right side it is shown how the solutions for different initial conditions converge to the image of the path in the Cartesian output space defined via (5.21g).

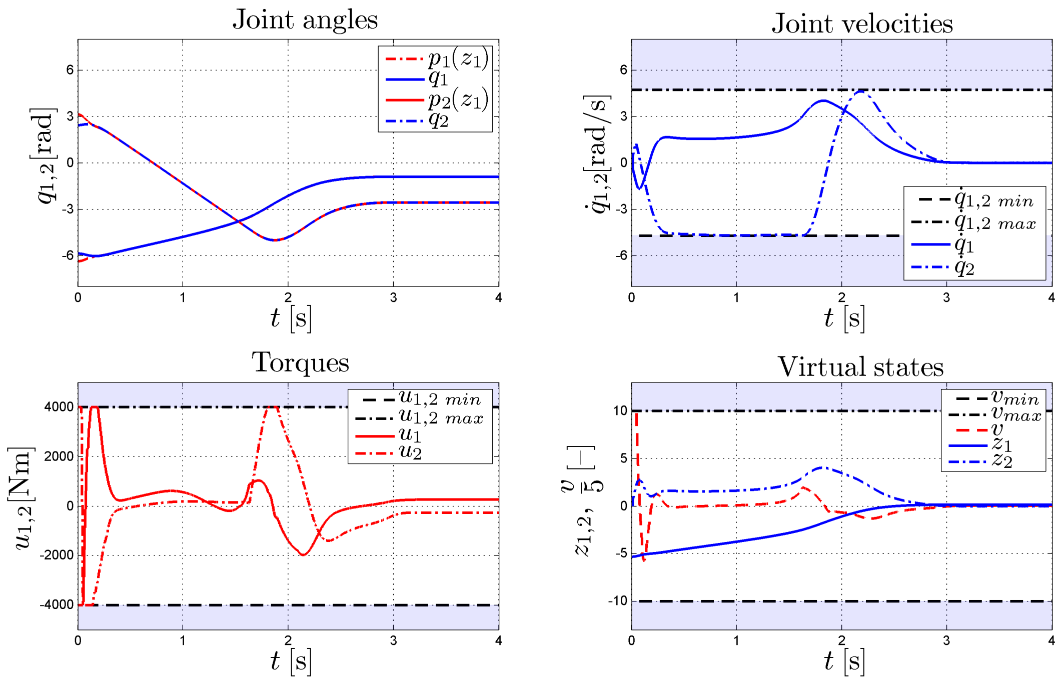


**Figure 5.7:** Simluation results for 2-DoF robot.

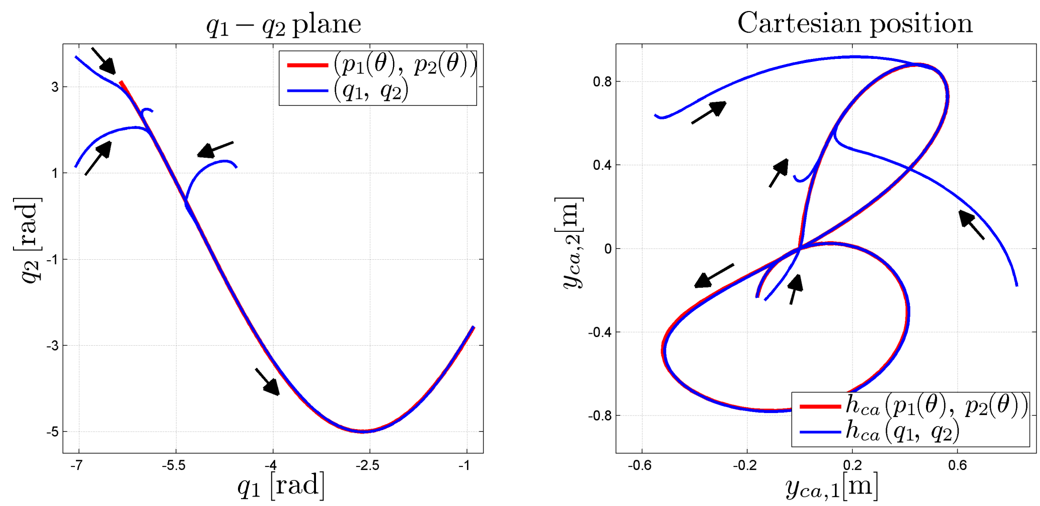


**Figure 5.8:** Path convergence in joint space (left) and cartesian output space (right).

Finally, we conclude from this example that the conditions of Theorem 5.2 can be used to design predictive path-following controllers. In presence of constraints on states and inputs the MPFC scheme stabilizes the motion of the system with respect to the path.

### 5.2.3 Example: Predictive Ship Course Control

To illustrate that the proposed MPFC scheme also works for systems without a non-square input-output structure we reconsider the ship course control problem from Example 4.1 and Section 4.3.2. Recall the augmented ship dynamics (4.37)

$$\begin{pmatrix}\dot{x}_1\\ \dot{x}_2\\ \dot{x}_3\\ \dot{x}_4\\ \dot{z}_1\\ \dot{z}_2\end{pmatrix} = \begin{pmatrix} w\cos x_3 - Lwx_4\sin x_3\\ w\sin x_3 + Lwx_4\cos x_3\\ x_4\\ \frac{1}{\tau}(-x_4+Ku)\\ z_2\\ v\end{pmatrix} \tag{5.26a}$$

$$e = \Big(x_1 - p_1(z_1),\ x_2 - p_2(z_1)\Big)^T \tag{5.26b}$$

$$\theta = z_1. \tag{5.26c}$$

The input $u$ is limited to $-0.85 \leq u \leq 0.85$. The system parameters are as introduced in Section 4.3.2. The path parameter input $v$ is subject to the constraint $-0.2 \leq v \leq 0.2$. As in (4.48) the path to be followed is given by the regular curve

$$p(\theta) = \begin{pmatrix}\theta\\ c_1\sin(c_2\theta)\end{pmatrix}^T, \quad c_1 = -10^3,\ c_2 = -1.5\cdot 10^{-3}.$$

The MPFC controller is designed according to the OCP (5.19) and Remark 5.2. As shown in Section 4.3.2 on the zero-path-error manifold the forward motion requirement determines unique inputs $u_{\mathcal{P}}(\cdot),\ v_{\mathcal{P}}(\cdot)$, i.e., the speed to move exactly along the path with $\dot{\theta} = z_2 \geq 0$ is not free. Thus we do not penalize the $u, v$ and $\theta$ explictly in the cost function $F$. To ensure forward motion along the path we introduce an extra constraint $z_2 \geq 1.5$. We penalize the path-following error $e$ as well as its time derivative $\dot{e}$ to enforce fast convergence to the zero-path-error manifold. $F$ is chosen as

$$F(e,\dot{e}) = \|(e,\dot{e})\|_Q^2, \quad Q = \mathrm{diag}(1,\ 1,\ 0.25,\ 0.25).$$

The prediction horizon is $T_p = 500$s, and the sampling time is $\delta = 60$s. For the computations the inputs are discretized as piecewise continous functions with $\delta t = 20$s. We do not consider terminal constraint nor terminal penalties.

After a suitable scaling of the states the simulation results are obtained with the ACADO Toolkit [Houska et al. 2011]. For several initial conditions the results are depicted in Figure 5.9. The ship movement and the reference path in the $x_1$–$x_2$ plane are illustrated in Figure 5.9. The black arrows indicate the direction of movement. For all initial conditions the solutions converge rapidly to the path. In Figure 5.10 the inputs to the augmented dynamics (5.26) are plotted over the path parameter $\theta$. The left side depicts the real system input $u$, the right side shows the path parameter

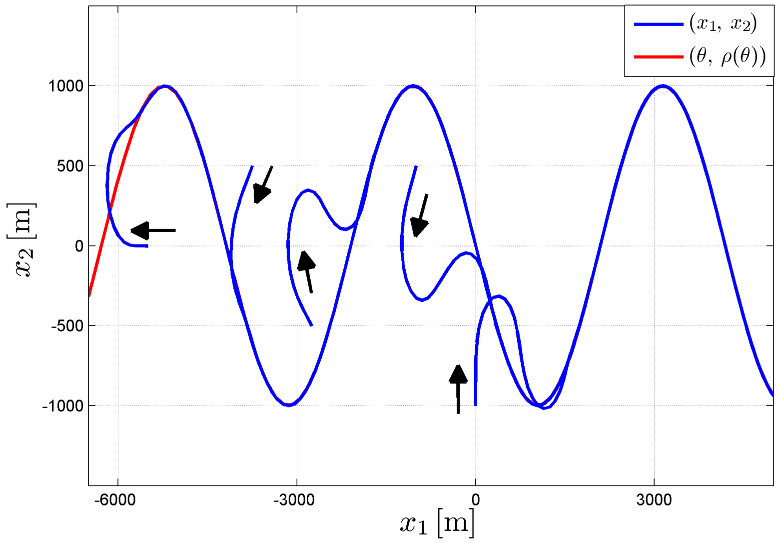


**Figure 5.9:** Ship movement and reference path in $x_1$–$x_2$ plane.

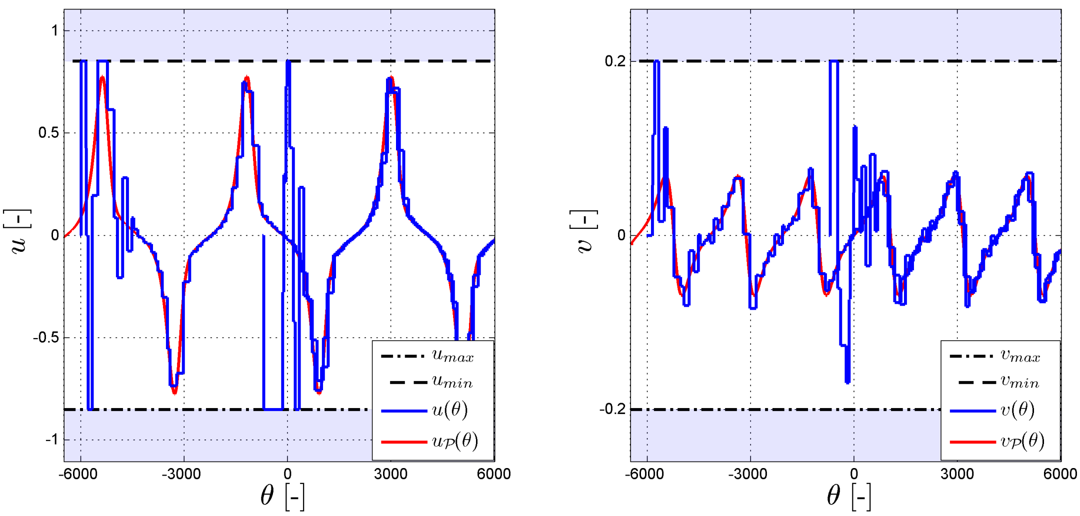


**Figure 5.10:** Path parameter input and system input obtained via MPFC scheme.

input $v$. The red curves are the nominal solutions $u_{\mathcal{P}}(\cdot)$, $v_{\mathcal{P}}(\cdot)$, i.e., the inputs which render $\mathcal{P}$ positively invariant with $\dot{z}_1 > 0$ as derived in Section 4.3.2. For sake of a clear presentation only the input trajectories corresponding to the first and the fourth initial condition are plotted. Both $u(\cdot)$ and $v(\cdot)$ obtained via the MPFC scheme converge rapidly to the unique path-following inputs.

Finally, in Figure 5.11 the phase plane of the internal dynamics of (5.26)—which have been derived in (4.45a)—is depicted. The red curve represents the nominal solution of the zero dynamics of (5.26). In other words, it depicts a solution where the unique exact path-following inputs $u_{\mathcal{P}}, v_{\mathcal{P}}$ from (4.47) are applied for an initial condition

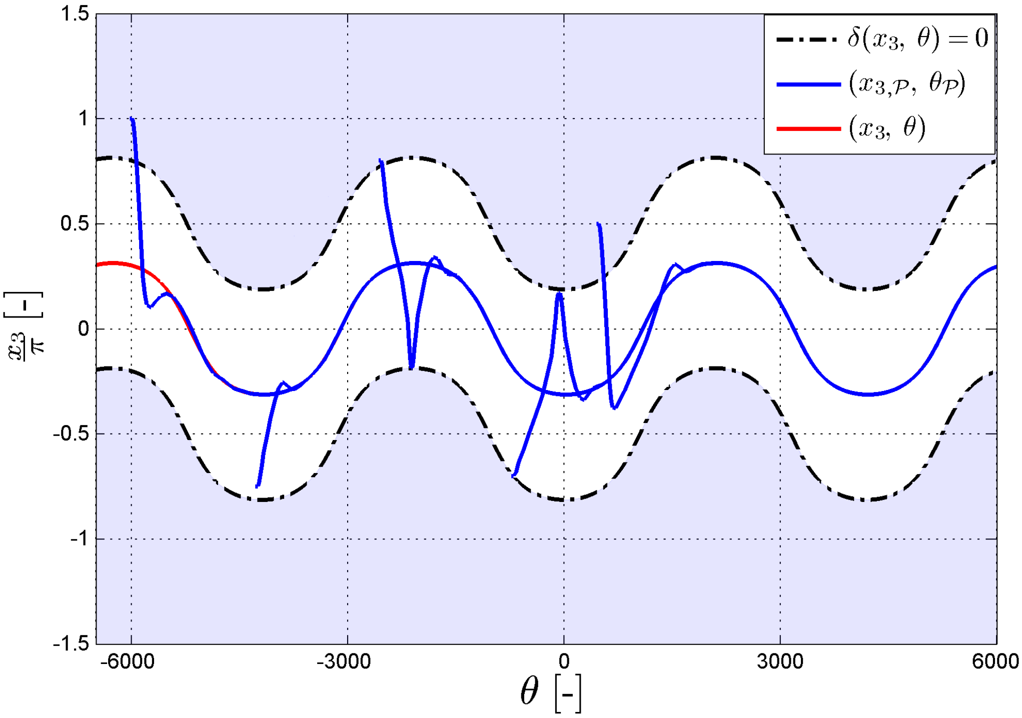


**Figure 5.11:** Phase plane of internal dynamics (4.45a) under MPFC scheme.

starting in the zero-path-error manifold. The blue curves depict the $(\theta, x_3)$ trajectories for the considered initial conditions. Again the solutions obtained with the proposed MPFC scheme converge rapidly to the nominal solution. The black dash-dot lines mark $\delta(x_3, \theta) = 0$, where $\delta$ is as in (4.40). As discussed in Section 4.3.2 a description of the path-following problem for (5.26) in the transverse normal coordinates (4.45) is restricted to the condition $\delta(x_3, \theta) \neq 0$. Note in Figure 5.11 the $(\theta, x_3)$ solutions for the first, third, and fifth considered initial condition start at points with $\delta(x_3, \theta) < 0$. Nevertheless, these solutions converge to the nominal trajectory plotted as red curve. Comparing this to the previous discussion of the ship example—cf. Figure 4.3 in Section 4.3.2—it is clear that such a behavior cannot be achieved by a controller designed in the transverse normal form coordinates (4.45). This is due to the fact that the transverse normal form coordinates (4.45) are not defined for $\delta(x_3, \theta) = 0$.

We can draw several conclusions from this example: The proposed MPFC scheme achieves path convergence in the presence of constraints. Note that the internal dynamics of (5.26) are unstable. This means that the MPFC scheme (5.19) stabilizes only the zero-path-error manifold but not the complete state. On this manifold the system moves in direction of increasing values of $\theta$. Moreover, our design is applicable to non-square input-output structures and avoids restrictions of purely geometric controller designs. Finally, we also see that the proposed MPFC scheme can achieve path convergence even if neither terminal constraints nor end penalties are considered.

## 5.3 Summary

In this chapter we presented a conceptual framework for model predictive path-following control. We derived rigorous stability conditions for path-following problems formulated in the state space as well as for output path following. We demonstrated that for state space path following exact path followability implies the existence of stabilizing terminal regions and end penalties. Furthermore, our examples from Sections 5.1.4, 5.2.2, and 5.2.3 demonstrate the applicability of the augmented system description, where the path parameter $\theta$ and several of its time derivatives are treated as virtual state variables.

For the 2-DoF robot from Section 5.2.2 we have shown how to obtain stabilizing terminal regions and end penalties. We have drawn upon an example from ship course control in Section 5.2.3 to illustrate that our predictive control approach to path following is applicable to non-square systems with less inputs than outputs.

# 6 Conclusions and Perspectives

By now model predictive control for set point stabilization of linear systems is a mature controller design technique which is widely applied in (process control) applications. Also nonlinear model predictive control for set point stabilization problems is well understood. However, not all control tasks are set point stabilization problems. In this thesis we discussed optimization-based approaches to trajectory-tracking and path-following problems extending the applicability of NMPC to these fields.

## 6.1 Trajectory Tracking

For trajectory-tracking problems we proposed an NMPC scheme based on time-varying terminal regions in Chapter 3. We considered output and state space trajectory tracking. The concept of time-varying terminal regions helps to overcome limitations of previous works [Magni and Scattolini 2007; Michalska 1996] on NMPC for trajectory tracking, for example, overly long prediction horizons or very small terminal regions. Moreover, the approach allows to explicitly consider input and state constraints. In case of reference trajectories defined in the state space we have shown how to compute terminal regions as time-varying level sets of a local Lyapunov function. If a system controlled by an affine feedback admits a quadratic time-varying Lyapunov function, it is possible to compute time-varying level sets via an infinite dimensional linear program.

Time-varying level sets can be interpreted as a tool to approximate the region of attraction of two-degrees-of-freedom (2-DoF) control structures in the presence of constraints. For future research it seems promising to consider specific nonlinearities in order to maximize not only the diameter of the time-varying level sets but also to optimize their shape. For example, one could combine the presented approach to time-varying level sets with results on computation of the region of attraction along uncontrolled trajectories of polynomial systems [Tobenkin et al. 2011]. This would lead to semi-definite programs to be solved. Using McCormick relaxations one can also handle non-polynomial nonlinearities at the expense of an increased state dimension [Gu 2009; McCormick 1976].

Furthermore, it would be interesting to combine the classic results on output regulation, where the reference is generated by an exogenous system [Isidori 1995], with NMPC. First steps in this direction are presented in [Magni et al. 2001]. However, it is still unclear how to handle constraints in such a framework. More closely related to the results presented in Chapter 3, one can ask how to consider periodic references for nonlinear systems, and how to avoid the use of terminal constraints by sufficiently long prediction horizons. The last question is challenging, since the usual results on NMPC for time-invariant systems without terminal constraints require quadratic bounds on the MPC value function or cost-controllability assumptions, cf . [Graichen and Kugi 2010; Grüne 2009; Jadbabaie and Hauser 2005; Jadbabaie et al. 2001]. In general, such assumptions are difficult to verify for time-varying systems.

## 6.2 Path Following

We discussed analysis and controller design aspects of path-following problems in the presence of constraints. In Chapter 4 we outlined path-following problems and introduced a notion of exact path followability. We propose considering path-following problems in an augmented system description which can be mapped locally into a Byrnes-Isidori normal form. As shown, this problem description allows investigation of the question of path followability. For differentially flat systems we presented sufficient conditions on exact path followability in presence of constraints on states and inputs. These results provide a framework to analyze path-following problems.

We briefly touched on the question of how to deal with non-square input-output structures. Extended path-following formulations—for example, geometric reference descriptions with more than one dimension—might provide a useful framework for detailed investigations. First steps in this direction are presented in [Faulwasser and Findeisen 2009a,b]. Such an approach leads to the problem of stabilizability of general output manifolds. In fact, path following can be seen as a special manifold stabilization task.

In Chapter 5 we presented novel NMPC schemes for model predictive path-following control (MPFC). The schemes rely on the augmented system description of path-following problems from Chapter 4. We discussed predictive path following in state and output spaces in presence of constraints on states and inputs. The novel aspect of our MPFC schemes is rigorously ensuring that the motion of a system is stabilized along the path. It is important to note that the presented convergence conditions for MPFC do not rely on specific system properties as, for example, differential flatness or square input-output structures. While overcoming existing limitations, it remains open how to design path-following specific NMPC schemes without terminal constraints. We want to mention, however, that first preliminary steps towards predictive path following without terminal cosntraints have been presented in [Faulwasser and Findeisen 2012].

Besides schemes without terminal constraints the question of suitable convexifing approximations to general MPFC schemes is of strong theoretical and practical interest. Even if the system dynamics and the output map are linear, general nonlinear path descriptions lead to non-convex optimization problems. To relax the computational demand one can also think of combining MPFC schemes with locally stabilizing controllers in a 2-DoF control structure. In such a setting the MPFC scheme would repeatedly assign reference trajectories to the path and these references would be stabilized with a very fast local controller. In contrast to usual control schemes with offline trajectory generation it would be rather easy to trigger the computations in the feedforward part by current information about the distance between reference and system output in an event-based fashion.

Finally, one could ask what is more challenging: path following in the state space or in an output space? Often path following in the state space can be reformulated as a set point stabilization problem in suitable coordinates, cf. Chapter 5. In contrast to that output path following is more challenging. It is not always possible to reconstruct complete state information from knowledge about the output path-following error and the path parameter. Hence we need extra care to ensure boundedness of the states and path convergence at the same time.

From a controllability or reachability point of view, the answer to this question might be a different one: Recall that $n_x, n_y, n_u$ are state, output, and input dimensions. Furthermore, all inputs and outputs are independent. For a general nonlinear MIMO system with $n_x > n_u$ the task to follow a path in the state space is challenging. The state dimension is usually much larger than the dimension of the inputs $n_x \gg n_u$. If the task is defined in an output space with $n_y < n_x$ reaching the path and rendering it positively invariant might be easier, since the ratio of independent inputs and outputs is more suitable.

Thus one can conclude that the answer to the question of whether path following in the state space is more difficult than in output spaces, depends on the point of view. Yet, there is no doubt that output path following is more relevant for applications. Beyond problems for robotic and vehicle-like systems certain process control problems can be regarded as (output) path-following problems. For example, consider tasks where it is required to track a temperature profile in batch or semi-batch reactors. One can formulate this as the problem of following a temperature path and at the same time maximizing the process yield along this path. We conclude that path following in general, and the results presented in this thesis, provide a framework for many challenging applications.

## 6.3 Concluding Remarks

The theoretical results on NMPC for set point stabilization are manifold. However, stabilization is only one aspect which is important in applications. For example, tasks such as rejection of measured/estimated disturbances, tracking of precomputed reference trajectories, optimization of economic process performance, or following of geometric references, are more general than set point stabilization problems. For these application-relevant problems suitable tools and methods are currently limited. Problem settings which are suitable from the NMPC point of view often include strong assumptions, for example, available state feedback, good system models with moderate state dimension, or availability of sufficient computational ressources. In fact, not all of these requirements can be met in applications. Thus design and implementation of predictive control schemes pose ongoing research challenges. This thesis has tackled some of these challenges by presenting new NMPC schemes which are specifically tailored to constrained trajectory-tracking and path-following problems.

# Bibliography


Abou-Kandil, H., G. Freiling, G. Jank, and V. Ionescu (2003). *Matrix Riccati equations in control and systems theory.* Systems & Control: Foundations & Applications. Birkhäuser, Basel.

Aguiar, A.P. (2005). *Performance Limitations in Reference-Tracking and Path-Following.* 44th IEEE Conference on Decision, Control, and European Control Conference, Workshop, Seville, Spain.

Aguiar, A.P. and J.P. Hespanha (2004). "Logic-based switching control for trajectory-tracking and path-following of underactuated autonomous vehicles with parametric modeling uncertainty". In: *Proceedings of the 2004 American Control Conference.* Vol. 4, pp. 3004–3010.

– (2007). "Trajectory-Tracking and Path-Following of Underactuated Autonomous Vehicles With Parametric Modeling Uncertainty". In: *IEEE Trans. Autom. Contr.* Vol. 52(8), pp. 1362–1379.

Aguiar, A.P., D.B. Dacic, J.P. Hespanha, and P.V. Kokotovic (2004). "PATH-FOLLOWING OR REFERENCE-TRACKING? An answer relaxing the limits to performance". In: *Proc. of 5th IFAC/EURON Symposium on Intelligent Autonomous Vehicles, Lisboa, Portugal 2004.*

Aguiar, A.P., J.P. Hespanha, and P.V. Kokotovic (2005). "Path-following for nonminimum phase systems removes performance limitations". In: *IEEE Trans. Automat. Contr.* Vol. 50(2), pp. 234–239.

– (2008). "Performance limitations in reference tracking and path following for nonlinear systems". In: *Automatica*, vol. 44(3), pp. 598–610.

Al-Hiddabi, S.A. and N.H. McClamroch (2002). "Tracking and maneuver regulation control for nonlinear nonminimum phase systems: application to flight control". In: *IEEE Trans. Contr. Sys. Tech.* Vol. 10(6), pp. 780–792.

Alamir, M. and G. Bornard (1995). "Stability of a truncated infinite constrained receding horizon scheme: the general discrete nonlinear case". In: *Automatica*, vol. 31(9), pp. 1353–1356.

Allgöwer, F. and A. Zheng, eds. (2000). *Nonlinear model predictive control.* Vol. 26. Progress in Systems and Control Theory. Birkhäuser.

Altafini, C. (2002). "Following a path of varying curvature as an output regulation problem". In: *IEEE Trans. Automat. Contr.* Vol. 47(9), pp. 1551–1556.

Anderson, B.D. and J.B. Moore (1969). "New results in linear system stability". In: *SIAM Journal on Control*, vol. 7(3), pp. 398–414.

Anderson, B.D. and J.B. Moore (1990). *Optimal control – linear quadratic methods.* Information and system science series. Prentice Hall, Englewood Cliffs, London.

Angeli, D., R. Amrit, and J.B. Rawlings (2009). "Receding horizon cost optimization for overly constrained nonlinear plants". In: *Proceedings of the 48th IEEE Conference on Decision and Control, 2009 held jointly with the 2009 28th Chinese Control Conference. CDC/CCC 2009.* IEEE, pp. 7972–7977.

Ariens, D., B. Houska, H. Ferreau, and F. Logist (2010-2011). *ACADO for Matlab User's Manual.* 1.0beta. Optimization in Engineering Center (OPTEC). `http://www.acadotoolkit.org/`.

Astolfi, A., P. Bolzern, and A. Locatelli (2004). "Path-tracking of a tractor-trailer vehicle along rectilinear and circular paths: a Lyapunov-based approach". In: *IEEE Trans. Robot. and Autom.* Vol. 20(1), pp. 154–160.

Athans, M. and P.L. Falb (1966). *Optimal Control - An Introduction to Theory and its Applications.* McGraw-Hill Book Company.

Aubin, J.-P. and H. Frankowska (1990). *Set-Valued Analysis.* Systems & Control: Foundations & Applications. Birkhäuser Basel, Boston, Berlin.

Balluchi, A., A. Bicchi, and P. Soueres (2005). "Path-following with a bounded-curvature vehicle: a hybrid control approach". In: *Int. J. Contr.* Vol. 78(15), pp. 1228–1247.

Banaszuk, A. and J. Hauser (1994). "Feedback linearization of transverse dynamics for periodic orbits". In: *Proceedings of the 33rd IEEE Conference on Decision and Control.* Vol. 2, pp. 1639–1644.

– (1995). "Feedback linearization of transverse dynamics for periodic orbits". In: *Sys. Contr. Lett.* Vol. 26(2), pp. 95–105.

Bemporad, A. and M. Morari (1999). "Robust model predictive control: A survey". In: *Robustness in identification and control.* Ed. by A. Garulli and A. Tesi. Vol. 245. Lecture Notes in Control and Information Sciences. Springer Berlin / Heidelberg, pp. 207–226.

Bensoussan, A., G. Da Prato, M. Delfour, and S. Mitter (1993). *Representation and control of infinite dimensional systems - Volume II.* Systems & Control: Foundations & Applications. Birkhäuser, Basel.

Berkovitz, L.D. (1974). *Optimal control theory.* Vol. 12. Applied Mathematical Sciences. Springer.

Bittanti, S., A.J. Laub, and J.C. Willems (1991). *The Riccati equation.* Communication and control engineering series. Springer Verlag.

Blanchini, F. and S. Miani (2008). *Set-theoretic methods in control.* Systems & Control: Foundations & Applications. Birkhäuser, Basel.

Boe, F. and B. Hannaford (1998). "Online improvement of speed and tracking performance on repetitive paths". In: *IEEE Trans. Contr. Sys. Tech.* Vol. 6(3), pp. 350–358.

Böhm, C. (2010). “Predictive Control using Semi-definite Programming – Efficient Approaches for Periodic Systems and Lur’e Systems”. PhD thesis. Universität Stuttgart.

Böhm, C., M. Lazar, and F. Allgöwer (2010a). “A relaxation of Lyapunov conditions and controller synthesis for discrete-time periodic systems”. In: *Proceedings of 49th IEEE Conference on Decision and Control (CDC)*, pp. 3277–3282.

– (2010b). “Stability analysis of periodically time-varying systems using periodic Lyapunov functions”. In: *Proc. IFAC Workshop on Periodic Control Systems (PSYCO)*. Citeseer.

Boyd, S.P. and L. Vandenberghe (2004). *Convex Optimization*. University Press, Cambridge.

Brenan, K.E., S.L. Campbell, and Petzold L.R. (1996). *Numerical Solution to Initial-Value Problems in Differential-Algebraic Equations*. Classics in applied mathematics 14. Society for Industrial and Applied Mathematics (SIAM).

Broeck, L. Van den (2011). “Time Optimal Control of Mechatronic Systems Through Embedded Optimization (Tijdsoptimale controle van mechatronische systemen door middel van ingebedde optimalisatie)”. PhD thesis. K.U. Leuven.

Bryson, A.E. and Y.-C. Ho (1969). *Applied Optimal Control*. Ginn and Company, Waltham, Massachusetts.

Bullo, F. and A.D. Lewis (2004). *Geometric control of mechanical systems – modeling, analysis, and design for simple mechanical control systems*. Springer, New York.

Charlet, B., J. Lévine, and R. Marino (1989). “On dynamic feedback linearization”. In: *Sys. Contr. Lett.* Vol. 13(2), pp. 143–151.

– (1991). “Sufficient conditions for dynamic state feedback linearization”. In: *SIAM Journal on Control and Optimization*, vol. 29, pp. 38–57.

Chen, H. and F. Allgöwer (1997). “A quasi-infinite horizon nonlinear predictive control scheme for stable systems: Application to a CSTR”. In: *Proc. IFAC ADCHEM*, pp. 471–476.

– (1998). “A quasi-infinite horizon nonlinear model predictive control scheme with guaranteed stability”. In: *Automatica*, vol. 34(10), pp. 1205–1217.

Chen, W.H., J. O’Reilly, and D.J. Ballance (2003). “On the terminal region of model predictive control for non-linear systems with input/state constraints”. In: *International journal of adaptive control and signal processing*, vol. 17(3), pp. 195–207.

Consolini, L. and M. Tosques (2005). “A path following problem for a class of non-holonomic control systems with noise”. In: *Automatica*, vol. 41(6), pp. 1009–1016.

Constantinides, A., J.L. Spencer, and Gaden E.L. (1970). “Optimization of batch fermentation processes. II. Optimum temperature profiles for batch penicillin fermentations”. In: *Biotechnology and Bioengineering*, vol. 12, pp. 1081–1098.

Dacic, D., D. Nesic, A. Teel, and W. Wang (2011). “Path folllowing for nonlinear systems with unstable zero dynamics: An averaging solution”. In: *IEEE Trans. Autom. Contr.* Vol. 56, pp. 880–886.

Dacic, D.B. and P.V. Kokotovic (2006). "Path-following for linear systems with unstable zero dynamics". In: *Automatica*, vol. 42(10), pp. 1673–1683.

Dacic, D.B., D. Nesic, and P.V. Kokotovic (2007). "Path-Following for Nonlinear Systems With Unstable Zero Dynamics". In: *IEEE Trans. Autom. Contr.* Vol. 52(3), pp. 481–487.

Dahl, O. and L. Nielsen (1990). "Torque-limited path following by online trajectory time scaling". In: *IEEE Trans. Robot. Autom.* Vol. 6(5), pp. 554–561.

de Oliveira Kothare, S.L. and M. Morari (June 2000). "Contractive model predictive control for constrained nonlinear systems". In: *IEEE Trans. Automat. Contr.* Vol. 45(6), pp. 1053 –1071. ISSN: 0018-9286.

Dieci, L. and T. Eirola (1994). "Positive definiteness in the numerical solution of Riccati differential equations". In: *Numerische Mathematik*, vol. 67(3), pp. 303–313.

– (1996). "Preserving monotonicity in the numerical solution of Riccati differential equations". In: *Numerische Mathematik*, vol. 74(1), pp. 35–47.

Diehl, M., R. Amrit, and J.B. Rawlings (2011). "A Lyapunov function for economic optimizing model predictive control". In: *IEEE Trans. Automat. Contr.* (99), pp. 703–707.

Dittmar, R. and B.M. Pfeiffer (2006). "Modellbasierte prädiktive Regelung in der industriellen Praxis (Industrial Application of Model Predictive Control)". In: *at-Automatisierungstechnik*, vol. 54(12), pp. 590–601.

Do, K.D. and J. Pan (2006). "Global robust adaptive path following of underactuated ships". In: *Automatica*, vol. 42(10), pp. 1713–1722.

Do, K.D., Z.P. Jiang, and J. Pan (2004). "Robust adaptive path following of underactuated ships". In: *Automatica*, vol. 40(6), pp. 929–944.

El-Hawwary, M.I. and M. Maggiore (2008). "Global Path Following for the Unicycle and Other Results". In: *Proceedings of the American Control Conference 2008, Seattle*, pp. 3500–3505.

Encarnaçao, P. and A. Pascoal (2001). "Combined trajectory tracking and path following: An application to the coordinated control of autonomous marine craft". In: *Proceedings of the 40th IEEE Conference on Decision and Control*, pp. 964–969.

Faulwasser, T. and R. Findeisen (2009a). "Ein prädiktiver Ansatz zur Lösung nichtlinearer Pfadverfolgungsprobleme unter Beschränkungen". In: *at - Automatisierungstechnik*, vol. 57(8), pp. 386–394.

– (2009b). "Nonlinear model predictive path-following control". In: *Nonlinear Model Predictive Control - Towards New Challenging Applications*. Ed. by L. Magni, D. Raimundo, and F. Allgöwer. Lecture Notes in Control and Information Sciences 384. Springer, Berlin, pp. 335–343.

– (2010). "Constrained Output Path-Following for Nonlinear Systems Using Predictive Control". In: *Proc. of 8th IFAC Symposium on Nonlinear Control Systems (NOLCOS), Bologna, Italy*, pp. 753–758.

– (2011). “A Predictive Control Approach to Trajectory Tracking Problems via Time-Varying Level Sets of Lyapunov Functions”. In: *Proc. of the 50th IEEE Conf. on Decision and Control and European Control Conference, Orlando, Florida, USA*, pp. 3381–3386.

– (2012). “Predictive Path Following without Terminal Constraints”. In: *Proc. of the 20th Int. Symposium on Mathematical Theory of Networks and Systems (MTNS), Melbourne, Australia.*

Faulwasser, T., B. Kern, and R. Findeisen (2009a). “Model predictive path-following for constrained nonlinear systems”. In: *Proc. 48th IEEE Conf. on Decision and Control held jointly with the 2009 28th Chinese Control Conf. CDC/CCC 2009*, pp. 8642–8647.

Faulwasser, T., B. Kern, P. Varutti, and R. Findeisen (2009b). “Prädiktive Regelung nichtlinearer Systeme unter asynchronen Mess- und Stellsignalen”. In: *at - Automatisierungstechnik*, vol. 57(6), pp. 279–287.

Faulwasser, T., V. Hagenmeyer, and R. Findeisen (2011). “Optimal Exact Path-Following for Constrained Differentially Flat Systems”. In: *Proc. of 18th IFAC World Congress, Milano, Italy*, pp. 9875–9880.

Ferramosca, A., D. Limon, I. Alvarado, T. Alamo, and E.F. Camacho (2009). “MPC for tracking with optimal closed-loop performance”. In: *Automatica*, vol. 45(8), pp. 1975 –1978.

Ferreau, H.J., P. Ortner, P. Langthaler, L. Re, and M. Diehl (2007). “Predictive control of a real-world diesel engine using an extended online active set strategy”. In: *Annual Reviews in Control*, vol. 31(2), pp. 293–301.

Ferreau, H.J., H.G. Bock, and M. Diehl (2008). “An online active set strategy to overcome the limitations of explicit MPC”. In: *Int. J. of Rob. and Nonl. Contr.* Vol. 18(8), pp. 816–830.

Findeisen, R. (2006). *Nonlinear Model Predictive Control: A Sampled-Data Feedback Perspective*. Fortschr.-Ber. VDI Reihe 8 Nr. 1087. VDI Verlag, Düsseldorf.

Findeisen, R., L. Imsland, F. Allgöwer, and B.A. Foss (2003). “State and output feedback nonlinear model predictive control: An overview”. In: *European Journal of Control*, vol. 9(2-3), pp. 190–206.

Findeisen, R., L. Biegler, and F. Allgöwer (2007). *Assessment and future directions nonlinear model predictive control*. Vol. 358. Lecture Notes in Control and Information Sciences. Springer Berlin.

Findeisen, R., L. Grüne, J. Pannek, and P. Varutti (2011). “Robustness of Prediction Based Delay Compensation for Nonlinear Systems”. In: *Proc. of 18th IFAC World Congress, Milano, Italy, 28.08.-02.09.2011.*

Fliess, M., J. Lévine, P. Martin, and P. Rouchon (1995a). “Design of trajectory stabilizing feedback for driftless flat systems”. In: *Proc. 3rd Eur. Contr. Conf., Rome, Italy*, pp. 1882–1887.

Fliess, M., J. Lévine, P. Martin, and P. Rouchon (1995b). “Flatness and defect of non-linear systems: introductory theory and examples”. In: *Int. J. Contr.* Vol. 61(6), pp. 1327–1361.

Fontes, F. (2001). “A General Framework to Design Stabilizing Nonlinear Model Predictive Controllers”. In: *Sys. Contr. Lett.* Vol. 42(2), pp. 127–143.

Frezza, R. (1999). “Path following for air vehicles in coordinated flight”. In: *Proc. IEEE/ASME Int Advanced Intelligent Mechatronics Conf*, pp. 884–889.

Frezza, R., A. Beghi, and A. Saccon (2004). “Model predictive for path following with motorcycles: application to the development of the pilot model for virtual prototyping”. In: *Proc. 43rd IEEE Conference on Decision and Control (CDC)*. Vol. 1, pp. 767–772.

Fujiwara, M., Z.K. Nagy, J.W. Chew, and R.D. Braatz (2005). “First-principles and direct design approaches for the control of pharmaceutical crystallization”. In: *J. Pro. Contr.* Vol. 15, pp. 493–504.

Ghabcheloo, R., A. Pascoal, C. Silvestre, and I. Kaminer (2005). “Coordinated path following control of multiple wheeled robots with directed communication links”. In: *Proc. 44th IEEE Conference on Decision and Control, 2005 and 2005 European Control Conference. CDC-ECC’05*. IEEE, pp. 7084–7089.

Ghaemi, R., S. Oh, and J. Sun (2010). “Path following of a model ship using Model Predictive Control with experimental verification”. In: *Proc. American Control Conf. (ACC)*, pp. 5236–5241.

Gondhalekar, R. and C.N. Jones (2011). “MPC of constrained discrete-time linear periodic systems–A framework for asynchronous control: Strong feasibility, stability and optimality via periodic invariance”. In: *Automatica*, vol. 47(2), pp. 326–333.

Graichen, K. and A. Kugi (2010). “Stability and Incremental Improvement of Sub-optimal MPC Without Terminal Constraints”. In: *IEEE Trans. Automat. Contr.* Vol. 55(11), pp. 2576–2580.

Grimm, G., M. J. Messina, S. E. Tuna, and A. R. Teel (2005). “Model predictive control: for want of a local control Lyapunov function, all is not lost”. In: *IEEE Trans. Automat. Contr.* Vol. 50(5), pp. 546–558.

Grimm, G., M.J. Messina, S.E. Tuna, and A.R. Teel (2007). “Nominally Robust Model Predictive Control With State Constraints”. In: *IEEE Trans. Automat. Contr.* Vol. 52(10), pp. 1856–1870.

Grüne, L. (2009). “Analysis and design of unconstrained nonlinear MPC schemes for finite and infinite dimensional systems”. In: *SIAM Journal on Control and Optimization*, vol. 48(2), pp. 1206–1228.

– (2011). “Optimal invariance via receding horizon control”. In: *Proceedings of the 50th IEEE Conference on Decision and Control and European Control Conference, Orlando, Florida, USA*, pp. 2668 –2673.

Grüne, L. and J. Pannek (2011). *Nonlinear Model Predictive Control: Theory and Algorithms.* Communication and Control Engineering. Springer Verlag.

Grüne, L., J. Pannek, M. Seehafer, and K. Worthmann (2010). “Analysis of unconstrained nonlinear MPC schemes with time varying control horizon”. In: *SIAM Journal on Control and Optimization*, vol. 48(8), pp. 4938 –4962.

Gu, C. (2009). “QLMOR: a new projection-based approach for nonlinear model order reduction”. In: *Proc. IEEE/ACM International Conference on Computer-Aided Design-Digest of Technical Papers, ICCAD 2009.* Pp. 389–396.

Gu, D.B. and H.S. Hu (2006). “Receding horizon tracking control of wheeled mobile robots”. In: *IEEE Trans. Contr. Sys. Tech.* Vol. 14(4), pp. 743–749.

Hagenmeyer, V. (2003). *Robust nonlinear tracking control based on differential flatness.* Fortschr.-Ber. VDI Reihe 8 Nr. 978, VDI Verlag, Düsseldorf.

Hagenmeyer, V. and E. Delaleau (2003). “Exact feedforward linearization based on differential flatness”. In: *Int. J. Contr.* Vol. 76(6), pp. 537–556.

Hagenmeyer, V. and M. Zeitz (2004). “Flachheitsbasierter Entwurf von linearen und nichtlinearen Vorsteuerungen”. In: *at - Automatisierungstechnik*, vol. 52, pp. 3–12.

Hamel, T., P. Soueres, and D. Meizel (2001). “Path following with a security margin for mobile robots”. In: *Int. J. Sys. Sci.* Vol. 32(8), pp. 989–1002.

Hauser, J. and R. Hindman (1995). “Maneuver regulation from trajectory tracking: Feedback linearizable systems”. In: *Proceedings IFAC Symp. Nonlinear Control Systems Design*, pp. 595–600.

– (1996). “Maneuver modified trajectory tracking”. In: *International Symposium on Mathematical Theory of Networks.*

– (1997). “Aggressive flight maneuvers”. In: *Decision and Control, 1997, Proceedings of the 36th IEEE Conference on.* Vol. 5, 4186–4191 vol.5.

Henson, M. and D. Seborg (1997). *Nonlinear Process Control.* Prentice Hall, Upper Saddle River, NJ.

Hladio, A., C. Nielsen, and D. Wang (2011). “Path following controller design for a class of mechanical systems”. In: *Proc. of 18th IFAC World Congress, Milano, Italy*, pp. 10331–10336.

Houska, B., H.J. Ferreau, and M. Diehl (2011). “ACADO toolkit – An open-source framework for automatic control and dynamic optimizationf”. In: *Optimal Control Applications and Methods*, vol. 32(3), pp. 298–312.

Ihle, I.-A., M. Arcak, and T.I. Fossen (2007). “Passivity-based designs for synchronized path-following”. In: *Automatica*, vol. 43(9), pp. 1508–1518.

Isidori, A. (1995). *Nonlinear control systems.* 3rd. Springer Verlag.

Jadbabaie, A. (2000). “Receding Horizon Control of Nonlinear Systems: A Control Lyapunov Function Approach”. PhD thesis. California Institute of Technology Pasadena, California.

Jadbabaie, A. and J. Hauser (2005). “On the stability of receding horizon control with a general terminal cost”. In: *IEEE Trans. Automat. Contr.* Vol. 50(5), pp. 674–678.

Jadbabaie, A., J. Yu, and J. Hauser (2001). “Unconstrained receding-horizon control of nonlinear systems”. In: *IEEE Trans. Automat. Contr.* Vol. 46(5), pp. 776–783.

Kalman, R.E. (1960). "Contributions to the theory of optimal control". In: *Bol. Soc. Mat. Mexicana*, vol. 5(2), pp. 102–119.
– (1963). "The theory of optimal control and the calculus of variations". In: *Mathematical optimization techniques*, pp. 309–331.
Kanjanawanishkul, K. and A. Zell (2009). "Path following for an omnidirectional mobile robot based on model predictive control". In: *Proc. IEEE International Conference on Robotics and Automation (ICRA'09).* IEEE, pp. 3341–3346.
Keerthi, S.S. and E.G. Gilbert (1988). "Optimal infinite-horizon feedback laws for a general class of constrained discrete-time systems: Stability and moving-horizon approximations". In: *Journal of Optimization Theory and Applications*, vol. 57(2), pp. 265–293.
Kehl, S., W.D. Posler, and M. Zeitz (2005). "Vehicle path-following with a GPS-aided inertial navigation system". In: *Control And Observer Design For Nonlinear Finite And Infinite Dimensional Systems.* Ed. by T. Meurer, K. Graichen, and E.D. Gilles. Vol. 322. Lecture Notes in Control and Information Sciences. Springer Berlin, pp. 285–300.
Kern, B., C. Böhm, R. Findeisen, and F. Allgöwer (2009). "Receding Horizon Control for Linear Periodic Time-Varying Systems Subject to Input Constraints". In: *Nonlinear Model Predictive Control - Towards New Challenging Applications.* Ed. by L. Magni, D. Raimondo, and F. Allgöwer. Vol. 384. Lecture Notes in Control and Information Sciences. Springer Berlin, pp. 109–117.
Khalil, H.K. (2002). *Nonlinear Systems.* 3rd. Prentice Hall, New Jersey.
Kögel, M. and R. Findeisen (2011). "A Fast Gradient Method for Embedded Linear Predictive Control". In: *Proceedings of the 18th IFAC World Congress, Milano, Italy.*
Kravaris, C., R.A. Wright, and J.F. Carrier (1989). "Nonlinear controllers for trajectory tracking in batch processes". In: *COMP. CHEM. ENG.* Vol. 13(1-2), pp. 73–82.
Kreindler, E. (1969). "On servo problems reducible to regulator problems". In: *IEEE Trans. Automat. Contr.* Vol. 14(4), pp. 413–415.
Krstic, M., I. Kanellakopoulos, and P. Kokotovic (1995). *Nonlinear and Adaptive Control Design.* John Wiley and Sons.
Kwakernaak, H. and R. Sivan (1972a). *Linear optimal control systems.* Vol. 188. Wiley-Interscience New York.
– (1972b). "The maximally achievable accuracy of linear optimal regulators and linear optimal filters". In: *IEEE Trans. Automat. Contr.* Vol. 17(1), pp. 79–86.
Lam, D., C. Manzie, and M. Good (2010). "Model predictive contouring control". In: *Proc. 49th IEEE Conf. Decision and Control (CDC)*, pp. 6137–6142.
– (2011). "Application of Model Predictive Contouring Control to an X-Y Table". In: *Proc. of 18th IFAC World Congress, Milano, Italy*, pp. 10325–10330.
Lapierre, L., D. Soetano, and A. Pascoal (July 2006). "Nonsingular path following control of a unicycle in the presence of parametric modelling uncertainties". In: *Int. J. Rob. Nonl. Contr.* Vol. 16(10), pp. 485–503.

Lee, E.B. and L. Markus (1967). *Foundations of optimal control theory*. The SIAM series in applied mathematics. John Wiley & Sons New York, London, Sydney.

Lévine, J. (2009). *Analysis and control of nonlinear systems: a flatness-based approach*. Mathematical Engineering. Springer, Berlin.

Li, Z., J. Sun, and S. Oh (2009). "Path following for marine surface vessels with rudder and roll constraints: An MPC approach". In: *Proc. of 2009 American Control Conference (ACC '09)*, pp. 3611–3616.

Limon, D., T. Alamo, F. Salas, and EF Camacho (2006). "On the stability of constrained MPC without terminal constraint". In: *IEEE Trans. Aut. Contr.* Vol. 51(5), pp. 832–836.

Limon, D., I. Alvarado, Alamo T., and E.F. Camacho (2008). "MPC for tracking piecewise constant references for constrained linear systems". In: *Automatica*, vol. 44(9), pp. 2382–2387.

Maciejowski, J.M. (2002). *Predictive control: with constraints*. Pearson Education Limited.

Magni, L. and R. Scattolini (2005). "On the solution of the tracking problem for nonlinear systems with MPC". In: *Int. J. Sys. Sci.* Vol. 36(8), pp. 477–484.

– (2006). "Stabilizing decentralized model predictive control of nonlinear systems". In: *Automatica*, vol. 42(7), pp. 1231–1236.

– (2007). "Tracking of non-square nonlinear continuous time systems with piecewise constant model predictive control". In: *J. Pro. Contr.* Vol. 17(8), pp. 631–640.

Magni, L., G. De Nicolao, and R. Scattolini (2001). "Output feedback and tracking of nonlinear systems with model predictive control". In: *Automatica*, vol. 37(10), pp. 1601–1607.

Magni, L., D.M. Raimondo, and F. Allgöwer, eds. (2009). *Nonlinear model predictive control: towards new challenging applications*. Vol. 384. Lecture Notes in Control and Information Sciences. Springer Berlin.

Martin, P., R.M. Murray, and P. Rouchon (1997). "Flat systems". In: *Proc. of the 4th European Control Conf*, pp. 211–264.

Mayne, D.Q. and H. Michalska (1990). "Receding horizon control of nonlinear systems". In: *IEEE Trans. Automat. Contr.* Vol. 35(7), pp. 814–824.

Mayne, D.Q., J.B. Rawlings, C.V. Rao, and P.O.M. Scokaert (2000). "Constrained model predictive control: Stability and optimality". In: *Automatica*, vol. 36(6), pp. 789–814.

McClamroch, H.N. (1990). "Feedback stabilization of control systems described by a class of nonlinear differential-algebraic equations". In: *Sys. Contr. Lett.* Vol. 15(1), pp. 53–60.

McCormick, G.P. (1976). "Computability of global solutions to factorable nonconvex programs: Part I–Convex underestimating problems". In: *Mathematical programming*, vol. 10(1), pp. 147–175.

Michalska, H. (1996). “Trajectory Tracking Control Using the Receding Horizon Strategy”. In: *Symposium on Control, Optimization and Supervision: CESA ’96 IMACS.*

Michalska, H. and D.Q. Mayne (1993). “Robust Receding Horizon Control of Constrained Nonlinear Systems”. In: *IEEE Trans. Automat. Contr.* Vol. 38, pp. 1623–1633.

Michalska, H. and R.B. Vinter (1994). “Nonlinear stabilization using discontinuous moving-horizon control”. In: *IMA Journal of Mathematical Control and Information*, vol. 11(4), pp. 321–340.

Michel, A.N. and R.K. Miller (1977). *Qualitative analysis of large scale dynamical systems.* Academic Press.

Miller, D.E. and R.H. Middleton (2008). “On Limitations to the Achievable Path Following Performance for Linear Multivariable Plants”. In: *IEEE Trans. Automat. Contr.* Vol. 53(11), pp. 2586–2601. ISSN: 0018-9286.

Nagy, Z.K. (2007). “Applications and application aspects of NMPC - from simulation to industrial implementation via OptCon”. In: *Proc. of the Int. Workshop on Nonlinear Model Predictive Control - Software and Applications (NMPC-SOFAP)*, pp. 35–36.

Nagy, Z.K., B. Mahn, R. Franke, and F. Allgöwer (2007). “Evaluation study of an efficient output feedback nonlinear model predictive control for temperature tracking in an industrial batch reactor”. In: *Control Engineering Practice*, vol. 15(7), pp. 839 –850. ISSN: 0967-0661.

Nagy, Z.K., J.W. Chew, M. Fujiwara, and R.D. Braatz (2008). “Comparative performance of concentration and temperature controlled batch crystallizations”. In: *Journal of Process Control*, vol. 18(3-4), pp. 399–407.

Nakamura, Y., H. Ezaki, Y. Tan, and W. Chung (2001). “Design of steering mechanism and control of nonholonomic trailer systems”. In: *IEEE Trans. Robot. Automat.* Vol. 17(3), pp. 367–374.

Nielsen, C. and M. Maggiore (2004). “Maneuver regulation via transverse feedback linearization: Theory and examples”. In: *Proceedings of the IFAC Symposium on Nonlinear Control Systems (NOLCOS), Stuttgart, Germany.*

– (2006). “Output stabilization and maneuver regulation: A geometric approach”. In: *Sys. Contr. Lett.* Vol. 55, pp. 418–427.

– (2008). “On local transverse feedback linearization”. In: *SIAM Journal on Control and Optimization*, vol. 47, pp. 2227–2250.

Nielsen, C., C. Fulford, and M. Maggiore (2010). “Path following using transverse feedback linearization: Application to a maglev positioning system”. In: *Automatica*, vol. 46(3), pp. 585–590.

Nijmeijer, H. and A.J. van der Schaft (1990). *Nonlinear dynamical control systems.* Springer.

Notarstefano, G., M. Pasquotti, and R. Frezza (2005). “Path Following of a Rolling Disk Using Throttle Only”. In: *Proc. IEEE Int. Symp. Control and Automation Mediterrean Conf Intelligent Control*, pp. 680–685.

Pannocchia, G., J.B. Rawlings, and S.J. Wright (2011). “Conditions under which suboptimal nonlinear MPC is inherently robust”. In: *Sys. Contr. Lett.* Vol. 60(9), pp. 747–755.

Parisini, T. and R. Zoppoli (1995). “A receding-horizon regulator for nonlinear systems and a neural approximation”. In: *Automatica*, vol. 31(10), pp. 1443–1451.

Phat, V.N. and V. Jeyakumar (2010). “Stability, stabilization and duality for linear time-varying systems”. In: *Optimization*, vol. 59(4), pp. 447–460.

Qin, S.J. and T.A. Badgwell (1997). “An overview of industrial model predictive control technology”. In: *AIChE Symposium Series*. Vol. 93. 316. New York, NY: American Institute of Chemical Engineers., pp. 232–256.

– (2000). “An overview of nonlinear model predictive control applications”. In: *Nonlinear model predictive control*. Ed. by F. Allgöwer and A. Zheng. Vol. 26. Progress in Systems and Control Theory. Birkhäuser, pp. 369–392.

Qui, L. and E.J. Davison (1993). “Performance limitations of non-minimum phase systems in the servomechanism problem”. In: *Automatica*, vol. 29(2), pp. 337–349.

Raczy, C. and G. Jacob (1999). “Fast and smooth controls for a trolley crane”. In: *Journal of Decision Systems*, vol. 8(3), pp. 367–388.

Raff, T., S. Huber, Z.K. Nagy, and F. Allgöwer (2006). “Nonlinear Model Predictive Control of a Four Tank System: An Experimental Stability Study”. In: *Proc. IEEE International Conference on Control Applications, 2006, (CCA ’06)*, pp. 237 –242.

Raimondo, D.R., L. Magni, and R. Scattolini (2007). “Decentralized MPC of nonlinear systems: An input-to-state stability approach”. In: *Int. J. Robust Nonlinear Contr.* Vol. 17, pp. 1651–1667.

Rawlings, J. and R. Amrit (2009). “Optimizing process economic performance using model predictive control”. In: *Nonlinear Model Predictive Control - Towards New Challenging Applications*. Ed. by L. Magni, D. Raimondo, and F. Allgöwer. Vol. 384. Lecture Notes in Control and Information Sciences. Springer Berlin, pp. 119–138.

Rawlings, J.B. and D.Q. Mayne (2009). *Model Predictive Control: Theory & Design*. Nob Hill Publishing, Madison, WI.

Reble, M. and F. Allgöwer (2011). “Unconstrained Nonlinear Model Predictive Control and Suboptimality Estimates for Continuous-Time Systems”. In: *Proc. IFAC World Congress 2011, Milano, Italy, 28.08.-02.09.2011*, pp. 6733–6738.

– (2012). “Unconstrained model predictive control and suboptimality estimates for nonlinear continuous-time systems”. In: *Automatica*, vol. 48(8), pp. 1812–1817.

Richter, S., C.N. Jones, and M. Morari (2009). “Real-time input-constrained MPC using fast gradient methods”. In: *Proceedings of the 48th IEEE Conference on Decision and Control and the 28th Chinese Control Conference, CDC/CCC*. IEEE, pp. 7387–7393.

Richter, S., S. Mariethoz, and M. Morari (2010). “High-speed online MPC based on a fast gradient method applied to power converter control”. In: *Proc. 2010 American Control Conference (ACC 2010)*, pp. 4737–4743.

Rothfuß, R. (1997). *Anwendung der flachheitsbasierten Analyse und Regelung nichtlinearer Mehrgrößensysteme.* Fortschr.-Ber. VDI Reihe 8 Nr. 664, VDI Verlag, Düsseldorf.

Rothfuß, R., J. Rudolph, and M. Zeitz (1996). “Flatness based control of a nonlinear chemical reactor model”. In: *Automatica*, vol. 32, pp. 1433–1439.

Rouchon, P., M. Fliess, J. Lévine, and P. Martin (1993). “Flatness, motion planning and trailer systems”. In: *Proc. 34th IEEE Conf. on Decision and Control, Piscataway, USA,* vol. 3, pp. 2700–2705.

Rutquist, P.E. and M.M. Edvall (2009). “PROPT-Matlab optimal control software”. In: *Tomlab Optimization Inc.*

Saccon, A., J. Hauser, and A. Beghi (2012). “Trajectory Exploration of a Rigid Motorcycle Model”. In: *IEEE Trans. Contr. Sys. Techn.* Vol. 20(2), pp. 424–437.

Samson, C. (1995). “Control of chained systems application to path following and time-varying point-stabilization of mobile robots”. In: *IEEE Trans. Automat. Contr.* Vol. 40(1), pp. 64–77.

Santos, L.O., P.A. Afonso, J.A. Castro, N. Oliveira, and L.T. Biegler (2001). “On-line implementation of nonlinear MPC: an experimental case study”. In: *Contr. Eng. Pract.* Vol. 9(8), pp. 847–857.

Seron, M., J. Braslavsky, P. V. Kokotovic, and D. Q. Mayne (1999). “Feedback limitations in nonlinear systems: from Bode integrals to cheap control”. In: *IEEE Trans. Automat. Contr.* Vol. 44(4), pp. 829–833.

Shin, K. and N. McKay (1985). “Minimum-time control of robotic manipulators with geometric path constraints”. In: *IEEE Trans. Automat. Contr.* Vol. 30(6), pp. 531 –541.

Siciliano, B., L. Sciavicco, and G. Villani L. Oriolo (2009). *Robotics: Modelling, Planning and Control.* Advanced Textbooks in Control and Signal Processing. Springer London.

Simon, L., Z. Nagy, and K. Hungerbuehler (2009). “Swelling constrained control of an industrial batch reactor using a dedicated NMPC environment: OptCon”. In: *Nonlinear Model Predictive Control - Towards New Challenging Applications.* Ed. by L. Magni, D. Raimundo, and F. Allgöwer. Lecture Notes in Control and Information Sciences 384. Springer, Berlin, pp. 531–539.

Sira-Ramírez, H.J and S.K. Agrawal (2004). *Differentially flat systems.* Control Engineering Series. Marcel Dekker Inc, New York.

Skjetne, R. (2005). “The Maneuvering Problem”. PhD thesis. Norwegian University of Science, Technology, Faculty of Information Technology, Mathematics, and Electrical Engineering, Department of Engineering Cybernetics, Trondheim, Norway.

Skjetne, R. and T.I. Fossen (2001). “Nonlinear maneuvering and control of ships”. In: *Proc. MTS/IEEE Conf OCEANS and Exhibition*. Vol. 3, pp. 1808–1815.

Skjetne, R., A. R. Teel, and P. V. Kokotovic (2002). “Nonlinear maneuvering with gradient optimization”. In: *Proceedings of the 41st IEEE Conference on Decision and Control, 2002*. Vol. 4, pp. 3926–3931.

Skjetne, R., T. Fossen, and P.V. Kokotovic (2004). “Robust output maneuvering for a class of nonlinear systems”. In: *Automatica*, vol. 40(3), pp. 373–383.

Skjetne, R., T.I. Fossen, and P.V. Kokotovic (2005). “Adaptive maneuvering, with experiments, for a model ship in a marine control laboratory”. In: *Automatica*, vol. 41(2), pp. 289–298.

Slotine, J.-J. and H.S. Yang (1989). “Improving the efficiency of time-optimal path-following algorithms”. In: *IEEE Trans. Robot. Automat.* Vol. 5(1), pp. 118–124.

Soroush, M. and C. Kravaris (1992). “Discrete-Time Nonlinear Controller Synthesis by Input/Output Linearization”. In: *AiChE Journal*, vol. 38, pp. 1923–1945.

Soueres, P., A. Balluchi, and A. Bicchi (2001). “Optimal feedback control for route tracking with a bounded-curvature vehicle”. In: *Int. J. Contr.* Vol. 74(10), pp. 1009–1019.

Su, W., L. Qiu, and J. Chen (2003). “Fundamental performance limitations in tracking sinusoidal signals”. In: *IEEE Trans. Autom. Contr.* Vol. 48(8), pp. 1371–1380.

Tobenkin, M.M., I.R. Manchester, and R. Tedrake (2011). “Invariant funnels around trajectories using sum-of-squares programming”. In: *Proc. of 18th IFAC World Congress, Milano, Italy*, pp. 9218–9223.

Topogonov, V.A. (2006). *Differential Geometry of Curves and Surfaces - A Concise Guide*. Birkhäuser, Boston.

Varga, A. (2008). “On solving periodic Riccati equations”. In: *Numerical Linear Algebra with Applications*, vol. 15(9), pp. 809–835.

Varutti, P., B. Kern, T. Faulwasser, and R. Findeisen (2009). “Event-based model predictive control for networked control systems”. In: *Proc. 48th IEEE Conference on Decision and Control held jointly with the 2009 28th Chinese Control Conference CDC/CCC 2009*, pp. 567–572.

Verscheure, D. (2009). “Contribution to contact modeling and identification and optimal robot motion planning”. PhD thesis. Katholieke Universiteit Leuven, Faculteit Ingenieurswetenschappen, Department Werktuigkunde.

Verscheure, D., B. Demeulenaere, J. Swevers, J. De Schutter, and M. Diehl (2009). “Time-Optimal Path Tracking for Robots: A Convex Optimization Approach”. In: *IEEE Transactions on Automatic Control*, vol. 54(10), pp. 2318–2327.

Wahl, A. and E.D. Gilles (2003). “Automatic Track-Keeping on Waterways Using Optimal Control”. In: *at - Automatisierungstechnik*, vol. 6. In German, pp. 255–264.

Wan, Z. and M.V. Kothare (2003). “An effcient on-line formulation of robust model predictive control using linear matrix inequalities”. In: *Automatica*, vol. 39, pp. 837–846.

Yu, S. (2011). "Robust Model Predictive Control of Constrained Systems". PhD thesis. Universität Stuttgart.

Yu, S., H. Chen, C. Böhm, and F. Allgöwer (2009). "Enlarging the terminal region of NMPC with parameter-dependent terminal control law". In: *Nonlinear Model Predictive Control - Towards New Challenging Applications*. Ed. by L. Magni, D. Raimondo, and F. Allgöwer. Vol. 384. Lecture Notes in Control and Information Sciences. Springer Berlin, pp. 69–78.

Zometa, P., M. Kögel, T. Faulwasser, and R. Findeisen (2012). "Implementation Aspects of Model Predictive Control for Embedded Systems". In: *Proceedings of the 2012 American Control Conference, Montreal, Canada*, pp. 1205–1210.

# Part IV

# Appendices

# A Proof of Theorem 2.1

Theorem 2.1 is a more general version of results on NMPC for autonomous systems [Chen and Allgöwer 1998; Findeisen 2006]. In essence, it is special case of a result presented in [Fontes 2001]. In order to simplify the proofs in Chapters 3 & 5 we give a detailed proof here. We first recall a modified version of Barbalat's Lemma, see e.g. [Khalil 2002]. The proof of the following result can be found in [Michalska and Vinter 1994, Lem. 4].

**Lemma A.1** (Barbalat's Lemma)**.**
*Let $M:\ \mathbb{R}^{n_x} \to \mathbb{R}_0^+$ be a continuous positive definite function and $x$ be an absolutely continuous function on $\mathbb{R}$. If*

$$x(\cdot) \in \mathcal{L}^\infty \quad \textit{and} \quad \dot{x}(\cdot) \in \mathcal{L}^\infty$$

*and*

$$\lim_{t\to\infty} \int_0^t M(x(\tau))d\tau < \infty$$

*then*

$$\lim_{t\to\infty} \|x(t)\| = 0.$$

The proof of Theorem 2.1 follows along the lines of [Findeisen 2006; Fontes 2001]. In step 1 we show recursive feasibility (part a)). In step 2 we establish convergence (part b)).

### Step 1: Recursive Feasibility

Consider a recalculation instant $t_k$, and assume that the OCP (2.3) is feasible. During the time span $t \in [t_k, t_k+\delta)$ the optimal input $u_k^\star : [t_k, t_k+T_p] \to \mathcal{U}$ is applied. Clearly, $u_k^\star(\cdot)$ is a an admissible input up to $t = t_k + T_p$, and can thus be applied up to this time instance. Since we consider no model-plant mismatch the real system trajectory is identical to the predicted one

$$\forall k \text{ and } \forall \tau \in [t_k, t_k + T_p]: \quad x(\tau, t_k, x(t_k)|u_k^\star(\cdot)) = \bar{x}(\tau, t_k, x(t_k)|u_k^\star(\cdot)).$$

Moreover, at $t_k + T_p$ the predicted state starting at time $t_k$ at $x(t_k)$ is in the terminal set $\bar{x}(t_k + T_p, t_k, x(t_k)|u_k^\star(\cdot)) \in \mathcal{E}$. Due condition ii) for all $x$ inside $\mathcal{E}$ and all $t$ the existence of an admissible input $u_\mathcal{E}(\cdot)$ is guaranteed for some time span $[t, t+\epsilon]$ with

$\epsilon \geq \delta$. Now, consider the concatenated input

$$\tilde{u}_{k+1}(\tau) = \begin{cases} u_k^\star(\tau) & \tau \in [t_k, t_k + T_p) \\ u_\mathcal{E}(\tau) & \tau \in [t_k + T_p, t_k + T_p + \delta]. \end{cases} \tag{A.1}$$

We have that $\tilde{u}_{k+1}(\cdot)$ is admissible. Moreover, by condition ii) $u_\mathcal{E}(\cdot)$ ensures that $\tilde{x}(t_{k+1} + T_p, t_{k+1}, x(t_{k+1})|\tilde{u}_{k+1}(\cdot)) \in \mathcal{E}$, and thus the OCP (2.3) at $t_{k+1}$ has a feasible solution. Hence, if (2.3) is feasible at $t_0$, it is feasible for all $t_k = t_0 + k\delta$.

Subsequently, we simplify the notation. We write $\tilde{x}_k(\cdot)$ and $x_k^\star(\cdot)$ instead of $\tilde{x}(\cdot, t_k, x(t_k)|\tilde{u}_k(\cdot))$ and $x^\star(\cdot, t_k, x(t_k)|u_k^\star(\cdot))$, respectively. Note that $\tilde{x}_k(\cdot)$ and $x_k^\star(\cdot)$ are predicted trajectories starting at time $t_k$ at $x(t_k)$. The input signal arising from the sequence of optimal inputs $u_k^\star(\cdot), k \in \mathbb{N}$ is denoted as $u^{mpc}(\cdot)$. The corresponding solution $x(\cdot, t_0, x(t_0)|u^{mpc}(\cdot))$ is briefly denoted as $x(\cdot)$.

### Step 2: Asymptotic Convergence

To show asymptotic convergence a strictly decreasing upper bound on the MPC value function will be constructed. The MPC value function is defined as

$$V_k(t_k, x(t_k)) := \int_{t_k}^{t_k+T_p} F(\tau, x_k^\star(\cdot), u_k^\star(\cdot))d\tau + E(t, x_k^\star(t))|_{t_k+T_p}. \tag{A.2}$$

We investigate the behavior of $V_k(t_k, x(t_k))$ over the time span of one control horizon $[t_k, t_k + \delta]$. We evaluate the value function which starts at $x(t) = x_k^\star(t, t_k, x(t_k)|u_k^\star(\cdot))$ at time $t$. We obtain

$$\begin{aligned} V_k(t, x(t)) &= \int_{t}^{t_k+T_p} F(\tau, x_k^\star(\cdot), u_k^\star(\tau))d\tau + E(t, x_k^\star(t))|_{t_k+T_p} \\ &= V_k(t_k, x(t_k)) - \int_{t_k}^{t} F(\tau, x_k^\star(\cdot), u_k^\star(\cdot))d\tau. \end{aligned} \tag{A.3}$$

Clearly, $V_k(t, x(t))$ decreases for $t \in [t_k, t_k + \delta]$.

Next we prove two technical lemmas which are helpful to conclude asymptotic convergence.

**Lemma A.2.**
*For all $k \in \mathbb{N}$*

$$V_{k+1}(t_{k+1}, x(t_{k+1})) - V_k(t_k, x(t_k)) \leq 0.$$

*Proof.* Consider the cost functional

$$J(t_k, x(t_k), \tilde{x}_k(\cdot), \tilde{u}_k(\cdot)) = \int_{t_k}^{t_k+T_p} F(\tau, \tilde{x}_k(\cdot), \tilde{u}_k(\cdot))d\tau + E(t, \tilde{x}_k(t))|_{t_k+T_p}$$

where $\tilde{u}_k(\cdot)$ is from (A.1) and $\tilde{x}_k(\cdot) = \tilde{x}(\cdot, t_k, x(t_k)|\tilde{u}_k(\cdot))$. Due to (A.2) $V_k(t_k, x(t_k))$ relies on the optimal solutions $x_k^\star(\cdot), u_k^\star(\cdot)$, and thus $V_k(t_k, x(t_k)) \leq$

$J(t_k, x(t_k), \tilde{x}_k(\cdot), \tilde{u}_k(\cdot))$. Hence it holds that

$$V_{k+1}(t_{k+1}, x(t_{k+1})) - V_k(t_k, x(t_k)) \leq J(t_{k+1}, x(t_{k+1}), \tilde{x}_k(\cdot), \tilde{u}_k(\cdot)) - V_k(t_k, x(t_k)). \quad \text{(A.4)}$$

From this we obtain

$$\begin{aligned} J(t_{k+1}, x(t_{k+1}), \tilde{x}_{k+1}(\cdot), \tilde{u}_{k+1}(\cdot)) - V_k(t_k, x(t_k)) = \\ \int_{t_{k+1}}^{t_{k+1}+T_p} F\left(\tau, \tilde{x}_{k+1}(\cdot), \tilde{u}_{k+1}(\cdot)\right) d\tau + E(t, \tilde{x}_{k+1}(t))|_{t_{k+1}+T_p} \\ - \int_{t_k}^{t_k+T_p} F\left(\tau, x_k^\star(\cdot), u_k^\star(\cdot)\right) d\tau - E(t, x_k^\star(t))|_{t_k+T_p}. \end{aligned}$$

Rearranging the right hand side leads to

$$\begin{aligned} J(t_{k+1}, x(t_{k+1}), \tilde{x}_{k+1}(\cdot), \tilde{u}_{k+1}(\cdot)) - V_k(t_k, x(t_k)) = \\ \int_{t_{k+1}}^{t_{k+1}+T_p} F\left(\tau, \tilde{x}_{k+1}(\cdot), \tilde{u}_{k+1}(\cdot)\right) d\tau - \int_{t_k}^{t_k+T_p} F\left(\tau, x_k^\star(\cdot), u_k^\star(\cdot)\right) d\tau \\ + E(t, \tilde{x}_{k+1}(t))|_{t_{k+1}+T_p} - E(t, x_k^\star(t))|_{t_k+T_p}. \quad \text{(A.5)} \end{aligned}$$

Due to the construction of $\tilde{u}_{k+1}(\cdot)$ in (A.1) we know that for $\tau \in [t_{k+1}, t_k + T_p]$ the inputs $\tilde{u}_{k+1}(\tau) = u_k^\star(\tau)$ are identical. Moreover, at time $t_{k+1}$ the trajectories $\tilde{x}_{k+1}(\cdot)$ and $x_k^\star(\cdot)$ are at $x(t_{k+1})$. Thus we have

$$\forall \tau \in [t_{k+1}, t_k + T_p]: \quad x_k^\star(\tau, t_k, x(t_k)|u_k^\star(\cdot)) = \tilde{x}_{k+1}(\tau, t_{k+1}, x(t_{k+1})|\tilde{u}_{k+1}(\cdot)). \quad \text{(A.6)}$$

Hence it holds that

$$\begin{aligned} \int_{t_{k+1}}^{t_{k+1}+T_p} F\left(\tau, \tilde{x}_{k+1}(\cdot), \tilde{u}_{k+1}(\cdot)\right) d\tau - \int_{t_k}^{t_k+T_p} F\left(\tau, x_k^\star(\cdot), u_k^\star(\cdot)\right) d\tau = \\ \int_{t_k+T_p}^{t_{k+1}+T_p} F\left(\tau, \tilde{x}_{k+1}(\cdot), \tilde{u}_{k+1}(\cdot)\right) d\tau - \int_{t_k}^{t_{k+1}} F\left(\tau, x_k^\star(\cdot), u_k^\star(\cdot)\right) d\tau. \end{aligned}$$

Subsitution of the last equation in (A.5) yields

$$\begin{aligned} J(t_{k+1}, x(t_{k+1}), \tilde{x}_{k+1}(\cdot), \tilde{u}_{k+1}(\cdot)) - V_k(t_k, x(t_k)) = - \int_{t_k}^{t_{k+1}} F\left(\tau, x_k^\star(\cdot), u_k^\star(\cdot)\right) d\tau \\ + \int_{t_k+T_p}^{t_{k+1}+T_p} F\left(\tau, \tilde{x}_k(\cdot), \tilde{u}_k(\cdot)\right) d\tau + E(t, \tilde{x}(t))|_{t_{k+1}+T_p} - E(t, x_k^\star(t))|_{t_k+T_p}. \quad \text{(A.7)} \end{aligned}$$

Note that for all $\tau \in [t_k + T_p, t_{k+1} + T_p]$ we have $\tilde{x}_{k+1}(\tau, t_{k+1}, x(t_{k+1})|\tilde{u}(\cdot)) \in \mathcal{E}$. Due to condition ii) of the Theorem (2.5) the last three terms are upper bounded by 0. Hence we have

$$J(t_{k+1}, x(t_{k+1}), \tilde{x}_{k+1}(\cdot), \tilde{u}_{k+1}(\cdot)) - V_k(t_k, x(t_k)) \leq - \int_{t_k}^{t_{k+1}} F\left(\tau, x_k^\star(\cdot), u_k^\star(\cdot)\right) d\tau.$$

Taking (A.4) into account we get

$$V_{k+1}(t_{k+1}, x(t_{k+1})) - V_k(t_k, x(t_k)) \leq -\int_{t_k}^{t_{k+1}} F\left(\tau, x_k^\star(\cdot), u_k^\star(\cdot)\right) d\tau \leq 0. \tag{A.8}$$

□

Denote as $V^\delta(t, x(t))$

$$V^\delta(t, x(t)) := V_k(t_k, x(t_k)) - \int_{t_k}^{t} F(\tau, x_k^\star(\cdot), u_k^\star(\cdot)) d\tau, \tag{A.9}$$

which is the remainder of the MPC value function for $x(t) = x_k^\star(t, t_k, x(t_k)|u_k^\star(\cdot))$. On the right hand side of the definition of $V^\delta(t, x_k^\star(t))$ the time instant is $t_k = k\delta$ with $k = \max_{k\in\mathbb{N}}\{k \mid t_k \leq t\}$, i.e., the closest previous sampling instant.

**Lemma A.3.**
*For all* $t \geq t_0$

$$V^\delta(t, x(t)) + \int_{t_0}^{t} F(\tau, x(\cdot), u^{mpc}(\cdot)) d\tau \leq V^\delta(t_0, x(t_0)).$$

*Proof.* First we evaluate $V^\delta(t_k, x(t_k)) - V^\delta(t_0, x(t_0))$.

$$V^\delta(t_k, x(t_k)) - V^\delta(t_0, x(t_0)) = V_k(t_k, x(t_k)) - V_0(t_0, x(t_0)) \tag{A.10}$$

Using (A.8) we have

$$\begin{aligned} &V_k(t_k, x(t_k)) - V_0(t_0, x(t_0)) \leq \\ &\qquad - \sum_{j=0}^{k} \int_{t_j}^{t_{j+1}} F\left(\tau, x_k^\star(\cdot), u_k^\star(\cdot)\right) d\tau = - \int_{t_0}^{t_k} F\left(\tau, x(\cdot), u^{mpc}(\cdot)\right) d\tau. \end{aligned}$$

Since we consider the nominal case without model-plant mismatch, the equality on the right hand side holds. Substitution of (A.10) into the last equation yields

$$V^\delta(t, x(t)) \leq V^\delta(t_0, x(t_0)) - \int_{t_0}^{t} F\left(\tau, x(\cdot), u^{mpc}(\cdot)\right) d\tau.$$

□

What we have shown so far is depicted in Figure A.1. From (A.3) we know that between two sampling instances $t_k$ and $t_{k+1}$ the function $V^\delta(t, x(t))$ is decreasing. From Lemma A.2 we know that $V_{k+1}(t_{k+1}, x(t_{k+1})) \leq V_k(t_k, x(t_k))$. Which means that the starting points for all the decreasing lines $V_k(t_k, x(t_k)) - \int_{t_k}^{t} F(\tau, x_k^\star(\cdot), u_k^\star(\cdot) d\tau$ are a decreasing sequence.

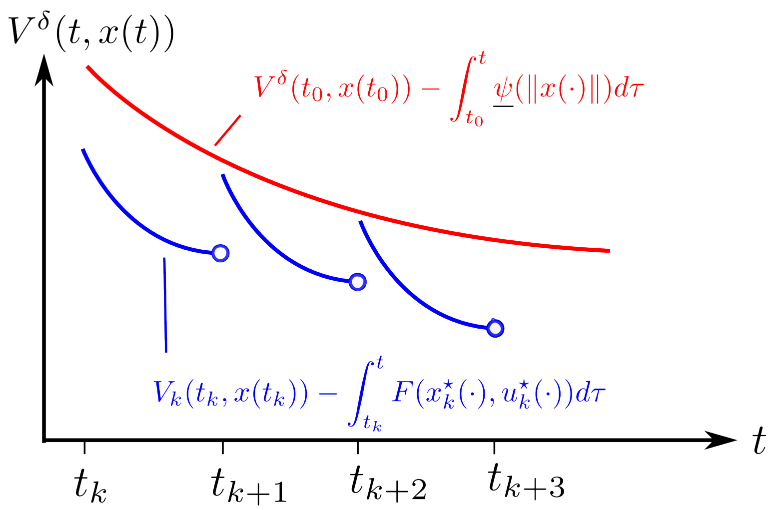


**Figure A.1:** Decreasing behavior of $V^\delta(t, x(t))$.

Now, we use Assumption 2.5, i.e., the cost function $F(\cdot)$ is lower bounded by a positive definite function $\underline{\psi}(\|x\|)$ and obtain

$$\forall t \geq t_0 : \quad V^\delta(t, x(t)) \leq V^\delta(t_0, x(t_0)) - \int_{t_0}^{t} \underline{\psi}(\|x(\cdot)\|)d\tau. \tag{A.11}$$

Due to supposition iii) of the Theorem the OCP (2.3) is feasible for $t = t_0$. Furthermore, we have $V^\delta(t_0, x(t_0)) < \infty$. Hence we deduce from Lemma A.3 that

$$\forall t \geq t_0 : \quad V^\delta(t, x(t)) \leq V^\delta(t_0, x(t_0)) < \infty.$$

From (A.11) we also have that

$$\forall t \geq t_0 : \quad \int_{t_0}^{t} \underline{\psi}(\|x(\cdot)\|)d\tau \leq V^\delta(t_0, x(t_0)) < \infty.$$

Since $\mathcal{U}$ is compact and by Assumptions 2.3–2.4 we have $x(\cdot)$ and $\dot{x}(\cdot) \in \mathcal{L}^\infty$. Hence we apply Lemma A.1 and conclude convergence to the steady state $\lim_{t\to\infty} \|x(t)\| = 0$.

# B Lyapunov Stability

We briefly recall some technical definitions and the notion of a Lyapunov function. A detailed description can be found in many textbooks as, for example, [Khalil 2002]. We consider a non-autonomous system

$$\dot{x}(t) = f(t, x(t)), \quad x(t_0) = x_0 \in \mathbb{R}^{n_x}. \tag{B.1}$$

We assume that $f$ is locally Lipschitz. Solutions starting at $t_0$ at $x_0$ are written as $x(t, t_0, x_0)$.

**Definition B.1** (Class $\mathcal{K}$ function)**.**
*A scalar function $\beta : \mathbb{R}_0^+ \to \mathbb{R}_0^+$ is said to belong to class $\mathcal{K}$, if it is continuous, strictly increasing, and $\beta(0) = 0$. $\beta : \mathbb{R}_0^+ \to \mathbb{R}_0^+$ is said to belong to class $\mathcal{K}_\infty$, if $\beta \in \mathcal{K}$ and if it is radially unbounded, i.e. $\beta(s) \to \infty$ as $s \to \infty$.*

**Definition B.2** (Class $\mathcal{KL}$ function)**.**
*A scalar function $\gamma : \mathbb{R}_0^+ \times \mathbb{R}_0^+ \to \mathbb{R}_0^+$ is said to belong to class $\mathcal{KL}$, if for each fixed $k \in \mathbb{R}_0^+$ it holds that $\gamma(s, k) \in \mathcal{K}$, and for each fixed $s \in \mathbb{R}_0^+$ it holds that $\gamma(s, k)$ is decreasing with respect to $k$ and* $\lim_{k\to\infty} = 0$.

Consider system (B.1). The origin $x = 0$ is called uniformly stable, if the following definition holds.

**Definition B.3** (Uniform stability)**.**
*The system* (B.1) *with $f(t, 0) = 0$ is said to be uniformly stable at $x = 0$, if for every $\epsilon > 0$ there exists an $\delta = \delta(\epsilon)$, which is independent from $t_0$, such that all solutions $x(t, t_0, x_0)$ of* (B.1) *fulfill*

$$\|x_0\| \leq \delta \quad \Rightarrow \quad \|x(t, t_0, x_0)\| \leq \epsilon \quad \textit{for all } t \geq t_0 \geq 0. \tag{B.2}$$

**Definition B.4** (Uniform asymptotic stability)**.**
*If $x = 0$ is a uniformly stable equilibrium of* (B.1)*, and there exists a positive constant $c = c(t_0)$, and additionally the solutions of* (B.1) *fulfill*

*i)*
$$\lim_{t\to\infty} \|x(t, t_0, x_0)\| = 0 \quad \textit{for all } \|x_0\| < c, \tag{B.3a}$$

*ii) and for each $\eta > 0$ there exists $T = T(\eta) > 0$ such that*

$$\|x(t, t_0, x_0)\| < \eta, \quad \textit{for all } t \geq t_0 + T(\eta), \quad \textit{for all } \|x_0\| < c, \tag{B.3b}$$

*then $x = 0$ is said to be uniformly asymptotically stable.*

**Definition B.5** (Exponential stability).
*The equilibrium* $x = 0$ *of* (B.1) *is said to be exponentially stable, if there exist positive constants* $k, \lambda, c$ *such that*

$$\|x(t, t_0, x_0)\| \leq k\|x(0)\|e^{-\lambda(t-t_0)} \text{ for all } \|x_0\| < c. \tag{B.4}$$

**Lemma B.1.**
*The equilibrium* $x = 0$ *of* (B.1) *is uniformly asymptotically stable if and only if there exists a class* $\mathcal{KL}$ *function* $\gamma$ *and a positive constant* $c$*, independent from* $t_0$*, such that for the solutions* $x(t, t_0, x_0)$ *of* (B.1) *it holds that*

$$\|x(t, t_0, x_0)\| \leq \gamma\left(\|x_0\|, t - t_0\right) \quad \text{ for all } t \geq t_0 \geq 0, \text{ for all } \|x_0\| < c. \tag{B.5}$$

**Lemma B.2.**
*Let* $\beta_1, \beta_2, \beta_3 \in \mathcal{K}$*, and system* (B.1) *fulfills* $f(t, 0) = 0$*. Consider some compact domain* $\mathcal{X}$ *containing* $x = 0$ *in its interior, and a function* $V : \mathbb{R}_0^+ \times \mathcal{X} \to \mathbb{R}_0^+$ *such that*

$$\beta_1(\|x\|) \leq V(t, x) \leq \quad \beta_2(\|x\|) \tag{B.6a}$$

$$\frac{\partial V}{\partial t} + \frac{\partial V}{\partial x} f(t, x) \leq -\beta_3(\|x\|) \tag{B.6b}$$

*holds for all* $t \geq 0$ *and all* $x \in \mathcal{X}$*. Then* $x = 0$ *is uniformly asymptotically stable in* $\mathcal{X}$*.*

**Lemma B.3.**
*Consider the suppositions of Lemma B.2. If the class* $\mathcal{K}$ *functions* $\beta_i, i \in \{1, 2, 3\}$ *are given by* $\beta_i(\|x\|) = k_i\|x\|^{a_i}$*, where* $k_i, a_i, i \in \{1, 2, 3\}$ *are positive constants, then* $x = 0$ *is exponentially stable.*

The proofs of the last three lemmas can, e.g., be found in [Khalil 2002]. Finally, we are ready to define a Lyapunov function.

**Definition B.6** (Lyapunov function).
*A function* $V : \mathbb{R}_0^+ \times \mathcal{X} \to \mathbb{R}_0^+$ *which fulfills the suppositions of Lemma B.2 is called a Lyapunov function of* (B.1) *on* $\mathcal{X}$*.*

# C Time-varying Sets

We introduce the notion of time-varying sets. The main idea is to define time-varying sets as point-wise in time projections from an augmented state space $\mathbb{R} \times \mathbb{R}^{n_x}$ to the usual state space $\mathbb{R}^{n_x}$. This is different to other approaches [Michel and Miller 1977] which define the time-varying sets directly in the state space. We work with projections to avoid the formalism of set-valued analysis, see [Aubin and Frankowska 1990]. The notion of time-varying sets plays a crucial role in our developments in Chapter 3.
We consider time-varying systems without control

$$\dot{x} = f(t, x), \quad x(t_0) = x_0 \in \mathbb{R}^{n_x}. \tag{C.1}$$

We assume that $f$ is locally Lipschitz. Solutions starting at $t_0$ at $x_0$ are written as $x(t, t_0, x_0)$.
We want to investigate the relation between the solutions to (C.1) and a time-varying set. To do this we have to introduce the notion of a time-varying set. Consider the extended states $(t, x)$ contained in a set $\Gamma \subset \mathbb{R} \times \mathbb{R}^{n_x}$, where $t$ refers to the time and $x$ refers to the state of (C.1). Corresponding to the set $\Gamma$ a projection $\Pi : \mathbb{R} \times \mathbb{R}^{n_x} \to \mathbb{R}^{n_x}$ is defined

$$\Pi : (t, x) \mapsto x \tag{C.2}$$

which projects any extended state $(t, x)$ onto $x \in \mathbb{R}^{n_x}$. Often it is helpful to work with a subset of $\Gamma$ where the coordinate $t$ is fixed

$$\Gamma_t := \Gamma \cap \{\{t\} \times \mathbb{R}^{n_x}\} \subset \mathbb{R} \times \mathbb{R}^{n_x}. \tag{C.3}$$

Based on this we define a time-varying set as follows.

**Definition C.1** (Time-varying set)**.**
*Given* $\Pi$ *from* (C.2) *and a non-empty set* $\Gamma \subset \mathbb{R} \times \mathbb{R}^{n_x}$. *The family of subsets of* $\mathbb{R}^{n_x}$ *given by*

$$\mathcal{G}_t := \{x \in \mathbb{R}^{n_x} \mid (t, x) \in \Gamma\} = \{\Pi(\Gamma_t) \mid t \in \mathbb{R}\} \tag{C.4}$$

*is called a time-varying set. Accordingly, we define the boundary of* $\mathcal{G}_t$ *point-wise in time*

$$\partial\mathcal{G}_t := \{\partial\Pi(\Gamma_t) \mid t \in \mathbb{R}\} \subset \mathbb{R}^{n_x}. \tag{C.5}$$

*A time-varying set* $\mathcal{G}_t$ *is called* {*open, closed, compact*}, *if for all* $t \in \mathbb{R}$ *the sets* $\Pi(\Gamma_t)$ *are* {*open, closed, compact*}.

Time-varying sets in $\mathbb{R}^{n_x}$ can be understood as point-wise in time projections of a higher dimensional sets living in $\mathbb{R}\times\mathbb{R}^{n_x}$. Similar to the usual time-invariant sets—see e.g. [Blanchini and Miani 2008]—one can define positive invariance of time-varying sets as follows.

**Definition C.2** (Positive invariance of time-varying sets).
*A time-varying set $\mathcal{G}_t \subset \mathbb{R}^{n_x}$ defined for all $t \geq t_0$ is said to be positively invariant w.r.t to* (C.1)*, if every solution $x(t, t_0, x_0)$ with $x_0 \in \mathcal{G}_{t_0}$ is globally defined, and for all $t > t_0$ it holds that $x(t, t_0, x_0) \in \mathcal{G}_t$.*

To study the positive invariance of time-varying sets we want to exclude cases, where the boundary $\partial\mathcal{G}_t$ does not evolve continuously with time. We adapt a definition, which was provided in [Michel and Miller 1977, p. 64] for open sets $\mathcal{G}_t$, such that it is applicable to open and closed sets $\Gamma \subset \mathbb{R} \times \mathbb{R}^{n_x}$.

**Definition C.3** (Property P of a time-varying set).
*A time-varying set $\mathcal{G}_t \subset \mathbb{R}^{n_x}$ defined for all $t \in [t_0, t_1]$ is said to have Property P, if for all $t \in [t_0, t_1]$ it holds*

$$\partial\Pi(\Gamma_t) = \Pi\left((\partial\Gamma)_t\right). \tag{C.6}$$

Note that on the right side of the above equality we firstly apply the boundary operation, secondly we fix $t$, and finally we project from $\{t\} \times \mathbb{R}^{n_x}$ to $\mathbb{R}^{n_x}$. This order of operations is crucial since $\partial(\Gamma_t) = \Gamma_t \subset \mathbb{R} \times \mathbb{R}^{n_x}$. An example of a set with Property P is $\Gamma^1 = \{(t, x) \in \mathbb{R} \times \mathbb{R}^{n_x} \mid \|x\| \leq e^{-t}\}$.

**Example C.1** (Time-varying set without Property P).
*To illustrate the difficulties which can arise from the time variance of sets consider*

$$\Gamma^2 = \{[0, a] \times \{x \in \mathbb{R} \mid 0 \leq x \leq b_2\}\} \cup \{[a, \infty) \times \{x \in \mathbb{R} \mid 0 \leq x \leq b_1\}\} \tag{C.7}$$

*for $a > 0, b_2 > b_1 > 0$. The set $\Gamma^2$ is depicted in Figure C.1. Note the discontinuity at $t = a$. On the one hand, we have $(\partial\Gamma^2)_{t=a} = \{(t, x) \mid t = a, (x \in [b_1, b_2]) \vee (x = 0)\}$. This yields $\Pi((\partial\Gamma^2)_{t=a}) = \{x \mid x \in [b_1, b_2]) \vee (x = 0)\}$. On the other hand, $\Gamma^2_{t=a} = \{(t, x) \mid t = a, 0 \leq x \leq b_2\}$ and $\partial\Pi(\Gamma^2_{t=a}) = \{0, b_2\} \subset \mathbb{R}$. We see that for this example $\partial\Pi(\Gamma^2_{t=a}) \neq \Pi((\partial\Gamma^2)_{t=a})$. $\Gamma^2$ does not have Property P.*

Clearly, one can ask for the reason to introduce Property P of a time-varying level set. This setting is motivated by the need to study the invariance of time-varying sets. Usually, positive invariance of time-invariant compact sets with respect to the flow of a dynamical systems is verified via *Nagumo's Theorem* [Blanchini and Miani 2008]. Under some technical assumptions this theorem states that the invariance of a compact set $\mathcal{S} \subset \mathbb{R}^{n_x}$ under the dynamics $\dot{x} = f(x)$ can be checked by evaluation of $f(x)$ for all boundary points $x \in \partial\mathcal{S}$.

However, checking the positive invariance of general time-varying sets can be tricky. This is illustrated by the following example.

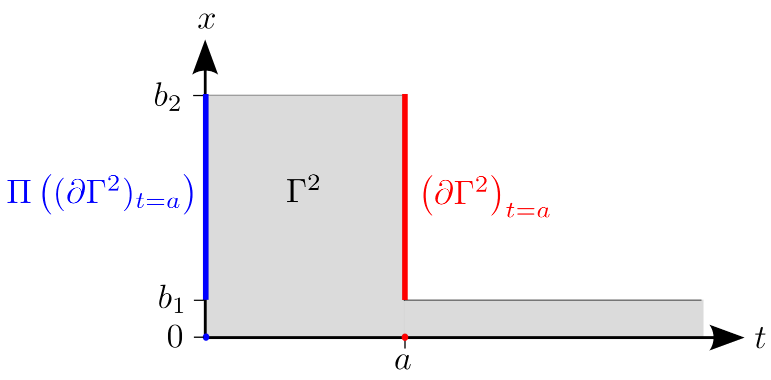


**Figure C.1:** Example set $\Gamma^2$ which has not Property P.

**Example C.2** (Positive invariance of time-varying sets).
*Recall the set* $\Gamma^2$ *from* (C.7)*, which is depicted in Figure C.1. As shown in Example C.1, this set does not have Property P. It is easy to check that for all* $t \in [0, a]$ *the time-varying boundary of* $\mathcal{G}_t$ *is* $\partial\mathcal{G}_t = \{0, b_2\}$*, and for all* $t \in (a, \infty) : \ \partial\mathcal{G}_t = \{0, b_1\}$*. Consider the trivial scalar dynamics*

$$\dot{x} = 0, \quad x(0) = x_0$$

*where* $b_1 < x_0 < b_2$*. Clearly,* $x(t, t_0, x_0) = x_0$*, and for all* $t \leq a$ *it holds that* $(t, x_0) \in \Gamma^2$*. For* $t > a$ *we have* $(t, x_0) \notin \Gamma^2$*. Consequently, for all* $t \leq a$ *it holds that* $(x_0) \in \mathcal{G}_t$*, and for* $t > a : x_0 \notin \mathcal{G}_t$*. This means that the set* $\mathcal{G}_t$ *is not positive invariant under the considered dynamics. However, for all* $t \geq 0$ *it holds that* $x(t) = x_0 \notin \partial\mathcal{G}_t$*. In other words, the trajectory* $x(t) = x_0$ *never passes the time-varying boundary* $\partial\mathcal{G}_t$*.*

Such cases, where trajectories can leave a time-varying set without being in the time-varying boundary $\partial\mathcal{G}_t$ for at least one time instance, are in general difficult to handle. If a time-varying set has Property P, things are simplified. This is expressed in the following lemma.

**Lemma C.1.**
*Given an either closed or open set* $\Gamma \subset \mathbb{R} \times \mathbb{R}^{n_x}$ *and a curve* $t \in [t_1, t_2] \mapsto (t, p(t)) \in \mathbb{R} \times \mathbb{R}^{n_x}$*, whereby* $p(t) \in \mathcal{C}^0$*. Suppose the corresponding time-varying set* $\mathcal{G}_t \subset \mathbb{R}^{n_x}$ *defined over* $[t_1, t_2]$ *has Property P.*
*If* $(t_1, p(t_1))^T \in \operatorname{int}\Gamma$ *and* $(t_2, p(t_2))^T \notin \Gamma$ *with* $t_2 > t_1$*, then there exists at least one* $\tilde{t} \in (t_1, t_2]$ *such that* $p\left(\tilde{t}\right) \in \partial\mathcal{G}_{\tilde{t}}$*.*

*Proof.* We have $p(t) \in \mathcal{C}^0$ and $(t_1, p(t_1))^T \in \operatorname{int}\Gamma$. Combined with $(t_2, p(t_2))^T \notin \Gamma$ this implies that there exists at least one $\tilde{t} \in (t_1, t_2]$ such that $(\tilde{t}, p(\tilde{t})) \in \partial\Gamma$. Hence it follows $(\tilde{t}, p(\tilde{t})) \in (\partial\Gamma)_{\tilde{t}}$. But since $\mathcal{G}_t \subset \mathbb{R}^{n_x}$ has Property P (C.6) we have that $\partial\mathcal{G}_{\tilde{t}} = \Pi\left((\partial\Gamma)_{\tilde{t}}\right)$. Projecting $(\tilde{t}, p(\tilde{t}))$ by $\Pi$ from (C.2) we yield $p(\tilde{t}) \in \partial\mathcal{G}_t$. $\square$

Verifying whether or not a general time-varying set has Property P can be tricky. If a time-varying set is an ellipsoid with time-varying shape, the following lemma holds.

**Lemma C.2** (Property P of ellipsoidally time-varying sets).
*Any set*

$$\Gamma = \{(t,x) \mid x^T P(t)x - \pi^2(t) \leq 0\} \subset \mathbb{R} \times \mathbb{R}^{n_x}, \tag{C.8}$$

*where $P(t) \in \mathcal{BC}^+(\mathbb{R}^{n_x} \times \mathbb{R}^{n_x})$ and $\pi(t) \in \mathcal{C}^0$ has Property P.*

*Proof.* On the one hand, the boundary of $\partial\Gamma$ is $\partial\Gamma = \{(t,x) \mid x^T P(t)x - \pi^2(t) = 0\}$. Fixing the time coordinate $t$ we have $(\partial\Gamma)_t$ which is an $n_x$-dimensional ellipsoid. The projection of the boundary set to the $\mathbb{R}^{n_x}$ yields the outer surface of the ellipsoid $\Pi((\partial\Gamma)_t) = \{x \mid x^T P(t)x - \pi^2(t) = 0\}$. On the other hand, $\Pi(\Gamma_t) = \{x \mid x^T P(t)x - \pi^2(t) \leq 0\}$. The boundary of this set is again the outer surface of the ellipsoid $\partial\Pi(\Gamma_t) = \{x \mid x^T P(t)x - \pi^2(t) = 0\}$. □

One can also ask for sufficient conditions on positive invariance of an ellipsoidally time-varying set with respect to (C.1). To this end we denote the upper right hand derivative of a function $\pi(t) \in \mathcal{C}^0$ as $D^+\pi(t)$, and the elementwise upper right hand derivative of $P(t) \in \mathcal{BC}^+(\mathbb{R}^{n_x} \times \mathbb{R}^{n_x})$ is written as $D^+P(t)$.

**Lemma C.3** (Local positive invariance of ellipsoidally time-varying sets).
*Consider system* (C.1) *and an ellipsoidally time-varying set* $\Gamma$ *from* (C.8) *where* $P(t) \in \mathcal{BC}^+(\mathbb{R}^{n_x} \times \mathbb{R}^{n_x}), D^+P(t) \in \mathcal{BC}^+(\mathbb{R}^{n_x} \times \mathbb{R}^{n_x})$, *and* $P(t), \pi(t)$ *are absolutely continuous. Assume that the solutions to* (C.1) *exist for all* $(t_0, x_0) \in \Gamma$ *on the interval* $[t_0, t_1]$.
*A solution* $x(t, t_0, x_0)$ *with* $(t_0, x_0) \in \Gamma$ *stays in* $\mathcal{G}_t$ *for all* $t \in [t_0, t_1]$, *if*

$$\forall t \in [t_0, t_1], \forall x \in \partial\mathcal{G}_t: \quad 2x^T P(t) f(t,x) + x^T D^+P(t)x - 2\pi(t)D^+\pi(t) \leq 0. \tag{C.9}$$

*Proof.* Consider

$$s(t) = x(t, t_0, x_0)^T P(t) x(t, t_0, x_0) - \pi^2(t).$$

By our assumptions this is an absolutely continuous function of $t$. Its value at time $t_1$ is

$$s(t_1) = s(t_0) + \int_{t_0}^{t_1} D^+s(\tau)\, d\tau.$$

Recall that $\mathcal{G}_t$ has Property P, hence we have to check only solutions starting at time $t_0$ at $x_0 \in \partial\mathcal{G}_{t_0}$, thus $s(t_0) = 0$. If condition (C.9) holds, we have for all $t \in [t_0, t_1]: \ D^+s(t) \leq 0$. Thus condition (C.9) is sufficient. □

This result is a generalization of Theorem 3.2 from Chapter 3, since $x^T P(t)x$ is not necessarily a Lyapunov function.

In this Appendix we briefly introduced a notion of time-varying sets as point-wise in time projections from an augmented space $\mathbb{R}^{n_x} \times \mathbb{R}$ to the state space $\mathbb{R}^{n_x}$. We have seen that Property P is helpful to investigate the positive invariance of time-varying sets.

# D Riccati Differential Equations

The purpose of this appendix is to collect several results on the existence of (symmetric non-negative definite) solutions to Riccati differential equations (RDE), which arise from optimal control problems of linear systems subject to quadratic cost functionals. Consider an LTV system

$$\dot{x} = A(t)x + B(t)u, \quad x(0) = x_0, \tag{D.1}$$

where $A(t) \in \mathcal{BC}(\mathbb{R}^{n_x \times n_x})$ and $B(t) \in \mathcal{BC}(\mathbb{R}^{n_x \times n_u})$. The Riccati differential equation associated to this system is

$$\dot{P}(t) = P(t)B(t)R^{-1}(t)B^T(t)P(t) - Q(t) - P(t)A(t) - A^T(t)P(t), \tag{D.2}$$

where $Q(t) \in \mathcal{BC}_0^+(\mathbb{R}^{n_x \times n_x})$ and $R(t) \in \mathcal{BC}^+(\mathbb{R}^{n_u \times n_u})$. Conditions guaranteeing the existence of symmetric positive semi-definite solutions to the RDE are of great interest, since

i) one can easily define a time-varying state feedback $u(t) = -R^{-1}(t)B^T(t)P(t)x$ which is optimal with respect to the cost functional

$$J(x_0, x(\cdot), u(\cdot)) = \int_0^T x(\tau)^T Q(\tau)x(\tau) + u(\tau)^T R(\tau)u(\tau)\ d\tau;$$

ii) if the solution $P(t)$ is positive definite a *natural* candidate of a time-varying Lyapunov function is $V(t,x) = x^T P(t)x$.

One way to guarantee the existence of symmetric non-negative definite solutions to the RDE (D.2) is to rely on stabilizability-like properties of the LTV system (D.1). The next definition and the subsequent lemma can be found in [Phat and Jeyakumar 2010].

**Definition D.1** ($Q$-stabilizability, [Phat and Jeyakumar 2010]**).**
*Consider the LTV system* (D.1) *and a matrix* $Q(t) \in \mathcal{BC}_0^+(\mathbb{R}^{n_x \times n_x})$. *We denote such a system as Q-stabilizable if for any initial condition* $x_0$ *there exists a control* $u(t) \in \mathcal{L}^2$ *such that the functional*

$$J_Q(x_0, x(\cdot), u(\cdot)) = \int_0^\infty \|u(\tau)\|^2 + x(\tau)^T Q(\tau)x(\tau)\ d\tau, \tag{D.3}$$

*is bounded.*

**Lemma D.1** (Existence of positive semi-definite RDE solutions).
*If the LTV system* (D.1) *is* $Q$*-stabilizable for some* $Q(t) \in \mathcal{BC}_0^+(\mathbb{R}^{n_x \times n_x})$*, then for all* $t \geq 0$ *the Riccati differential equation* (D.2) *with* $R(t) = I$ *has a solution* $P(t) \in \mathcal{BC}_0^+(\mathbb{R}^{n_x \times n_x})$*.*

As the term $Q$-stabilizability implies the existence of symmetric positive semi-definite solutions to the RDE depends on the stabilizability or controllability properties of the considered LTV system. Of particular importance for the existence of symmetric positive strictly definite solutions to the RDE is the following property which dates back to [Anderson and Moore 1969; Kalman 1960].

**Definition D.2** (Uniform complete controllability).
*The LTV system* (D.1) *is denoted as uniformly completely controllable if for some* $\sigma > 0$ *any two of the subsequent conditions hold*

$$\alpha_1 I \leq \mathcal{G}(s, s+\sigma) \leq \alpha_2 I, \tag{D.4a}$$

$$\alpha_3 I \leq \Phi(s, s+\sigma)\mathcal{G}(s, s+\sigma)\Phi^T(s, s+\sigma) \leq \alpha_4 I, \tag{D.4b}$$

$$\|\Phi(s, \omega)\| \leq \alpha_5(|s-\omega|) \tag{D.4c}$$

*where*

$$\mathcal{G}(s, s+\sigma) = \int_s^{s+\sigma} \Phi(s,\tau)B(\tau)B^T(\tau)\Phi^T(s,\tau)\; d\tau$$

*is the controllability Grammian and* $\Phi(\cdot)$ *denotes the flow of* (D.1)*. Furthermore,* $\alpha_i, i \in \{1,2,3,4\}$ *are positive constants, and* $\alpha_5(\cdot)$ *maps* $\mathbb{R}$ *onto* $\mathbb{R}$ *and is bounded on bounded intervals.*

The next existence result is a slight reformulation of a very early result presented in [Kalman 1960].

**Lemma D.2** (Existence of symmetric strictly positive definite RDE solutions).
*If the LTV system* (D.1) *is completely uniformly controllable, and the weight matrices* $Q(t) \in \mathcal{BC}^+(\mathbb{R}^{n_x \times n_x})$ *and* $R(t) \in \mathcal{BC}^+(\mathbb{R}^{n_u \times n_u})$ *are strictly positive definite and bounded, then the RDE* (D.2) *has a unique strictly positive definite solution* $P(t)$ *which is defined for all* $t \geq 0$*.*

For further details on this subject the reader is refered to the monographs [Abou-Kandil et al. 2003; Anderson and Moore 1990; Bensoussan et al. 1993; Bittanti et al. 1991; Kwakernaak and Sivan 1972b] and to [Anderson and Moore 1969; Kalman 1960; Phat and Jeyakumar 2010]. Details on the numerical solution to Riccati differential equations can be found in [Dieci and Eirola 1994, 1996; Varga 2008].

# E Existence of Optimal Controls

In this appendix we recall a specific result on existence of optimal solutions to optimal control problems. This result is needed to prove Theorem 4.3 in Chapter 4. The result and its proof can be found in [Lee and Markus 1967, Thm. 4, p. 259]. Similar results and extensions to relaxed controls can be found in [Berkovitz 1974; Bryson and Ho 1969].

Consider a cost functional

$$J\left(t_0, t_1, x(\cdot), u(\cdot)\right) = \int_{t_0}^{t_1} F\left(t, x(t), u(t)\right) dt + E\left(t_1, x(t_1)\right), \tag{E.1}$$

and an optimal control problem to be solved:

$$\underset{t_0,\ t_1,\ u(\cdot)}{\text{minimize}}\ J\left(t_0, t_1, x(\cdot), u(\cdot)\right) \tag{E.2a}$$

subject to

$$\begin{aligned}
& x(t) && = f(t, x(t), u(t)) && \text{(E.2b)}\\
\forall t \in [t_0, t_1]: \quad & x(t) && \in \mathcal{X} && \text{(E.2c)}\\
\forall t \in [t_0, t_1]: \quad & u(t) && \in \mathcal{U} \ \subseteq \mathbb{R}^{n_u} && \text{(E.2d)}\\
& x(t_0) && \in \mathcal{X}_0 \subseteq \mathbb{R}^{n_x} && \text{(E.2e)}\\
& x(t_1) && \in \mathcal{X}_1 \subseteq \mathbb{R}^{n_x}. && \text{(E.2f)}
\end{aligned}$$

Note that the start and end time may vary within the fixed compact interval $\tau_0 \leq t_0 \leq t_1 \leq \tau_1$. We assume that the problem data are as follows:

1. The sets $\mathcal{X}_0$ and $\mathcal{X}_1$ are nonempty and compact.
2. The input constraint set $\mathcal{U}$ is nonempty and compact.
3. The state constraints $\mathcal{X}$ are described by a finite or infinite family of continuous functions $h^i : \mathbb{R}^{n_x} \to \mathbb{R}$ such that $\mathcal{X} = \{x \in \mathbb{R}^{n_x} \mid h^i(x) \leq 0, i = 1, \ldots, i_{max}\}$.
4. The family $\mathcal{F}$ of admissible controllers consists of all measurable functions $u : [t_0, t_1] \to \mathcal{U}$, defined on various time intervals $[t_0, t_1] \subseteq [\tau_0, \tau_1]$, such that
   - each $u(\cdot)$ has a response $x(t, t_0, x_0 | u(\cdot))$ steering $x(t_0) \in \mathcal{X}_0$ to $x(t_1, t_0, x_0 | u(\cdot)) \in \mathcal{X}_1$;
   - for all $t \in [t_0, t_1]: \quad u(t) \in \mathcal{U}$;
   - and for all $i = 1, \ldots, i_{max}$ it holds that $h^i(x(t, t_0, x_0 | u(\cdot))) \leq 0$.
5. The cost $F : \mathbb{R} \times \mathbb{R}^{n_x} \times \mathbb{R}^{n_u} \to \mathbb{R}$ is $\mathcal{C}^1$ and $E : \mathbb{R}^{n_x} \to \mathbb{R}$ is continuous.

The following result states sufficient conditions for the existence of optimal controls.

**Theorem E.1** (Lee and Markus 1967)**.**
*Given OCP* (E.2)*. Assume*

*i) The family $\mathcal{F}$ of admissible controllers is not empty.*
*ii) There exists a uniform bound $\|x(t, t_0, x_0|u(\cdot))\| < \infty$ on $t_0 \leq t \leq t_1$ for all solutions $x(t, t_0, x_0|u(\cdot))$ driven by admissible $u(\cdot) \in \mathcal{F}$.*
*iii) The extended velocity set*

$$\mathcal{S} := \left\{ s \in \mathbb{R}^{n_x+1} \mid u \in \mathcal{U} \mapsto (F(t, x, u), f(t, x, u))^T \right\}$$

*is convex in $\mathbb{R}^{n_x+1}$ for fixed $(t, x)$.*

*Then there exists an optimal control $u^\star(\cdot) \in \mathcal{F}$ on $t_0^\star \leq t \leq t_1^\star$.*

# F Terminal Region and End Penalty for the Robot Example

In this appendix we derive a terminal region and an end penalty for the 2-DoF robot from Section 5.2.2. Our goal is to compute these objects such that the fulfill the conditions of Theorem 5.2. Our main idea is to exploit the exact feedback linearizability of the robot dynamics. We proceed in four steps:

1. We rewrite the problem in a feedback linearized transversal normal form.
2. We design a local controller and a terminal region for the path parameter dynamics, which are the internal dynamics of the normal form.
3. We design a locally stabilizing controller for the transversal states. A terminal region is obtained as a level set of local Lyapunov function.
4. Finally, we derive an end penalty such that the conditions of Theorem 5.2 are fulfilled.

**Step 1:** Recall the augmented system description of the path-following problem (5.24)

$$\begin{aligned}
\dot{x} &= \begin{pmatrix} x_2 \\ B^{-1}(x_1)\left(u - C(x_1, x_2)x_2 - g(x_1)\right) \end{pmatrix} \\
\dot{z} &= \begin{pmatrix} 0 & 1 \\ 0 & 0 \end{pmatrix} z + \begin{pmatrix} 0 \\ 1 \end{pmatrix} v \\
e &= x_1 - p(z_1) \\
\theta &= z_1.
\end{aligned}$$

Note that $x_1 = (q_1, q_2)^T$ and $x_2 = (\dot{q}_1, \dot{q}_2)^T$ are the vector of joint positions and the vector of joint velocities, respectively. Subsequently, we derive a continuous feedback to solve the path-following problem. In contrast to Example 4.2 the path parameter dynamics are chosen as an integrator chain of length two. Since we derive continuous feedbacks this causes no difficulties, cf. Remark 4.3. Clearly, the control $u_{lin} : \mathbb{R}^4 \times \mathbb{R}^2 \to \mathbb{R}^2$

$$u_{lin}(x, w) = C(x_1, x_2)x_2 + g(x_1) + B(x_1)w \tag{F.1}$$

achieves exact static feedback linearization of the augmented system. The variable $w \in \mathbb{R}^2$ is the input of the feedback linearized system. Application of $u_{lin}$ leads to

$$\left(\dot{x}_1, \dot{x}_2, \dot{z}_1, \dot{z}_2\right)^T = \left(x_2, w, z_2, v\right)^T, \quad \begin{pmatrix} e \\ \theta \end{pmatrix} = \begin{pmatrix} x_1 - p(z_1) \\ z_1 \end{pmatrix}.$$

We map these augmented dynamics into a transversal normal. We use $\xi_1 = e \in \mathbb{R}^2, \xi_2 = \dot{e} \in \mathbb{R}^2, \eta_1 = z_1, \eta_2 = z_2$, and obtain

$$\begin{pmatrix} \dot{\xi}_1 \\ \dot{\xi}_2 \\ \dot{\eta}_1 \\ \dot{\eta}_2 \end{pmatrix} = \left(\begin{array}{c|c} A_\xi & \mathbf{0}^{4\times 2} \\ \hline \mathbf{0}^{2\times 4} & A_\eta \end{array}\right) \begin{pmatrix} \xi_1 \\ \xi_2 \\ \eta_1 \\ \eta_2 \end{pmatrix} + \left(\begin{array}{c|c} B_\xi & \mathbf{0}^{4\times 1} \\ \hline \mathbf{0}^{2\times 2} & B_\eta \end{array}\right) \begin{pmatrix} w - \ddot{p}(\eta_1(t)) \\ v \end{pmatrix} \tag{F.2a}$$

$$\begin{pmatrix} e \\ \theta \end{pmatrix} = \begin{pmatrix} \xi_1 \\ z_1 \end{pmatrix}. \tag{F.2b}$$

The system matrices are given by

$$A_\xi = \left(\begin{array}{c|c} \mathbf{0}^{2\times 2} & \mathbf{I}^{2\times 2} \\ \hline \mathbf{0}^{2\times 2} & \mathbf{0}^{2\times 2} \end{array}\right), B_\xi = \begin{pmatrix} 0 & 0 & 1 & 1 \\ 0 & 0 & 1 & 1 \end{pmatrix}^T, \quad A_\eta = \begin{pmatrix} 0 & 1 \\ 0 & 0 \end{pmatrix}, B_\eta = \begin{pmatrix} 0 \\ 1 \end{pmatrix}.$$

**Step 2:** Now, we are ready to design constraint consistent feedbacks which will lead to terminal regions. Note that the $\eta$-dynamics are not influenced by the $\xi$-dynamics. Thus we begin the feedback design with the path parameter dynamics. Recall that the state constraints for $\eta = z$ are given by the set

$$\mathcal{Z} = \{\eta \in \mathbb{R}^2 \mid \eta_1 \in [\theta_0, 0],\ \eta_2 \in [0, \infty)\}.$$

Subsequently, we construct a feedback $v_\mathcal{E} = K_\eta \eta$ such that the closed loop driven by $A_\eta + B_\eta K_\eta$ is asymptotically stable, and a closed-loop solution with $\eta_0 \in \mathcal{E}_\eta \subset \mathcal{Z}$ satisfies the state constraints for all times. In the phase plane of the $\eta$-dynamics the state constraints $\mathcal{Z}$ require to design a feedback such that the 2nd quadrant is positively invariant. In other words, we have to design a feedback which guarantees convergence to the origin of the $\eta_1$–$\eta_2$ plane while $\eta_2 \geq 0$ holds, cf. Figure F.1.
It is easy to see that for the double integrator $\dot{\eta} = A_\eta \eta + B_\eta v$ we cannot render the complete 2nd quadrant positively invariant with a continuous asymptotically stabilizing feedback $v = K_\eta \eta$. The reasons for this are as follows: Consider the cases where $A_\eta + B_\eta K_\eta$ is asymptotically stable with conjugate complex eigenvalues. This case has to be ruled out, since it leads to solutions with convergent oscillations around the origin. Also the case of non-asymptotic stability is not helpful, since solutions starting in $\mathcal{Z}$ should converge to the origin. So it remains to choose $K_\eta$ such that we obtain two stable and real eigenvalues. This is achieved if the coefficients $K_\eta = (k_1, k_2)$ satisfy $k_1, k_2 < 0$ and $k_2^2 > -4k_1$. Such a feedback leads to the situation depicted in Figure F.1. We have two stable eigenspaces (blue lines) in the 2nd and 4th quadrant. The fact that the eigenspaces cannot lie in the 1st and 3rd quadrant is easily verified by calculation of the eigenvectors for $k_1, k_2 \leq 0$. A solution of $\dot{\eta} = (A_\eta + B_\eta K_\eta)\eta$ starting anywhere in the cone spanned by the eigenspaces in the 2nd quadrant converges to the origin with $\eta_2 = \dot{\theta} \geq 0$.

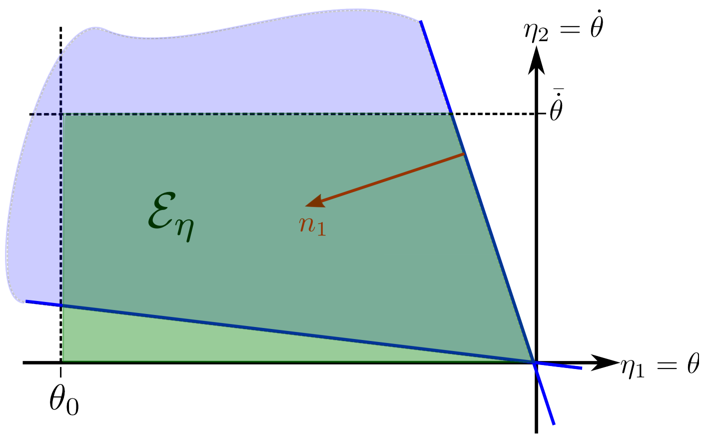


**Figure F.1:** Terminal region for the path parameter dynamics.

Consider the case that a solution starts on the negative $\eta_1$-axis. We have

$$\dot\eta = \begin{pmatrix} 0 & 1 \\ k_1 & k_2 \end{pmatrix} \begin{pmatrix} -\alpha \\ 0 \end{pmatrix} = \begin{pmatrix} 0 \\ -\alpha k_1 \end{pmatrix}, \quad \alpha \geq 0.$$

Thus $k_1 \geq 0$ implies that such a solution converges to the origin with $\dot\theta \geq 0$. However, if the solution starts on the positive $\eta_2$-axis, we have

$$\dot\eta = \begin{pmatrix} 0 & 1 \\ k_1 & k_2 \end{pmatrix} \begin{pmatrix} 0 \\ \alpha \end{pmatrix} = \begin{pmatrix} \alpha \\ \alpha k_2 \end{pmatrix}, \quad \alpha \geq 0.$$

That means that such a solution leaves the 2nd quadrant, no matter how the coefficients $k_1, k_2$ are chosen. From these observations we conclude that only a subset of the 2nd quadrant can be used as terminal region for the $\eta$-dynamics.
We use as a feedback

$$v_{\mathcal{E}} = K_\eta \eta, \quad K_\eta = (k_1, k_2),\ k_1, k_2 < 0,\ k_2^2 > -4k_1,\ k_2 \leq -k_1\theta_0 \left(\bar{\dot\theta}\right)^{-1} < 0. \tag{F.3}$$

The additional condition $k_2 \leq -k_1\theta_0/\bar{\dot\theta}$ ensures that a closed-loop solution starting anywhere on the line $\eta = (\alpha, \bar{\dot\theta}), \alpha \in [\theta_0, 0]$ points towards the $\eta_1$-axis. Based on this feedback we choose the terminal region for the $\eta$-dynamics as

$$\mathcal{E}_\eta := \left\{\eta \in \mathbb{R}^2 \mid \eta_1 \in [\theta_0, 0],\ \eta_2 \in \left[0, \bar{\dot\theta}\right],\ n_1 \cdot \eta \geq 0\right\} \subset \mathcal{Z}. \tag{F.4}$$

Here, $n_1$ is the normal vector corresponding to the upper eigenspace of $A_\eta + B_\eta K_\eta$. The terminal region is sketched in green color in Figure F.1. The verification of positive invariance of $\mathcal{E}_\eta$ with respect to $\dot\eta = (A_\eta + B_\eta K_\eta)\eta$ follows directly from the considerations above. The boundary $0 \leq \eta_2 \leq \bar{\dot\theta}$ is introduced to $\mathcal{E}_\eta$ in order to simplify the design of a terminal region for the $\xi$-dynamics.

**Step 3:** We proceed with the design of a suitable feedback for the $\xi$-part of the transversal dynamics (F.2a). We consider the control

$$w = K_\xi \xi + \ddot{p}(\eta_1(t)) = K_\xi \xi + \frac{\partial^2 p}{\partial \eta_1^2}\eta_2^2 + \frac{\partial p}{\partial \eta_1} v.$$

The first part is a feedback to stabilize the zero-path-error manifold. The second part can be understood as a feedforward control. If this feedback is applied, the $\xi$ part of the dynamics is governed by $\dot{\xi} = (A_\xi + B_\xi K_\xi)\xi$. W.l.o.g. we assume that we have designed a stabilizing gain matrix $K_\xi$, and that

$$V(\xi) = \xi^T P_\xi \xi, \quad P_\xi > 0 \tag{F.5}$$

is a corresponding Lyapunov function. To derive a terminal region we substitute the feedback from above into the exact linearizing feedback (F.1). This yields

$$u_\mathcal{E}(x,z) = C(x_1,x_2)x_2 + g(x_1) + B(x_1)\left(K_x \xi + \ddot{p}(\eta_1(t))\right). \tag{F.6}$$

Note that the transversal states $\xi$ depend on $x$ and $z$. We want to compute a terminal region $\mathcal{E}_\xi \subset \mathbb{R}^4$ such that for all $\xi(x,z)$ inside the region $u_\mathcal{E}(x,z) \in \mathcal{U}$, $x \in \mathcal{X}$ and $z \in \mathcal{Z}$. The main idea is to upper bound the feedback (F.6), and to obtain a terminal region as a level set of $V(\xi)$. The terms $B : \mathbb{R}^2 \to \mathbb{R}^{2\times 2}, C : \mathbb{R}^2 \times \mathbb{R}^2 \to \mathbb{R}^{2\times 2}$ and $g : \mathbb{R}^2 \to \mathbb{R}^2$ from (5.21d-f) can be upper bounded by

$$\forall x \in \mathcal{X}: \quad \|B(x_1)\| \le \bar{B}, \quad \|C(x_1,x_2)\| \le \bar{C}, \quad \|g(x_1)\| \le \bar{g}.$$

To upperbound $\ddot{p}(z_1(t)) \in \mathbb{R}^2$ we restrict ourselves to the set $\mathcal{E}_\eta$ from (F.4). Since the path parametrization $p$ is smooth and $\mathcal{E}_\eta$ is compact, we obtain

$$\forall \eta \in \mathcal{E}_\eta: \quad \|\ddot{p}(\eta_1(t))\| \le \left\|\frac{\partial^2 p}{\partial \eta_1^2}\eta_2^2 + \frac{\partial p}{\partial \eta_1} v\right\| \le \left\|\frac{\partial^2 p}{\partial \eta_1^2}\right\| \left(\bar{\dot{\theta}}\right)^2 + \left\|\frac{\partial p}{\partial \eta_1}\right\| \left\|k_1\theta_0 + k_2\bar{\dot{\theta}}\right\| = \bar{\ddot{p}}.$$

Here, we have used that in the set $\mathcal{E}_\eta$ the $\eta$-dynamics are controlled via $v = K_\eta \eta$. To simplify the further considerations we work with tightened constraints $\bar{\mathcal{U}} \subset \mathcal{U}$, $\bar{\mathcal{X}} \subset \mathcal{X}$

$$\bar{\mathcal{U}} = \left\{u \in \mathbb{R}^2 \mid \|u\| \le \bar{u}\right\} \tag{F.7a}$$

$$\bar{\mathcal{X}} = \left\{x = (x_1,x_2) \in \mathbb{R}^4 \mid \|x_2\| = \|(\dot{q}_1,\dot{q}_2)\| \le \bar{\dot{q}}\right\} \tag{F.7b}$$

where in comparison to (5.22) the 2-norm is used instead of $\|\cdot\|_\infty$.
We apply the bounds from above to the feedback $u : \mathbb{R}^4 \times \mathbb{R}^2 \to \mathbb{R}^2$ from (F.6)

$$\forall (x,z)^T \in \bar{\mathcal{X}} \times \mathcal{E}_\eta: \quad \|u_\mathcal{E}(x,z)\| \le \bar{C}\bar{\dot{q}} + \bar{g} + \bar{B}\left(\bar{\ddot{p}} + \|K_\xi \xi(x,z)\|\right).$$

Reordering the last inequality leads to

$$\frac{\|u_{\mathcal{E}}(x,z)\| - \bar{C}\bar{\dot{q}} - \bar{g}}{\bar{B}} - \bar{\ddot{p}} \leq \|K_\xi\| \cdot \|\xi(x,z)\|.$$

We use the constant $\bar{u}$ as upper bound on the left side, and solve for $\|\xi\|$. Thus

$$\forall (x,z)^T \in \bar{\mathcal{X}} \times \mathcal{E}_\eta: \quad \|\xi(x,z)\| \leq \frac{\bar{u} - \bar{C}\bar{\dot{q}} - \bar{g} - \bar{B}\bar{\ddot{p}}}{\bar{B}\|K_\xi\|} \quad \Rightarrow \quad u(x,z) \in \bar{\mathcal{U}} \subset \mathcal{U}. \quad \text{(F.8)}$$

Subsequently, we derive $\mathcal{E}_\xi$ as a suitable level set of the Lyapunov function $V(\xi)$ from (F.5). In general, the level set is

$$\mathcal{L}_c := \left\{ \xi \in \mathbb{R}^4 \mid \xi^T P_\xi \xi \leq c^2 \right\}.$$

The constant $c$ can be computed as follows

$$\underset{c>0}{\text{maximize}}\ c \quad \text{(F.9a)}$$

subject to

$$\forall \xi \in \mathcal{L}_c: \quad \|\xi\| \leq \frac{\bar{u} - \bar{C}\bar{\dot{q}} - \bar{g} - \bar{B}\bar{\ddot{p}}}{\bar{B}\|K_\xi\|} \quad \text{(F.9b)}$$

$$\forall \xi \in \mathcal{L}_c: \quad \|\xi_2\| \leq \bar{\dot{q}} - \bar{\dot{p}}. \quad \text{(F.9c)}$$

Here $\bar{\dot{p}}$ is a bound on $\dot{p}(\eta_1(t))$ which can be obtained for $\eta \in \mathcal{E}_\eta$ in a similar fashion as $\bar{\ddot{p}}$. Given $K_\xi$ and $P_\xi$ this is a simplified version of the (convex) problem to compute a maximum volume ellipsoid contained in a convex set, cf. [Boyd and Vandenberghe 2004]. This problem has a solution $c^\star > 0$, if $\bar{\dot{q}} - \bar{\dot{p}} > 0$ and the constant on the right side of (F.9b) is positive. This means that the input bounds $\bar{u}$ and $\bar{\dot{q}}$ have to be sufficiently large.

We use the model data from Table 5.1 and the path (5.23). The bound on $\eta_2$ is set to $\bar{\dot{\theta}} = 0.4$, and the feedback matrix for the $\eta$-dynamics is $K_\eta = (-0.1, -1.33)$. This leads to the terminal constraint for $\eta$

$$\mathcal{E}_\eta = \left\{ \eta \in \mathbb{R}^2 \mid \eta_1 \in [-5.3, 0],\ \eta_2 \in [0, 0.4],\ (-0.78,\ -0.63)\eta \geq 0 \right\}.$$

The Lyapunov function and the feedback matrix for the $\xi$-dynamics

$$V(\xi) = \xi^T \begin{pmatrix} 1.73 & 0 & 1 & 0 \\ 0 & 1.73 & 0 & 1 \\ 1 & 0 & 1.73 & 0 \\ 0 & 1 & 0 & 1.73 \end{pmatrix} \xi, \quad K_\xi = \begin{pmatrix} 1 & 0 & 1.73 & 0 \\ 0 & 1 & 0 & 1.73 \end{pmatrix}.$$

are computed via an LQR controller with $Q_\xi = \mathbf{I}^{4\times 4}, R_\xi = \mathbf{I}^{2\times 2}$. Solving (F.9) with these values leads to $c = 1.59$. Thus the terminal region for the $\xi$-dynamics is

$$\mathcal{E}_\xi = \left\{\xi \in \mathbb{R}^4 \mid \xi^T P_\xi \xi \le 2.53\right\}.$$

Recall that $e = x_1 - p(z_1)$ and $\dot{e} = x_2 - \frac{\partial p}{\partial z_1} z_2$. Rewriting the terminal constraints in $(x, z)$ coordinates leads to

$$\mathcal{E} = \left\{(x,z) \in \mathbb{R}^6 \mid (e,\dot{e})^T P_\xi (e,\dot{e}) \le 2.53),\ z \in \mathcal{E}_\eta\right\} \subset \mathcal{X} \times \mathcal{Z}. \tag{F.10}$$

**Step 4:** It remains to derive an end penalty such that the conditions of Theorem 5.2 are satisfied. Recall condition (5.20), which expresses a relation between the cost $F$ and the end penalty $E$. For the MPFC controller we use a cost function according to Remark 5.2

$$F(e,\dot{e},\theta,u,v) = \|(e,\ \dot{e},\ \theta)\|_Q^2 + \|(u-\tilde{u},\ v)\|_R^2,$$
$$Q = \mathrm{diag}(10^5,\ 10^5,\ 10,\ 10,\ 5),\ R = \mathrm{diag}(10^{-6},\ 10^{-6},\ 10^{-4}).$$

This means we penalize the path error as well as its time derivative. The offset

$$\tilde{u} = (263.0, -262.5)^T = g(p(0))$$

corresponds to the torque required to keep the robot at the final path point $p(0)$.
We derive an end penalty as follows: Firstly, we derive exponential convergence bounds on the states $\xi, \eta$. Secondly, we use this bounds to derive bounds on the terminal control laws (F.3) and (F.6). Finally, we apply all these bounds to derive convergence of the cost function $F$ on $\mathcal{E}$ if the system is controlled via (F.3) and (F.6).
It is easy to see that on $\mathcal{E}_\xi \times \mathcal{E}_\eta$ system (F.2a) controlled via (F.6) admits a quadratic Lyapunov function

$$V(\xi,\eta) = \xi^T P_\xi \xi + \eta^T P_\eta \eta.$$

The existence of such a function implies that on $\mathcal{E}_\xi \times \mathcal{E}_\eta$ the states $\xi$ and $\eta$ converge exponentially, cf. Lemma B.3. Hence the application of (F.6) and $v_\mathcal{E} = K_\eta \eta$ ensure that path-following error $e$ and its time derivative $\dot{e}$ converge exponentially. Thus we have exponential bounds on $\xi = (e,\dot{e}), \eta$ and $v_\mathcal{E} = K_\eta \eta$. Recall that $\dot{p} = \frac{\partial p}{\partial \eta_1}\eta_2$ and $\ddot{p} = \frac{\partial^2 p}{\partial \eta_1^2}(\eta_2)^2 + \frac{\partial p}{\partial \theta} v_\mathcal{E}$, thus we also have exponential bounds on $\dot{p}, \ddot{p}$ and $x_2 = \xi_2 + \dot{p}_1$:

$$\forall(\xi,\eta) \in \mathcal{E}: \quad \|\eta\| \le \alpha_\eta e^{-\beta_\eta t}, \quad \|v_\mathcal{E}\| \le \|K_\eta\|\alpha_\eta e^{-\beta_\eta t} \tag{F.11a}$$
$$\|\xi\| \le \alpha_\xi e^{-\beta_\xi t} \tag{F.11b}$$
$$\|\dot{p}\| \le \alpha_{\dot{p}} e^{-\beta_{\dot{p}} t}, \quad \|\ddot{p}\| \le \alpha_{\ddot{p}} e^{-\beta_{\ddot{p}} t} \tag{F.11c}$$
$$\|x_2\| \le \alpha_{x_2} e^{-\beta_{x_2} t}. \tag{F.11d}$$

The constants $\alpha_i, \beta_i$ in these bounds are strictly positive. Now, we consider solutions to the augmented dynamics (F.2a) which are controlled via the terminal feedbacks (F.3) and (F.6). In other words, we restrict ourselves to solutions $\xi(t, \xi_0 | u_{\mathcal{E}}(\cdot)), \eta(t, \eta_0 | u_{\mathcal{E}}(\cdot))$ with $(\xi_0, \eta_0) \in \mathcal{E}$. Using the bounds on $\xi, \eta$ and $v_{\mathcal{E}}$ we obtain that along these solutions

$$\|u_{\mathcal{E}}(x(t), z(t)) - \tilde{u}\| \leq \underbrace{\|C(x_1, x_2)x_2\|}_{\leq \bar{C}\alpha_{x_2} e^{-\beta_{x_2} t}} + \underbrace{\|B(x_1)\left(K_x \xi + \ddot{p}(\eta_1(t))\right)\|}_{\leq \bar{B}\left(\|K_\eta\| \alpha_\eta e^{-\beta_\eta t} + \alpha_{\ddot{p}} e^{-\beta_{\ddot{p}} t}\right)} + \underbrace{\|g(x_1) - g(p(0))\|}_{\leq \alpha_g e^{-\beta_g t}}$$

The bounds on the first two terms are straightforward. The estimate from above on $g(x_1) - g(p(0))$ is more complicated. Note that $x_1 = \xi + p(\eta_1)$. For $p : [\theta_0, 0] \to \mathbb{R}^2$ from (5.23) one can show that exponential convergence of $\eta$ to 0 implies exponential convergence of $p(\eta_1)$ to $p(0)$. Using this we see that for $t \to \infty$ also the state $x_1$ converges exponentially to $p(0)$ since $x_1 = \xi + p(\eta_1)$. Finally, we use that in $g : \mathbb{R}^2 \to \mathbb{R}^2$ from (5.21f) only cos-functions appear, and conclude that $g(x_1) - g(p(0))$ converges exponentially to 0. Summarizing the last considerations, we have seen that along the solutions generated by the terminal control laws

$$\forall t \geq 0 : \quad \|u_{\mathcal{E}}(x(t), z(t)) - \tilde{u}\| \leq \alpha_u e^{-\beta_u t}, \quad \alpha_u > 0. \tag{F.11e}$$

We proceed by deriving a bound on the cost function inside the terminal region $\mathcal{E}$. $\mathcal{E}$ is compact. $F$ and the terminal feedbacks $u_{\mathcal{E}}(x, z), v_{\mathcal{E}}(z)$ are continuous. Hence there exists a finite constant $\hat{F}$ such that

$$\forall (x, z) \in \mathcal{E} : \quad 0 \leq F(e, \dot{e}, u_{\mathcal{E}}(x, z), v_{\mathcal{E}}(z)) \leq \hat{F}.$$

Recall that $\xi = (e, \dot{e})^T$. We apply the exponential bounds (F.11) to estimate from above the behavior of $F$ on $\mathcal{E}$ along the trajectories $\xi(t, \xi_0 | u_{\mathcal{E}}(\cdot))$ and $\eta(t, \eta_0 | u_{\mathcal{E}}(\cdot))$. It follows

$$\forall t \geq 0 : \quad F(e(t), \dot{e}(t), u_{\mathcal{E}}(t), v_{\mathcal{E}}(t)) \leq \hat{F} e^{-\beta_F t}$$

with $\beta_F > 0$. Now, one can apply a simliar reasoning as in Remark 3.5 and conclude that purely time dependent end penalties $E(t)$ which satisfy the conditions of Theorem 5.2 exist.[1] For example, a suitable choice is $E(t) = \frac{\hat{F}}{\beta_F} e^{-\beta_F t}$. Recall that we have seen in the proof of Lemma 3.6 that such an end penalty can be dropped during optimization. Thus we use $E(x, z) = 0$.

Finally, we conclude that terminal regions and terminal penalties, which satisfy the conditions of Theorem 5.2, can be derived. However, one needs to mention that it is not straightforward to generalize this approach. We used the global static feedback linearizability of the robot dynamics and its specific structure to obtain bounds on the linearizing feedback.

[1] To be precise the time-dependent end penalty would satisfy an immediate extension of Theorem 5.2 to time-varying end penalties $E(t, x, z)$. To avoid technicalities we do not investigate this further.